A novel geometry based approach for casting process optimisation.

Sood, Minkesh Paul

CIVIL & COMPUTATIONAL ENGINEERING CENTRE
SCHOOL OF ENGINEERING
UNIVERSITY OF WALES SWANSEA

A NOVEL GEOMETRY BASED APPROACH FOR CASTING PROCESS OPTIMISATION

MINKESH PAUL SOOD
B.Sc., M.Phil (*Wales*)

SUBMITTED TO THE UNIVERSITY OF WALES IN FULFILMENT OF THE REQUIREMENTS FOR THE DEGREE OF DOCTOR OF PHILOSOPHY OF ENGINEERING

SWANSEA UNIVERSITY
2006

SUMMARY

The work presented in this thesis constitutes the main body of research carried out to develop a new technique for solidification simulation by using the Medial Axis Transformation (MAT) technique in combination with other geometric reasoning and numerical methods. The aspects of casting solidification researched include a review of existing geometric reasoning techniques and employability of MAT in combination with other methods. In the first phase of research, MAT was used to present a one-dimensional interpolation scheme that provided quick results compared to the numerical methods and evolving temperature solutions in time when compared to modulus method. The scheme successfully predicted the location of hotspots and provided an acceptable temperature distribution. Learning from, and owing to limitations posed by the interpolation scheme, a new innovative and hybrid technique was then proposed that for the first time unifies geometric and numerical methods, thereby inheriting their advantages and overcoming their respective limitations. The inscribed radius and other relevant geometric information were extracted from MAT. This was then combined with the Heuvers' Circle method. A new equation, based on Chvorinov's classic rule and modulus method, was derived that enabled the proposed technique to utilise the radius information of the casting to obtain effective interface boundary conditions for an optimal solution. The proposed method was then tested on a range of casting geometries, including those from the foundries. The problems arising from complexity of the medial axes were resolved by developing a sorting technique to select the most effective Heuvers' radii and a scaling framework was also developed to obtain realistic values. Finally the application of this technique to 3D castings was conceptualised and demonstrated through a case study. Thus an effective technique has been developed that not only retains the simplicity, ease of use, speed of the conventional geometric reasoning techniques but also the accuracy and sensitivity to material properties and boundary conditions offered by the numerical methods. The proposed method is capable of providing optimal solutions in two FE simulations.

DECLARATIONS AND STATEMENTS

This work has not previously been accepted in substance for any degree and is not being concurrently submitted in candidature for any degree.

Signed ... ...(candidate)

Date .....1-12-2006.....

STATEMENT 1

This thesis is being submitted in partial fulfilment of the requirements for the degree of Doctor of Philosophy.

Signed .... ..(candidate)

Date .....1-12-2006.....

STATEMENT 2

This thesis is the result of my own investigations, except where otherwise stated. Other sources are acknowledged by footnotes giving explicit references. A bibliography is appended.

Signed ... ...(candidate)

Date .....1-12-2006.....

STATEMENT 3

I hereby give consent for my thesis, if accepted, to be available for photocopying and for inter-library loan, and for the title and summary to be made available to outside organisations.

Signed ..... .(candidate)

Date .....1-12-2006.....

CONTENTS

Chapter 5: A Novel Approach using Modified Heuvers' Circle Method for Solidification Simulation

Chapter 6: Coupled Thermal Optimisation using Modified Heuvers' Circle Method – Results and Discussions

Chapter 7: Conclusions

List of Figures

LIST OF TABLES

ACKNOWLEDGEMENTS

I would like to express the utmost gratitude to my supervisor, Dr. R. S. Ransing for his invaluable guidance, support, vision and wisdom. The work would not have been possible had it not been for his continuous patience, advice and support. I would also like to extend my sincere thanks to Prof. R. W. Lewis for his support during the initial period of my research. It has been a distinct privilege to have worked under the tutelage of such accomplished and eminent academics.

Many thanks to colleagues in the casting research group Dr. Meghana Ransing, Dr. W. K. S. Pao and Dr. C. Lin who always offered help and willingly shared their knowledge on issues related to my research and their contribution is greatly valued and appreciated. Thanks are also due to Mrs. D. M. Cook, Mrs. M. A. Fox and Ms. Jacqui Evans for their logistic support during the research period. I have been very fortunate during my research to meet an excellent group of friends, Farooq, Ian and Arnaud amongst others, who have had an enriching effect on my PhD experience and many of whom I now regard as close friends.

I would also like to thank my employer for providing me leave. Thanks to Engineering and Physical Sciences Research Council for the partial financial support. Thanks are due to Dr. G. Butlin at Transcendata Europe Ltd for providing licences and technical support for using CADfix. Thanks also to Triplex Components Group and Zeus Foundry for providing casting geometries.

Finally, my deepest gratitude goes to my wife Sarita and children, Ishaan and Rimjhim, my loving parents, family and in-laws for their patience and unwavering support. Your constant encouragement and love has been my sustenance through it all.

ABBREVIATIONS AND NOMENCLATURE

FDM	Finite Difference Method.
FEM	Finite Element Method.
H	Enthalpy of the casting
H_{int}	Interfacial heat transfer coefficient.
h_H	Modified value of interfacial heat transfer coefficient.
h_{inf}	Interfacial heat transfer coefficient
h_o	Original value of interfacial heat transfer coefficient.
IHTC	Interfacial heat transfer coefficient.
$IHTC_{min}$	Minimum value of interfacial heat transfer coefficient
$IHTC_{max}$	Minimum value of interfacial heat transfer coefficient
IBC	Interface boundary conditions.
M	Modulus.
MAT	Medial Axis Transformation.
MA	Medial axis.
MO	Medial object.
MST	Medial Surface Transform.
R_o	Original radius at a section of casting.
R_H	Heuvers' radius at a particular section.
SM	Section Modulus.
K_c	Thermal conductivity of the casting.
K_m	Thermal conductivity of the mould.
c_m	Heat capacity of the mould material.
ρ_c	Mass density of the casting.
ρ_m	Mass density of the mould.
T_m	Mould temperature.
ξ	Normalised radius

Chapter 1

INTRODUCTION

1.1 BACKGROUND

The manufacture of defect free components at low cost and high productivity is of paramount importance to the casting industry. The casting process has many inherent advantages over other shaping methods such as machining, forging, welding, stamping, hot working etc. and remains a preferred choice for metal forming. It took centuries before casting emerged as a science from an early age of primitive art form that was held a captive secret by local craftsmen [1]. In the past, experience was gained either by using a 'trial and error' method or by undertaking expensive experiments. Many 'dos' and 'don'ts' have evolved in the casting process over a period of its development through ever evolving foundry practices. Solidification of liquid metal in a casting is an important phase in the casting process influencing quality and yield of products. The last freezing sections and locations are often the most likely and probable locations of defects such as shrinkage cavities or porosity. Even until the middle of last century, the feeding of cast metal was guided by experience and relied heavily on the intuitive knowledge and skills of the foundrymen.

Location, number and size and shape of feeders, pouring rate, varying rate of heat transfer in different parts of the mould and the complex geometry of industrial castings, values of physical and thermal properties that change non-linearly over a range of temperatures involved make the solidification analysis a complex process. Owing to increasing need to understand these processes, increased effort, time and resources were invested into this sector. Foundry engineers and researchers continuously strived to enhance levels of understanding and develop tools and techniques to assist foundrymen. The casting research community often communicated with foundrymen by

prescribing a series of empirical rules, simple heuristics, design criteria and process guidelines ([2]-[5]). These rules and criteria-based casting designs challenged and generated interests amongst simulation experts to model and simulate these designs using computers. This also coincided with the great advances made in computing powers of personal computers (PCs).

The researchers who were interested in quantitative understanding used various numerical methods to develop computer software to capture and simulate the physics involved in casting solidification. After the pioneering development of SOLSTAR, a 3D diagnostic software, in the 1980s, many other types of software using numerical techniques have been adopted by foundries worldwide [6]. Whereas, a parallel research fraternity, interested in qualitative analysis, opted for using geometry of the casting to hypothesise their methods and techniques. These methods assumed that solidification in casting is driven by the casting geometry and this essentially influences the sequence of solidification. These approaches linked geometric parameters with the thermal properties of the metal, mould and heat transfer systems [7]. One of the earliest casting optimization methods was based on modulus principle that had its origin in Chvorinov's classic rule [8] that related solidification time of a casting to its modulus. Derivatives of Chvorinov's rule have since been investigated and expanded by many researchers ([9]-[15]). These methods succeeded in reducing cost of computations and also offered 'ease of use' to foundrymen who have traditionally shown little inclination to adopt modern casting simulation software due to their inherent complexity and pre-requisites of knowledge for their use. Despite their advantages, these geometry based methods remained insensitive to material properties and boundary conditions and also had limited success in providing transient solidification profiles.

Often the software developed for the product design following these two parallel approaches were standalone software systems managed at different locations by experts who have the required domain knowledge and specialised skills. Although such disparate standalone software systems provided accurate results, these also require greater number of simulations

and often produce incompatible data. This is in contrast with the growing popularity of Product Life cycle Management (PLM) approach which is described as a succession of strategies used by PLM designers as a particular product goes through its lifecycle [16]. PLM supports the development and management of the product right from its 'idea' stage to its 'retirement' in its entirety (Figure 1.1).

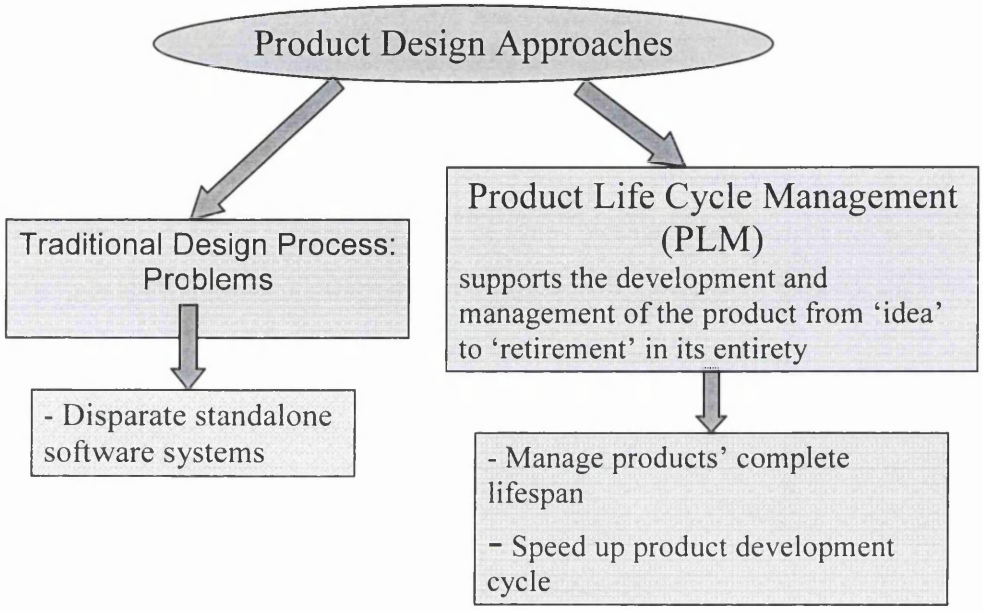

Figure 1.1: Product design approaches

The PLM approach enables a designer to develop a product using digital mockups and provide quick access to a portfolio of software systems to undertake manufacturability assessment of different components of that particular product. Such an approach encourages innovation, enhances productivity and helps the designer to manage the products' complete lifespan ensuring regulatory compliance as well. This speeds up the product development cycle and reduces the lead time to the development of new models of that product by almost half.

If we consider a case of a PLM designer who is not a foundry expert but is contemplating a new model of a car. The designer has on his screen say e.g. a cylinder block for which he needs to undertake a quick manufacturability

assessment and find out whether a sound casting can be obtained without a hotspot (Figure 1.2). Now the problem in this case has been reduced to a casting solidification problem. He now has the option of accessing through a suite of softwares say e.g. a finite element based software that he uses to find a solution to this problem. The software provides him a quick assessment and the solution informs that the desired component can be manufactured if e.g. steps 1, 2, 3, ... are followed. The PLM designer's objective is achieved and with the knowledge that this component can be manufactured, the details are then delegated to the respective experts.

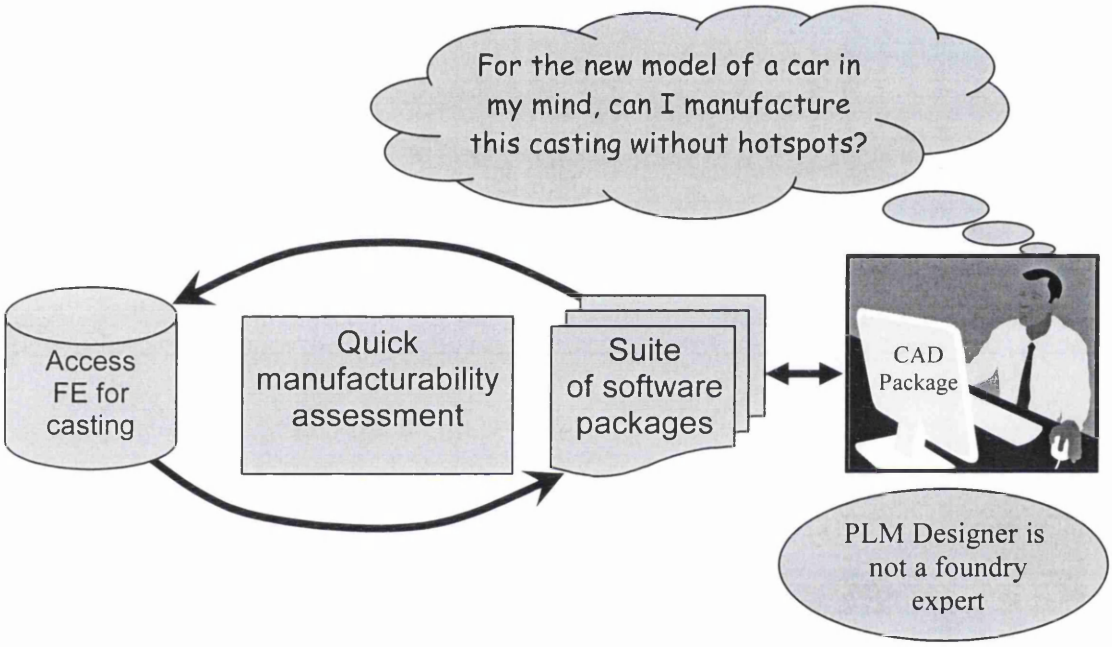

Figure 1.2: PLM for quick manufacturability assessment

Thus it is observed that there are various methods and techniques with their respective limitations and advantages e.g. the trial and error methods rely heavily on individual skills and intuitive knowledge and experience of foundrymen and are not an efficient approach. Even though FE based optimisation methods provide accurate solutions, these are computationally expensive e.g. gradient based methods can require 100s of FE simulations and do not guarantee global optimal solution and evolutionary methods are even more expensive often requiring 1000s of FE simulations. Then there are geometry reasoning methods that are based on simplistic physical models. Although solution time is comparatively less, these remained insensitive to

material properties and boundary conditions. On the other hand there is an ever growing need to speed up the product development cycle by reducing the number of FE simulations required for casting process optimisation.

The present study originates within this overall context and framework. In the Casting Research Group, alongside strongly mandated projects on numerical modelling, there was another important project, which focused on using the medial object technique to simulate casting solidification. This provided an opportunity to choose this particular line of research for the current research study presented in this thesis.

Transcendata Europe Ltd. developed a Medial Axes Transformation (MAT) tool in CAD based software called CADfix. The medial object (MO) technique has been used for the subdivision of complex solids into simpler pieces for automatic mesh generation and also for the generation of simpler idealised models ([17], [18]). Ever since its first known use in 1967 to describe the biological shapes ([19]-[23]), MAT technique remained unexplored in the field of engineering. However, recently the technique has been utilised for obtaining substituted equivalent structures for massive engineering structural analysis ([24]-[27]). Motivated by this background and the project objectives, it was decided to investigate the use of the MAT for solidification simulation.

The research problem to be resolved through this research study thus narrowed down to combine these two parallel streams of research (geometric and numerical) and develop a technique that retains advantages of both. The review of the literature revealed that this has not been achieved previously. The aim and the challenge was to develop a computational method for solidification analysis that was simple, easy to use, quick to provide solutions at low computational cost and at the same time, delivered the same degree of accuracy as numerical methods. The proposed methods would therefore, endeavour to reduce the number of FE simulations during the design cycle. The proposed geometry based method will rather combine with and depend on the FE based simulation software to make use of the physics simulated by

the FE solidification solver, implying therefore, that the quality of its prediction will be driven by the quality of the FE solvers. If FE method provides better quality results, the proposed method will provide same quality results in lesser number of simulations.

The development of such a technique was therefore, divided into three main tasks viz. review of literature on use of geometric techniques in the field of casting and assessment of their respective strengths, weaknesses and possible opportunities for their enhancements or modifications; develop a new method based on one or more of such techniques and incorporate numerical method to build in elements of accuracy; and finally test and validate solution obtained by this new unified method by comparing its results with conventional geometric methods and finite element based solutions.

1.2 SCOPE OF WORK AND RESEARCH CONTRIBUTIONS

The work documented in this thesis constituted the phase in the development of a technique for using Medial Axis Transformation technique in combination with other geometric and numerical methods for solidification simulation. The main research activities were:

- Acquiring knowledge of various techniques and methods employed in the field of casting for solidification analysis and develop a current understanding of their advantages and limitations regarding their applicability to contemporary casting problems.

- Develop techniques for employing MAT and associated geometric information and demonstrate a geometry based interpolation technique to predict hotspots and temperatures during the casting solidification process. Learning from its application to casting geometries and resulting limitations or failures, bring about enhancements for better results.

- Develop a new effective technique based on Heuvers' Circle method [3],[8], MAT and combine it with FE based simulation software and test and validate results on a variety of arbitrary and realistic casting geometries.

A summary of research contributions made during the above activities follows:

- MAT based single interpolation technique is presented that can simulate the casting solidification process. This involved the use of CAD based software known as CADfix [18].

- Enhancements were implemented in the interpolation scheme to overcome limitations posed by its first version. The method was improved to account for effect of mould in the cast-mould assembly and in addition to distance ratio used for earlier algorithm, a radius ratio was also incorporated.

- Case studies were carried out to test the method on foundry castings applying realistic material properties and boundary conditions and the results were compared with numerical solutions.

- Learning from and building on the understanding gained during this development, the MAT was then further used with another popular geometry based technique called Heuvers' Circle method ([3],[8]). Based on Chvorinov's classic rule and modulus method, a new equation was derived for using radius information of the casting to obtain effective interface boundary conditions for optimal solution. This development was validated using FE based solidification simulation software - Merlin [28].

- The newly developed method was tested on a range of two-dimensional casting geometries and the technique was further improved to account for problems posed by each of these cases. A

sorting technique was developed for selecting effective Heuvers' radii and scaling of values of interface heat transfer coefficients was adopted to provide realistic solutions for its application to three-dimensional casting objects. The applicability of this technique was conceptualised and demonstrated for a 3D casting geometry.

- Finally an effective novel technique was developed that can now provide an optimal solutions in two FE simulations.

The research outputs during the entire course of study period were documented and a number of publications, as a result, originated or are forthcoming and are listed next.

1.3 LIST OF PUBLICATIONS

The following publications were produced during the course of the research study period.

- W. K. S. Pao, C. Lin, M. P. Sood, R. S. Ransing and R. W. Lewis, "Medial Axis Based Interpolation Tool-Kit for an Approximate Estimation Of Casting Temperature", in Bonet J. et al. (Editors), *Proceedings 10th Annual Conference of the Association for Computational Mechanics in Engineering*, University of Wales Swansea, UK, 14th-17th April, 2002, pp. 89-92.

- M. P. Sood, R. S. Ransing and R. W. Lewis, "Casting Process Optimisation based on Heuvers' Circle Method coupled with Medial Axis Transformation" in Wheel Marcus A (Editor), *Proceedings (Extended Abstracts) of the 11th Annual Conference of the Association for Computational Mechanics in Engineering*, University of Strathclyde, Glasgow, UK, 24th-25th April 2003, pp. 17-20.

- R. S. Ransing, W. K. S. Pao, C. Lin, M. P. Sood and R. W. Lewis, "An Enhanced Interpolation Algorithm using Medial Axis and its Application to Hotspot Prediction in a Mould-Casting Assembly",

International Journal of Cast Metals Research, February 2005, Vol. 18, No. 1, pp. 1-12.

- R. S. Ransing, M. P. Sood and W. K. S. Pao, "Computer Implementation of Heuvers' Circle Method for Thermal Optimization in castings, *International Journal of Cast Metals Research,* 2005, Vol. 18, No 2, pp. 119-126.

- R. S. Ransing and M. P. Sood, "Review Of Optimization Methods For Casting Simulation", *Shape Casting: The John Campbell Symposium*, Edited by M. Tiryakioglu and P. N. Crepeau, Proceedings of the Symposium sponsored by Aluminum Committee of Light Metal Division (LMD) and Solidification Committee of Material Processing and Manufacturing Division (MPMD) of TMS (The Minerals, Metals and Materials Society) held at 2005 TMS Annual Meeting, San Francisco, California, USA, Feb 13-17, 2005, ISBN: 087339-583-2, pp. 327-336.

- R. S. Ransing, M. P. Sood, "Optimization in Castings – An Overview of Relevant Computational Technologies and Future Challenges", Accepted for publication: Metallurgical and Materials Transactions B, March 2005.

1.4 OUTLINE OF THE THESIS

The thesis is subdivided into seven chapters, including an introduction and conclusion. The following is the synopsis of each chapter.

- *Chapter One: Introduction*. Apart from providing an outline of the thesis, this chapter contains an overview of the background to research work, scope and research contributions made during the period of study.
- *Chapter Two: Casting Solidification and Geometric Techniques: A Literature Review*. In this chapter, the relevant literature in the field of casting solidification and optimisation is reviewed with an aim to

develop an understanding of various methods and techniques. A theoretical context and framework is presented and a historical over view of casting practices and their emergence from an earlier 'black art' form to a better understood science is provided. After briefly describing the choices that are available to foundrymen for taking decision for various types of casting processes and the challenges and dilemma that these poses, an overview of various numerical optimisation techniques and an evaluation of their performance is provided. The contributions from various researchers in the field of casting optimisation using geometric reasoning techniques are then summarised. Then a detailed description of different geometric techniques to explain solidification process is given. After outlining the limitations posed by these geometry based techniques and methods, conclusions are drawn and the research direction identified for pursuing this study is presented.

- *Chapter Three: Solidification Simulation Using Medial Axis Based Interpolation Scheme*. This chapter builds on the discussion on geometric techniques and the methods are further investigated to provide a solidification pattern in castings with an aim to predict casting temperatures and likely locations of hotspots. The medial axis transformation (MAT) technique for castings is explained. A case study using the MAT based interpolation scheme is then presented and its feasibility as a useful tool for understanding solidification behaviour and as an aid in casting design cycle is illustrated. The advantages and limitation of this scheme are brought out and improvements sought.
- *Chapter Four: Enhanced Interpolation Scheme*. The work on the MAT based interpolation scheme initiated in Chapter 3 is carried forward. Improvements made to the scheme in the interest of improved accuracy are discussed. An improved double interpolation scheme is presented that introduces a concept of radius ratio and also takes into account the effect of the mould in a cast-mould assembly for predicting casting temperatures and hotspots. The enhanced scheme is then tested and validated using geometries of different

shapes and thicknesses. The results from this scheme are compared with numerical solutions for same castings. A study on point (mesh) density is presented and discussion on error in the solution provided by the double interpolation scheme is undertaken. The Interpolation results are then compared with numerical solutions for accuracy, run time and requirements for human intervention. The advantages and limitations of the double interpolation scheme are highlighted. Based on lessons learnt from limitations posed by the scheme and versatility offered by the MAT technique, a further line of research to develop a more efficient and practical geometry based method for studying and analysing behaviour of solidifying castings is sought.

- *Chapter Five: A Novel Approach Using Modified Heuvers' Circle Method For Solidification Simulation*. Building on the understanding on MAT technique, a new method based on geometric reasoning techniques is proposed to predict hot spots. The new method for the first time uses geometric parameters of the castings to obtain effective interface boundary conditions. Two conventional geometry based methods, MAT and Heuvers' Circle methods, are combined using a classic Chvorinov's rule and then coupled with FE simulation techniques to retain ease of use, speed and simplicity of the former and accuracy offered by the latter. The newly developed method is then tested on a simple casting geometry.
- *Chapter Six: Coupled Thermal Optimisation Using Modified Heuvers' Circle Method: Results and Discussions*. The new approach developed in the previous chapter is further validated and its effectiveness and accuracy is tested on a range of casting geometries. The coupled approach is tested on geometries of different shape and thicknesses and is then further validated on more practical real life geometries including case studies on castings/geometries obtained from published literature and foundries. The issues pertaining to complexity provided by branched medial axes and scaling of modifying factors to obtain realistic results are tackled. The results from all these case studies are validated using FE based simulations. The application of the new method to a three-dimensional casting object is conceptualized and a

case study is presented to advocate its applicability to 3D objects. The results are then discussed for their interpretation and implementation through various design decisions in actual foundry situations.

- *Chapter Seven: Conclusion*. The novel research contributions are summarised and recommendations are made for continuation of work through future research.

REFERENCES

[1] H. F. Taylor, M.C. Flemings and J. Wulff, "*Foundry Engineering*", John Wiley & Sons, New York, USA, 1959.

[2] J. Campbell, *Castings Practice: The Ten Rules of Castings,* Butterworth-Heinemann, Oxford, UK, ISBN: 0750647914, May 2004.

[3] J. Campbell, *Castings 2nd Edition* Butterworth-Heinemann, Oxford, UK, 2003.

[4] G. Upadhya and A. J. Paul, "Rational Design of Gating and Risering for Castings: A New Approach Using Knowledge base and Geometric Analysis", *AFS Transactions*, 1993, Vol. 113: 919-925.

[5] J. G. Bralla, "*Design for Manufacturability*", 2nd Edition, McGraw-Hill, NY, USA, pp. 1.20, 1998.

[6] M. Jolly, "State of the Art Review of Use of Modelling Software for Shape Casting", *Shape Casting: The John Campbell Symposium*, Edited by M. Tiryakioglu and P. N. Crepeau, Proceedings of the Symposium sponsored by TMS (The Minerals, Metals and Materials Society), San Francisco, California, USA, Feb 13-17, 2005, ISBN: 087339-583-2, pp. 337-346.

[7] B. Ravi and M. N. Srinivasan, "Casting Solidification Analysis by Modulus Vector Method", *International Journal of Cast Metals Research*, 1996, 9: 1-7.

[8] R. Wlodawer, "*Directional Solidification of Steel Castings*", Pergamon Press, Oxford, 1966

[9] B. Ravi and M. N. Srinivasan. "Feature-Based Castability Evaluation", *International Journal of Production Research*, 1995, Vol. 33 (12): 3367-3380.

[10] B. Ravi and M. N. Srinivasan, "Casting Solidification Analysis by Modulus Vector Method", *International Journal of Cast Metals Research*, 1996, 9: 1-7.

[11] M. Tiryakioglu, E. Tiryakioglu and D. R. Askeland, "The Effect of Casting Shape and Size on Solidification Time: A New Approach", *International Journal of Cast Metals Research*, 1997, 9, 259-267.

[12] M. Tiryakioglu and E. Tiryakioglu, "A Comparative Study of Optimum Feeder Models for Castings", *International Journal of Cast Metals Research*, 2001, 14, 25-30.

[13] M. Tiryakioglu, E. Tiryakioglu and J. Campbell, "Mass and Heat Transfer during Feeding of Castings", *International Journal of Cast Metals Research*, 2002, 14, 371-375.

[14] R. W. Heine and J. J. Uicker, "Risering by Computer assisted Geometric Modeling", *AFS Transactions*, 1983, 91, 127-136.

[15] S. J. Neises, J. J. Uicker and R. W. Heine, "Geometric Modeling of Directional Solidification based on Section Modulus", *AFS Transactions*, 1987, 95, 25-30.

[16] A. Saaksvuori and A. Immonen, "*Product Lifecycle* Management", 2nd Edition, Springer, Berlin, pp: 2, 2005.

[17] Transcendata Europe Medial Object Technical Paper from their website http://www.fegs.co.uk/motech.html, 2002-2005, last accessed on 16th Jan 2006.

[18] http://www.fegs.co.uk/medial.html, 2002-2005, last accessed on 16th Jan 2006.

[19] G. Evans, A. Middleditch and N. Miles, "Stable computation of the 2D medial axis transform", *International Journal Comp. Geom. and Application*, 1998, **8** (5), 577-598.

[20] N. Miles, G. Evan, and A. Middleditch, "*Proc. of the 6th International Aluminum Extrusion Technology Seminar*", Chicago, Illinois, May 1996.

[21] S. Fortune, "A sweepline algorithm for Voronoi diagrams", *Algorithmica*, 1987, **2**, 133-174.

[22] H. N. Gursoy, and N. M. Patrikalakis, "Automated interrogation and adaptive subdivision of shape using the medial axis transform", *Adv. Eng. Soft*, 1991, **13**, 287-302.

[23] D. J. Sheehy C. G. Armstrong and D. J. Robinson, "Shape description by medial surface construction", *IEEE Transaction on Visualization and Computer Graphics,* 1996, **2**(1), 62-72.

[24] K. W. Shim, D. J. Monaghan and C. G. Armstrong, "Mixed dimensional coupling in finite element stress analysis", *10th Int.*

Meshing Roundtable, 2001, Sandia National Laboratories, Newport Beach, California, 269-277.

[25] C. G. Armstrong, D. J. Robinson, R. M. Mckeag, T. S. Li, S. J. Bridgett and R. J. Donaghy, "Application of the medial axis transform in analysis modeling", *Proceedings of 5th International Conference on Reliability of FE Methods for Engineering Applications*, NAFEMS, May 1995, 514-426,

[26] T. Tam and C. G. Armstrong, "2D finite element mesh generation by medial axis subdivision", *Adv Eng. Software,* 1991, **13**, 312-324.

[27] http://sog1.me.qub.ac.uk/Research/medial/medial.php, last accessed on 16th Jan 2006 and 12th June 2006.

[28] http://www.swan.ac.uk/civeng/Research/casting/merlin/index.html, accessed in May 2005.

Chapter 2

CASTING SOLIDIFICATION AND GEOMETRIC TECHNIQUES: A LITERATURE REVIEW

CHAPTER LAYOUT
This chapter reviews the literature in the field of casting solidification and analysis with an aim to set a theoretical context for defining a research problem for the thesis. The chapter starts with an overview of casting practices and their emergence from the earlier 'mystique' days of local craftsmen to a better understood science. The next section then describes the choices that are available to foundrymen for taking decision for various types of casting processes and the challenges and dilemma that this poses. An historical overview of various casting optimisation techniques and methods deployed in the past by various streams of researchers is then provided along with an analysis of their strengths and disadvantages. Various numerical optimisation techniques are briefly described along with evaluation of their performance. The fifth section then summarises contributions from various researchers in the field of casting optimisation using geometric reasoning techniques. A detailed description is provided here on how the geometry of a casting can be used as a basis to compare different research methods for analysing the casting solidification process. The next section then describes the simulation techniques used to study solidification patterns in castings. The penultimate section outlines some of the limitations posed by these geometry based techniques and methods. Finally, conclusions are drawn from this literature review to choose a research direction for pursuing this study.

2.1 INTRODUCTION

Use of metals and various alloys in today's modern world and our day to day lives is indispensable. The manufacture of defect free components at low cost and high productivity is important to the casting industry. Most of these useful metal parts and goods are made from metals and alloys by metal forming through forging, welding, machining, casting etc or a combination of these methods. Only the casting process has been dealt within this research study. A casting can be defined as a "metal object obtained by allowing molten metal to solidify in a mould" and the shape of this metal object is determined by the shape of the mould cavity. The process of forming these metal objects by melting metal and pouring it into moulds is known as founding or casting [1]. The casting process has many inherent advantages over other shaping methods such as machining, forging, welding, stamping, hot working etc. Casting practices have been used since 4000 B.C. but even then it took several millennia before it emerged as a science from the shackles of primitive art form that was held a captive secret by local craftsmen [2].

Solidification is an important phase in the casting process influencing quality and yield of products. Solidification is defined as the discontinuous change of state from liquid to crystalline solid [3]. The solid and liquid portions of cast metal are separated by the solidification front that advances from surface to the center of the casting. The analytical and approximation methods have been described by Ruddle [4] to gain an understanding of the solidification problems. The last freezing sections and locations are the most likely and probable locations of defects such as shrinkage cavities or porosity. Even until the middle of last century, the feeding of cast metal (also known as risering) was guided by experience and "cut and try" method. But as foundry practices have evolved and matured over the period, the shrinkage defects are now minimised and restricted and contained within the feeders (which act as reservoirs of molten metal attached to a casting to compensate for the shrinkage as it solidifies) by providing feeders at appropriate locations, or by providing insulations and chills at suitable locations to ensure a desired directional solidification.

Heat transfer during the solidification process is a non linear transient phenomenon in which energy is transferred from the molten metal to the environment involving all the three modes of heat transfer viz. conduction, convection and radiation. Thermodynamics not only explains how this energy is transferred but it also predicts the rate at which the heat exchange will take place under specified conditions. The heat transfer rate is proportional to the normal temperature gradient [5]. Location of ingates, pouring rate, varying rate of heat transfer in different parts of the mould and the temperature dependent non-linear thermo physical properties make the solidification simulation a complex process.

In the past, experience was gained either by using a 'trial and error' method or by undertaking expensive experiments. Many 'dos' and 'don'ts' have evolved in the casting process over a period of time. However, the important ones that come to mind are so fundamental that they challenge the 'academic mind' to think all over again. The rules proposed by Campbell [6] are classic examples. The message is simple: mathematical complexity in computer models needs to go hand in hand with the rules derived from 'first principles'. But over the years casting research community all over the world accepted this challenge to enhance understanding of casting process and develop tools and techniques to aid foundrymen. In the field of casting optimisation, a variety of methods have been proposed over a period of years. At the start of optimisation study, the foundryman's first choice is to use simple but well established methods such as the use of orthogonal arrays for optimal design of process conditions or the famous "inscribed" or Heuvers' circle method [7] for optimal feeding design.

The computer simulation software has been based on a variety of computational methods ranging from geometric reasoning techniques (the famous Chvorinov rule and its variants ([8]-[13]) to solving complex partial differential equations using one of the numerical methods. Optimisation methods based on solving partial differential methods was an active area of research in mid nineties ([14]-[19]). This chapter will review a variety of

casting optimisation methods including - probably for the first time - geometric reasoning methods. The contribution from various computational methodologies is highlighted with particular emphasis on characterising 'objective functions' and 'constraints'.

2.2 CHOICES FOR DIFFERENT CASTING PROCESSES – A CHALLENGE FOR CASTING OPTIMISATION

Achieving high quality control over solidifying castings is of paramount importance for the manufacturing of critical components that are made up of very expensive metals and super alloys. The design of casting process often depends on a combination of trial and error methods based on foundrymen's many years of accumulated non-quantitative experience and intuition. For many decades, researchers have communicated with the foundrymen by developing and prescribing a series of process guidelines, simple heuristics, empirical rules and criteria based guidelines.

Researchers in casting industry conventionally communicated with practicing foundrymen using a series of simple rules and criteria based guidelines which were based on their foundry practice and the emerging learning experience. The classic example of such work is reflected in Campbell's feeding rules and subsequently published ten rules ([6],[7],[20],[21]), which incorporate the latest technological developments for producing high quality and reliable castings. Bralla's [22] design rules are another example of such interaction between researchers and practicing foundrymen. Campbell's six feeding rules [7] that satisfy the heat transfer, volume, feed path, thermal, geometrical and pressure criteria are an example of work that has led and attracted further research in this field. The evolution of "dos and don'ts" in a casting process in the form of simple rules (e.g. Part Orientation Rules, Parting Plane Rules, Gate Rules, Runner Rules, Sprue Rules and Riser Rules) are some of the well-documented examples of such interaction between foundrymen and researchers ([22],[23]). Good casting designs are assessed using these established rules. Engineers have to make a series of design decisions to obtain a defect free quality casting at low cost. Table 2.1 provides an insight

into some of the decision-making choices that confronts Foundrymen at the time of casting.

Type of Casting / **Design Decisions**	Sand Casting	Gravity Die Casting	Pressure Die Casting	Investment Casting	Squeeze Casting
Feeder (Number, Size, Shape and Location)	●	●	●	●	
Interface Conditions (Heat Transfer Coefficients, Chills, Insulations, padding)	●	●		●	
Mould (Cooling Channels, Chills, Heating the mould)	●	●	●	●	●
Filling and Running System	●	●	●	●	●

Table 2.1: A partial list of design choices for different casting processes

The casting research fraternities developed simple rules and criteria and challenged the simulation community to model, simulate and implement the criteria-based castings designs on computers. Two parallel streams of research strategies emerged that took on the challenge, and these two streams of researchers worked to achieve nearly similar objectives. The objectives are to enhance the quality of castings, reduce wastage and scrap, modernize and facilitate decision making on various important aspects during the casting process and reduce the cost. While many academic researchers, practioners, foundry engineers adopted numerical techniques to obtain answers to various phenomena involved in casting process, many others followed a parallel strong thinking of using geometry of the castings to make research progress in the field of casting. The next sections will describe the progress made in this direction during the last three decades.

2.3 AN OVERVIEW OF CASTING OPTIMISATION TECHNIQUES

In engineering terminology, optimisation is understood as a set of strategies to determine process parameters that maximize or minimize some aspect of a process (casting in this case), while ensuring that the process operates within established limits or constraints [24]. Casting process optimisation has facilitated foundrymen in making right choices but still remains a very challenging area that has drawn attention of many researchers during last two decades. Many aspects of physics involved in casting are now well established and understood and have been successfully modeled. The numerical modeling community is continuously working to capture and simulate less understood phenomena of physics e.g. Oxide Film, Bubble Damage and provision of high quality liquid melt.

This section will now focus on various optimisation techniques developed by researchers over the decades and put into use in foundry industry. Table 2.2 provides an overview of some of the achievements/milestones attained in the field of casting optimisation by various researchers. Dantzig and his associates made significant contribution to casting optimisation through their pioneering work in the mid nineties that is reflected in a series of publications ([14]-[18]) defining objective functions for optimal feeder/riser design. On the other hand, researchers like Heuvers [8], Ravi *et al.* ([9],[25]) Tiryakioglu *et al.* ([10],[26],[27]) and Upadhya *et al.* [23] based their methods on geometric reasoning techniques to achieve similar objectives in order to produce defect-free castings.

Optimised Design Decisions / **Method for Optimisation**	Feeders (Number, Size, Shape Location)	Interface Conditions (Chills, Insulations, Die-coating thickness)	Mould (Cooling Channels, Chills, Heating mould)	Filling and Running System
Modulus Method [8]	●	●	●	
Heuvers' Circle Method ([7], [8])	●	●	●	
Tiryakioglu *et al.* ([10]-[26],[27])	●			
Upadhya *et al.* [23]	●			
Dantzig, Tortorelli *et al.* ([14]-[18])	●	●	●	●
Morthland *et al.* [15]	●			
Ransing *et al.* ([19], [28],[29], [30])	●	●	●	●

Table 2.2: Casting optimisation at a glance

2.4 NUMERICAL OPTIMISATION

Table 2.3 shows some of the objective functions defined and used by different authors over the years. Haftka and Grandhi [31] resolved problems of structural shape optimisation in the mid 1980s and Tortorelli *et al.* [14] went on to apply it to casting. The latter introduced methods for optimizing solidification processes through shape and process parameters modifications. Sensitivity analysis is an important aspect of optimisation procedures using gradient-based methods. The authors presented the shape sensitivity analysis for the thermal system and coupled this analysis with nonlinear programming to optimise the design of a sand casting. Morthland *et al.* [15] combined FE analysis of the solidification process with sensitivity analysis based on efficient direct differentiation method and numerical optimisation to optimise feeder dimensions and volume. Ebrahimi *et al.* extended this approach for the investment casting and their numerical optimisation

algorithm used the direct differentiation/adjoint variable methods to calculate the gradient information and upgrade the design until an optimum was found [16]. Chen and Tortorelli [17] investigated a problem facing unification of CAD and FEM packages i.e. relating the finite element nodal coordinates to the CAD solid model dimensions. They developed the critical link between these CAD and FEM data and successfully optimised a three-dimensional connecting rod model to exemplify their method for shape optimisation.

Considering that interfacial heat transfer is a critical controlling parameter for gravity die casting, Ransing [32] proposed a regression equation so that the temporal variation of interfacial heat transfer coefficients could be optimised to produce a desired solidification path. This equation allowed the temporal variation of heat transfer coefficients to be used as design variables in the subsequent optimisation analysis ([19],[28]). Later this model was linked with a 'thermal stress model' [29] to give realist initial values for interface heat transfer coefficients. These values were predicted by calculating air gap widths at corresponding locations at the interface. Lewis *et al.* [33] proposed an efficient method for interpolating sensitivity values from previous time steps and used this method to optimally design chill locations for a sand casting process. Recently, Ransing *et al.* [34] numerically modeled the tilt casting phenomenon by keeping the mould stationary and rotating the gravitational force vector. A mathematical expression relating tilting angle with the tilting speed was proposed so that an optimal value of tilting speed could be predicted by minimizing splashing effects.

Author	Objective Function/Fitness Function/Cost Function	
Tortorelli *et al.* [14]	$G=\frac{1}{2}\left[\begin{matrix}\left(T_1-T_2+b_{19}\right)^2+\left(T_2-T_3+b_{20}\right)^2\\+\left(T_3-T_4+b_{21}\right)^2\end{matrix}\right],$	The cost function ensured a positive vertical temp. gradient from casting to feeder to eliminate porosity in the casting
Morthland *et al.* [15]	$G(b)=\sum_{e=1}^{N_r}\int_{\Omega_{0_e}}\lvert J_e\rvert dV_0$	Where G is the volume of Nr elements in the riser region that is minimized
Ebrahimi *et al.* [16]	$G=G(T(b),b)$ and $F_i=F_i(T(b),b)$	G represents the riser volume that is minimized while constraint function Fi enforces directional solidification
McDavid *et al.* [18]	$G=\sum_{i=1}^{N_A}\int_0^{tf} f_i dt$	G represents the amount of fluid in contact with runner wall and is maximized thus minimizing pocket formation
Ransing *et al.* [19]	$Cost=\sum_{i=1}^{S_n-1} p\max\left[\left(t_{f_{i+1}}-t_{f_i}\right),0\right]$	Cost function is the deviation from user defined feed metal flow path
Ransing *et al.* [34]	$\begin{cases}\omega=\omega_{min} & if\ 0\le\theta<\theta_{in}\\ \omega=\dfrac{k_1}{\arctan\left(\frac{k_2}{s}\right)}\cdot\arctan\left(\dfrac{\theta-k_3}{s}\right)+k_4 & if\ \theta_{in}\le\theta\le\theta_{fin}\\ \omega=\omega_{max} & if\ \theta>\theta_{fin}\end{cases}$	The function describes the relation between the tilting speed ω and the tilting angle θ. This function also allows to change the shape of the function $\omega = \omega\ (\theta)$ with only one shape parameter s.
Lewis *et al.* [33]	$F(X)=\{T_A-T_B+C\}+W\times\left\{\dfrac{\text{Vol. of Feeder}}{\text{Max Vol. of Feeder}}\right\}$	$F(X)$ included both thermal and vol. components

Table 2.3: Objective functions used in optimisation research using numerical methods

2.4.1 Performance of various methods and need for robustness

It is thus gathered from above discussion that research in casting technology has been labouring towards achieving 'near optimal' solutions while attempting to keep the computational cost to minimum possible. Trial and error methods based on experiments and intuitive and accumulated hands-on experience are quicker and easy to implement but they don't necessarily always provide the optimal solution. Gradient-based methods provide near optimal designs with higher computational costs. The newly emerging Evolutionary computing techniques, however, may lead us towards the optimal designs and solutions but are computationally very expensive (See Figure 2.1). The availability of skilled foundrymen, computing power, relative need for higher quality components and ease of implementation then influences the decision making on choosing one of these methods.

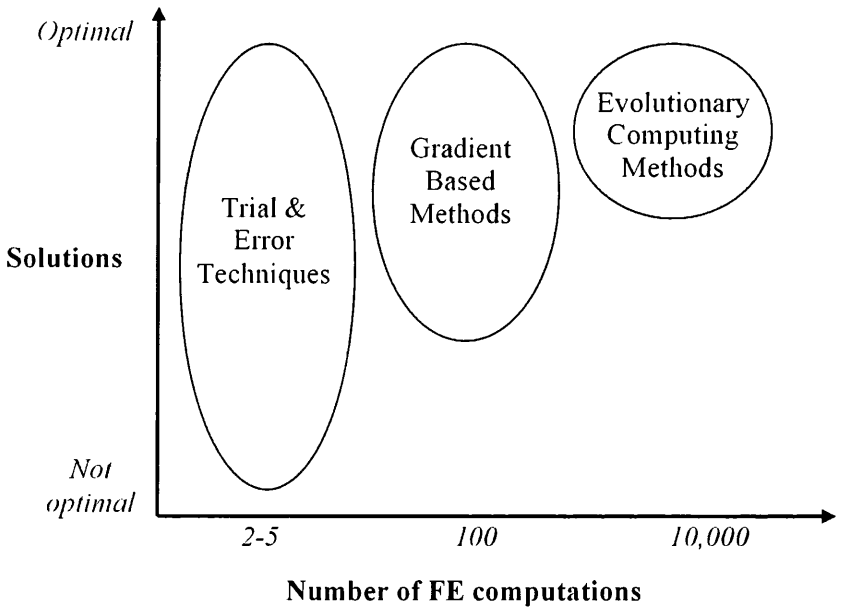

Figure 2.1: Performance of various optimisation methods

As illustrated in Figure 2.2, even though gradient-based methods provide local or global minima, it is advisable to avoid a region of steep gradients of the objective function (A in Figure 2.2). The aim should rather be to obtain robustness in casting process designs by seeking and opting for relatively less steep gradient of the objective function that is achieved at (B). This will ensure a robust casting design that is more stable to fluctuations or small

changes in design variables or process parameters as the change in the objective function value is minimum (e.g. as in region B).

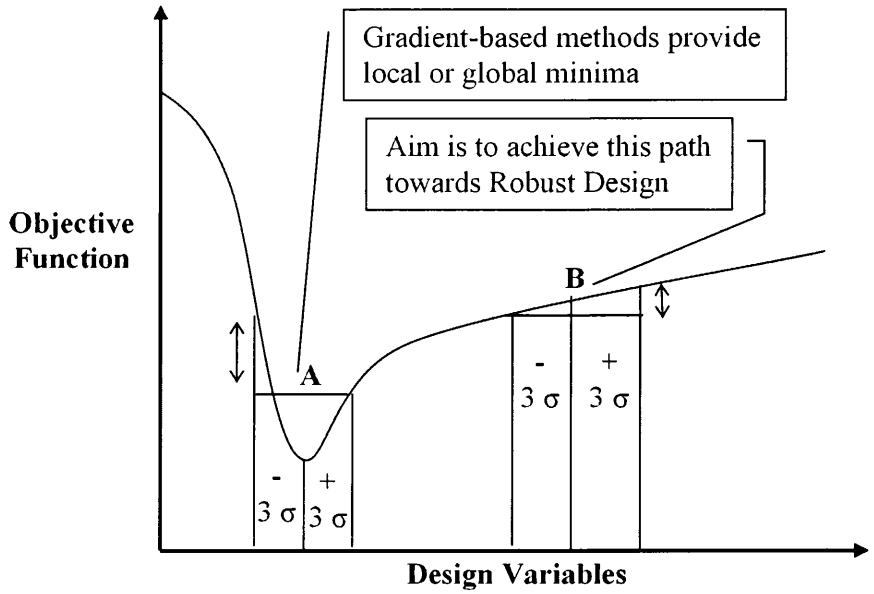

Figure 2.2: Aiming for robustness in casting designs

2.5 GEOMETRIC TECHNIQUES FOR SOLIDIFICATION ANALYSIS AND GEOMETRIC OPTIMISATION

2.5.1 Background

In parallel with evolution of numerical optimisation methods, some conventional approaches to solidification analysis and optimisation have been driven by the casting geometry. These approaches were motivated by the need to reduce the cost of computations as the time required to develop the finite element grid, the requirements for computer power and time contribute to cost problems. Since geometric methods are fast and easy to use, they are also used for complex shapes for preliminary analysis before carrying out a detailed numerical simulation for further validation.

The geometric methods are based on the premise that the sequence of solidification and thus the location of hotspots are driven by the shape of geometry. This second approach simulates the solidification process using geometric parameters and assumes that these parameters dominate the thermal properties of the metal, mould and heat transfer systems. The relative value of temperature and solidification time assume greater

significance than the actual values associated with any point inside the casting for predicting shrinkage defects and for designing appropriate feeders [35]. Simulation programs based on geometric models have another advantage over those built on FEM and FDM as errors resulting from inaccuracy or non-linearity in the thermal properties of the mould medium or liquid metal are avoided. Table 2.4 recaptures a summary of achievements in this stream of optimisation research.

Author	Proposal	Description of work
Chvorinov's Rule [38] (Section 2.5.5)	*Solidification time* $t_s = k\left(\frac{V}{A}\right)^m$	Chvorinov's classic rule related the solidification time of the casting to its modulus which is the ratio of its heat content volume to heat transfer area.
Wlodawer [8] (Section 2.5.7)	$M_{CASTING} : M_{NECK} : M_{FEEDER}$ 1 : 1.1 : 1.2	Used Chvorinov's rule to design the feeders in such a way that the modulus (M) of the feeder is greater than that of the casting and it must increase by 10% from casting across the ingate to the feeder for ensuring adequate feeding.
Tiryakioglu *et al.* ([10],[26], [27]) (Section 2.5.8)	$t = B' k^{1.31} V^{0.67}$ $k = \frac{A_s}{A} = \frac{4.837 V^{\frac{2}{3}}}{A}$ $t_t = t_f = a\, t_c$	Pointing to limitations in Chvorinov's Rule, authors proved that the modulus includes the effect of both, casting shape and size and proposed that shape factor *(k)* separate these two independent factors. Using their own superheat model, authors found that the solidification time of optimum-sized feeders in a feeder-casting combination was only fractionally longer than that of the casting. (a = 1.046 for Al-12%Si alloy and 1.005 for steel castings)
Upadhya *et al.* [23]	$PM = \frac{2}{\sum_{i=1}^{N} \frac{1}{d_i}}$	Used Chvorinov's rule to determine continuous modulus for complex shapes discretised in a three-dimensional grid and Point Modulus was then used to calculate solidification time map.
Ravi *et al.* [25] (Section 2.5.10 and 2.5.11)	$M = \sum_i w_i c_i$	Authors developed 30 criteria functions to assess the influence of various features in a casting and then gave this relationship to assess manufacturability of casting design by a weighted evaluation of all the features using all the criteria.

Table 2.4: Achievements made by researchers using geometric techniques

Upadhya and Paul [23] incorporated foundrymen's intuitive skills and accumulated experience and developed a knowledge-based integrated design system to optimise gating and risering. They applied some empirical heuristics to the discretised solid model and performed a geometric analysis to determine the natural flow path for liquid metal. The risering routine then used solidification time map to find hotspots and locate feeders at these spots to ensure adequate feeding. Ravi and Srinivasan [25] studied various guidelines and rules on geometric features employed by practicing engineers and came up with a list of thirty Castability criteria. The authors then described manufacturability assessment for casting by presenting these criteria as equations in term of influencing parameters.

2.5.2 A simple geometric method -Largest inscribed circle

A simple geometric method for locating a hotspot in a casting assume that last point to solidify lies in the zone of maximum concentration, represented or recognized by the largest inscribed circle in a cross section of the casting. This particularly holds true for axi-symmetric solids.

2.5.3 A Methods for shrinkage prediction

Niyama *et al.* [36] have shown that for steel castings and short freezing range alloys, the temperature gradient can be a simple and effective parameter of shrinkage prediction, but since the critical temperature gradient had to be determined empirically for each casting, this method could not make comprehensive predictions. The same authors further developed and demonstrated through a laboratory experiment effect of casting size on the critical temperature gradient. The observation led to the selection of a new parameter, $G/\sqrt{R}$, the temperature gradient divided by the square root of cooling rate at the end of solidification at each point within a casting. Although not representing an accurate physical model of shrinkage formation, it has been used as a tool for connecting design in routine foundry works. The common critical value of the parameter was independent of the alloy and shape and size of castings in range studied.

2.5.4 Solid Fraction Gradient Method

Imafuku [37] proposed a method, which predicts the shape of a shrinkage cavity and is analytically formulated as the function of solid fraction and shrinkage cavity ratio. This method is based on the idea that porosities are generated by the solidification shrinkage of a large quantity of molten metal. This method enables a more rational casting design using numerical analysis as it allows quantitative prediction of shrinkage defects.

2.5.5 Chvorinov's Rule

Most of these geometric methods stem from Chvorinov's rule [38] that was the first to answer the basic question: how long does it take for a casting or a given part of casting to solidify? Chvorinov's equation relates solidification time of a casting with its modulus. Solidification time, t_s, is determined by

$$\textit{Solidification time } t_s = k\left(\frac{V}{A}\right)^m \tag{2.1}$$

where k is a material constant depending on the cast metal and mould material and $\left(\frac{V}{A}\right)$ is the modulus (M), which pertains to ratio of heat content volume (V) to its heat transfer area (A), and m is a constant and is 2 in Chvorinov's work.

$$\textit{Modulus } (M) = \frac{\textit{Heat content volume of casting}}{\textit{Heat transfer area}} \tag{2.2}$$

The application of this classic rule will be discussed later in this and subsequent chapters of the thesis.

2.5.6 Unit Area Approach

Ozdemir and Atasoy [39] proposed this new approach called "Unit Area" method to calculate the solidification time of the castings and for dimensioning of the feeders. They defined unit area of the casting as the ratio of the casting volume to the resultant of the dimensions of the casting. SR (structural resultant) is the resultant of the columnar grain dimensions,

which is opposite to the resultant of heat flow directions e.g. SR for a prism with dimensions *a, b and c* will be $SR = \sqrt{a^2 + b^2 + c^2}$. Since the structural resultant of the casting is known, the authors calculated the unit area using this expression

$$UA = \frac{V}{SR} \tag{2.3}$$

where UA is unit area (cm^2), V is volume of the casting (cm^3) and SR is structural resultant (cm). They conducted experiments to suggest that this method produces better results for finding solidification time than using only Chvorinov's approach, which require correction in order to produce sound castings.

2.5.7 Section Modulus Method

Wlodawer [8] used Chvorinov's rule to design the feeder in such a way that the modulus of the feeder is greater than that of the casting. This ensured adequate feeding although it is to be noted that this work was limited at that time to fairly heavy steel castings in steel mould. The more complex geometry is divided into a number of simpler shapes and the modulus for each portion is calculated. Largest value of modulus will indicate the last freezing point. The solidification proceeds as the thickness and corresponding section modulus (SM) increases throughout the casting until the final endpoint of solidification is reached. This progression of solidification towards the final point of solidification in the casting is known as directional solidification.

The concept of modulus can be further explained by casting 10 kg of steel, first as a sphere and then as a plate. The plate solidifies first because the heat contained in 10 kg of cast steel is dissipated over a much larger surface area. This will also imply that two bodies with the same modulus will solidify in the same time. Say a cube (of length 3cm, with volume V = $(3)^3$ = 27 cm^3, area A = 6 $(3)^2$ = 54 cm^2) will have a modulus M = V/A = 0.5 cm. This cube will solidify in the same time as any other body having the same ratio of volume to cooling surface area.

The modulus has units of length, and if the relationships are known, the modulus can be measured with a scale without any calculation. In the example cited above, the modulus of cube with a length of 3 cm was 0.5 cm, i.e. the modulus of cube with six cooling surfaces is equal to 1/6 of the length of the side. Similarly the plate of 1 cm thickness had a modulus of 0.5 cm, thus it can be said that the modulus of plates is equal to half the plate thickness. Such relationship also exists for other fundamental bodies thus rendering separate calculations unnecessary. This is further explained using a Cube of say length "a" or its inscribed cylinder or sphere:

$$\text{For cube, } V = a^3,\ A = 6a^2 \text{ thus modulus } M = \frac{V}{A} = \frac{a}{6} \tag{2.4}$$

$$\text{For inscribed cylinder, } V = \frac{a^3\pi}{4},\ A = a^2\frac{\pi}{2} + a^2\pi \quad \text{thus modulus } M = \frac{V}{A} = \frac{a}{6} \tag{2.5}$$

$$\text{For inscribed sphere, } V = \frac{a^3\pi}{6},\ A = a^2\pi \text{ thus modulus } M = \frac{V}{A} = \frac{a}{6} \tag{2.6}$$

It is thus seen that moduli for a cube will be same as its inscribed sphere or cylinder i.e. a/6 where is "a" the length of side or the diameter. This conveys that each of these bodies will take same time to solidify.

Similarly many castings are made up of bars that either form a closed ring or have no cooling surfaces at the end, as they merge into parts of the casting having heavier walls. Semi-infinite bodies like rings have neither beginning and nor end although their thickness can be measured. If say a 1 cm long section from a bar having side lengths a and b is considered, then its volume $V = a.b.1$ and cooling surface area $A = 2.1.(a+b)$. The imaginary surfaces of separation are not included in calculations. Its modulus will then be

$$Modulus\ (M) = \frac{V}{A} = \frac{ab}{2(a+b)} \tag{2.7}$$

$$Hence\ Modulus\ (M) = \frac{cross\text{-}sectional\ area\ (A)}{perimeter\ of\ the\ cross\text{-}section\ (P)} \qquad (2.8)$$

Equation (2.8) substitutes the detailed calculations of volume and surface area by simpler determination of area and perimeter. The 3D value of SM is replaced by a 2D cross section recognizing that V/A = A/P. Wlodawer created a log-log diagram for finding modulus of bars with rectangular cross section. If a bar is bent around neutral axis, the total surface area remains unaffected as the outer curved side increases by same amount that the inner surface contracts. Modulus for rings of all types can thus be determined by the use of above equation.

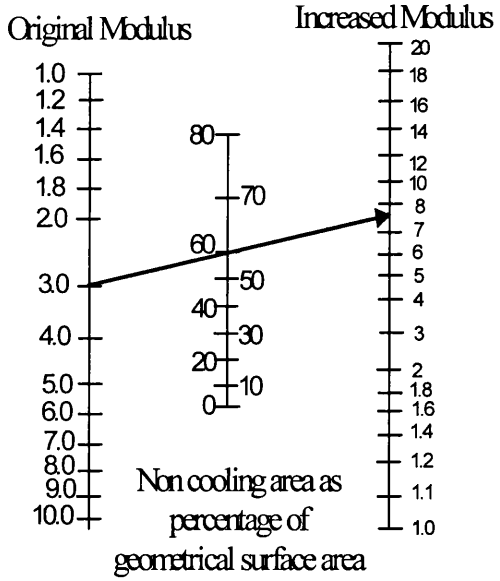

Figure 2.3: Increase in the Modulus with reduction in the cooling surface area – Source [8]

More complex casting bodies like beater cross casting (a stair shaped cross casting) are first resolved in to simpler basic components. The common "boundary surfaces" do not enter the calculation, as they are only imaginary. If the actual cooling surface is only a fraction of the original geometrical surface, the modulus increases thus increasing the solidification time for the casting. The nomogram as given in Figure 2.3 shows these changes in modulus with change in actual cooling area. Many other complicated castings such as bearing components are circumscribed by a simple

parallelepiped as a simulation and the modulus is calculated in the same way as for bars and is then corrected using Figure 2.3. This technique of using simplified equivalents is of immense practical importance for foundry men and saves time and resources without having to undergo the costly "trial and error" techniques that result in foundry scrap.

The essence of the modulus method consists in dividing the actual casting into basic geometric bodies and calculating the ratio 'volume/surface area' for each basic body. Only the casting surfaces in contact with the mould (e.g. sand) are included as surface area. The contact surfaces of the basic body at which it joins other components of the casting are not included, since for long periods little or no cooling takes place at these surfaces. According to the approach outlined by Wlodawer [8], the modulus of the feeder is taken as 1.2 times that of the casting assuming that the feeder solidifies later than the casting.

2.5.8 Shape Factor

Berry *et al.* [11] however, argued that Chvorinov's approach as explained by Wlodawer does not satisfactorily express the solidification time. They conducted experiments to show that solidification time changes with the geometry even for castings with same modulus values.

Jamar [40] also reported that the modulus, as calculated by Chvorinov and Wlodawer is also influenced by shape. He argued that the geometric modulus must be multiplied by a factor before being used to calculate the true solidification time. If the shape of the casting varied from zone to zone e.g. from cuboid to bar or to plate shaped, then the deviations in solidification time suggested by Jamar must be considered.

Tiryakioglu *et al.* ([10],[26],[27]) also argued that feeder efficiency ratio has a linear correlation with the feeder-casting shape factor ratio. Pointing to limitations because of assumptions in Chvorinov's Rule, which did not take the shape of the casting in to consideration, the authors proved that the modulus includes the effect of both casting shape and size. These two

independent factors were separated from each other by the use of a shape factor, k;

$$t = B' k^{1.31} V^{0.67} \tag{2.9}$$

where B' is the mould constant. V represents the amount of heat that needs to be dissipated for complete solidification and k represents the relative ability of the casting shape to dissipate heat under the given mould conditions. The shape factor, k, is the ratio of the surface area of sphere of same volume as that of casting to the surface area of the casting;

$$k = \frac{A_S}{A} = \frac{4.837 V^{\frac{2}{3}}}{A} \tag{2.10}$$

where A_s is the surface area of the sphere, A is the surface area of the casting and V is the volume of the casting.

Using experimental data, Tiryakioglu and Tiryakioglu [10] examined and characterized the effectiveness of nine feeder models and rewrote these models to separate the effects of shape and size of casting. They then determined optimum feeder sizes for a variety of casting volumes and shapes for Al-Si eutectic alloy. The authors then went on to test the validity of the assumption that casting and feeder solidify simultaneously and analysed the heat and mass exchange between feeder and casting during solidification and its effect on solidification time of castings. This challenged the conventional mindset of researchers that considered the feeders and castings separately for calculating solidification times and only accounted for mass transfer from feeder to casting assuming that the transfer takes place isothermally and at pouring temperature, Tiryakioglu *et al* [27] treated casting-feeder combination as a single total casting and argued that the thermal centre of this combination should be in the feeder. They used a superheat model that is based on the equality of the solidification times of feeder and total casting. This contribution allowed the geometric reasoning methods to ensure that the thermal centre of the total casting is retained in the feeder.

2.5.9 Thermal gradient and modulus

In a solidifying casting, the metal in the thicker section remains liquid for longer because of the greater amount of heat that is required to be dissipated, or it can be said, due to the difference in moduli. As temperature falls towards the solidified ends of the casting, a temperature gradient develops that drives the solidification towards the feeder. Pellini (1952) quoted in Wlodawer [8] suggested that to obtain a sound casting, the temperature gradient in a plate must be at least 0.5°C/cm length of the casting as the solidifying casting can still be fed from an adjoining section of the casting that is 0.5°C hotter. These results also strictly apply to steel castings in sand moulds. A section with a longer solidification time also has a larger modulus. Experiments showed that the modulus must be larger by a factor of about 1.1 to ensure the directional solidification with adequate feeding from thicker sections to thinner sections. Similarly the modulus for the feeder head must be at least 1.2 times larger than that of the casting or the modulus must increase by 10% from casting across the ingate to the feeder as is evident from equation (2.11) [8]

$$M_{casting} : M_{neck} : M_{feeder} = 1 : 1.1 : 1.2 \qquad (2.11)$$

The approach suggested by Kotschi and Plutshack, [41] comprises the slicing of the casting model into a number of cross sections and computing the section modulus (SM) at different points in each section. The loci of points with same SM was plotted to visualize the progress of solidification front with the innermost loop identifying the hot spot.

Neises, Uicker and Heine ([12],[13]) also simulated the course of solidification using geometric parameters that essentially influence the thermal properties of the metal, mould and heat transfer systems. Chvorinov's rule given in equation (2.1) states

$$Log\ t = k \log (V / A) + b \qquad (2.12)$$

Where V is total casting volume, A is total surface area, t is solidification time and b and k are constants. Based on Chvorinov's original relationship, the time to the end of the solidification after pouring from approximately 1575°C was found to be proportional to V/A, which has been referred earlier as section modulus (SM). Thus it is appropriate to assume that solidification proceeds as the thickness and corresponding SM increases throughout the casting until the final endpoint of solidification is reached. Instead of using the complete casting volume, the SM principle use 2D cross-sections such as circles, squares, polygons etc. The 3D value of SM is substituted by a 2D cross-section recognizing that V/A = A/P as described by Equation (2.8) earlier. This concept can be visualized by using a cross-section of an infinite cylinder as shown in Figure 2.4 which is taken from [12]. D is the cross-sectional diameter and aD is the diameter of cross-section still in liquid phase.

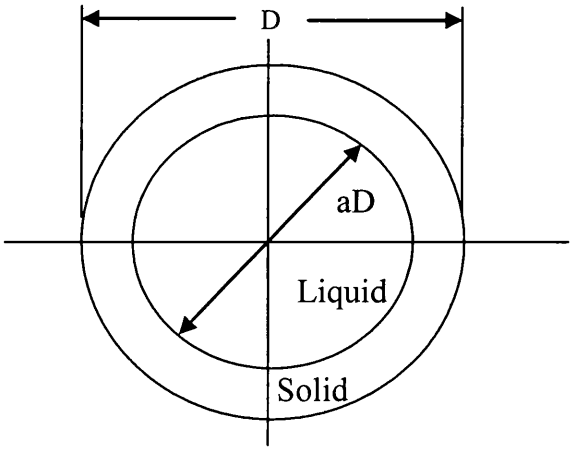

Figure 2.4: Section Modulus in a cross-section of an infinite cylinder

In a 2D analysis, the perimeter P is the heat transfer area and the area of thickness frozen at any distance from the surface is the volume solidified. Therefore, in SM =A/P, the value of P is fixed and the value of A increases as solidification thickness increases. The final SM is thus D/4. If D is chosen, then the end of solidification time for steel could be read from Chvorinov's original expression. For the abovementioned case

$$Thickness\ Solidified = \frac{D - aD}{2} \tag{2.13}$$

$$Section\ Modulus\ (TF) = \frac{V}{A} = \frac{A}{P} = \left(\frac{\pi D^2}{4} - \frac{\pi a^2 D^2}{4}\right) \div \pi D \qquad (2.14)$$

$$\frac{V}{A} = \frac{D\,(1-a^2)}{4} \qquad (2.15)$$

Thus it is observed that Neises *et al.* [13] also computed the moduli of 2D sections using a generalized equation based upon an area/perimeter value for the section modulus.

2.5.10 Hotspot detection and modulus calculation using computer graphics

Ravi and Srinivasan [42] developed another method for identification of hotspots at regions of mass concentration in a casting section using only the geometric elements of the component (inscribed circle method) based on computer graphics. The variation in section area normal to the specified planes was assessed to locate heavier sections in the solid. Rays were projected from a given point inside a section in all directions and their intersections with the section boundary were computed. It was found that the resultant vector along these rays pointed toward the hotspot. This ray tracing technique assisted in determining the mass concentration center and the effective boundary, which was then used to compute the areas and cooling perimeter in 2D for calculating the modulus. By further integrating the moduli of the three orthographic sections taken through the hotspot, the specific modulus of a 3D region is determined for designing appropriate feeders.

The same authors [43] then went on to validate the above-mentioned geometry driven computational technique for predicting hotspots by undertaking experimental verification. They divided the casting section in to a number of wedges each subtending the same angle with its apex at a selected point with the section. The thermal vector for each wedge is computed and the resultant of these determined. If this resultant is zero, then the hot spot is the same as the selected point or else the point is shifted

along the resultant and the process is continued till the resultant is zero. The initial point is taken at the area of mass concentration to reduce the number of such iterations. This program, run on MS DOS environment, also determined the significant section boundary and the corresponding modulus for designing the feeders. The hot spot was located in 6-8 iterations depending on the complexity of the section geometry and the initial location of the chosen point. The experiments were repeated with several sections having external and re-entrant edges and corners, convex and concave surfaces, cylindrical cores and fins for identifying the hot spots. The authors used disposable mould prepared in sodium silicate bonded CO_2 – hardened sand compacted around foamed polystyrene patterns. Aluminum 12% silicon alloy melted in a graphite cubicle was poured at 710°C. The castings were sectioned and radiographically inspected. The shrinkage cavity or the porosity region was found to be in a small zone around the hot spot that was located through the computation in all the 15 test castings investigated. The results were then compared using a FEM program. The hotspot so obtained was within 1% of the maximum section dimension with respect to the hotspot located using the thermal vector technique.

2.5.11 Modulus Vector Method

Ravi and Srinivasan [35] came up with this technique while implementing the above-mentioned program. This approach used the direction of the thermal gradient at any point inside a casting to move along a path that leads to the location of hot spot. They considered a section of the casting showing iso-solidification time contours. If T_i is the temperature at a particular contour at the time before the complete solidification occurs and p_i is the point on the contour. The direction of the largest temperature gradient $\bar{G}_i$ at p_i is given by the normal to the contour of T_i at p_i. The intersection of a line in the direction of $\bar{G}_i$ with the next isothermal contour T_{i+1} gives a point p_{i+1} that has temperature higher than p_i. By repeating the above step and proceeding in this manner, the last point p_{i+n} is reached where the temperature is the maximum and gradient tend to be zero. This represents the location of the hotspot p_h. When the temperature T_i of molten metal at a location p_i reaches the solidus value, the nearest location p_{i+1} along the

temperature gradient is likely to supple p_i with liquid metal to compensate for solidification shrinkage. Thus the path connecting the points p_i, p_{i+1}, p_{i+2},.... P_h represents the feeding path in reverse. This approach reduces the complexity of computation as the temperature values at all the points inside a casting are no longer required to be calculated exhaustively.

This method was implemented in a software package called SOFTCAST that comprised three modules for casting input, solidification analysis and feeder design. The solid modeler creates 3D models of castings and details of any feeders, ingates and cores are entered. The analysis module identifies the hotspot, traces feed metal flow paths and generates colour-coded contours of relative temperature or solidification time. The computation time for a casting of medium complexity on a 486 PC was between 5-10 minutes. The method was first tried on 2D cross sections and later on 3D sections and was validated in laboratory and industrial settings.

2.5.12 Heuvers' Circle Method

This method is based on the modulus principle described earlier and implies that the modulus of a cross section must increase continuously in the direction of the feeder, if the freezing is to be prevented or steered directionally. Heuvers was the first to suggest a practical method consisting of inscribing a series of circles (spheres when implemented three-dimensionally) the diameter of which increases in the direction of the feeder head ([7],[8],[20]), The underlying assumption is that larger the radius of the inscribed circle, longer is the time required for complete solidification in that particular part or section of the casting geometry. Despite its limitations, the method remained very popular with the foundry engineers. This method will be discussed in detail later in Chapter 5.

2.5.13 Medial object technique

The medial object of a solid is defined as a skeletal representation that provides comprehensive information, which can be further used for a variety of geometric reasoning applications. Blum was the first to introduce medial

axis transform (MAT) of a 2D region in 1967 to describe biological shapes [44].

2.5.13.1 Medial object

For a two-dimensional object, its medial axis is the locus of the centre of an inscribed disc of maximal diameter as it rolls within the domain by maintaining the contact with the domain boundary as is illustrated in Figure 2.5. It is thus seen that the MAT is a one-dimensional entity of the region in case of 2D casting sections.

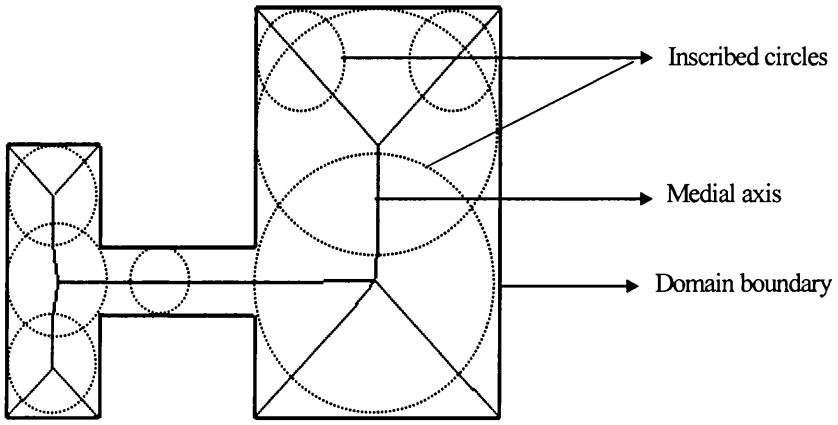

Figure 2.5: Diagram showing medial axis of a casting cross section

Transcendata Europe Ltd. (earlier known as FEGS Ltd. UK) has developed a Medial Axes Transformation (MAT) tool in CAD based software marketed as CADfix and the medial object (MO) technique has been used for the subdivision of complex solids into simpler pieces for automatic mesh generation and also for the generation of simpler idealised models such as shells and beams for stress analysis ([45],[46]). Robust and reliable algorithms are now available for computation of the medial object and its generation. This has allowed users to access and use it without requiring expert knowledge in the mathematical techniques for generating it. The Application Programmers Interface (API) provides a set of tools for accessing the data contained in the medial object. These tools present the data in a readily understandable form such as aspect ratio and minimum thickness values.

2.5.13.2 An example of application of MAT for rapid approximation of casting solidification

Houser [47] demonstrated the feasibility of using MAT (referred by him as Medial Surface Transformation - MST) for quicker approximation of solidification patterns of convex faceted solid models of castings. MST was used to automate the greatest included sphere approach. He extracted the MST by computing the model's Voronoi diagram to identify hotspots and cooling pattern. Voronoi diagrams, named after George Voronoi [48], are also called a Voronoi tessellation or a Voronoi decomposition [49]. Hoff III *et.al.* [50] gave an historical timeline of their development since 1850 (Dirichlet tessellation) to 1908 (Voronoi diagram) and to 1911 (Theissen polygons). *The* Voronoi diagram of a point set P is a subdivision of the plane with the property that each Voronoi cell of vertex p contains all locations that are closer to p than to every other vertex of P [51]. The vertices P are also called Voronoi generators. Each edge of a Voronoi cell is the bisector of the connection of p to the corresponding neighbour cell. Each intersection of Voronoi edges belongs to at least three Voronoi cells and is the center of the circle through the generators of these three cells (Figure 2.6). These three vertices form a Delaunay triangle.

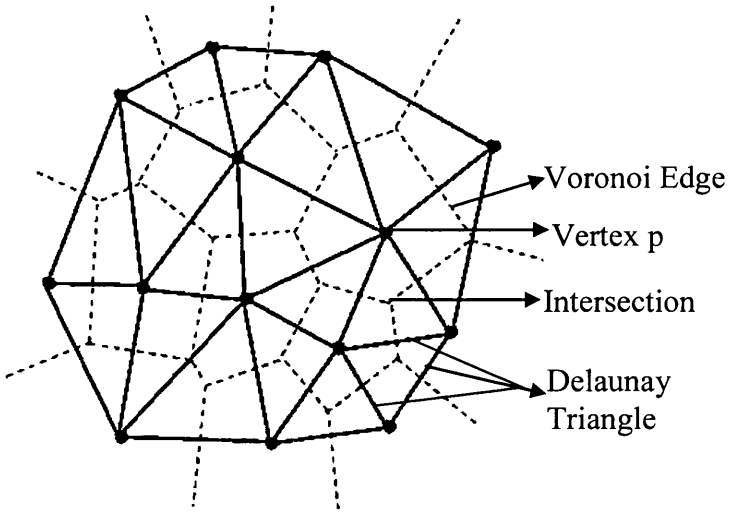

Figure 2.6: An illustration of Voronoi diagram [52], [53]

This method builds on the greatest included sphere method (which is a 2D hand-performed technique) and similarly assumes that the larger the sphere included in a given section of a casting, the longer is the time required to

solidify that section and it also assumes that the center of any included circle/sphere will take longer time to solidify than any other point in the circle. Thus the relative solidification time taken by the various included circles is directly related to its radius. MST, which is the set of the centers of all the locally maximal included spheres in 3D casting object, provided a mathematical method for identifying regions of likely defects in a casting.

The author used a Voronoi diagram for calculating the intersections of the cooling and freezing wave fronts, which in fact is also the medial surface transform for that particular casting section. He further made use of Delaunay tetrahedralisation to exploit its positive relationship with Voronoi diagrams. The results were compared with models generated by explicit finite difference method. It is observed from the above discussion that the predicted relative temperature solution from MST method was consistent with explicit FDM solutions for different tested geometries. Voronoi diagram greatest sphere method made accurate predictions of temperature profiles for 2D cross-sections. However the method was tested only for convex faceted solid models and it did not work for general faceted solid models.

Chapter 3 will take this discussion on MAT forward and describe medial axis transformation technique in detail and also explain how this technique can be used with other geometric methods to achieve directional solidification in castings.

2.6 SIMULATION OF SOLIDIFICATION PROCESS

As mentioned earlier, the hotspots are the most likely locations of casting defects. Efforts were then directed to identify and visualize these last freezing regions or hotspots and predict the casting defects by simulating the solidification process. Such simulations were aimed at predicting hotspots and thus help in placement of feeders, chills, insulations etc thereby, ensuring maximum yield, higher quality castings and lesser production of casting scrap. But uncertainties of metal and mould properties, solidification temperature ranges, changes in the heat transfer system of the liquid; liquid-solid phase, solid phase and air gap formation increase the difficulties of

numerical calculations and the accuracy of their predictions. With the advent of PCs and the computing power that these computers offered, the numerical simulation of castings process moved from research to practical application.

SOLSTAR was the first 3D PC software launched in market in the mid-1980s. This modelling software was developed by a foundryman and was based on a series of rules to model casting solidification ([54],[55],[56]). SOLSTAR is a diagnostic software programme that predicts the solidification pattern in a casting. Based on various data imported from client's plant and fed into it, the programme is capable of providing a visual representation of the casting structure during solidification [57]. Since its launch, many other types of software have been developed to capture and simulate the physics involved in casting solidification process. Some of the commercially used FEM based solidification modeling packages are ProCAST, PATRAN/ANSYS, and CADCAST. Two of the commonly used FDM based packages from American Foundrymen Society are 2D AFSolid and 3D AFS Solidification System [47] and SIMULOR [56]. Softwares like SOLSTAR, MAGMAsoft™ Flow-3D™ have been effective in enabling foundrymen see graphical representation of what they see in the real casting [54].

Although the FEM based numerical simulation approach is computationally expensive, it is accurate and reliable, and is widely preferred and applied in engineering applications as it allows a wider choice of elements shape and accuracy [58]. Such a numerical analysis also allows a better understanding of the phase transformation phenomenon especially the study and modeling of heat transfer process [59]. Automatic preprocessing and adaptive re-meshing for better accuracy have also gained acceptability in recent past. The location and shape of shrinkage cavity can also be visualized from the innermost isotherm or iso-solidification time contour obtained from such simulations.

Several packages based on various numerical methods are currently being used by the industry. A typical iteration comprises solid modeling, mesh generation, material selection, specification of boundary conditions, numerical computations and finally post processing for viewing the results. The latter usually involves plotting of colour-coded temperatures at different time steps and displaying macro and micro-shrinkage cavities. The accuracy of such simulations depends on the size of mesh, the material property data and the heat transfer coefficients specified for the casting/mould interface. Despite their increasing popularity, the percentage of foundries in West using such software in 2002 was still less than 25% [55] and 15% worldwide [56]. Foundrymen have been slow to adopt such simulation tools initially but then they started to realize that such tools are to aid and help them perform their jobs more efficiently and are not a threat to their employment.

In a useful contribution to our knowledge about various softwares and their capabilities and usefulness to foundry industry, Jolly ([55],[56]) studied and reviewed efficiency of current software packages as to how best they achieve the objective of predicting casting defects. The author took into account the underlying physical phenomenon, practical defects, capability of the software packages to accurately represent boundary conditions and thermo-physical data, and issues pertaining to post processing that are hugely relevant to a layperson. The author concluded that no single software is capable of completely meeting the foundry requirements and it is highly unlikely any single numerical technique can take into account the range of problems that foundrymen face in the casting industry. However hybrid software packages that combine experimental data with numerical analysis and optimisation approach are most likely to succeed and gain popularity amongst foundrymen.

2.7 LIMITATIONS OF GEOMETRIC METHODS

Despite their advantages of simplicity of use, reduction in cost and time, the geometry based methods suffer from following limitations:

1. The geometric methods remain restricted in their application, as most of these only provide a qualitative analysis that is insensitive to material properties and boundary conditions. Geometric techniques like Heuvers' Circle would give similar results for different materials and boundary conditions.

2. These methods for example MAT based temperature approximation assume that boundary conditions are uniform because greatest included method also relies on symmetry to predict the relative solidification times.

3. Geometric methods including the classic Chvorinov's rule only provide an acceptable estimate of total solidification time of a casting without giving information on local solidification times.

4. Foundrymen using some of the geometry based methods e.g. Modulus Method, Inscribed Circle/Heuvers' Circle Method often applied additional padding to influence the modulus for directional solidification. Such padding ultimately increased the size of the feeder and usually has to be removed through dressing operations resulting in wastage and affecting yields.

2.8 CLOSURE

Foundrymen and researchers have continuously sought to improve the modelling of the solidification patterns and behaviour of casting metals. Most of these programmes and commercial software packages comprise of 2D and 3D FEM or FDM based heat transfer/solidification simulation softwares that provide detailed information on cooling and freezing behaviour of castings. These applications have often been expensive to procure and had greater cost attached to them in terms of time and pre requisites of knowledge of material properties that was required to run and understand the results. It is however, pertinent to point out here that although such applications provide precise results that are accurate; these have been found wanting where there

was a need for foundrymen to seek quicker design iterations to optimize the solidification process for casting soundness.

The review of the relevant literature has revealed that geometric methods do provide another effective option other than numerical simulations for predicting the solidification pattern and shrinkage defects in castings. The various methods using geometric parameters described in this chapter provide an alternative approach that combine speed with ease of use to pave a way for development of applications that are accurate too. Most of these applications based on geometric reasoning use feature-based reasoning i.e. sectioning of the complex casting geometry into simple components. Some of these are capable of performing 3D calculations but mostly they are 2D simplifications of 3D models. CADfix [45] is one such commercial application package.

The discussions from examples of use of MAT reveal that medial axis transformation is a very unique and useful data structure that can be utilized for solidification modelling. The MAT provides a unique representation of an object in a compressed manner from which the original geometry of the object can be retrieved. It is proposed to make use of this scope that exists for further research to investigate the use of MAT combined with other geometry-based methods (e.g. Modulus method and Inscribed circle method) to predict temperatures in solidifying castings and seek solution to various problems that occur during the solidification process and are currently relevant to the foundrymen. The findings and results from such innovation from geometry-based methods will then be compared and validated with the solutions obtained from FE based simulations.

The subsequent chapters will take this discussion forward and describe MAT technique in detail and also explain how this technique is used with other geometric methods to predict casting temperatures and hot spots (Chapter 3 and 4) and achieve directional solidification in castings with very few numerical simulations (Chapter 5 and 6).

REFERENCES

[1] R. W. Heine and P. C. Rosenthal, "*Principles of Metal Casting*", McGraw-Hill Book Company, Inc, New York, USA, 1955.

[2] H. F. Taylor, M.C. Flemings and J. Wulff, "*Foundry Engineering*", John Wiley & Sons, New York, USA, 1959.

[3] B. Chalmers, "*Principles of Solidification*", John Wiley & Sons, Inc. New York, USA, 1964.

[4] R. W. Ruddle, "T*he Solidification of Castings*", The Institute of Cast Metals, London, 1957.

[5] J. P. Holman, "*Heat Transfer*", 7th Edition, McGraw-Hill Book Company, London, 1992.

[6] J. Campbell, *Castings Practice: The Ten Rules of Castings,* Butterworth-Heinemann, Oxford, UK, ISBN: 0750647914, May 2004.

[7] J. Campbell, *Castings 2nd Edition* Butterworth-Heinemann, Oxford, UK, 2003.

[8] R. Wlodawer, "*Directional Solidification of Steel Castings*", Pergamon Press, Oxford, 1966

[9] B. Ravi and M. N. Srinivasan, "Casting Solidification Analysis by Modulus Vector Method", *International Journal of Cast Metals Research*, 1996, 9: 1-7.

[10] M. Tiryakioglu and E. Tiryakioglu, "A Comparative Study of Optimum Feeder Models for Castings", *International Journal of Cast Metals Research*, 2001, 14, 25-30.

[11] J. Berry, V. Kondic and G. Martin, "Solidification times of simple shaped castings in sand models", *Modern Castings*, 1959, 36, 39

[12] R. W. Heine and J. J. Uicker, "Risering by Computer assisted Geometric Modeling", *AFS Transactions*, 1983, 91, 127-136.

[13] S. J. Neises, J. J. Uicker and R. W. Heine, "Geometric Modeling of Directional Solidification based on Section Modulus", *AFS Transactions*, 1987, 95, 25-30.

[14] D. A. Tortorelli, J. A. Tomasko, T. E. Morthland and J. A. Dantzig, "Optimal-Design of Nonlinear Parabolic-Systems.2. Variable Spatial Domain with Application to Process Optimisation", *Computer*

Methods in Applied Mechanics and Engineering, 1994, 113 (1-2): 157-172.

[15] T. E. Morthland, P. E. Byrne, D. A. Tortorelli and J. A. Dantzig, "Optimal riser design for metal castings", *Metallurgical and Materials Transactions,* 1995, 26B: 871-885.

[16] S. A. Ebrahimi, D. A. Tortorelli, J. A. Dantzig, "Sensitivity analysis and nonlinear programming applied to investment casting design, *Applied Mathematical Modeling,* Feb 1997, 21 (2): 113-123.

[17] S. Chen, D. A. Tortorelli, "Three-dimensional shape optimisation with variational geometry", *Structural* Optimisation, 1997, 13 (2-3): 81-94.

[18] R. M. McDavid and J. A. Dantzig, "Fluid Flow in Casting Rigging Systems: Modeling, Validation and Optimal Design", *Metallurgical and Materials Transactions-B*, 1998, Vol. 29 B: 679-690.

[19] R. S. Ransing and R. W. Lewis, "Optimal Design of the Die Coating Thickness Using the Lewis-Ransing Correlation", *International Journal of Cast Metals Research*, 1997, Vol. 9: 269-277.

[20] J. Campbell, *Castings.* Reprinted series, Butterworth-Heinemann, Oxford UK, 1997.

[21] J. Campbell, "10 Rules for good casting", *Modern Castings*, 1997, **97 (4)**, pp. 36-39.

[22] J. G. Bralla, *"Design for Manufacturability"*, 2nd Edition, McGraw-Hill, NY, USA, pp. 1.20, 1998.

[23] G. Upadhya and A. J. Paul, "Rational Design of Gating and Risering for Castings: A New Approach Using Knowledge base and Geometric Analysis", *AFS Transactions*, 1993, Vol. 113: 919-925.

[24] B. Lally, L. T. Biegler and H. Henein, "Optimisation and Continuous-casting. 1. Problem Formulation and Solution Strategy, *Metallurgical Transactions B - Process Metallurgy*, Oct 1991, 22 (5): 641-648.

[25] B. Ravi and M. N. Srinivasan. "Feature-Based Castability Evaluation", *International Journal of Production Research*, 1995, Vol. 33 (12): 3367-3380.

[26] M. Tiryakioglu, E. Tiryakioglu and D. R. Askeland, "The Effect of Casting Shape and Size on Solidification Time: A New Approach", *International Journal of Cast Metals Research*, 1997, 9, 259-267.

[27] M. Tiryakioglu, E. Tiryakioglu and J. Campbell, "Mass and Heat Transfer during Feeding of Castings", *International Journal of Cast Metals Research*, 2002, 14, 371-375.

[28] R. S. Ransing, R. W. Lewis and D. T. Gethin, "Lewis-Ransing Correlation to Optimally Design the Metal-Mould Heat Transfer", *International Journal of Numerical Methods in Heat and Fluid Flow*, 1999, Vol. 9, no. 3: 318-332.

[29] R. S. Ransing and R. W. Lewis, "A Thermo-elasto-visco-plastic Analysis for Determining Air Gap and Interfacial Heat Transfer Coupled with the Lewis-Ransing Correlation for Optimal Feeding Design", *Modeling of Casting, Welding and Advanced Solidification Processes VIII*, Ed. BG Thomas and C. Beckermann, San Diego, USA, 1998: 731-738.

[30] R. S. Ransing, M. P. Sood and W. K. S. Pao, "Computer Implementation of Heuvers' Circle Method for Thermal Optimisation in Castings", *International Journal of Cast Metals Research,* 2005, Vol. 18, no 2, 119-126.

[31] R. T. Haftka and R. V. Grandhi, "Structural shape optimisation—A survey", *Computer Methods in Applied Mechanics and Engineering*, 1986, Vol. 57, Issue 1: 91-106.

[32] R. S. Ransing, "An Approach for the Causal Analysis in Casting Processes based on Probabilistic Analysis, Neural Network and Design Optimisation", PhD Thesis, University of Wales Swansea, UK, 1996.

[33] R. W. Lewis, M. T. Manzari, R. S. Ransing and D. T. Gethin, "Casting shape optimisation via process modeling", *Materials and Design* 2000, 21 (4): 381-386.

[34] R. S. Ransing, S. Savino and R. W. Lewis, "Numerical Optimisation of a Tilt Casting Process", *International Journal of Cast Metals Research,* 2005, Vol. 18, no 2, 109-118.

[35] B. Ravi and M. N. Srinivasan, "Casting Solidification Analysis by Modulus Vector Method", *International Journal of Cast Metals Research*, 1996, **9**, 1-7.

[36] E. Niyama, T. Uchida, M. Morikawa and S. Saito, "A method of shrinkage prediction and its application to steel casting practice", *International Journal of Cast Metals Research*, 1982, **9**, 52-63.

[37] I. Imafuku and K. Chijiiwa, "A Mathematical Model for Shrinkage Cavity Prediction in Steel Castings", *AFS Transactions*, 1983, **91**, 527-537.

[38] N. Chvorinov, "Theory of Solidification of Castings", *Giesserei*, 1940, **27**, 177-225. (This is not a original reference but was referred to by many authors e.g. Ravi and Srinivasan , 1996; Wlodawer, 1966).

[39] S. Ozdemir and E. Atasoy, "A new approach to feeder dimensioning" *Cast Metals*, 1995, **8** (3), 129-137.

[40] J. Jamar, http://www.eildonr.demon.co.uk/software.htm, 1975, accessed in Aug.-Nov. 2002 and again on 18th Jan. 2006.

[41] R. M. Kotschi and L. A. Plutshack, "An easy and inexpensive technique to study the solidification of castings in three dimensions", *AFS Transactions,* 1981, **89**, 601-610.

[42] B. Ravi and M. N. Srinivasan, "Hot spot detection and modulus computation by computer graphics", *Proceedings of 56th World Foundry Congress*, Dusseldorf, May 19-23, 1989, 12.1-12.7.

[43] B. Ravi and M. N. Srinivasan, "Hot spots in Castings: Computer-aided location and experimental validation", *AFS Transaction,* 1990, **98**, 353-357.

[44] G. Evans, A. Middleditch and N. Miles, "Stable computation of the 2D medial axis transform", *Int J Comp. Geom. & Application*, 8(5), 577-598, 1998.

[45] Transcendata Europe Medial Object Technical Paper from their website http://www.fegs.co.uk/motech.html, 2002-2005, last accessed on 16th Jan 2006.

[46] http://www.fegs.co.uk/medial.html, 2002-2005, last accessed on 16th Jan 2006.

[47] S. A. Houser, "*Medial Surface Transformations for Rapid Approximation of Casting Solidification*", MS thesis, Virginia Polytechnic Institute and State University, USA, July 1996.

[48] G. Voronoi, J. R. Angew, *Math*, 1908, 134, pp: 198-287.

[49] http://www.answers.com/topic/voronoi-diagram, accessed on 30th Jun 2006.

[50] K. E. Hoff III, T. Culver, J. Keyser, M. Lin and D. Manocha, "Fast computation of generalised Voronio diagrams using graphics hardware", a MS PowerPoint presentation, University of North Carolina at Chapel Hill, SIGGRAPH 1999.

[51] Riky Subrata, A. Y. Zomaya, "Some results on the computation of Voronoi diagrams on a mesh with multiple broadcasting", *Journal of Parallel and Distributed Computing*, December 2003, Vol. 63 (12), pp: 1300–1314, Academic Press, Inc., Orlando, FL, USA, accessed on 30th June 2006 through the website: http://portal.acm.org/citation.cfm?id=965266&dl=GUIDE&coll=GUIDE.

[52] http://www.cs.cornell.edu/Info/People/chew/Delaunay.html, accessed on 30th Jun 2006.

[53] http://www.pi6.fernuni-hagen.de/GeomLab/VoroGlide/, accessed on 30th Jun 2006.

[54] M. Jolly, S. Wen and J. Campbell, "An Overview of Numerical Modelling of Casting Processes", *Modelling and Simulation in Metallurgical Engineering and Material Science*, June 11-13, Metallurgical Press, Beijing, China, 1996, p. 540.

[55] M. Jolly, "Casting Simulation: How well do reality and virtual casting match? State of the art review", *International Journal of Cast Metals Research*, 2002, **14**, 303-313.

[56] M. Jolly, "State of the Art Review of Use of Modelling Software for Shape Casting", *Shape Casting: The John Campbell Symposium*, Edited by M. Tiryakioglu and P. N. Crepeau, Proceedings of the Symposium sponsored by TMS (The Minerals, Metals and Materials Society), San Francisco, California, USA, Feb 13-17, 2005, ISBN: 087339-583-2, pp. 337-346.

[57] http://www.fosecosteel.com/steel/products_and_services/ingot_casting/amitec_solstar.php, accessed in May 2005 and 18th Jan 2006.

[58] I. Minkoff, "*Solidification and Cast Structure*", John Wiley & Sons, Chichester, England, 1986.

[59] R.W. Lewis, K. Morgan, H.R. Thomas and K.N. Seetharamu, "*The Finite Element Method in Heat Transfer Analysis*", Reprint Series, John Wiley & Sons, Chichester, England, 1997.

Chapter 3

SOLIDIFICATION SIMULATION USING MEDIAL AXIS BASED INTERPOLATION SCHEME

CHAPTER LAYOUT
This chapter builds on the discussion on geometric reasoning techniques from previous chapter. The objective now is to investigate these geometric methods with an aim to predict casting temperatures and likely locations of casting defects, known as hotspots. After introducing the chapter, the next three sections of the chapter provide information on medial axis transformation (also known as MAT) technique and briefly discuss how MAT is derived along with its potential for use in the field of casting. A case study is then presented to illustrate the technique and feasibility of using such geometric information and applicability of MAT based interpolation scheme for understanding solidification behaviour and as an aid in casting design cycle. The chapter then discusses the advantages and limitation of this scheme and brings out conclusions in the last section.

3.1 INTRODUCTION

The previous Chapter 2 described and discussed various geometric reasoning techniques to analyse the process of solidification in castings. Along with other geometric reasoning methods, the Medial Axis Transformation (MAT) technique was also briefly discussed in Section 2.3.13 of Chapter 2. This chapter now aims to explain how the important geometric information provided by MAT can be used to predict casting temperatures and aid solidification analysis. The radius information provided by the MAT for various points on medial axis is used to develop an interpolation scheme to meet the objective outlined above. This chapter first introduces the MAT technique and then briefly describes how it has been constructed by different researchers. The later half of the chapter then focuses on explaining the usefulness of MAT technique in studying and analyzing solidification pattern and predicting hotspots in a freezing casting by using a novel interpolation scheme.

3.2 THE MEDIAL AXIS TRANSFORMATION TECHNIQUE

As described in Section 2.3.13 of Chapter 2, the medial object of a solid is defined as a skeletal representation that provides comprehensive information that can be further used for a variety application based on geometric reasoning. The medial axis transform of a 2D region was first introduced in 1960s to describe biological shapes [1]. The medial object is constructed by rolling a disc around inside a face, or a sphere incase of a volume. Thus the medial axis transform of a two-dimensional region is a locus of the center of an inscribed disc of maximal diameter as it rolls within the domain while maintaining contact with the domain boundary on at least two points, as shown in Figure 3.1 and Figure 3.2[2]. The centres of all these interior maximal discs are known as medial points. Medial axis becomes a medial surface for a three dimensional object (Figure 3.2). The medial object is a complete representation of the original object as it carries radius information of the object. It is thus seen that the MAT is a one-dimensional entity of the region in case of 2D casting sections. The term medial object represents both, the medial axis of a surface and the medial surface of a solid (referred in the literature collectively as the medial axis transform - MAT). The term

MAT has been used widely as an alternative representation of an object that is capable of providing important geometric information contained with in that particular solid object e.g. MAT provides the radius information associated with a particular medial point on the medial axis or the radii of all the inscribed circles or spheres with in that solid object.

The first known use of MAT was made in 1967 by Blum as an aid to describe the biological shapes ([1],[3]-[6]). Although the existing literature suggests many uses of the medial axis technique for geometry interrogation, mesh generation and constructions of three-dimensional objects like the human body, biological entities possessing very odd shapes but its utility in obtaining engineering solution remained unexplored for long time.

However, Armstrong and co-workers ([6]-[10]) made perceptible progress in this direction since 1990s using the medial objects as *substituted equivalent structures* for massive engineering structural analysis e.g. in an offshore platform that requires expensive computational efforts and time. The work by Armstrong and his colleagues demonstrated that medial objects have significant potential to reduce the simulation time and cost in practical engineering applications. Some potential applications have also been given by Quadrose *et al.* [11].

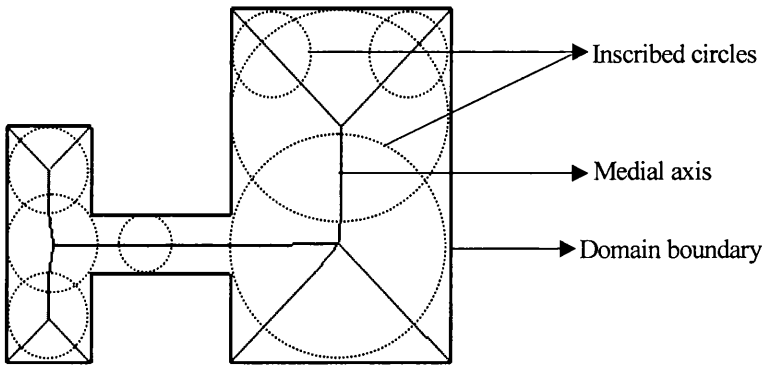

Figure 3.1: Medial axis and maximal inscribed circles in a two-dimensional geometry

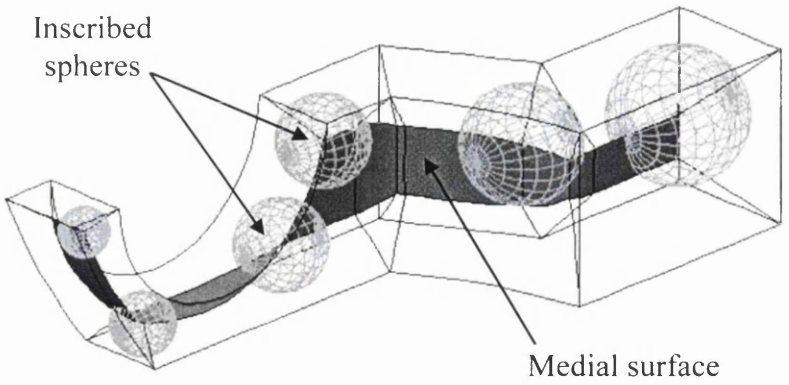

Figure 3.2: Medial surface and maximal inscribed spheres in a three-dimensional object [2]

3.3 OBTAINING MAT OF AN OBJECT

Owing to its manifold uses, many researchers have tried to develop the skeletal representation of two- and three-dimensional solids using the medial axis transformation technique. Reddy and Turkiyyah [12] showed that a generalized Voronoi diagram (See Section 2.5.13.2 on page 41) derived from a set of boundary entities of a polyhedron is the exact skeleton of the polyhedron. They computed an abstract Delaunay triangulation from which the skeleton (MAT) could be derived. The circumcentres of the Delaunay tetrahedral approximately lie on the skeleton. Ramamurthy and Farouki [13] adopted an incremental approach for computing the Voronoi Diagram of the planar domain wherein a single boundary segment is added to an existing boundary-segment set at each step. When all such boundary segments have been included and Voronoi regions have been constructed, the Voronoi diagram of the boundary is obtained as the union of the Voronoi polygons for each boundary segment. The medial axis is then obtained from the Voronoi diagram by removing certain edges of the Voronoi diagram that do not belong to the medial axis and adding some edges that do belong to it.

However, it is acknowledged here that for the purpose of the research carried out in this and the following chapters, extensive use was made of medial axis transformation (MAT) tool that was available in CADfix system software provided by TranscenData Global Europe Ltd [2]. MAT was used to generate medial axes for various case studies undertaken in this thesis.

Medial axes generated for two casting geometries using CADfix is shown in Figure 3.3 (a) and (b).

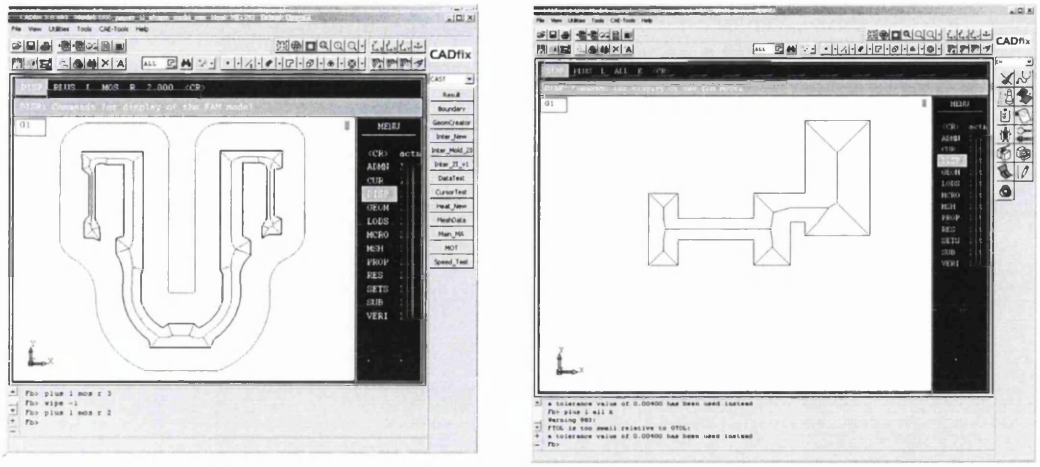

(a) Medial axis of a U-shaped casting geometry adopted from [14]

(b) Medial axis of a Gear blank casting adopted from [15]

Figure 3.3: Examples of automatic medial-axis generation using CADfix

3.4 MEDIAL AXIS TRANSFORM AND ITS APPLICATIONS

3.4.1 Motivation for this research

The ability to achieve high quality control over solidifying castings is of paramount importance issue for the manufacturing of critical components used in aerospace and other key industries [16]. Very often, these components are made up of very expensive metals and alloys. Metal casting is a complex process and is sometimes known as *black art* amongst the foundrymen. This is because the quality control of the casting technology not only depends on a trial and error method in selecting the optimum manufacturing parameters, but also on many person-years of accumulated hand-on experience. This old-fashioned approach is very unreliable and inconsistent because it relies heavily on individual foundrymen's non-quantitative experience and intuition. However, in the last two decades, emphasis has shifted to more scientific and quantitative approaches and in particular the numerical method, to enhance the understanding about the casting processes ([17]-[20]).

The growing need for shorter product development cycles has witnessed widespread popularity of using computer based simulation methods to achieve various goals in castings processes, ranging from castings designs, quality control to cost reduction ([21],[22]). One of the major problems during a casting design cycle is the time taken to perform the numerical simulation for predicting solidification patterns, hot spots and thermal stresses. Very often, this design-simulation-evaluation cycle is performed many times before a final satisfactory geometry is obtained or sound cast-mould assemblies are put together. This cycle can be expensive and irritatingly annoying as well if the simulation time required for the re-evaluation is significantly large in comparison to the time taken to change the part geometry on a CAD system. Here the efficiency of the numerical software plays a key role. As was discussed in Chapter 2 (Section 2.2); most commercially available software use conventional numerical methods such as the finite element (FEM), finite difference (FDM) and finite volume (FVM) methods ([23]-[27]) that usually involves solving a large set of simultaneous physical equations. In this way, the duration of the simulation time depends largely on the speed at which the matrix equations are solved in these codes.

As pointed out in previous chapter, alternative to the numerical simulation methods are various geometric reasoning techniques. From the detailed literature review on such techniques given in Chapter 2, it is noted that none of the developed geometric methods is able to predict evolution of temperature profiles in time or take into account the sensitivity of the material properties. The case study explained in next section details an interpolation scheme that provides these evolving temperature profiles and predicts the hot spots in a solidifying casting.

3.5 CASE STUDY: A MEDIAL AXIS BASED INTERPOLATION FOR AN APPROXIMATE ESTIMATION OF CASTING TEMPERATURES

3.5.1 Background

During visits to foundries, the discussions with experienced foundrymen and other industrial collaborators revealed that on many occasions, the accuracy of prediction is not a critical issue and the knowledge of the relative temperature profile and the location of a hot spot in a casting assume greater significance. It is not uncommon for the engineers to re-run the simulation overnight even for a slight change in the geometry. The need to improve upon the computational speed by developing a useful, comprehensive and simple technique led to the research being presented in this case study. The aim however, is not to substitute the conventional numerical software, but to develop a technique that will shorten the design time while retaining nearly same order of accuracy. The tool developed may serve as an add-on to a CAD system rather than any numerical simulation software. With this objective in mind, the possibility of using a medial axes transformation on a simplified geometric representation of complex geometrical object to achieve this task is investigated.

3.5.2 MAT, one-dimensional domain and heat conduction

It has been discussed in Section 3.2 earlier that in 2D, the MAT is a one-dimensional entity of the region. The purpose here is to explore the use of MAT entities in obtaining approximate temperature solutions in a solidifying casting. The governing equations for temperature diffusion in a solid can be written as [28]:

$$\nabla \cdot (K \nabla T) + \rho c \frac{\partial T}{\partial t} - Q = 0 \tag{3.1}$$

where K is thermal conductivity of the material (W/mK), ∇T is the temperature gradient in the direction of the heat flow, ρ is density (kg/m^3) and c is the specific heat of material (J/kgK).

It was assumed that (i) all the boundaries of the casting are homogeneous and that (ii) the heat flux emanates normally from the medial axes. First assumption follows directly from the Chvorinov rule. The second assumption is due to the observation that during uniform solidification, all heat flux vectors in a casting originate from the highest temperature in the cast and heat flows perpendicularly towards the mould-cast interface. In a two-dimensional solidifying casting, the highest temperature is usually located in the vicinity of the medial axes as depicted schematically in Figure 3.4. The dotted arrows along a cross-section A-A' cut perpendicularly through the medial axis Figure 3.4 in thus represents approximately the heat flow path. This assumption is essentially one-dimensional (Figure 3.5) and analytical solutions to such problems are given by Carslaw and Jaeger [29].

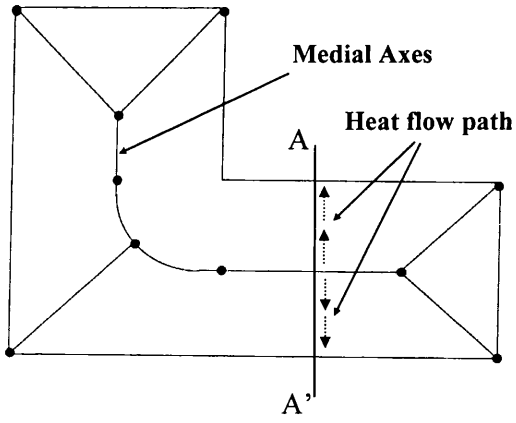

Figure 3.4: A two-dimensional object diagrammatically showing that heat flux emanates from medial axis only and does not cross the medial axis. The arrows show the heat flow path assuming equal boundary conditions

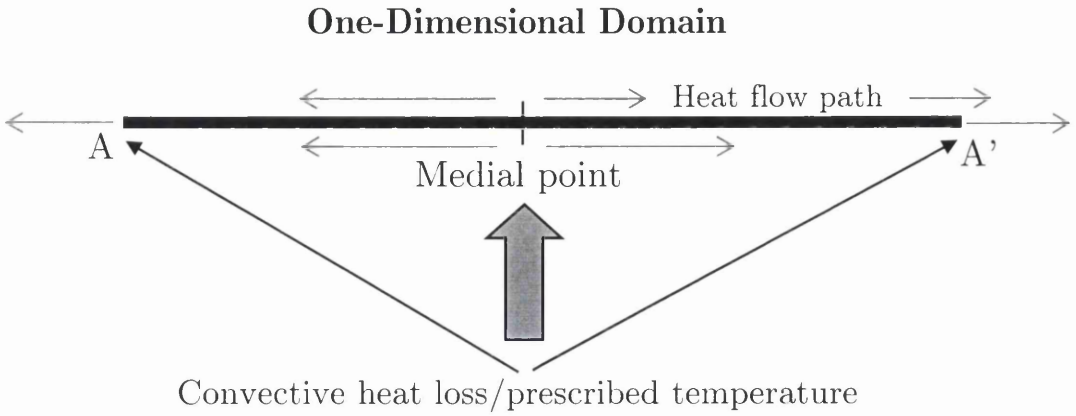

Figure 3.5: Reduction to 1D Heat Conduction

3.5.3 Implementation of interpolation scheme

3.5.3.1 Predicting transient temperature using MAT

The first step in implementing the proposed 1D interpolation scheme was to study the transient temperature profiles for one one-dimensional bar and then more bars of varying lengths. For this purpose, an existing FE based research code developed in house by a research team was used to simulate the solidification process for 10 one dimensional bars of various lengths with material properties and boundary conditions as shown in Figure 3.6 and given in Table 3.1. Initially, there were many unknowns and hence simplified values for boundary conditions and material properties were used. Also, simplified unit values for properties for testing purpose were assumed so that the code was easy to debug [30]. After the testing phase, simulation was carried out using realistic values for material properties and boundary conditions.

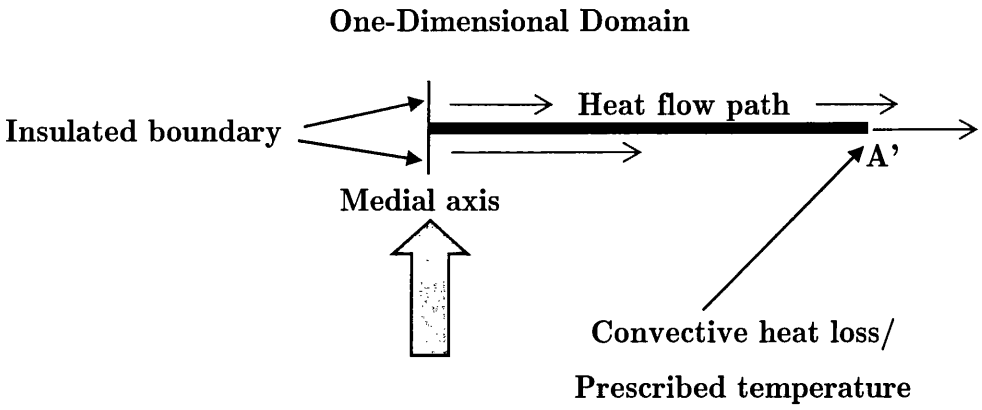

Figure 3.6: Schematic of one-dimensional bar taken for FE analysis

Initial temperature in the domain	100°C
Ambient temperature (Fixed boundary condition)	25°C
Conductivity of cast material (K)	1 W/mK
Volumetric Energy Density of casting (ρc)	1 J/m^{3}K
Simulation time span	2.5 seconds
Time step size	0.1 seconds

Table 3.1: Input data for FE simulation of one-dimensional bar

A schematic representation of temperature profile for a single one-dimensional bar at different time steps is shown in Figure 3.7 and the same temperature profile in normalised space (0,1) is shown in Figure 3.8

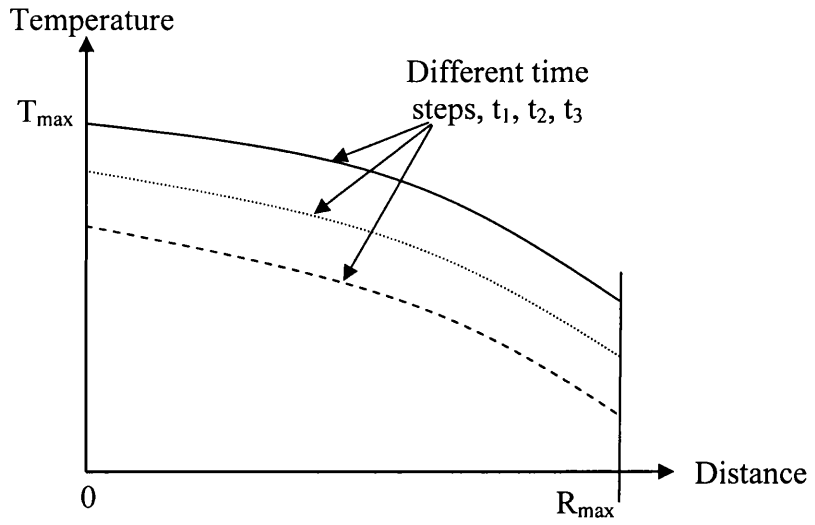

Figure 3.7: A schematic of temperature profile of a 1D Bar from cast only (at different time steps)

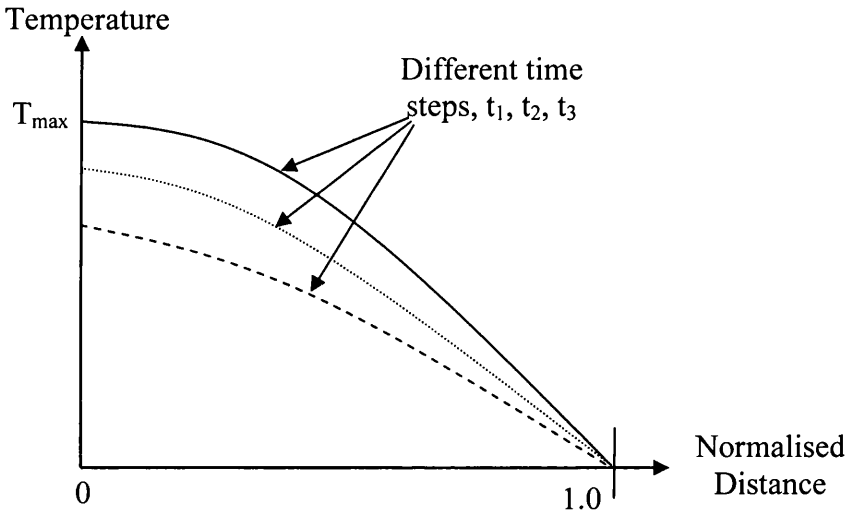

Figure 3.8: A schematic of 1D Bar with different time steps in normalised space (0, 1)

On undertaking similar FE analysis for more one-dimensional bars of varying lengths, it was observed that the temperature profile exhibits the same pattern as illustrated schematically in Figure 3.9 for same time step and Figure 3.10 for different time steps.

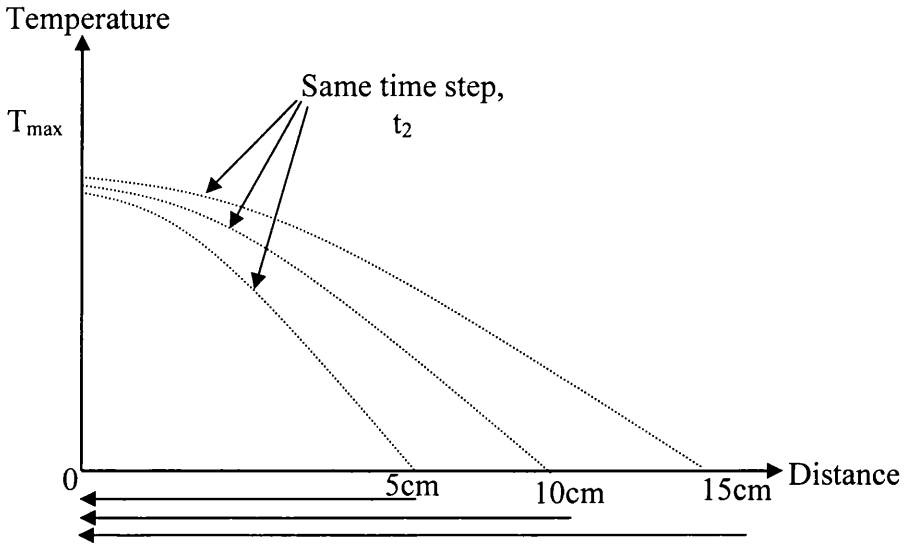

Figure 3.9: A schematic of temperature solution for 1D bars of varying lengths at same time step

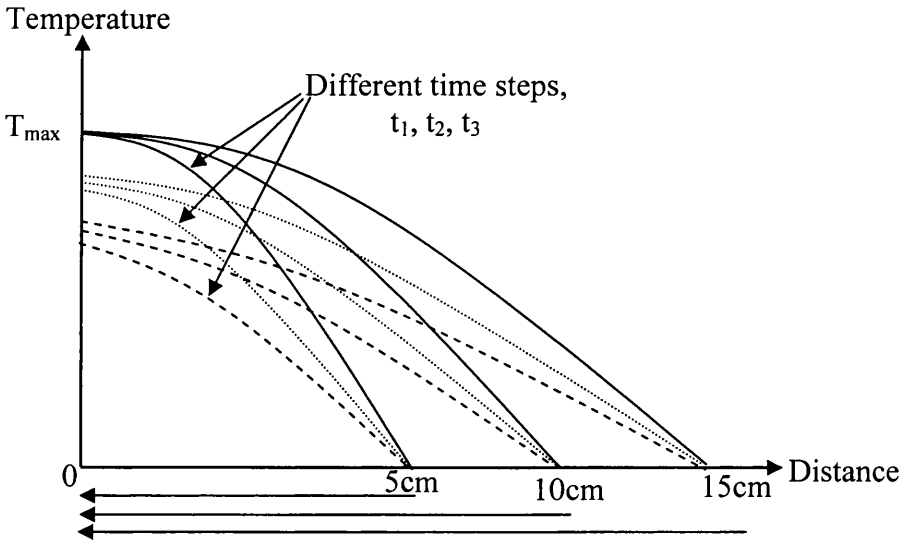

Figure 3.10: A schematic of temperature solution for 1D bars of varying lengths at different time step

The temperature solutions for one-dimensional bars of above mentioned three lengths (Figure 3.10) at different time steps in normalised space (0,1) are shown schematically in Figure 3.11. The actual temperature solutions for

ten 1D bars using boundary conditions and material properties from Table 3.1 are shown in Figure 3.12 [30]. It is observed that the transient solutions exhibited similar temperature profiles for all ten lengths of one-dimensional bars.

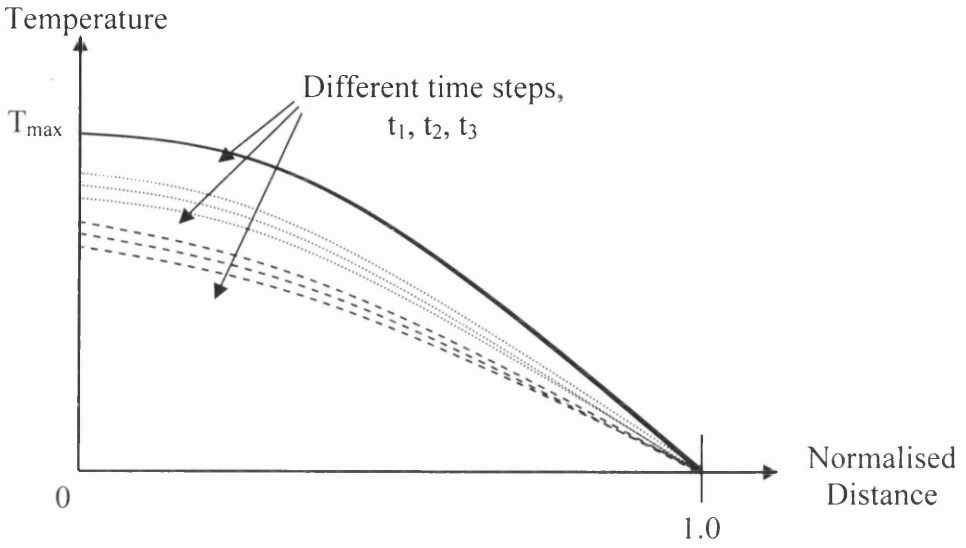

Figure 3.11: A schematic of temperature solution for different bars in normalised space (0,1)

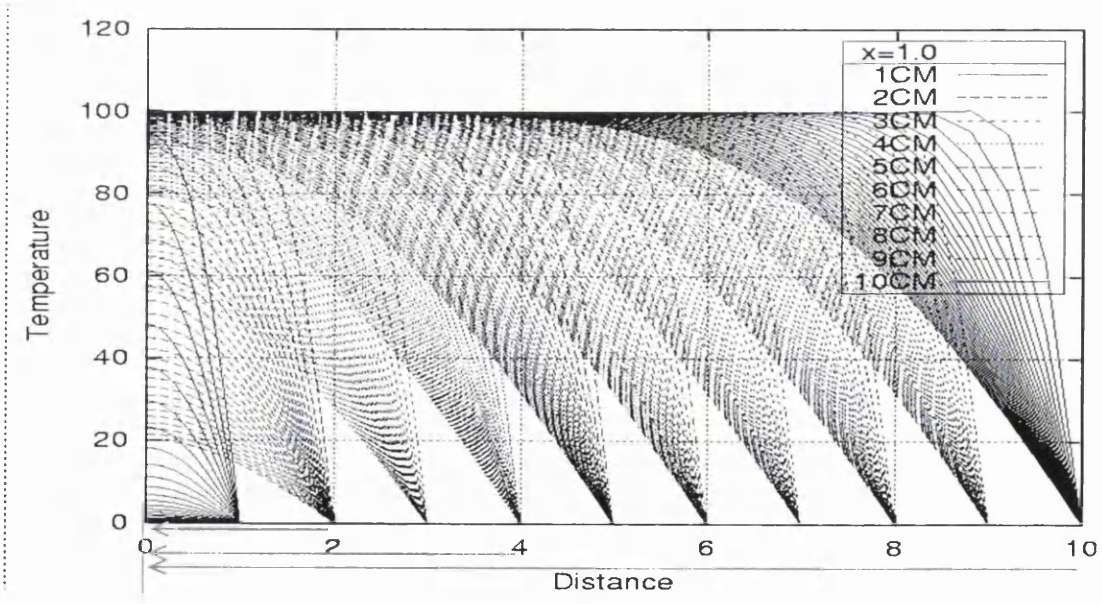

Figure 3.12: Solution for 1D heat conduction

By observing that the transient solutions are similar for a particular case of homogeneous boundary condition, the temperature (T) can be expressed as a function of normalised space, x, and time, t, such that:

$$T = T\left(\frac{x}{L}, \frac{t}{t_{\max}}\right) \tag{3.2}$$

where L and $t_{\max}$ are the maximum medial-radius of the cast domain and total time of simulation, respectively.

The MAT now provides the radius information which gives the maximum radius of the inscribed circle, R. By generating an array of arbitrary points with distance d_i normal to the medial axis, the transient temperature 'T_i' at any arbitrary point in the casting could be found by interpolation using Equation (3.2) and as shown in Figure 3.13 as

$$T_i = T\left(\xi = \frac{d_i}{R}, \tau = \frac{t}{t_{\max}}\right) \tag{3.3}$$

where ξ is the normalised radius in the geometry. It is noticed that Equation (3.3) represents a three-dimensional curve in (T, ξ, τ) space. The temperatures at $t = t_{\max}$ are unknown until the solutions at the last time step have been resolved. Therefore to normalise the temperature solution in both space and time, the solutions in both space and time are first required. This required additional programming effort which would have defeated the very objective of effecting time savings to predict temperatures in a solidifying cast-mould assembly. In the implementation of this equation, it is assumed that the temperature is only a function of ξ at each time step, thus simplifying the implementation scheme. The interpolation method is compromised here due to this assumption and as a result only a sequence of temperature distribution snapshots is obtained rather than the full transient temperature solutions as provided by the FE based techniques.

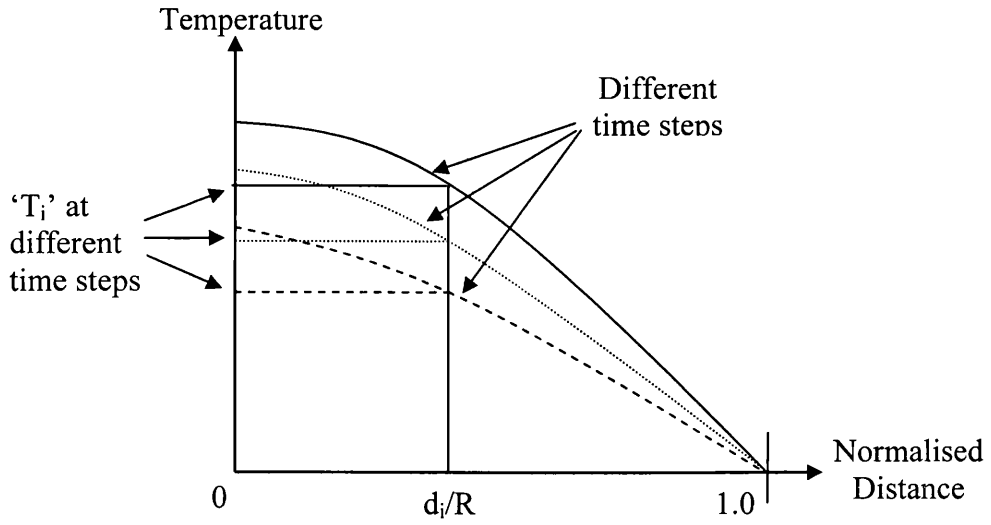

Figure 3.13: A schematic illustration of Single interpolation algorithm for cast at different time steps

Based on and using the concept described above, the interpolation method is then implemented through the following steps.

3.5.3.2 Step 1: Creating date bank from temperature profile of one dimensional bar

A one dimensional bar perpendicular to the medial axis is taken from a casting geometry. The created one dimensional bar is then meshed and solidification simulation is carried out using FE simulation code and temperature profile is obtained prescribing the assumed material properties and boundary condition Figure 3.14(a). This data bank from 1D bar is stored for further use by the interpolation algorithm later.

3.5.3.3 Step 2: Generating MAT and obtaining medial radii

The model of the casting is then created using CADfix and the medial axes and medial-radii of a given casting are obtained using CADfix, as shown in the first illustration in Figure 3.14(b). Assuming now that all the medial axes are available, together with their radius function at the junction points, it is now possible to find the maximum radius, R, in the medial object.

3.5.3.4 *Step 3: Obtaining all coordinate points using mesh*

The whole assembly is now meshed, which provides all the co-ordinate points for the interpolation algorithm, as shown in the second illustration in Figure 3.14(c). In fact, the coordinate points can be generated randomly within the domain but meshing is also conveniently used later for plotting temperature contours and for validating the interpolated solution against a finite-element solution.

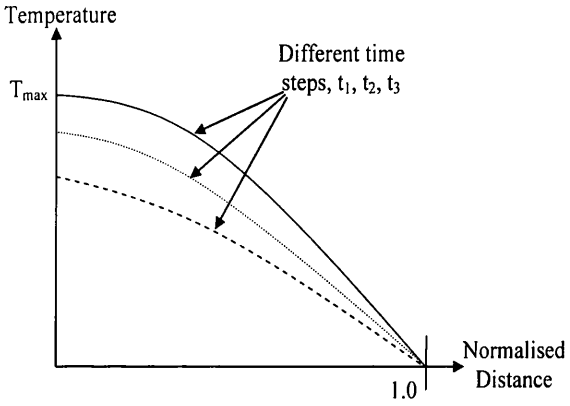

(a) Creation of temperature databank from FE simulation of one-dimensional bar

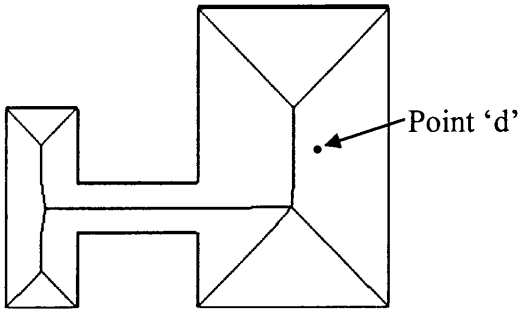

(b) Medial axis transformation of casting geometry

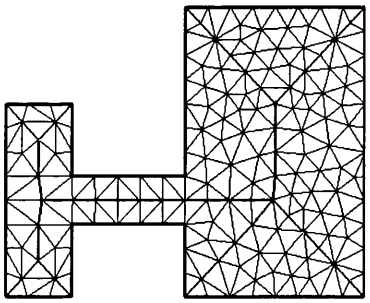

(c) Casting geometry meshed to get all co-ordinate points

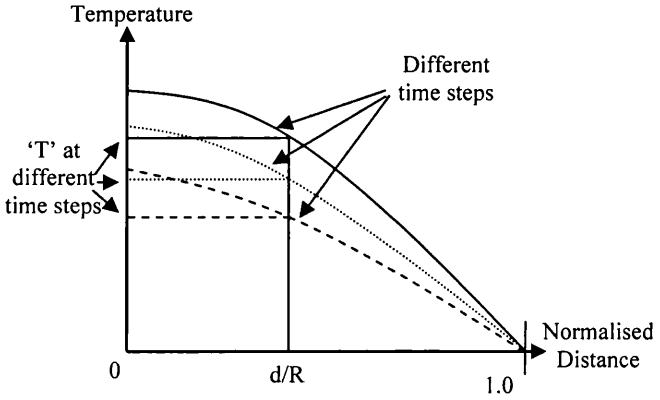

(d) Interpolated temperatures at point 'd' for different time steps

Figure 3.14: Schematic procedure for temperature interpolation

3.5.3.5 Step 4: Applying interpolation algorithm and obtaining temperature profiles

All the coordinate points, *d*, *perpendicular* to the medial axes in the casting can now be normalised with respect to the maximum radius R. Finally, the one-dimensional temperature solution, which is already computed for the domain [0,1] and stored in a databank is retrieved and used as an interpolation temperature database (Figure 3.14(d) to obtain the temperature values at different time steps.

3.6 NUMERICAL EXAMPLES OF COMPARISON OF INTERPOLATION RESULTS WITH FINITE ELEMENT SOLUTION

3.6.1 Example 1

This section investigates the feasibility of the medial axes interpolation method by comparing its solution to a finite element solidification software package. With this in view, an L-shaped casting with varying thickness was selected to test the workability, efficiency and accuracy of the interpolation scheme. The reason for varying the thickness is to ensure that the method is capable of correctly interpolating the temperature profile under generalised geometry conditions. The FE analysis was carried using same boundary conditions and material properties as given in Table 3.1.

The evolving temperature profiles at different stages of solidification were obtained using the medial axes based interpolation method and are compared with the solution obtained from the finite element method and these are shown in Figure 3.15 (a)-(d). It is observed from Figure 3.15 (a & b) and (c & d) that medial axis interpolation method has correctly predicted the location of hotspot. At different stages, the proposed method exhibit an acceptable pattern of temperature distribution in the L-shaped casting section compared to a finite element solution for same casting.

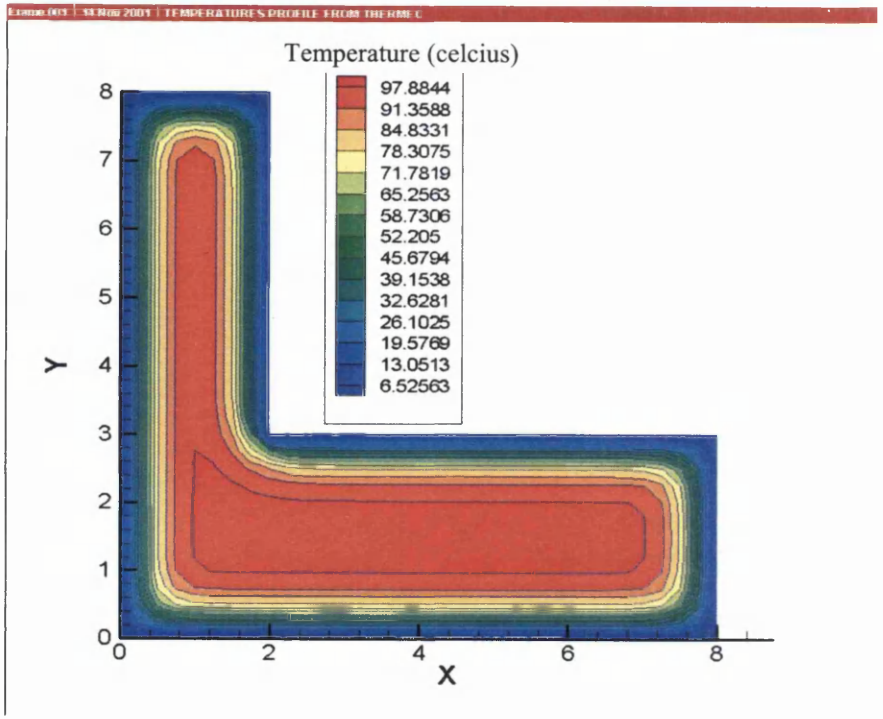

(a) Finite Element Simulation

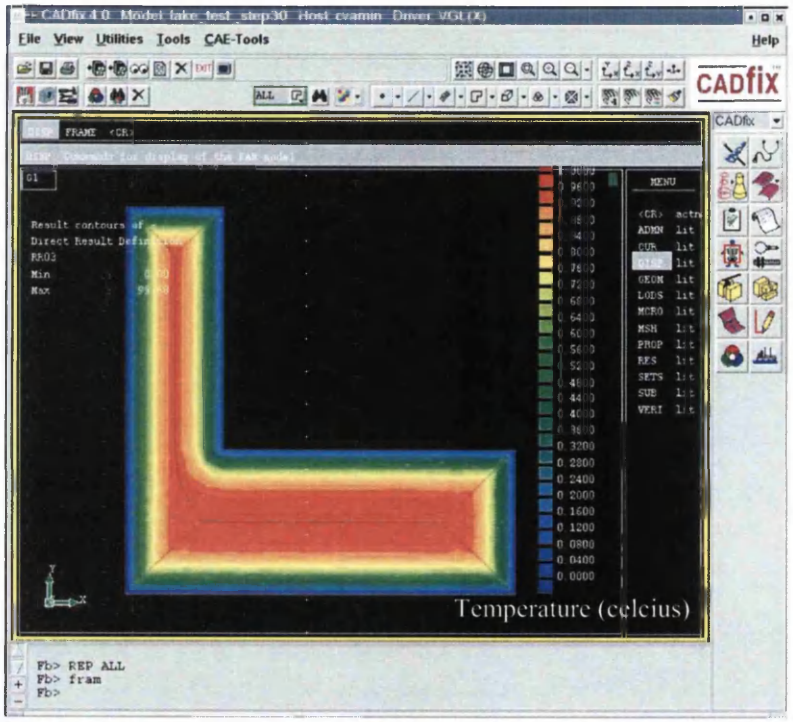

(b) Medial Axis based interpolation solution

Figure 3.15: Example 1 - Comparison of Finite Element with the evolving interpolated solution

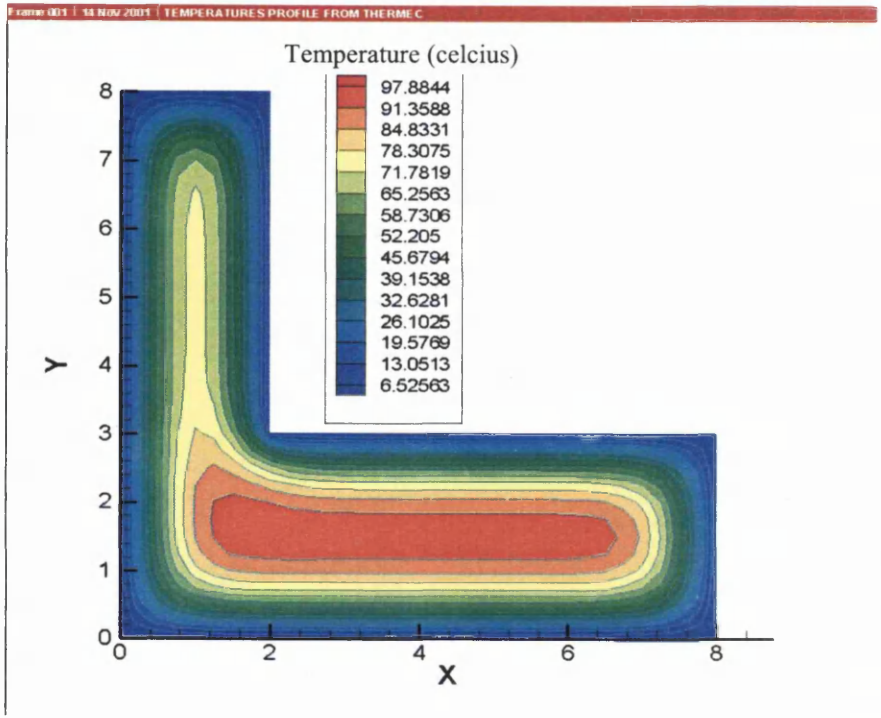

(c) Finite Element Simulation

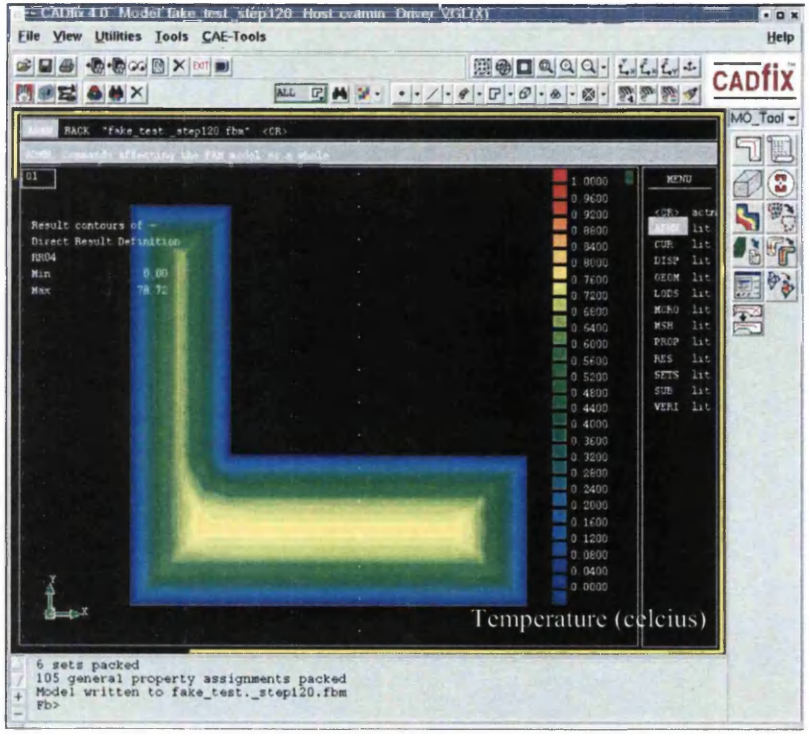

(d) Medial Axis based interpolation solution

Figure 3.15: Example 1 - Comparison of Finite Element with the evolving interpolated solution

3.6.2 Example 2, 3 and 4

With an aim to check the applicability of this method on more generalised geometry shapes, the method was further tested on two more arbitrary casting geometries. Following the same procedure as outlined earlier and with same material properties and boundary conditions as in L-shaped example, the results were obtained. Figure 3.16 and Figure 3.17 show the temperature distribution in these different casting sections at different time levels while Figure 3.18 shows the location of hotspot in a more general casting section predicted using the medial axes interpolation method.

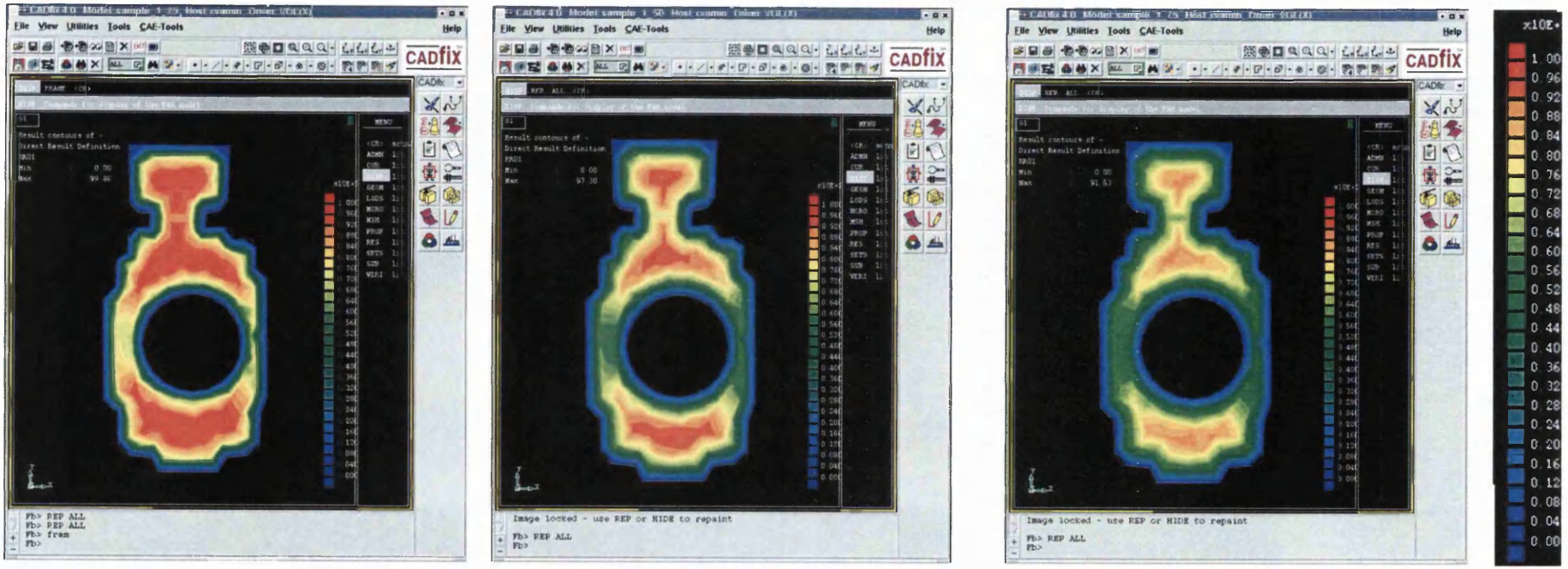

Figure 3.16: Example 2 - Solidifying temperature profile in an arbitrary section at different stages of solidification using the interpolation scheme. The scale for temperature in Celcius is given on the right.

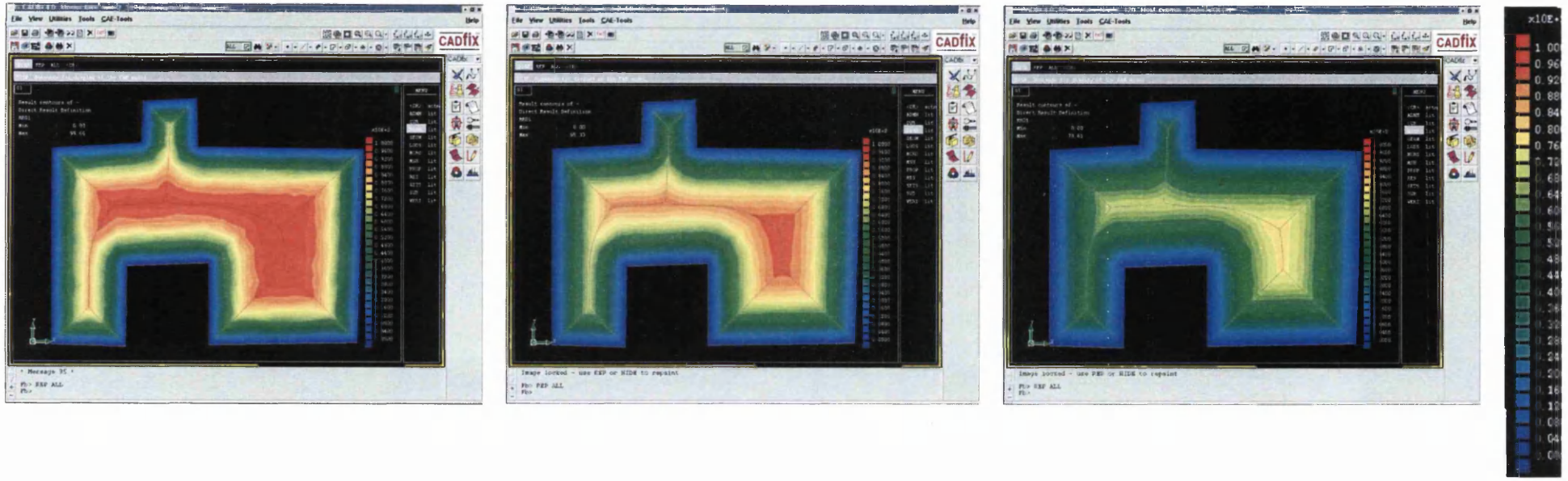

Figure 3.17: Example 3 - Solidifying temperature profile in an arbitrary section at different stages of solidification using the interpolation scheme. The scale for temperature in Celcius is given on the right.

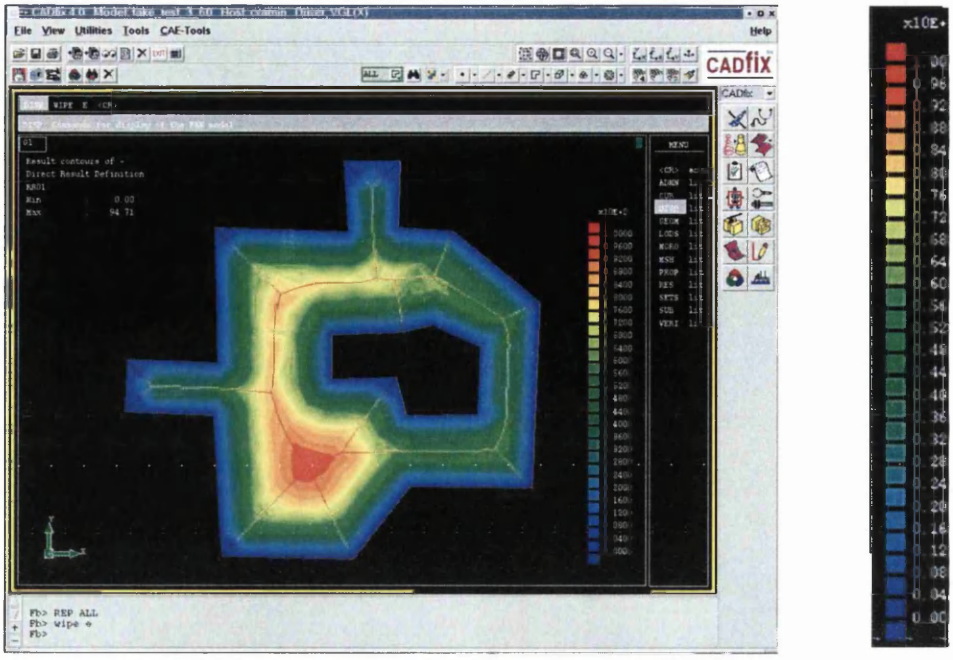

Figure 3.18: Example 4 - Predicting hotspot location in another general geometry. The scale for temperature in Celcius is given on the right.

3.6.3 Example 5 – U-shaped casting

A U-shape casting, as shown in Figure 3.19, with varying thickness was analysed as a test case [30]. The same finite element mesh was used for the continuum simulation and the interpolation method. As described earlier in Section 3.5.3.1, for the sake of simplicity and for comparison purposes, the initial temperature in the domain were chosen as 100°C, the ambient temperature was assumed to be 25°C, k=0.01 W/mK, $\rho c = 100$ J/m^{3}K, and $h_{inf} = 1$ W/m^{2}K [30]. As shown in Figure 3.19, two reference points A and B were chosen within the U-shaped casting. The simulation was performed for a time span of 1.5 seconds, with a time step size of 0.01 seconds. These values were applied by the authors to simplify the interpolation procedure for obtaining normalised solution in space and time. The normalised temperature at different time levels, obtained using the proposed method, was compared with the solution obtained by the finite element method. It is evident from Figure 3.20 that the temperature interpolated at reference point A matches almost exactly to that of the continuum solution. This result is expected since the point A is located within the region where the maximum

medial radius is found. As one departs further away from the location of the maximum medial radius, the accuracy of the interpolated temperature degenerates and the error accumulates as time increases. This is shown by comparing the temperature values at the reference point B.

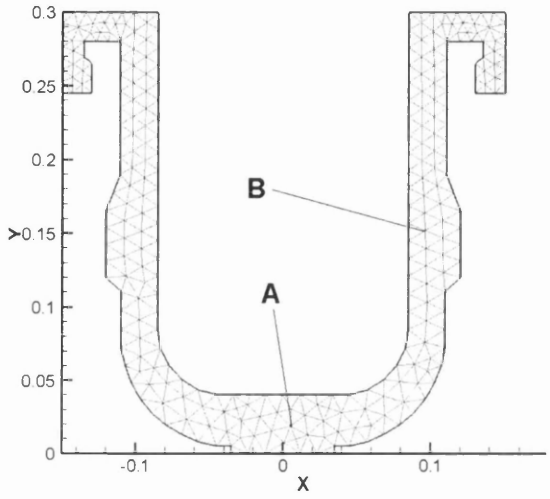

Figure 3.19: U-shaped geometry used for validation test

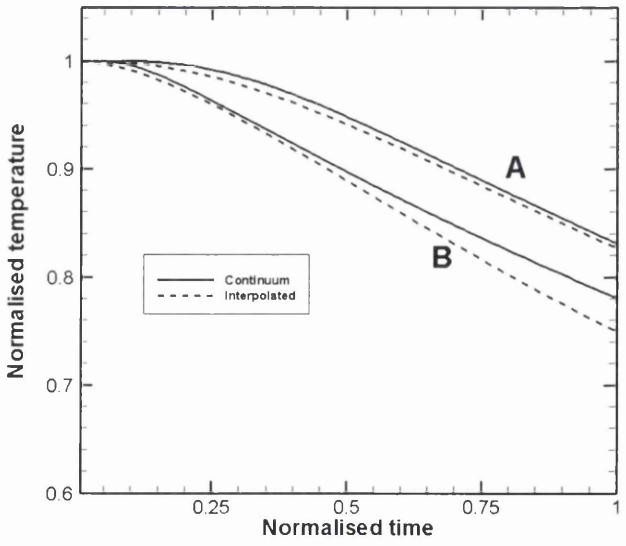

Figure 3.20: Comparison between FE (solid line) and interpolation (dashed line) results [30]

3.7 ADVANTAGES AND LIMITATIONS OF INTERPOLATION METHOD

The method is quick and suitable for rapid evaluation of the temperature profiles and hot spot prediction. However, normalization of spatial solution only provides evolution of temperature profiles in time unlike the FE solution which provides more accurate temperature profiles at each time step. Therefore, it is observed that the interpolation method provides a sequence of temperature snapshots in time during the solidification rather transient temperature solutions given by FE simulations. The interpolated solutions also over predict the size of the hot spot. The method is also limited as only one type of boundary conditions can be specified e.g. convective heat flow or prescribed temperature at cast boundary.

The major advantages of this method are that it is fast and comprehensive compared to conventional numerical simulations since the number of performed computer operations is linearly proportional to the number of mesh points in the casting. The method gives a rapid "feel" of the design which is an important step during the interrogation stage. The purpose of this method is to aid the technicians/draftsmen to make changes in the components, and is not intended to replace the conventional numerical software.

3.8 CLOSURE

This chapter set an aim to utilise medial axis transformation technique for solidification simulation using an interpolation scheme. The MAT generated using CADfix was investigated here and based on the radius information provided by the MAT; a one-dimensional interpolation scheme was implemented. It is clear from the case study that the method provided an acceptable pattern of temperature distribution in casting sections compared to a finite element solution for same casting. The method also always predicted correct location of the hotspots. However, the interpolation method was implemented for only cast in this case study and subsequent examples.

There was thus need to apply the same interpolation technique to a cast-mould assembly to further validate the usefulness of the method. The method also needs to be tested using realistic material properties and boundary conditions.

In this chapter, it was discovered that a realistic sequence of temperature snapshots can be created using interpolation method. The next chapter will take this research forward and discuss methodology and the improvements that are brought about in its implementation to obtain solutions for cast-mould assembly using realistic material properties and boundary conditions and improving the accuracy of each temperature snapshot. This is illustrated through more case studies in Chapter 4.

REFERENCES

[1] G. Evans, A. Middleditch and N. Miles, "Stable computation of the 2D medial axis transform", *International Journal Comp. Geom. and Application*, 1998, **8** (5), 577-598.

[2] http://www.fegs.co.uk/CAE.html, accessed on 16th Jan. 2006 and http://www.fegs.co.uk/medial.html, last accessed on 16th Jan. 2006.

[3] N. Miles, G. Evan, and A. Middleditch, "*Proc. of the 6th International Aluminum Extrusion Technology Seminar*", Chicago, Illinois, May 1996.

[4] S. Fortune, "A sweepline algorithm for Voronoi diagrams", *Algorithmica*, 1987, **2**, 133-174.

[5] H. N. Gursoy, and N. M. Patrikalakis, "Automated interrogation and adaptive subdivision of shape using the medial axis transform", *Adv. Eng. Soft*, 1991, **13**, 287-302.

[6] D. J. Sheehy C. G. Armstrong and D. J. Robinson, "Shape description by medial surface construction", *IEEE Transaction on Visualization and Computer Graphics,* 1996, **2**(1), 62-72.

[7] K. W. Shim, D. J. Monaghan and C. G. Armstrong, "Mixed dimensional coupling in finite element stress analysis", *10th Int. Meshing Roundtable,* 2001, Sandia National Laboratories, Newport Beach, California, 269-277.

[8] C. G. Armstrong, D. J. Robinson, R. M. Mckeag, T. S. Li, S. J. Bridgett and R. J. Donaghy, "Application of the medial axis transform in analysis modeling", *Proceedings of 5th International Conference on Reliability of FE Methods for Engineering Applications*, NAFEMS, May 1995, 514-426,

[9] T. Tam and C. G. Armstrong, "2D finite element mesh generation by medial axis subdivision", *Adv Eng. Software,* 1991, **13**, 312-324.

[10] http://sog1.me.qub.ac.uk

[11] W. R. Quadros, B. Gurumoorthy, K. W. Ramaswami and F. B. Prinz, "Skeleton representation and reasoning in engineering application" *Engineering with Computers,* 2001, **17**(2), 186.

[12] J. M. Reddy and G. M. Turkiyyan, "Computation of 3D skeletons using a generalized Delaunay triangulation technique", *Computer-Aided Design*, 1995, **27**(9), 677-694.

[13] R. Ramamurthy and R. T. Farouki, "Voronoi diagram and medial axis algorithm for planar domains with curved boundaries I. Theoretical foundations" *Journal of Computational and Applied Mathematics*, 1999, 102, 119-141.

[14] R. Wlodawer, "*Directional Solidification of Steel Castings*", Pergamon Press, Oxford, 1966.

[15] R. W. Heine and J. J. Uicker, "Risering by Computer assisted Geometric Modeling", *AFS Transactions*, 1983, **91**, 127-136.

[16] Casting: Metals Handbook Vol. 15, 9th edition, ASM International, Metals Parks, Ohio, USA. 1988.

[17] H.D. Brody and D. Apelian (Eds.), *Modeling of Casting and Welding Processes.* The Metallurgical Society of AIME, PA, USA. 1981.

[18] J.A. Dantzig and J.T. Berry JT (Eds.), *Modeling of Casting and Welding Processes II.* The Metallurgical Society of AIME, PA, USA. 1984.

[19] S. Kou and Mehrabian (Eds.), *Modeling of Casting and Welding Processes II.* The Metallurgical Society of AIME, PA, USA. 1986.

[20] A.F. Giamei and G.J. Abbaschian (Eds.), *Modeling of Casting and Welding Processes IV.* The Metallurgical Society of AIME, PA, USA. 1988

[21] T.E. Morthland, P.E. Byrne, D.A. Tortorelli and J.A. Dantzig, "Optimal Riser Design for Metal Castings", *Metallurgical and Materials Transactions*, 1995, 26**B**, 871-885.

[22] T.S. Piwonka, V.R. Voller and L. Katgerman, *Modelling of Casting, Welding and Advanced Solidification Processes VI.* T.S. Piwonka *et al.* (Eds.), TMS-AIME, Warrendale, PA, USA, 1993.

[23] A.B. Shapiro, "*Topaz-a finite element heat conduction code for analyzing 2D solids*", Lawrence Livermore Laboratory, California, 1984.

[24] ANSYS - *Engineering Analysis System*, Version 4.3, Swanson Analysis Systems, Inc., PA, 1987.

[25] ABAQUS, Hibbitt, Karlsson and Sorenson, Inc., Rhode Island, 1985.

[26] ProCAST - *The Professional Casting Simulation System User Manual*, Universal Energy Systems Inc., Ohio, 1988.

[27] M. Jolly, "Casting Simulation: How well do reality and virtual casting match? State of the art review", *International Journal of Cast Metals Research*, 2002, **14**, 303-313.

[28] J. P. Holman, "*Heat Transfer*", 7th Edition, McGraw-Hill Book Company, London, UK, 1992, pp 2-3.

[29] H. S. Carslaw and J. C. Jaeger, "*Conduction of Heat in Solids*", 2nd Ed., reprinted series, Oxford Sc. Pub., Oxford, UK, 2000.

[30] R. S. Ransing, W. K. S. Pao, C. Lin, M. P. Sood and R. W. Lewis, "An Enhanced Interpolation Algorithm using Medial Axis and its Application to Hotspot Prediction in a Mould-Casting Assembly", *International Journal of Cast Metals Research*, February 2005, Vol. 18, No. 1, pp. 1-12.

Chapter 4

AN ENHANCED INTERPOLATION SCHEME FOR PREDICTING CASTING HOTSPOTS

CHAPTER LAYOUT

This chapter is a rational attempt to carry forward the research tasks outlined in the concluding observations of Chapter 3. In this chapter, the MAT based interpolation scheme will be tested on a cast-mould assembly. The second section of this chapter therefore, first highlights the limitations of using MAT based one-dimensional interpolation schemes and stresses on the need to bring about improvements in its implementation. Next two sections then describe the scheme that incorporates mould effects and discusses the improvements effected on the previous version of interpolation technique. Section five then describes the enhancements made and the implementation of two-stage double linear interpolation scheme that introduces a concept of radius ratio and also takes into account the effect of mould to predict casting temperatures and hotspots. Section six provides results from case studies on geometries of different shapes and thicknesses and compares their results with the numerical solutions for same castings. Section seven discusses the results from these case studies and compares results with solutions obtained using numerical and geometric techniques. Section eight describes the point (mesh) density study and undertakes a discussion on the estimation of error in the solution provided by the double interpolation scheme. The Interpolation results are then compared with numerical solutions for accuracy, run time and requirements for human intervention. The next two sections then highlight the advantages and limitations of the interpolation scheme with regard to their applicability in a foundry scenario. The conclusions are then drawn in the last section to guide further research using geometry based techniques for studying and analysing the behaviour of solidifying castings.

4.1 INTRODUCTION

This chapter essentially builds on the work discussed in Chapter 3 and is an extension of previous work, which was only valid for a casting geometry without mould. Therefore, an enhancement and modification to the previous work is described to take into account the effect of mould and to consider the interaction of the whole mould-casting assembly. The feasibility of the proposed temperature interpolation technique is further illustrated by comparing its solutions with a geometric reasoning technique and the finite element method. The results are then further validated using real-life casting geometries with realistic material properties and boundary conditions. It will be demonstrated in this chapter that once a data bank comprising temperature solutions from one dimensional bars for a set of boundary conditions and particular material properties is created, the proposed interpolation scheme can provide instant solutions for casting geometries of any shape and size.

4.2 LIMITATIONS IN USE OF MAT BASED ONE DIMENSIONAL INTERPOLATION SCHEME AND NEED FOR IMPROVEMENT

4.2.1 Limitations

The interpolation scheme described in the previous chapter was initially devised to compute only casting temperature. This single interpolation scheme only took distance ratio into account and thus could not link with the actual size of casting models. It was also discovered that the single interpolation scheme was particularly less accurate for casting models with varying thicknesses. There was also a need to consider and incorporate further information for predicting hotspots in the castings *e.g.* different material properties or different initial temperature values.

4.2.2 Need For Improvement of Interpolation Scheme

As stated above, there was thus a need to develop and improve upon the interpolation scheme that not only predicts the casting temperature and hot spots in solidifying castings but also has following improvements.

- The scheme provides temporal variations of temperature in a cast-mould assembly
- The improved scheme is sensitive to material properties
- The scheme is able to work when realistic boundary conditions are applied
- The scheme accurately models the variation in casting thickness.

4.3 IMPROVED TWO-STAGE HOTSPOT PREDICTION BASED ON THE DOUBLE LINEAR INTERPOLATION SCHEME FOR 2D CAST-MOULD ASSEMBLY

As the name suggests, this method involves a two-stage interpolation procedure. The *two*-stage here refers to the casting domain interpolation and the mould domain interpolation. The interpolation technique used in these two domains is the same but it becomes necessary to identify whether the current interpolating point belongs to casting or mould and associate this point correctly in a one-dimensional domain [0,1]. By double linear interpolation scheme, it is meant that two linear interpolations are undertaken based on radius and distance ratio respectively.

4.3.1 The Approach

- In an effort to overcome the limitations discussed in Section 4.2.1 and take into account the actual casting size, another set of geometric information was used. The radii of the included circles or spheres within the casting section are introduced as a measure of casting thickness so that the actual size and the relative thickness of each part of the casting model can be taken into account and incorporated into the interpolation scheme.

- Also, the finite element simulation was undertaken for a series of one-dimensional bars and temperature databases were created for different sets of material properties and boundary conditions in order to demonstrate the applicability of the proposed technique.

The double interpolation method proposed in this chapter to calculate temperature profiles is briefly described below.

1. The casting model is partitioned based on section thicknesses and radius information is obtained using the MAT function of the CADfix software to calculate radius ratios.

2. Using the first linear interpolation, a new temperature profile is estimated based on these radius ratios and pre-calculated FE simulation results stored in the database.

3. A mesh is created for the casting model. The use of this mesh is to obtain a distribution of points in the casting and mould that are required to calculate the distance ratios used by the interpolation scheme.

4. Finally using second linear interpolation, the new temperature profiles are obtained based on distance ratios and the interpolated temperatures estimated from first linear interpolation.

4.3.2 One-dimensional heat conduction with the mould

In addition to the two assumptions made earlier in Section 3.5.2 in Chapter 3, it is also assumed that the mould is relatively thin compared to the casting, *e.g.*, as found in the investment casting process. An illustration shown in Figure 4.1 further clarifies the necessity for this assumption. Figure 4.1 shows a casting-mould assembly along with the corresponding medial-axis for the casting. A line drawn perpendicular to the medial axes of the casting will extend directly from the medial-axis and into the mould. In this particular case, the outer boundary condition for the resulting one-dimensional model is simply the convective heat flow condition and because of second assumption that heat flux emanates normally from the medial axis of the casting, the medial axis is an insulated boundary.

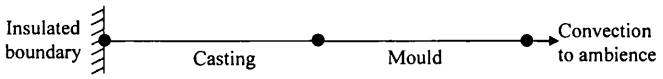

(b) One-dimensional heat conduction

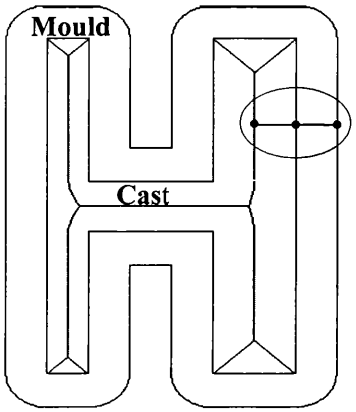

(a) Casting model with mould and medial axis

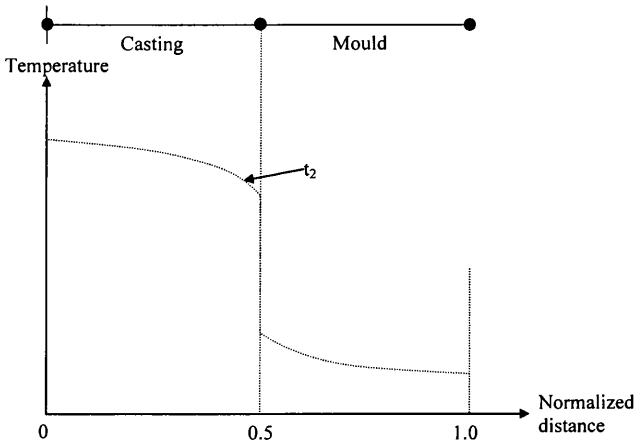

(b) A schematic of a temperature profile of a 1D Bar from a cast-mould assembly

Figure 4.1: An example of cast-mould geometry to illustrate assumptions made in Section 3.5.2 in Chapter 3

A two-dimensional FE solver was used to obtain the 1D temperature solution by applying boundary conditions as shown in Figure 4.2.

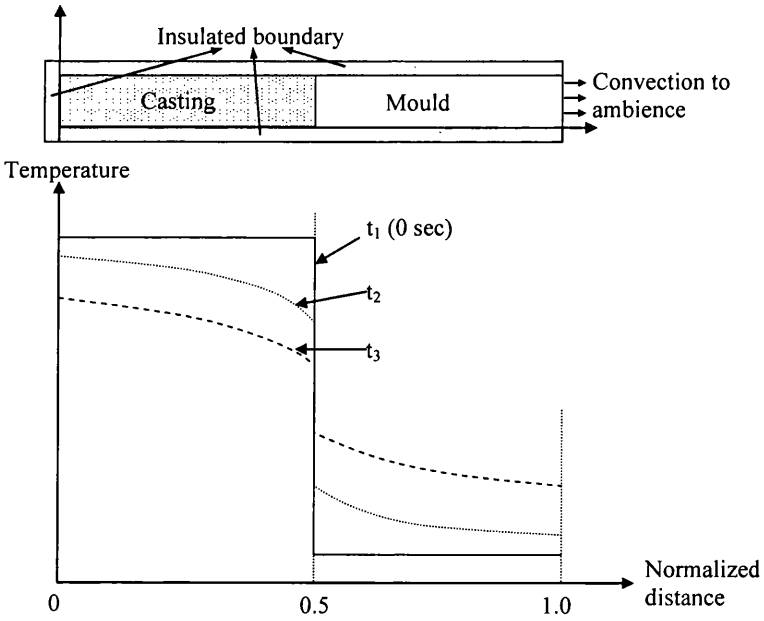

Figure 4.2: A schematic of a temperature profile of a 1D Bar from a cast-mould assembly at different time steps

By observing that the transient temperature solutions are similar for a particular case of boundary condition (See Figure 3.12 on page 66), one can again express the temperature as a function of normalised space x, and time t, such that

$$T = T\left(\frac{x}{L}, \frac{t}{t_{max}}\right) \tag{4.1}$$

where L and t_{max} are the maximum medial-radius in the mould-cast domain and total time of simulation, respectively (See Equation 3.2 on page 66). Figure 4.2 represents the temperature profile in normalised space (0,1) for a one dimensional bar at different time steps in case of casting with mould. Therefore, the temperature, T, at any point within the cast-mould domain at a given time step is a function of normalised space (Figure 4.3).

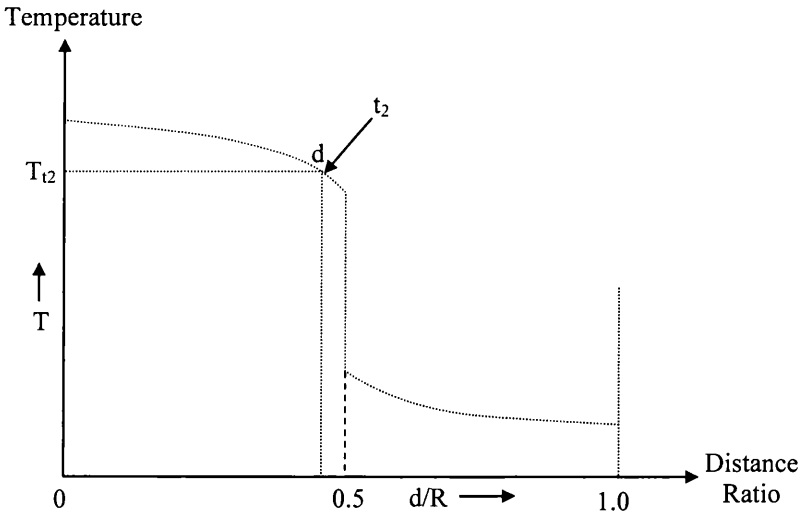

Figure 4.3: A schematic showing interpolation algorithm for cast-mould assembly

Similarly, the temperature values (T_{t1}, T_{t2}, T_{t3}) at same point, d at different time steps (t_1, t_2, t_3) can be found out by using the same expression (4.1) and as illustrated in Figure 4.4.

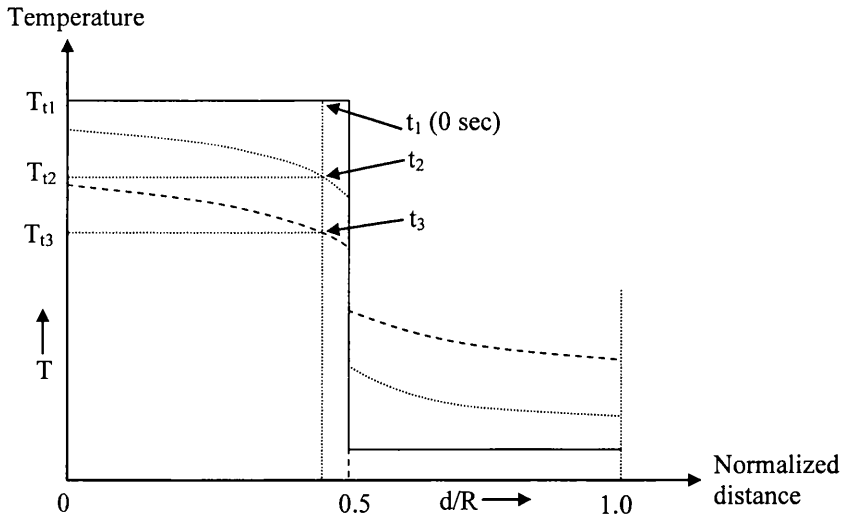

Figure 4.4: Using interpolation algorithm for different time steps

4.3.3 Creating a databank of temperature solutions from one-dimensional bars using FE simulation

As discussed earlier, in the interpolation scheme described in Chapter 3 earlier, only one 1D bar was used to create the temperature data bank for applying interpolation algorithm to the casting simulation. Therefore, in an effort to increase the accuracy of temperature predictions through the interpolation scheme, instead of generating a data bank based on FE simulation of only one 1D bar, 15 such one-dimensional bars were simulated (ranging from 1cm to 110 cm long with interface at the centre). The temperature data generated from 1D FE based temperature solutions for 15 bars now constitute the data bank that is utilised by the interpolation algorithm for temperature prediction. The rationale behind bringing about this improvement was the fact that different castings have different shapes (varying thicknesses at different sections) and thus a degree of variation in their medial radii. Creating a data bank based on fifteen one-dimensional bars takes into account this variation and enriches the data bank to provide more accurate temperature prediction. This number however, can vary depending on section thicknesses of the casting models. Similar to Figure 4.2, the temperature profiles for bars of varying lengths (e.g. d_1 and d_2) at time step, t_2, is shown in Figure 4.5.

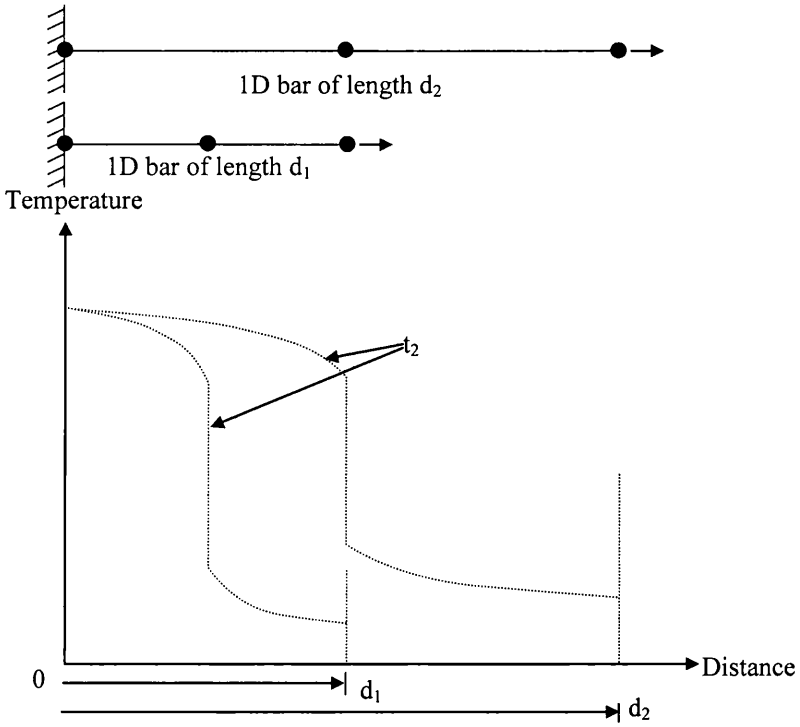

Figure 4.5: A schematic of temperature profiles for 1D bars of varying lengths at same time step

It was shown earlier that the transient temperature solutions are similar for a particular case of boundary conditions and this similarity is illustrated schematically in Figure 4.6 for the temperature profiles of 1-D bars of two lengths at different time steps for cast-mould assembly.

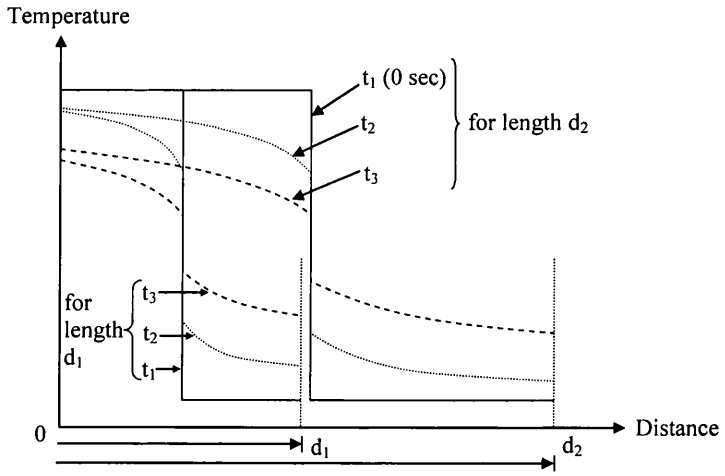

Figure 4.6: A schematic of temperature profiles for 1D bars of varying lengths at different time step

The temperature solutions for various lengths of one dimensional bars for cast-mould assembly at various time steps in normalised space (0,1) are illustrated schematically in Figure 4.7.

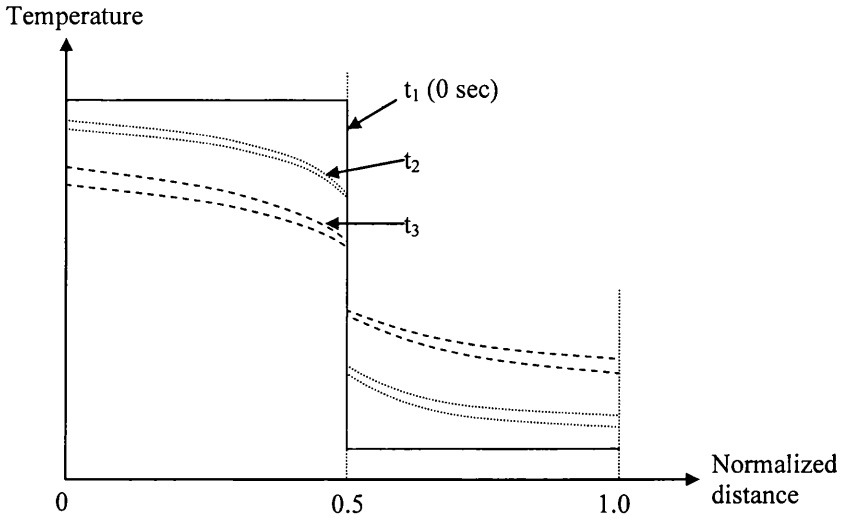

Figure 4.7: A schematic of temperature profiles for different bars in the normalised space (0,1)

Building on the understanding of temperature profiles exhibited in Figure 4.6, the interpolation scheme and algorithm is further elaborated by an illustration shown in Figure 4.8. The shaded area represents a surface generated from the temperature solutions of two one dimensional bars (cast thickness R_1 and R_2) at time step, t=n. This solution is used by the interpolation algorithm for seeking temperature for any points lying between these two thicknesses. The number of such one-dimensional bars will depend on the variation in the thickness of the casting at different sections.

Figure 4.9 takes the implementation procedure illustrated through Figure 4.7 forward into the next step and schematically represents the surface generated by temperature solutions obtained for different cast thicknesses (1D bars) in normalised space (0,1). Now we have a data bank comprising temperature solutions obtained from fifteen one-dimensional bars for all time steps.

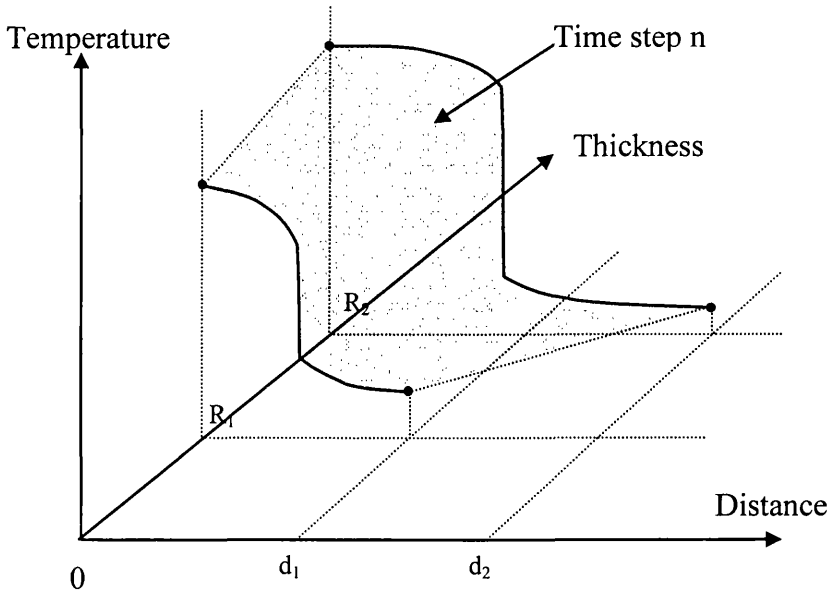

Figure 4.8: A schematic of temperature solution of single casting at different thicknesses at same time step

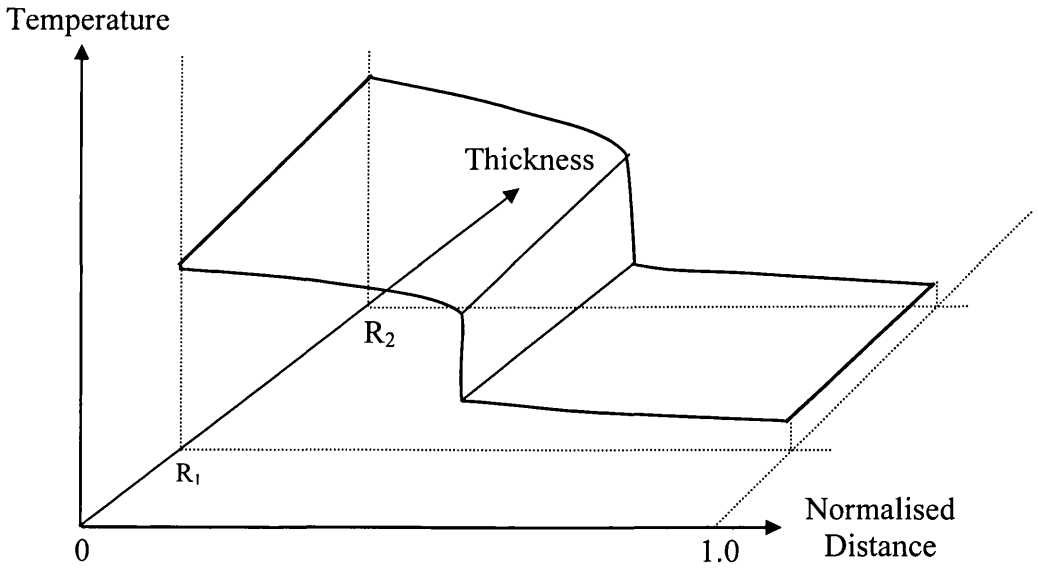

Figure 4.9: A schematic of temperature solution of single casting at different thicknesses in the normalised space for n^{th} time step

4.3.4 One-dimensional bar and FE based temperature solution

This sub-section takes the discussion forward and provides an example of one of the fifteen 1D bars that are simulated using a FE solver to create the

database of temperature profiles. This profile is used by the interpolation scheme using geometric information to predict the interpolated temperature profiles. This 1D bar is 10 cm long and 5 mm thick with an interface at the centre. The bar was meshed and it had 40 nodes and 36 elements including an interface element (Figure 4.10). It should be noted that although the bar has finite thickness, it still approximates to 1D solution as adiabatic conditions apply on both sides of the thickness. Typical properties for the aluminium casting alloy (LM25) and sand casting process were used. The properties for aluminium cast were: solid density, $\rho_c = 2680$ kg/m^3, thermal conductivity, $k_c = 186.3$ W/mK and specific heat, $C_p = 1093$ J/kgK and for the sand mould were: $\rho_m = 1000$ kg/m^3, $k_m = 0.8$ W/mK and $C_{pm} = 709$ J/kgK [5]. The imposed boundary condition to the exterior of the mould is convection ($h_\infty = 200$ W/m^2K) to air at $T_\infty = 30^oC$. The sand was initially at 30^oC while the initial temperature of the molten aluminium (LM25) was at 650^oC. The simulation was run for 5000 seconds and the two-dimensional temperature profile obtained from FE simulation at three different time steps is shown in Figure 4.11. The three-dimensional profile is also presented in Figure 4.12. It is observed that the temperature profiles exhibit similarity with the schematic profiles shown earlier in Figure 4.7. This temperature database is then further expanded with similar temperature profiles created from 1D bars of varying thicknesses using FE simulations.

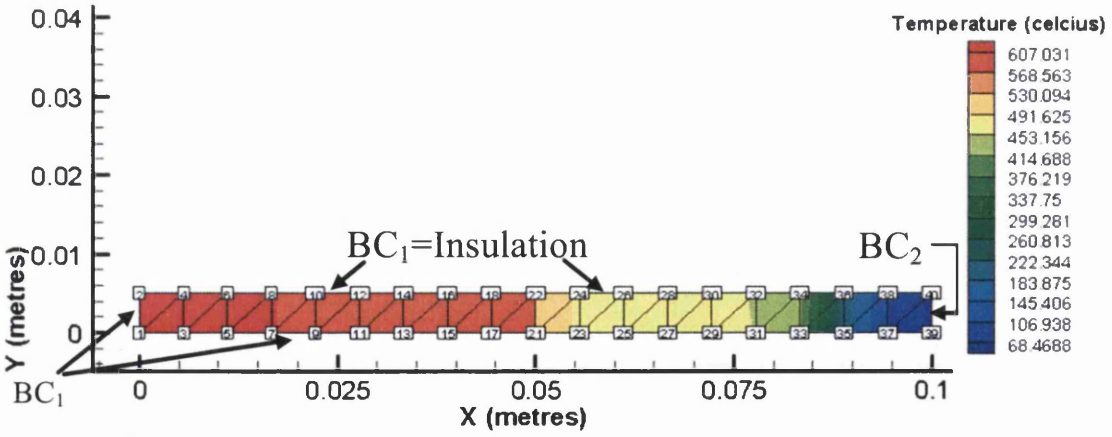

Figure 4.10: One dimensional bar used for FE simulation for creating temperature database (10 cm long). BC_1 = Insulation boundary conditions and BC_2 = Convection to ambience

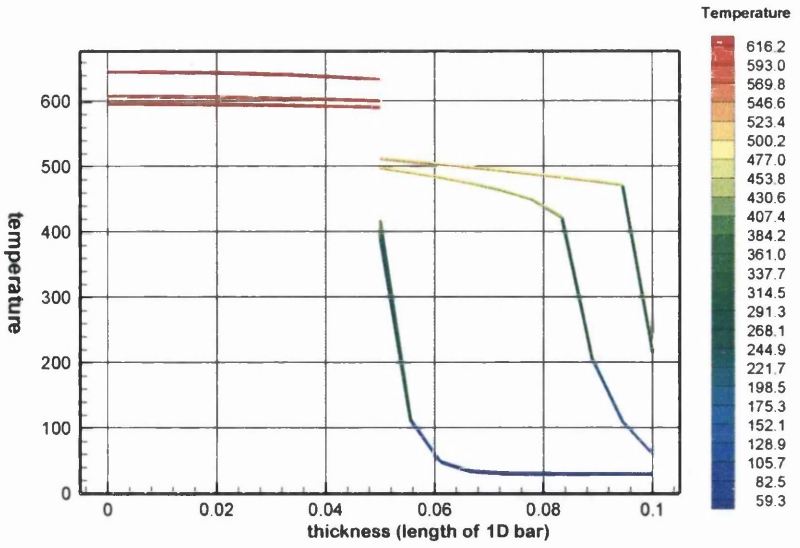

Figure 4.11: 2D Temperature profiles of a one-dimensional bar using FE solver at time step 1, 20 and 40

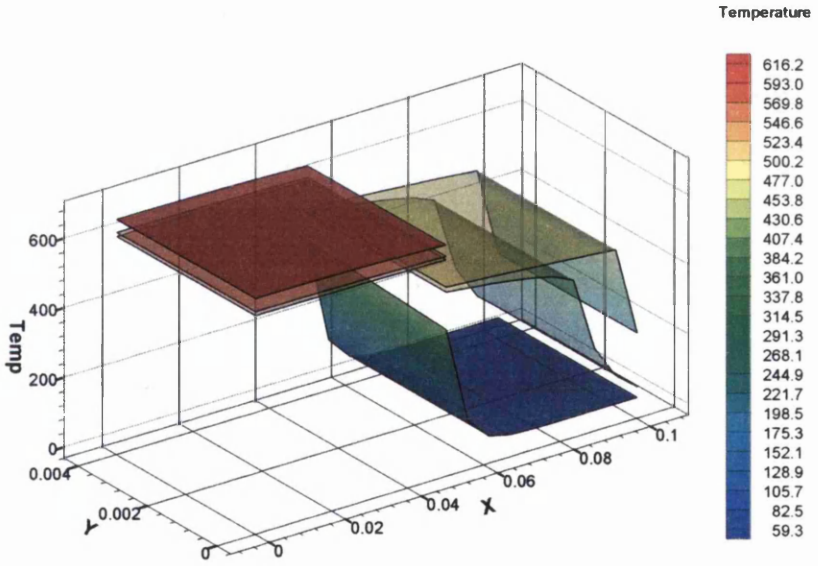

Figure 4.12: Three-dimensional temperature profile of a one-dimensional bar using FE solver at time step 1, 20 and 40

Another bar of 20 cm length and 5 mm thickness with an interface at the centre was created. FE simulation was carried out with the same material properties and boundary conditions that were used for the first 1D bar. The temperature profiles for cast-mould assembly for these two 1-D bars (10 cm and 20 cm long) at time steps 1, 10 and 20 are shown in Figure 4.13. This

FE solution with realistic material properties and boundary conditions supports the schematic illustration shown in Figure 4.6 in Section 4.3.3 and it is observed that transient temperature solutions are similar for these two bars of varying lengths. This similarity achieved after applying realistic material properties and boundary conditions lends support to argument presented in Section 3.5.3.1 and Figure 3.12 in Chapter 3. The solutions presented in Figure 3.12 were obtained assuming unit values of material properties for the sake of simplicity for implementing single interpolation scheme in its early development.

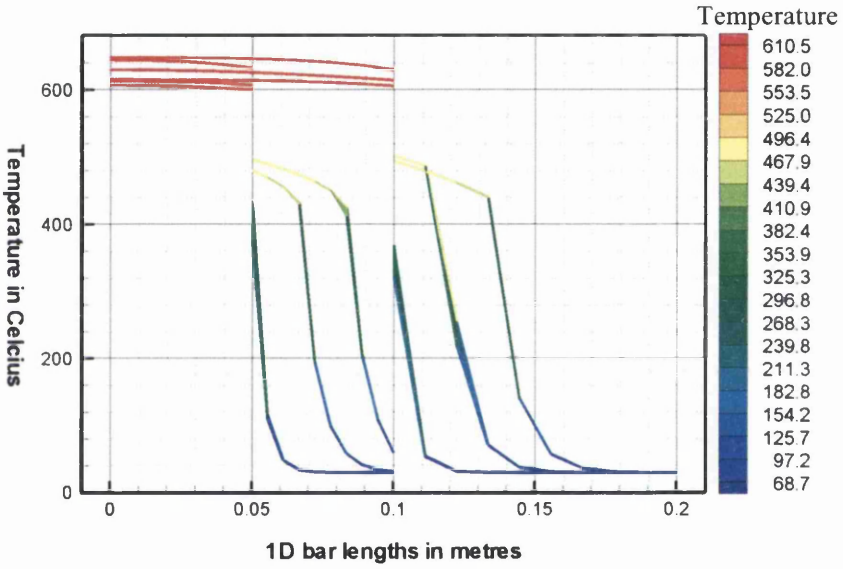

Figure 4.13: 2D temperature profiles of two 1D bars (10 cm and 20 cm long) using FE solver at time step 1, 10 and 20

4.3.5 Implementation of two-stage double linear interpolation scheme

From here onwards, a similar procedure is followed as was earlier described in Section 3.5.3 and Figure 3.14 in Chapter 3. All the models and their medial axes are generated using CADfix ([3],[4]). The radius information is obtained from the medial axis transformation. The whole cast mould assembly is then meshed and an array of arbitrary points 'n' with distance d_i normal to the medial axis are generated.

The transient temperature at any arbitrary point in the casting can now be found by interpolation (see Figure 4.14) using Equation (4.1) as

$$T_i = T\left(\xi = \frac{d_i}{R_{\max}}, \tau = \frac{t}{t_{\max}}\right) \tag{4.2}$$

where ξ is the normalised radius in the geometry (See Equation 3.3 on page 66). It is noticed that Equation (4.2) represents a three-dimensional curve in (T, ξ, τ) space. The implementation of Equation (4.2) required additional programming to normalise temperature solution in both space and time. Therefore, as described in Chapter 3, with an aim to achieve a *qualitative* comparison of the temperature solutions, Eq. (4.2) is simplified as

$$T_i = T(\xi, t) \tag{4.3}$$

Now therefore, for a particular time step, the temperature, T, at any point normal to medial axis is only a function of the normalised space coordinate between 0 and 1.

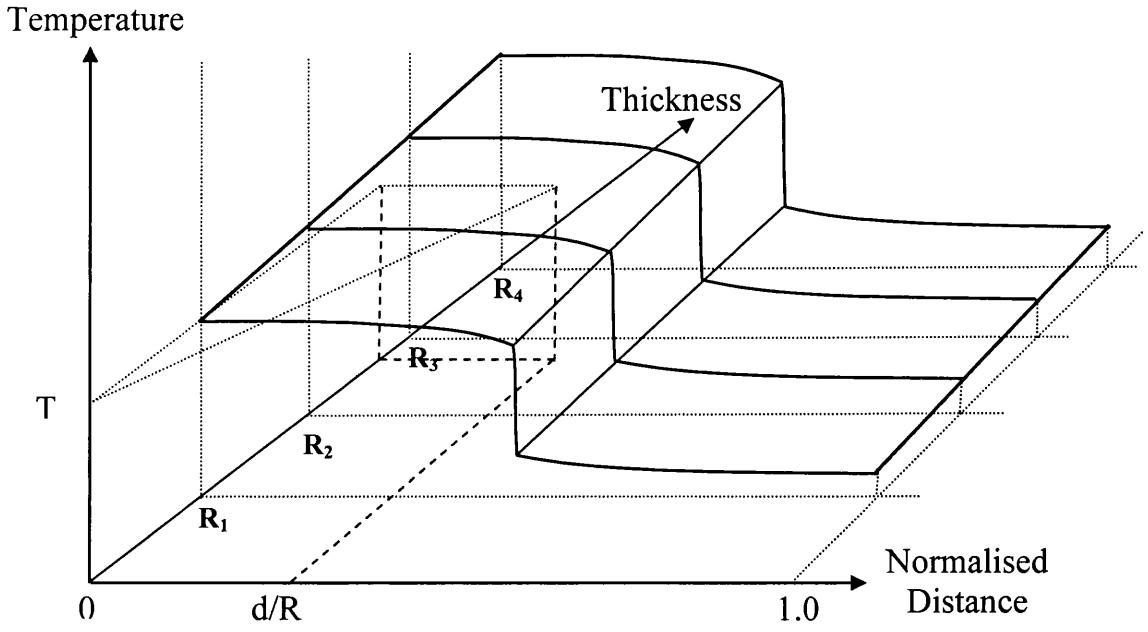

Figure 4.14: A Schematic procedure for temperature prediction using interpolation scheme for cast-mould assembly

Now to initiate the interpolation algorithm, the temperature databank is first prepared by solving *two* one-dimensional heat conduction equations for time $n\Delta t$ where 'n' is a positive integer and Δt is the time step size. These two one-dimensional problems consist of the domain (i) $R_{max} + L^m_{max}$ and (ii) $R_{min} + L^m_{min}$ as shown in Figure 4.18. The temperature solutions for various cast thicknesses (1D bars) are stored in data bank and are recalled by the interpolation algorithm for providing temperatures at various points in the casting and mould at different time steps. These temperature solutions are illustrated schematically as 3D surfaces in Figure 4.15.

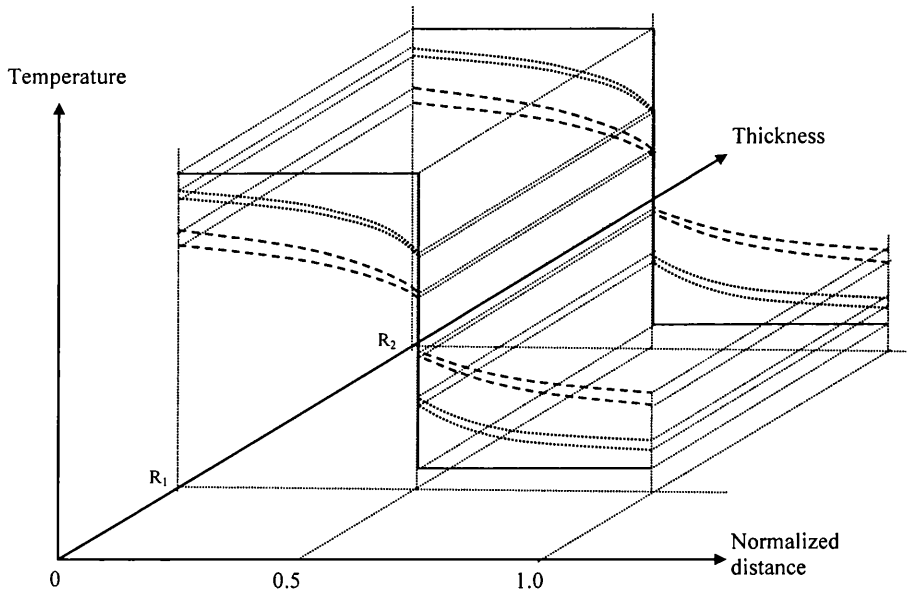

Figure 4.15: Three-dimensional schematic representation of a temperature solution at different time steps in the normalised space (0,1)

In addition to the distance ratio earlier taken into consideration for the single interpolation technique, a radius ratio is also taken into account. The radius of a point on the medial axis, in fact, is its distance from the nearest domain boundary. After medial axes are generated in a casting model, the radii at different points on medial axis are known. The mesh result provides the distance information associated with each node of the casting model.

It is noted here that in the first stage of interpolation, the mesh is only used for determining co-ordinates of points in the casting-mould assembly for calculating geometric information associated with these points. In the second stage, after the interpolation scheme has generated the temperature profiles based on this geometric information and FE based temperature databank, the mesh is again conveniently used to plot temperature contours.

The approach outlined in Section 4.3.1 (Para 1, 2, 3 and 4) is now implemented and the radius and distance ratios and the new interpolated temperature profiles are calculated as described in the following sub-sections. Any arbitrary point 'n' in the domain can only belong to either (i) casting or (ii) mould or (iii) interface, and for each of these sub domains, the temperatures *e.g.* T_{11}, T_{12}, T_{21}, T_{22} (Figure 4.17) are always defined and are available from the databank.

4.3.5.1 Radius ratio

The radius information is obtained using the MAT technique. The radius ratio values (Figure 4.16 and Figure 4.17) are calculated as follows:

$$r_{radius}\ (r_R) = \frac{R_{new} - R_q}{R_{q+1} - R_q} \tag{4.4}$$

where R_{new} is the radius associated with node n whose temperature is being interpolated, R_q and R_{q+1} are the radii associated with the adjoining nodes for which temperatures T_{11} and T_{12} are available from the FE based temperature databank.

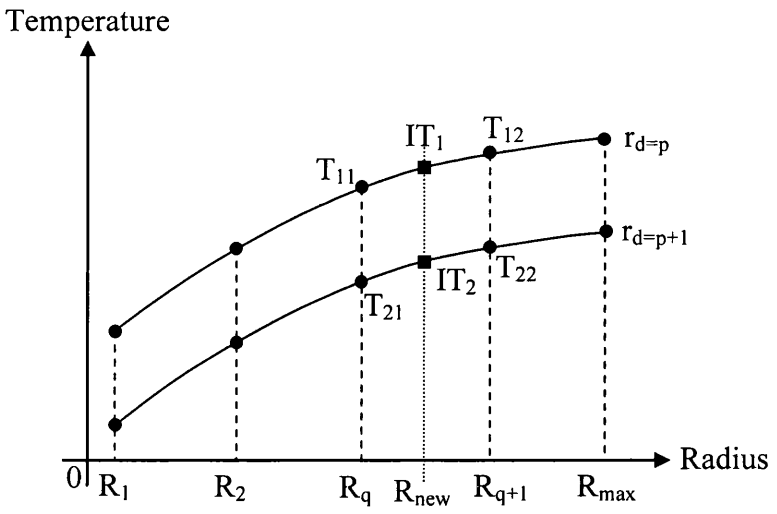

Figure 4.16: A schematic illustration of the first linear interpolation using radius ratio

4.3.5.2 First linear interpolation

Now using the radius ratio (r_R) calculated in Equation(4.4), the interpolated temperature, IT_1, is first obtained by undertaking linear interpolation (Figure 4.16 and Figure 4.17) using

$$IT_1 = r_R(T_{12} - T_{11}) + T_{11} \tag{4.5}$$

Similarly interpolated temperature, IT_2, is then obtained

$$IT_2 = r_R(T_{22} - T_{21}) + T_{21} \tag{4.6}$$

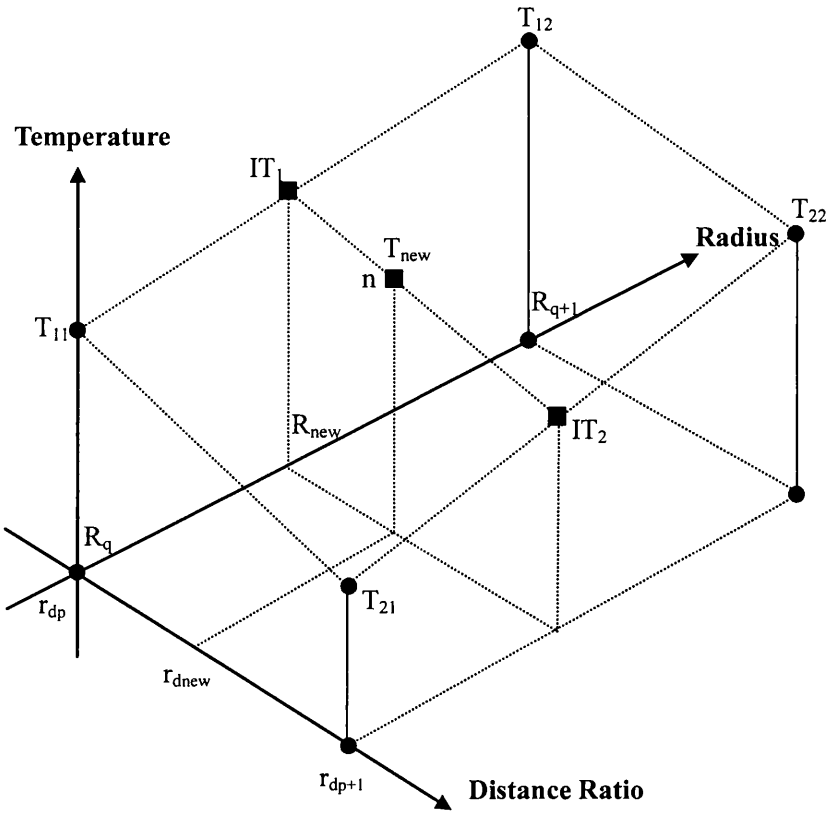

Figure 4.17: A schematic of two-stage double linear interpolation scheme

4.3.5.3 Distance ratio

The mesh of the casting model provides all the coordinate points ('n') which are used to calculate the distance ratios. Figure 4.18 illustrates how the distance ratio is calculated using Equation (4.7). This is further clarified in Figure 4.19.

$$r_{\text{distance}}\ (r_d) = \frac{\text{distance } (d)}{\text{radius associated to node n } (R_n)} \tag{4.7}$$

where d is the distance of the node 'n' from the medial axis and radius associated with node 'n' (R_n) is the radius at a point on medial axis where a perpendicular drawn from node *n* intersects the medial axis.

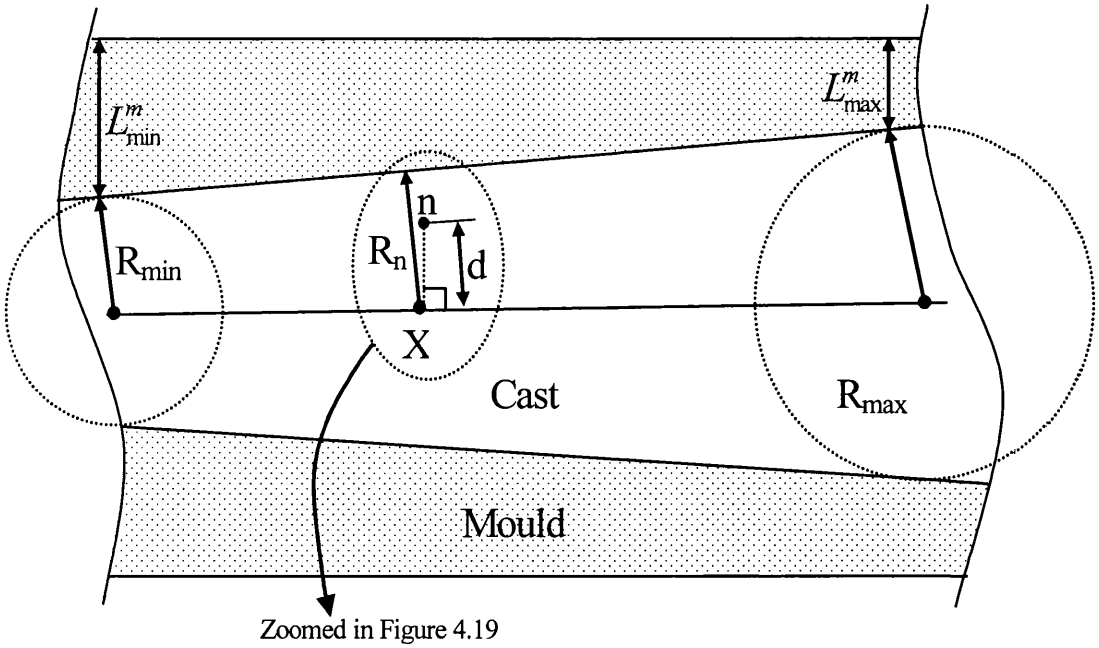

Figure 4.18: A schematic illustration of variables involved in calculating the distance ratio

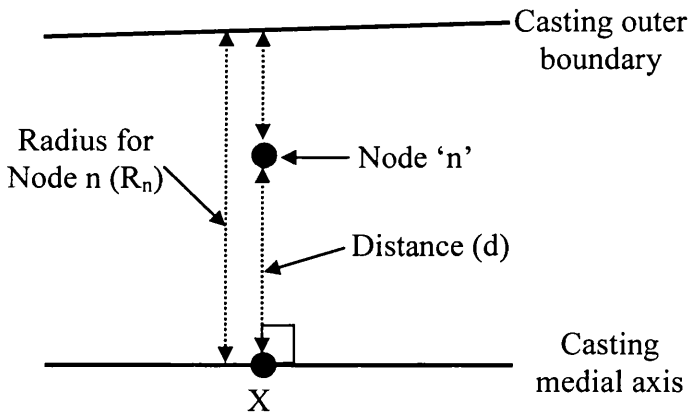

Figure 4.19: A zoomed schematic showing variables used for calculating distance ratio

4.3.5.4 Second linear interpolation

The interpolated temperatures, IT_1 and IT_2, are already calculated using Equations (4.5) and (4.6) in Section 4.3.5.2. Now a second linear interpolation is undertaken as shown in Figure 4.20 and the temperature at node 'n' (T_n) is then interpolated (Figure 4.17) as under

$$T_n = \frac{r_{d_{new}} - r_{d_p}}{r_{d_{p+1}} - r_{d_p}} \times (IT_2 - IT_1) + IT_1 \qquad (4.8)$$

where $r_{d_{new}}$ is the distance ratio at node 'n', r_{d_p} and $r_{d_{p+1}}$ are the known distance ratios intervals for which interpolated temperatures (IT_1 and IT_2) are already calculated using first linear interpolation in Section 4.3.5.2.

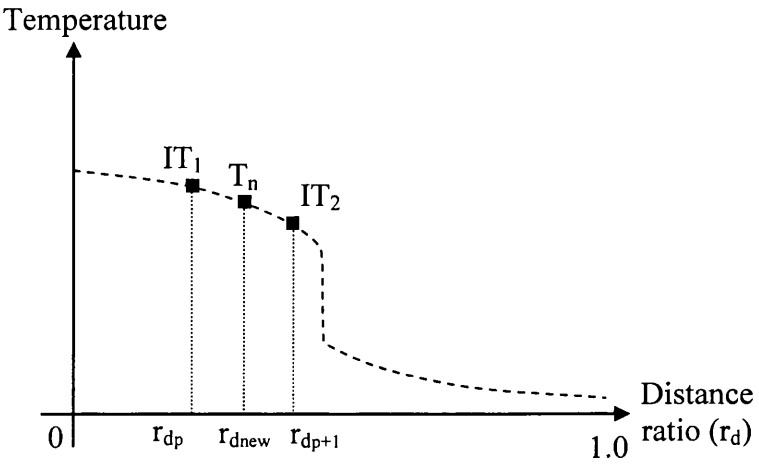

Figure 4.20: A schematic illustration of second linear interpolation using distance ratios

4.3.6 Execution of the Double Interpolation Scheme

The implementation of the double interpolation approach using the CADfix software package and the casting solidification code is illustrated through a flow diagram in Figure 4.21. The double linear interpolation scheme has been implemented using a CADfix software (Figure 4.22), which provided the medial axis, the radius information and distribution of points in the casting mould assembly and the geometric information associated with these points. The whole simulation can be executed and animated almost instantaneously. This can provide a quick idea of the feasibility of the design to its creator during the interrogation stage.

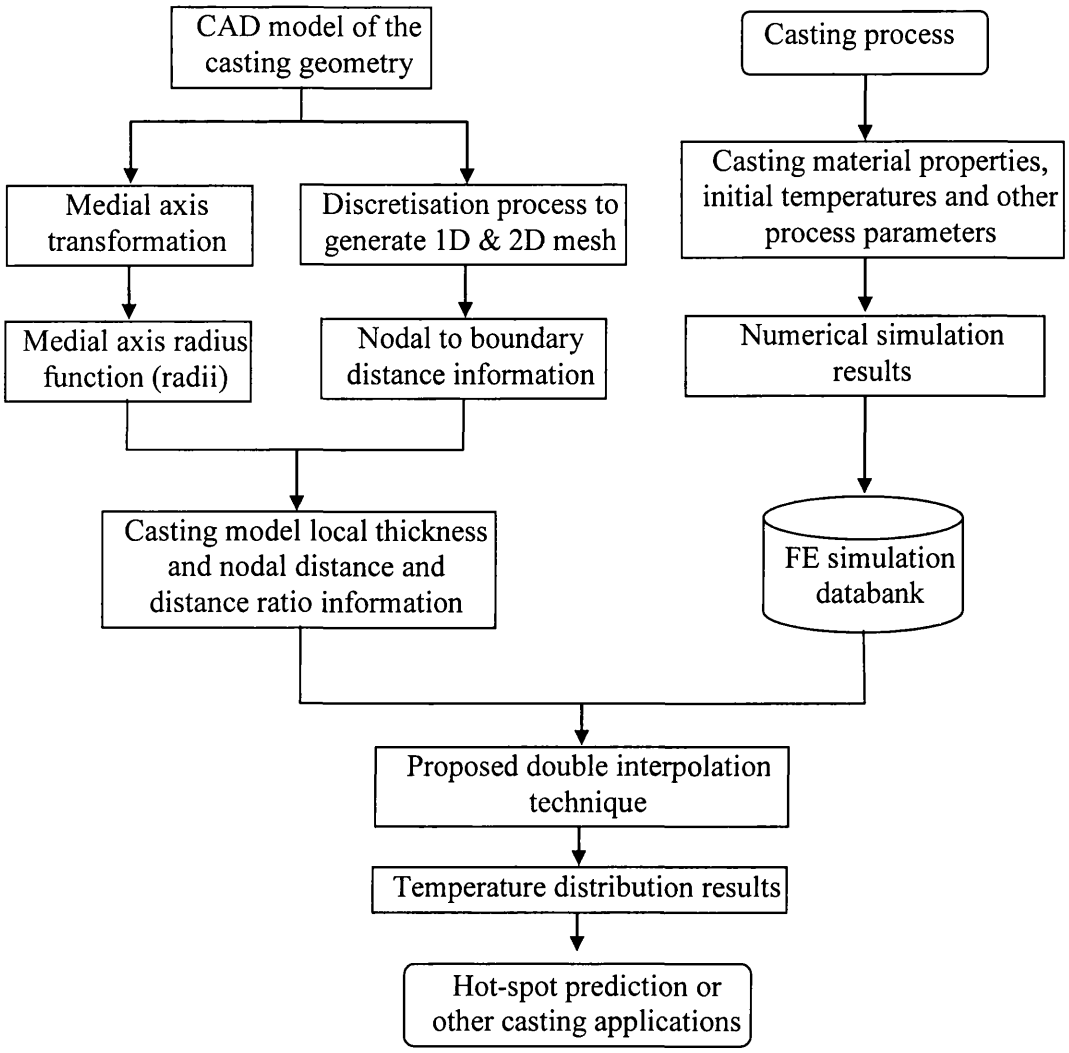

Figure 4.21: Flow chart describing steps involved in predicting hotspots using the proposed double interpolation technique

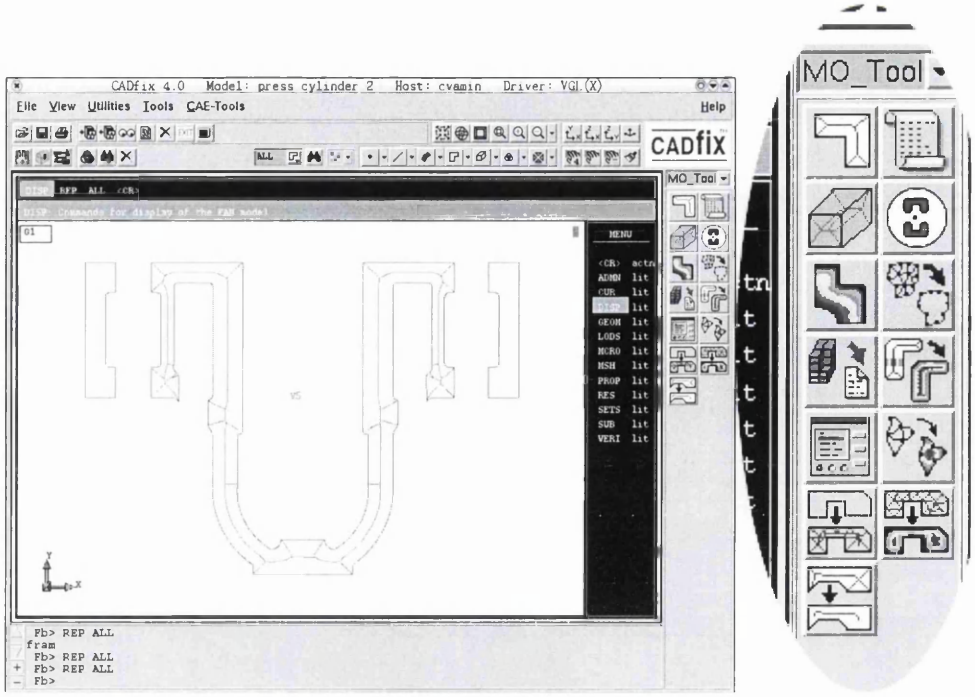

Figure 4.22: CADfix and its interface button for one-dimensional interpolation

4.4 RESULTS FROM CASE STUDIES

In this section, the feasibility and utility of the medial axis based interpolation method is assessed on a few casting examples. In the first example, a Gear Blank casting is used to explain the double interpolation method which was described in Section 4.3 and further illustrated through a flow chart in Figure 4.21. The casting model, its medial axis, the 2D mesh that provides the coordinate points, the distribution of distance and radius ratios are shown to explain the proposed scheme. The results obtained from the proposed double interpolation method are compared with solutions obtained from the geometric reasoning technique and the FE simulation. The proposed method is then further validated through two more examples by comparing their results with the actual castings. All the medial axis transformations used in these examples are provided by the CADfix software [3] and [4].

4.4.1 Example 1 – Gear blank casting

The proposed double interpolation scheme was first tested on a Gear Blank casting geometry taken from a published result [2]. The casting model and

the mesh for this particular casting are shown in Figure 4.23 and Figure 4.24 respectively. The mesh created by 2D mesh generator provides a distribution of points in the casting and mould as shown in Figure 4.25. The geometric information associated with these points is used to calculate radius and distance ratios as explained earlier in Section 4.3.5.1 and 4.3.5.3 and also on left hand side of the flow chart in Figure 4.21. The medial axis for this geometry is shown in Figure 4.26 (a). The medial axis comprises of the main medial axis and its side branches which touch the corners. Since the main medial axis is sufficient to provide the local thickness of the casting at various sections, these side branches of the medial axis are removed. The main medial axis for gear blank casting is shown in Figure 4.26 (b).

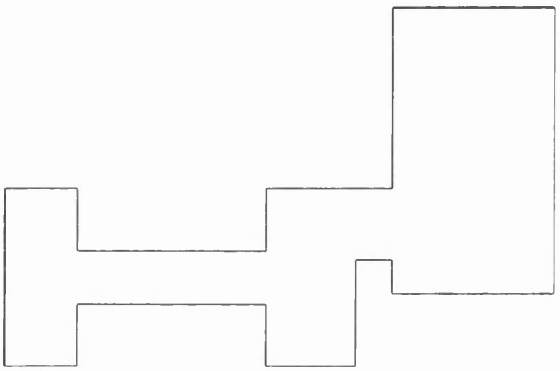

Figure 4.23 : Gear Blank casting model

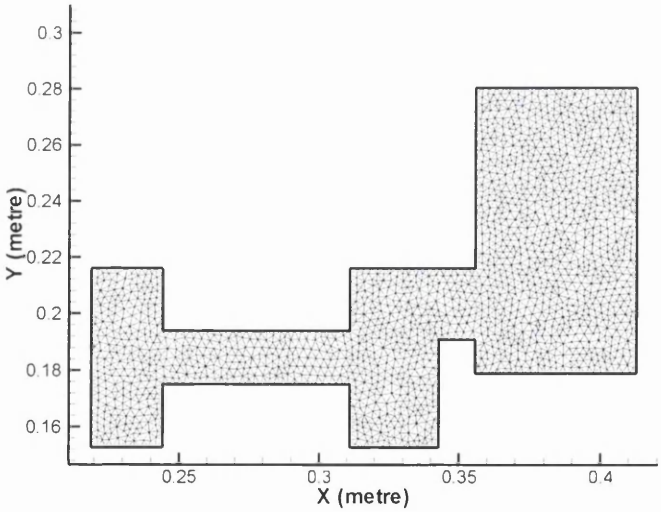

Figure 4.24 : Gear Blank casting model with mesh used to obtain distribution of points for calculating radius and distance ratios

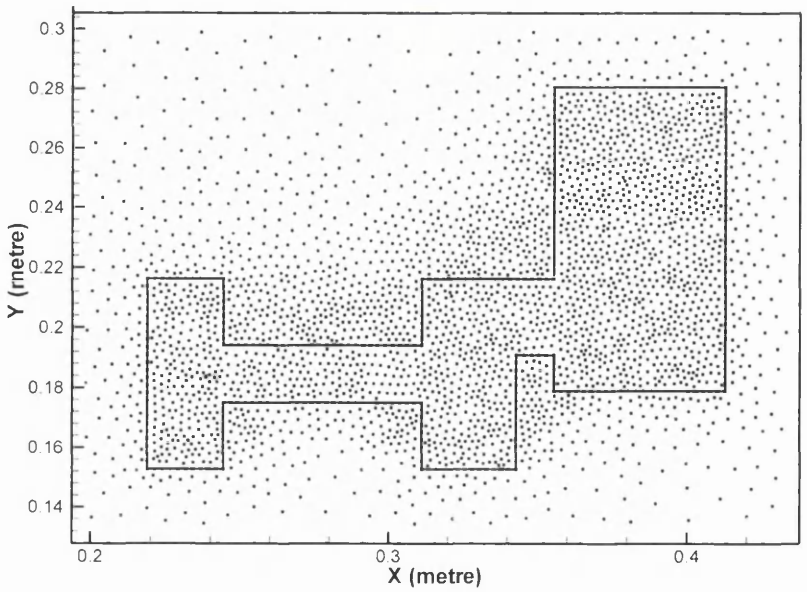

Figure 4.25 : Gear Blank casting model showing all the points generated by the mesh for calculating radius and distance ratios used by the proposed double interpolation scheme

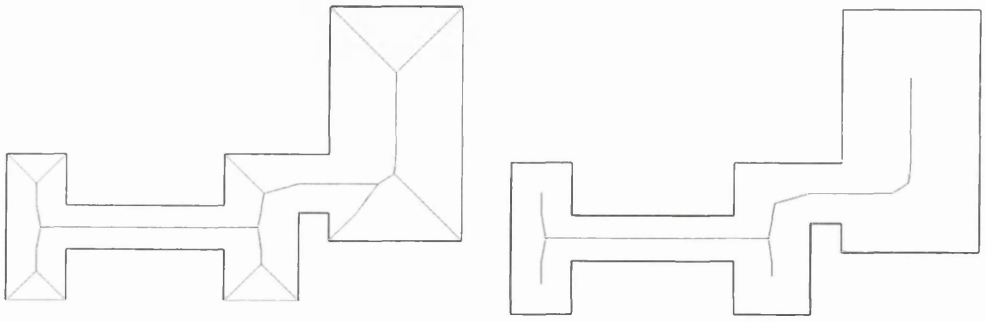

(a) Casting model with the complete medial axis

(b) Casting model with main medial axis (the side branches are removed)

Figure 4.26 : The Gear Blank casting model with medial axis

As explained earlier, the mesh result provides all the coordinate points (*e.g.* point 'n' in Figure 4.17 - Figure 4.19) with in the casting and the mould and these are used to calculate the distance of each of these points ('n') from the main medial axis. The distance contours obtained for this casting are shown in Figure 4.27.

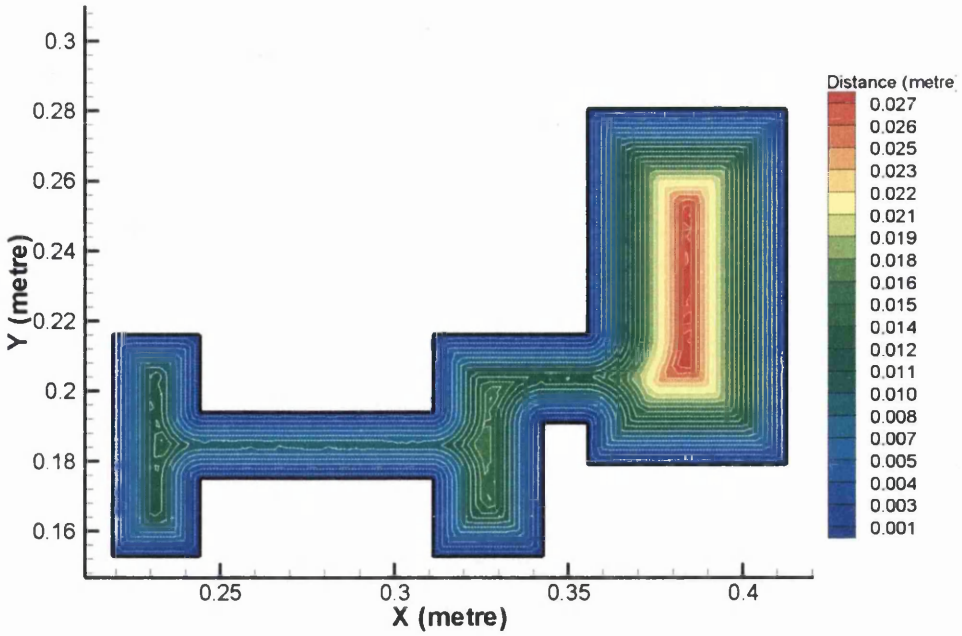

Figure 4.27 : Gear blank casting showing distance contours (distance between the points and the casting boundary)

The distance ratios as explained in Section 4.3.5.3 using Equations (4.7) (Section 4.3.5.3) are then calculated and the distribution of the distance ratios (d/R) for this casting is shown in Figure 4.28.

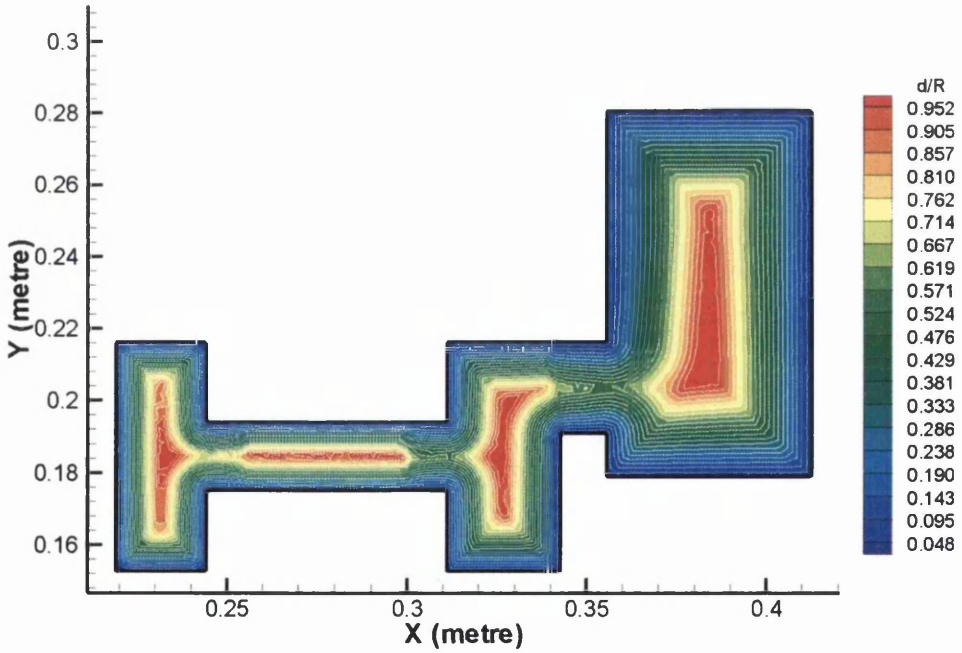

Figure 4.28: Gear Blank casting showing distance ratio (distance from casting boundary divided by maximum radius)

As illustrated in the flow chart (Figure 4.21), the medial axis transformation provides the radius information associated with these points. Figure 4.29 shows the radius contours thus obtained for this casting example. This radius information is then used to calculate the radius ratios using Equation (4.4) as explained earlier in Section 4.3.5.1.

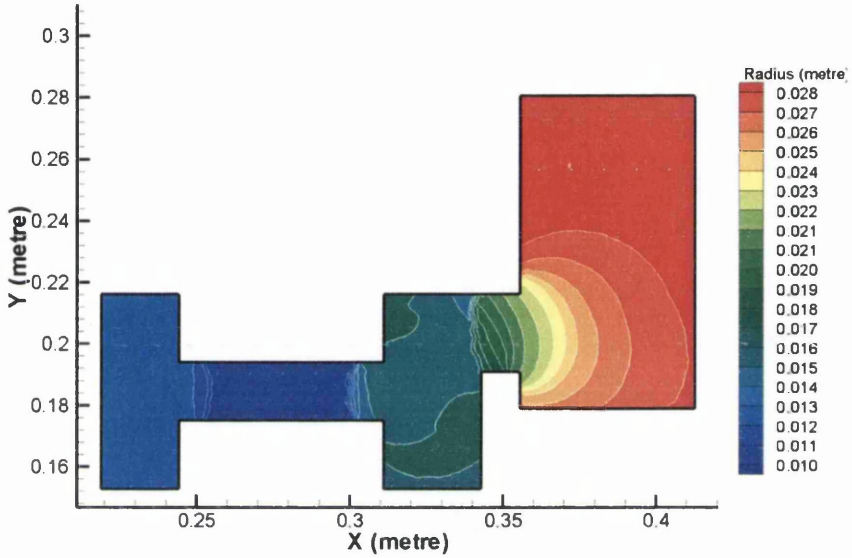

Figure 4.29: Gear blank casting showing radius contours (medial radius inside the casting)

The temperature solution obtained from the proposed double interpolation method for casting and mould is shown in Figure 4.30 and Figure 4.31 for coarse and medium point (mesh) density respectively. The temperature contours in the thinner section (marked with A in Figure 4.30) of casting are not smooth and factors contributing to this asymmetry will be discussed in next section. The hotspot is located in the thickest section of the casting on the right hand side. This solution compares favourably with the solution obtained using another geometric method *i.e.* Modulus method and with solution predicted by the FE simulation.

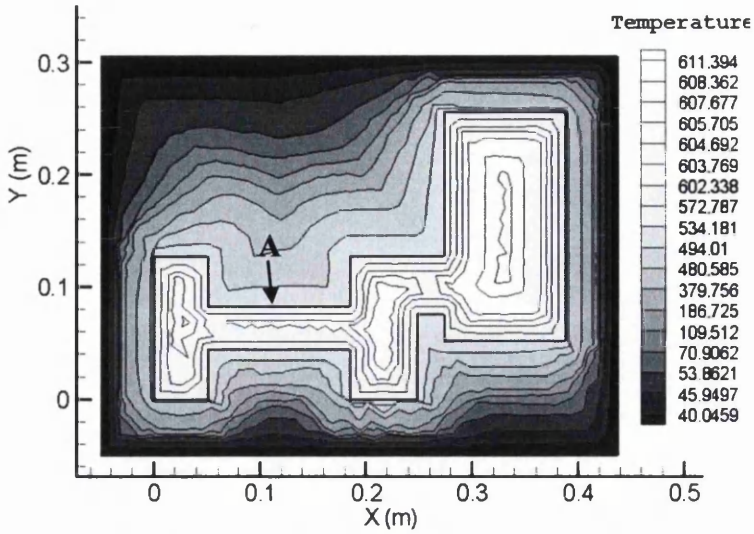

Figure 4.30: Temperature contours obtained using double interpolation method with coarse point (mesh) density

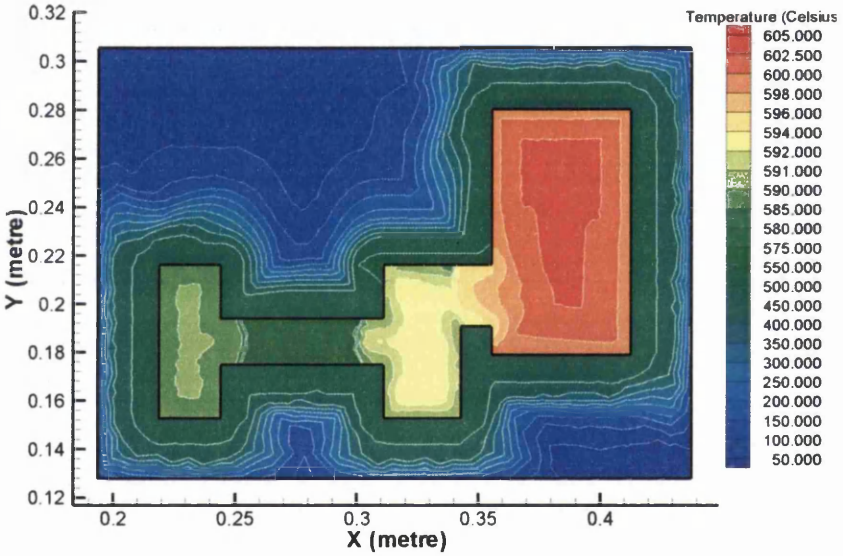

Figure 4.31: Temperature contours obtained using double interpolation method with medium point (mesh) density

Figure 4.32 shows the solidification wave front predicted by Heine and Uicker [2]. The wave-front technique, however, can not show transient solutions, whereas the proposed technique is able to provide the evolution of temperature profiles in time and also retain the main advantage of geometric reasoning methods – higher computational efficiency.

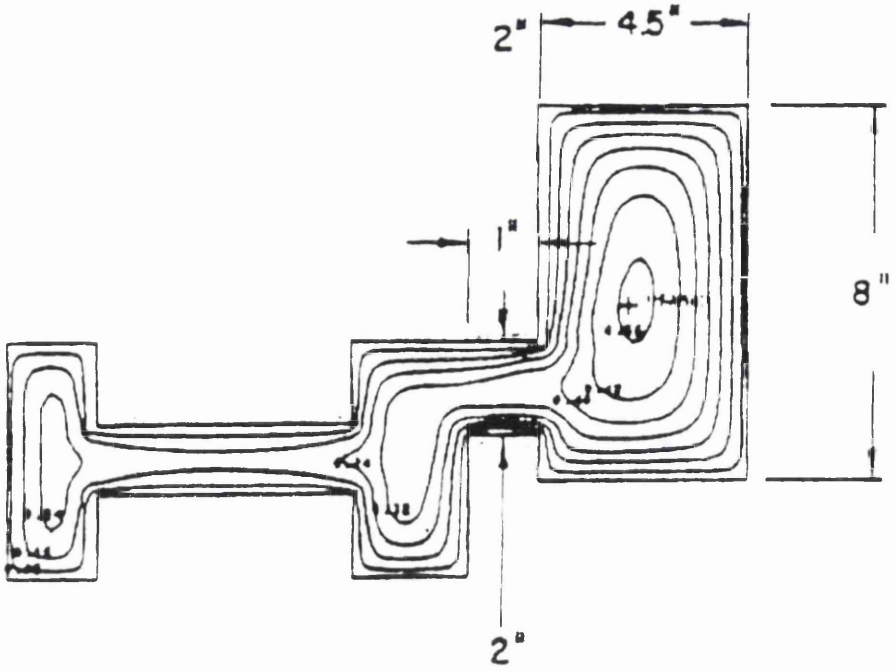

Figure 4.32: Freezing wave solution using a geometric method [2]

It can be seen that even though the results are not as accurate as the finite element solution (Figure 4.33), they are qualitatively similar. The location of hotspot compares favourably between two methods. For this geometry, the hotspots are located in the section that has largest inscribed radius value. It is also noted that the temperature contour distribution exhibits similarity for both the solutions, both in the cast and in mould.

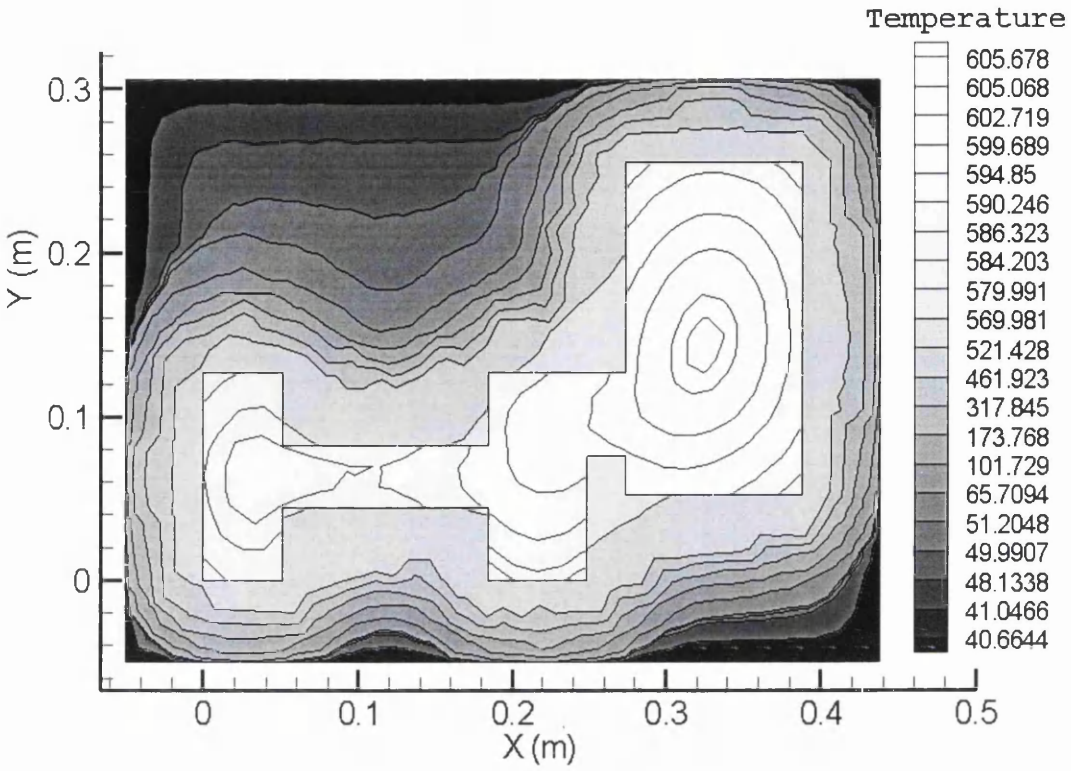

Figure 4.33: Finite-element solution for the gear blank casting

4.4.2 Example 2 – Aluminium Sand casting 1

The second casting component chosen is depicted in Figure 4.34, which is an aluminium sand casting problem, where the enlarged locations A, B and C show the porosity formation in the final product. These locations indirectly point to the locations of the hotspot during the solidification process. Figure 4.35 shows the medial axes of the casting component geometry.

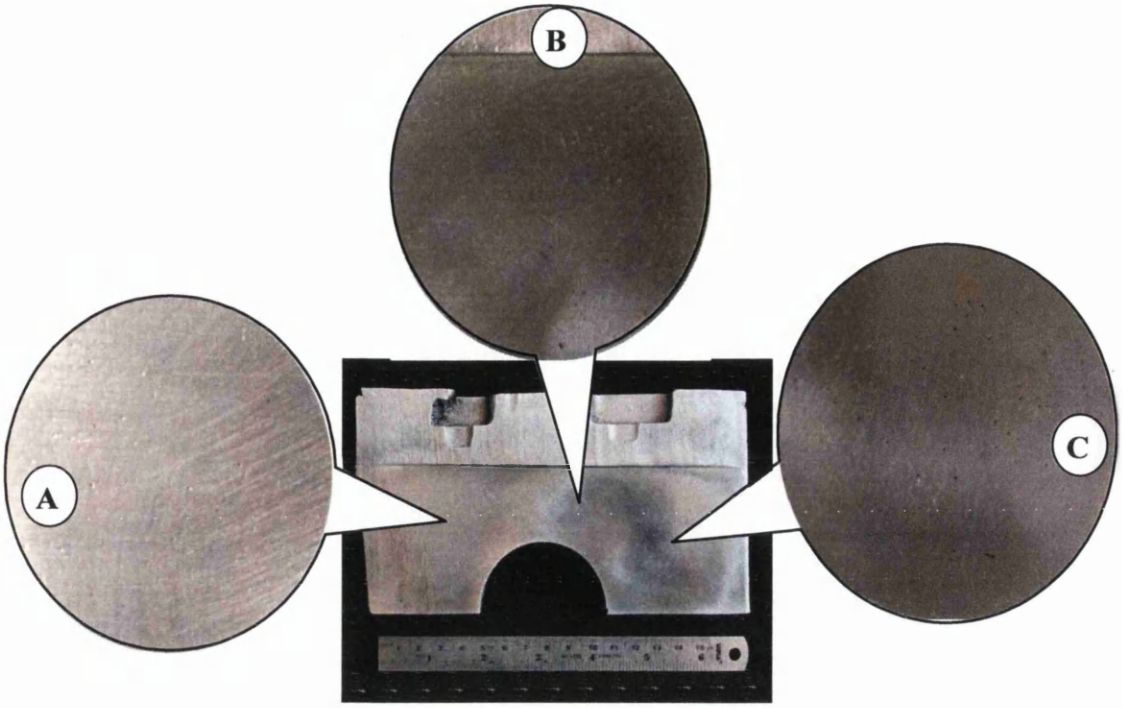

Figure 4.34: Photograph of Aluminium sand casting showing its dimension and locations of porosity formation

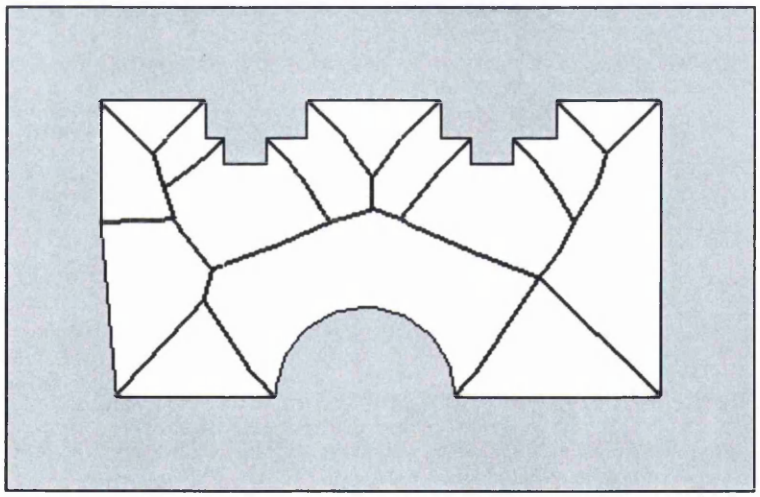

Figure 4.35: Medial axis for the Aluminium sand casting used in Example 2

Typical properties for the aluminium sand casting process are used for the one-dimensional solidification solver and are given in Table 4.1 [5]. The variation of enthalpy with temperature is tabulated in Table 4.2.

Solid density for the aluminium cast	$\rho_c = 2680$ kg/m^3
Thermal conductivity of aluminium cast	$k_c = 186.3$ W/mK
Density of the sand mould	$\rho_m = 1000$ kg/m^3
Thermal conductivity of sand	$k_m = 0.8$ W/mK
Specific heat for sand mould	$C_{pm} = 709$ J/kgK
Initial temperature of the molten aluminium alloy	650^oC
Initial temperature of the sand mould	50^oC
Inter-facial heat transfer coefficient value between the casting and the sand	$h_{\text{inf}} = 500$ W/m^2K
Imposed boundary condition for the exterior of the sand mould is convection	$h_\infty = 25$ W/m^2K to air at $T_\infty = 30^oC$

Table 4.1: Material properties and boundary conditions for aluminium alloy (LM24) and sand mould

$T(^oC)$	k(W/mK)	Enthalpy (J/kg)
0	186.3	0.0
550	186.3	601 150
615	186.3	998 150
800	186.3	1200 000

Table 4.2: Thermal properties of aluminium [5]

The proposed double interpolation method was then tested for the Aluminium sand casting and Figure 4.36 shows the temperature contours. It is seen that the proposed method rightly predicts the location of hotspots: the three hotspots accurately correspond to the porosity defect locations A, B and C in the Aluminium casting (Figure 4.34). It is to be noted that the solution of the temperature may not be quantitatively accurate as compared to numerical simulation technique but the predicted temperature profile is qualitatively correct.

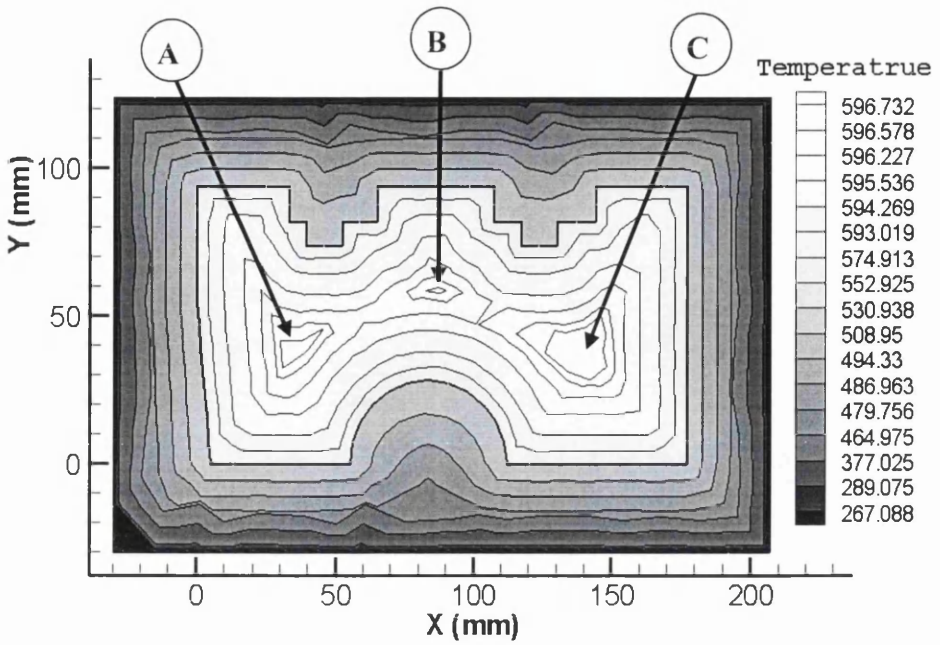

Figure 4.36: Temperature contours obtained using Double Interpolation method

4.4.3 Example 3- Aluminium Sand casting 2

Figure 4.37 shows the third example which is again an aluminium sand casting industrial component but this sample had a hole in the casting as shown in Figure 4.37. As a result of the third assumption in Section 4.3.2, the double interpolation method could not be directly applied. The locations of porosity defects which were noticed in casting sample can be clearly seen as A, B and C in Figure 4.37 and these corresponds to the locations of the hotspots. Due to the non-uniformity of the casting, only the cross-sectional area of the model was chosen. The medial axis for this casting geometry is shown in Figure 4.38, where the grey area represents the mould.

To overcome the difficulty posed by the hole, it was assumed that there is no mould material inside the hole. No special treatment was made to handle the boundary conditions at the interface along the circumference of the hole and the simulation was carried out 'as is'. The same temperature databank as used in the previous example was used. The method again accurately predicted the possible locations of hotspots locations A, B and C as shown in

Figure 4.39, which correctly correspond to the location of defects in the real casting component in Figure 4.37.

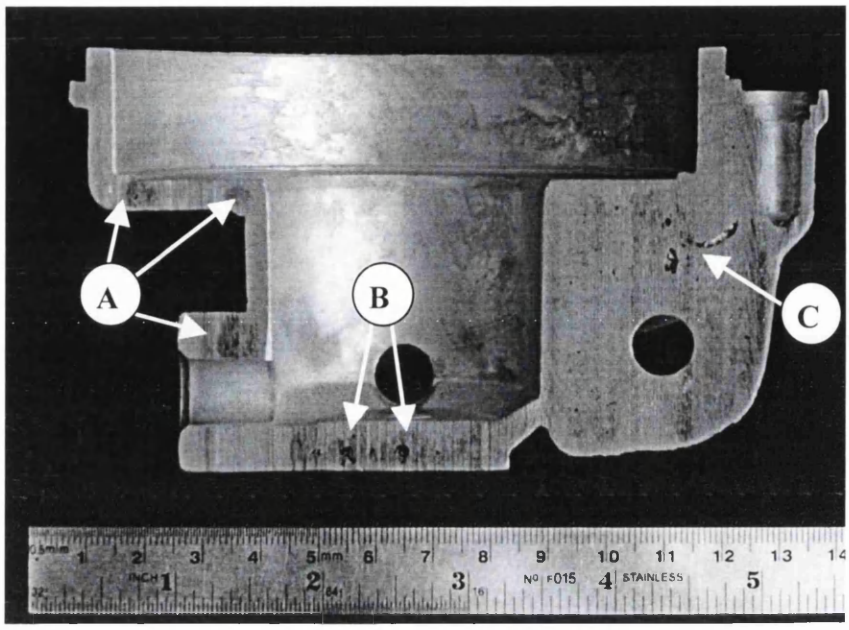

Figure 4.37: Photograph of test piece 2 showing its dimension and location of porosity formation

It is worthwhile mentioning here that the entire simulation for both examples takes between 60-90 seconds (Pentium 4 with 1500 MHz CPU and 512 MB RAM) which was less than half the time required for an equivalent FE simulation. In fact, the actual time required for the interpolation method would be much less than 60-90 seconds. This rather long CPU time is due to the time delay in command interfacing between the Tcl/Tk script and the CADfix software. The program, which was written in Tcl/Tk, needs to prompt CADfix continuously for the geometric and medial-axes information. Once the pre-processing of the geometric entities is completed, the interpolation algorithm itself can be completed within matter of seconds. This feature could be of use to engineers who want a quick simulation of the casting design while interacting with a CAD based software.

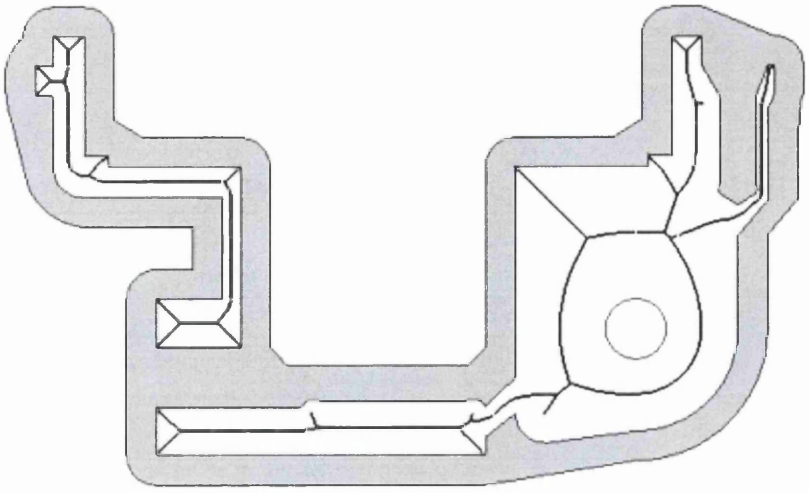

Figure 4.38: Model setup for test piece 2 showing the mould-cast assembly and its medial-axes

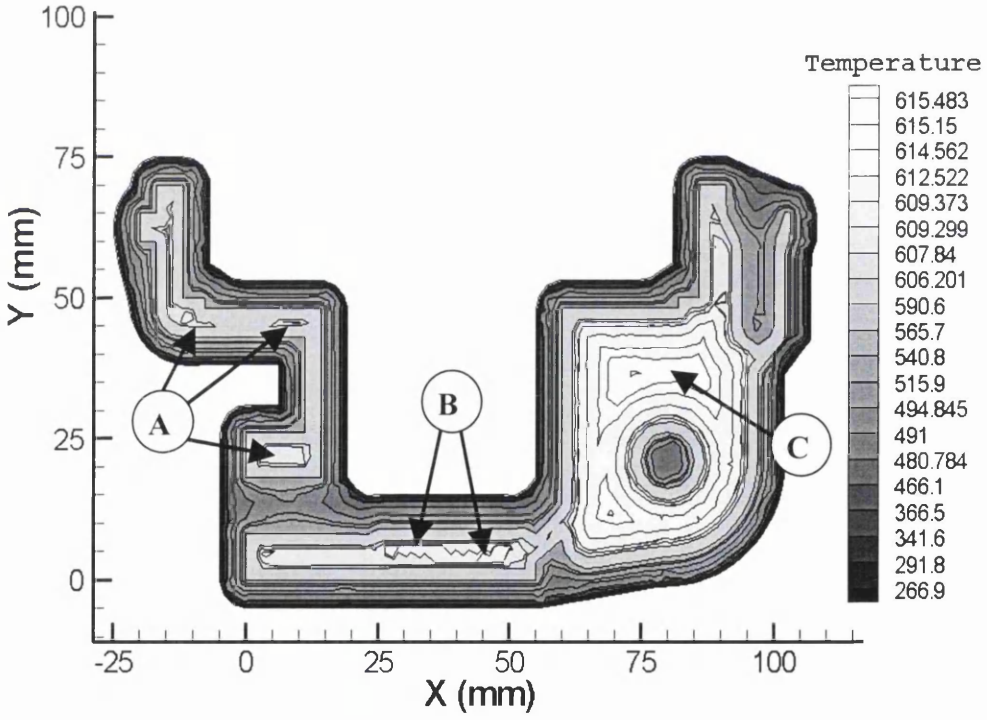

Figure 4.39: Temperature contours obtained using Double Interpolation method

4.5 POINT (MESH) DENSITY STUDY AND DISCUSSION ON ERROR

4.5.1 Discussion on error generated by the double interpolation technique

The temperature contours shown in Figure 4.30 are not smooth at section A. This section will explore the reasons for the error that generates 'zigzag behaviour' of temperature contours at some locations. It is estimated that the following two factors contribute to this error.

1. The method for calculating the value of "d" in Equation (4.7) in order to determine the distance ratio.
2. Error caused by the distribution of points generated by the mesh

As described in section 3.5.3.4 and 4.3.5.3, the sampling points required by the interpolation algorithm are obtained by meshing the whole casting-mould assembly. The points are then classified into three parts. The points on the main medial axis are stored in a separate point set (Point set A) and the points on the boundary are stored in another point set (Point set B). The rest of the points are also stored separately. This is illustrated by a schematic Figure 4.40.

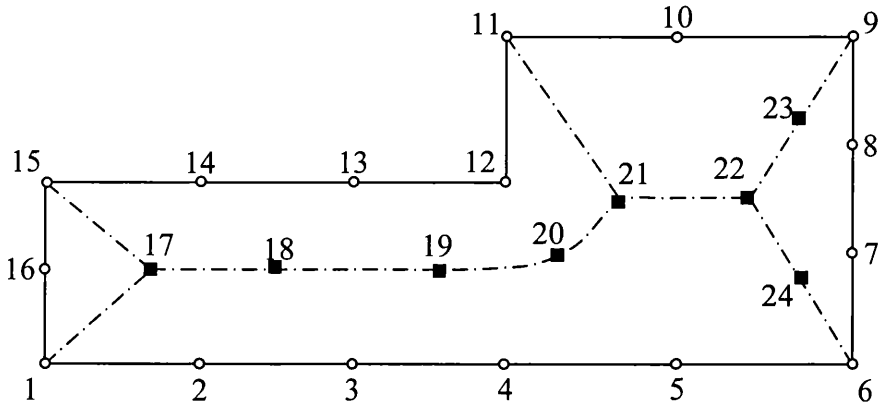

Figure 4.40: A schematic of points generated by the medial axis transformation technique for calculating distance and radius ratios

Point set A (On main medial axis): 17, 18, 19, 20, 21, 22, 23 and 24

Point set B (On boundary segments): 1, 2, 3, 4, 5, 6, 7, 8, 9, 10, 11, 12, 13, 14, 15 and 16

In Equation (4.7) and Figure 4.18, R_n is the medial-radius associated with point 'n' i.e. it is the medial radius at point X on the medial axis where a perpendicular line drawn from node n' intersects the medial axis. In other words, the distance d' is the minimum distance of the node 'n' from the medial axis. However, it is very difficult to calculate this minimum distance and the interpolation algorithm therefore, takes into account the distance d which is the distance between point n and the point on the medial axis that is nearest to point n. This results in an error as shown schematically in Figure 4.41. The distance ratio (r_d) at node n is thus greater than the distance ratio ($r_{d'}$) at node n'. This thus results in lower interpolated temperature value (Tr_d) at node n compared to the interpolated temperature value ($Tr_{d'}$) at node n'.

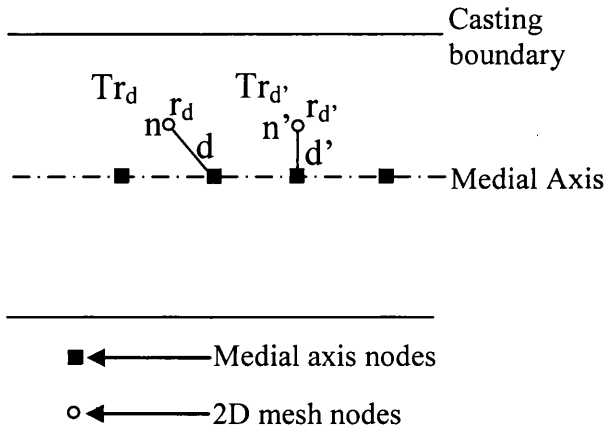

Figure 4.41: Diagrammatic explanation of the error observed in double interpolation solution

This error however can be calculated. Assuming that minimum section thickness of the casting is equal to at least three times the 2D mesh for a specific case (i.e. minimum medial radius = 3L or say k times the L as shown in Figure 4.42) and that average distance between two nodes on medial axis equals half the element length (L/2), the percentage error can be calculated using Equations (4.9) and (4.10).

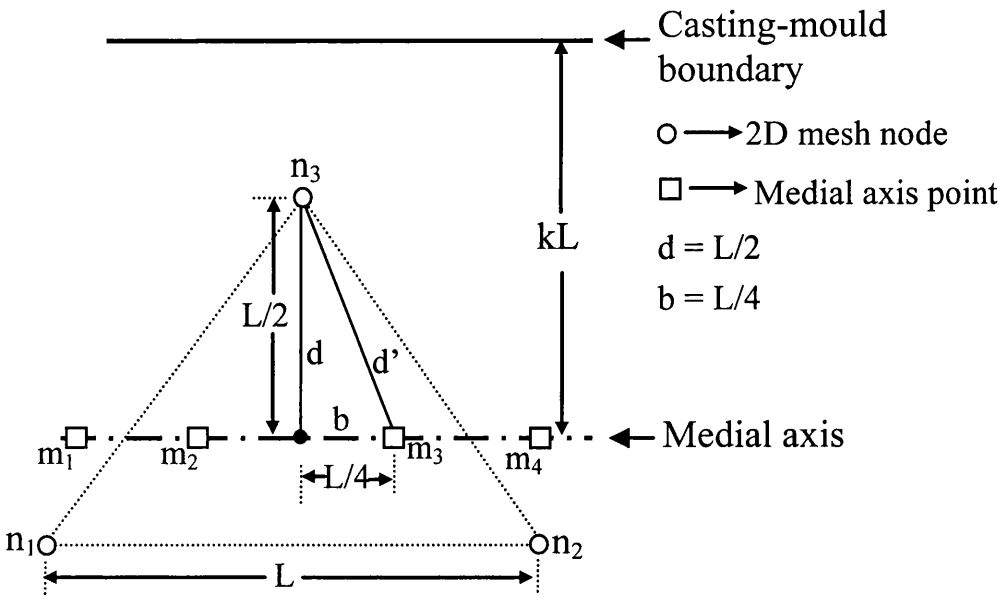

Figure 4.42: A schematic illustration of calculation of percentage error

$$d' = \sqrt{d^2 + b^2}$$

$$= \sqrt{L^2 . \left(\frac{1}{4} + \frac{1}{16}\right)}$$

$$= L\sqrt{\frac{5}{16}} = \frac{L}{4}\sqrt{5} \qquad (4.9)$$

$$\Delta d = d' - d \quad = \left(\frac{\sqrt{5}}{4} - \frac{1}{2}\right) L$$

$$= \frac{\sqrt{5} - 2}{4} L \quad \approx \frac{2.236 - 2}{4} L$$

$$\Delta d = \frac{0.236}{4} \times 100\% \times L \quad = \Delta d = 5.9\% L \qquad (4.10)$$

If we consider that the casting thickness is k times the size of 2D mesh (kL), then the corresponding error in distance ratio Δr_d can then be calculated as in Equation (4.11)

$$\Delta r_d = \frac{\Delta d}{R} = \frac{\frac{\sqrt{5}-2}{4}L}{kL}$$

$$\Delta r_d = \frac{\sqrt{5}-2}{4} \times \frac{1}{k}$$

$$\Delta r_d = \frac{1}{k} 5.9\% \tag{4.11}$$

The error is maximum when the casting has one layer of elements on either side of the medial axis and the maximum value of error is 5.9%. As the density of the points generated by mesh increases, the error reduces and the resultant zigzag in temperature contours smoothes out. This is shown in Table 4.3 and the corresponding graph is plotted in Figure 4.43. The relationship of point density to this zigzag contours is further shown by the interpolation solutions obtained for different point densities for a case of gear blank casting in Section 4.5.2.

Value of k	Percentage error
1	5.90
2	2.95
3	1.97
4	1.48
5	1.18
6	0.98

Table 4.3: Table showing values of k (point density) and error (%) in distance ratio

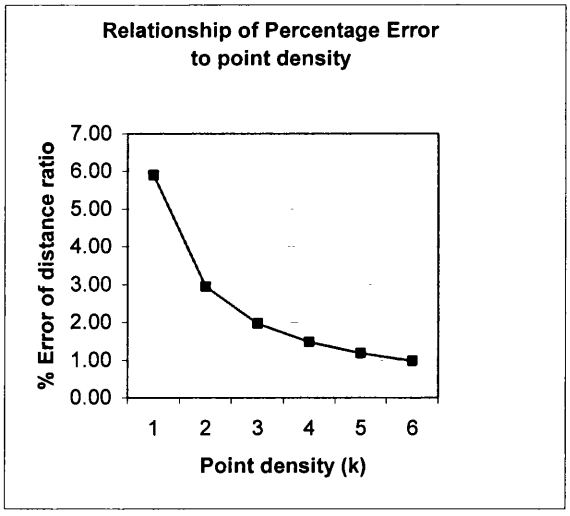

Figure 4.43: Relationship of percentage error of distance ratio to point density

The second source of error is the 2-dimensional mesh used to obtain points for collecting geometric information for double interpolation. This happens when the 2D mesh crosses the medial axis as shown in Figure 4.44 (b) where element with nodes (P_1, P'_1, P_2) crosses the medial axis.

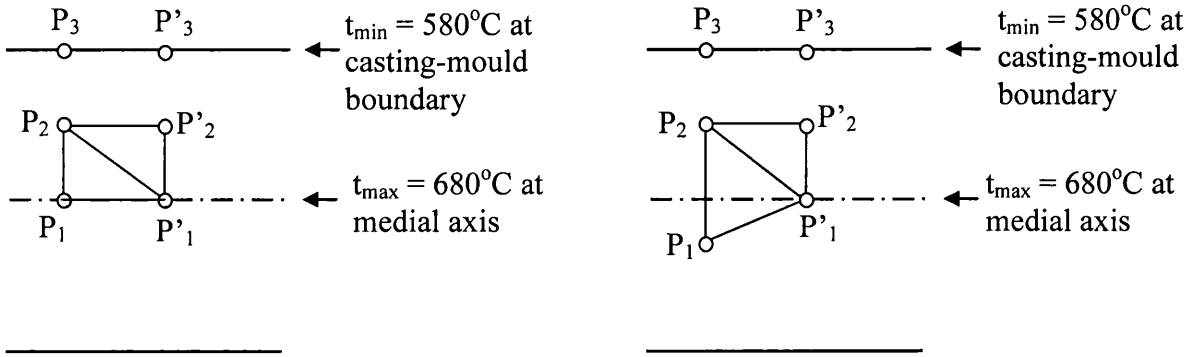

$tempP'_1 = tempP_1 = 680°C$
$tempP'_2 = tempP_2 = 630°C$
$tempP'_3 = tempP_3 = 580°C$

(a) F.E. Solution

$tempP'_1 = 680°C$
$tempP_1 = 650°C$
$tempP'_2 = tempP_2 = 630°C$
$tempP'_3 = tempP_3 = 580°C$

(b) Interpolation Solution

Figure 4.44: A schematic explanation of error created by mesh in double interpolation method

Due to the nature of interpolation algorithm, area with such elements which cross the medial axis show lower temperatures thereby resulting in an asymmetry and zigzag amongst temperature contours. This is further explained in Figure 4.45 and Figure 4.46. Such error however, can be eliminated by assuming medial axis as a boundary and then by obtaining points on medial axis.

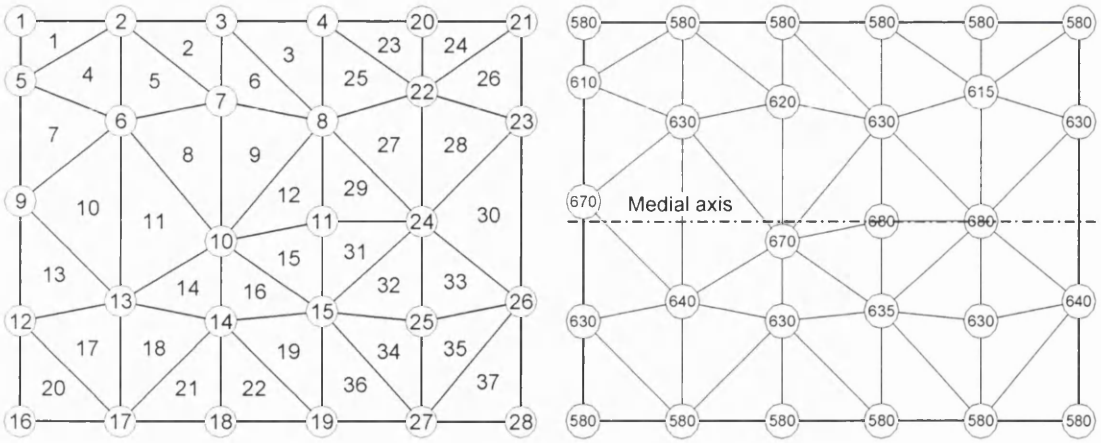

(a) Casting showing mesh result (b) Temperature at the nodes

Figure 4.45: Explanation of zigzag pattern in double interpolation solution

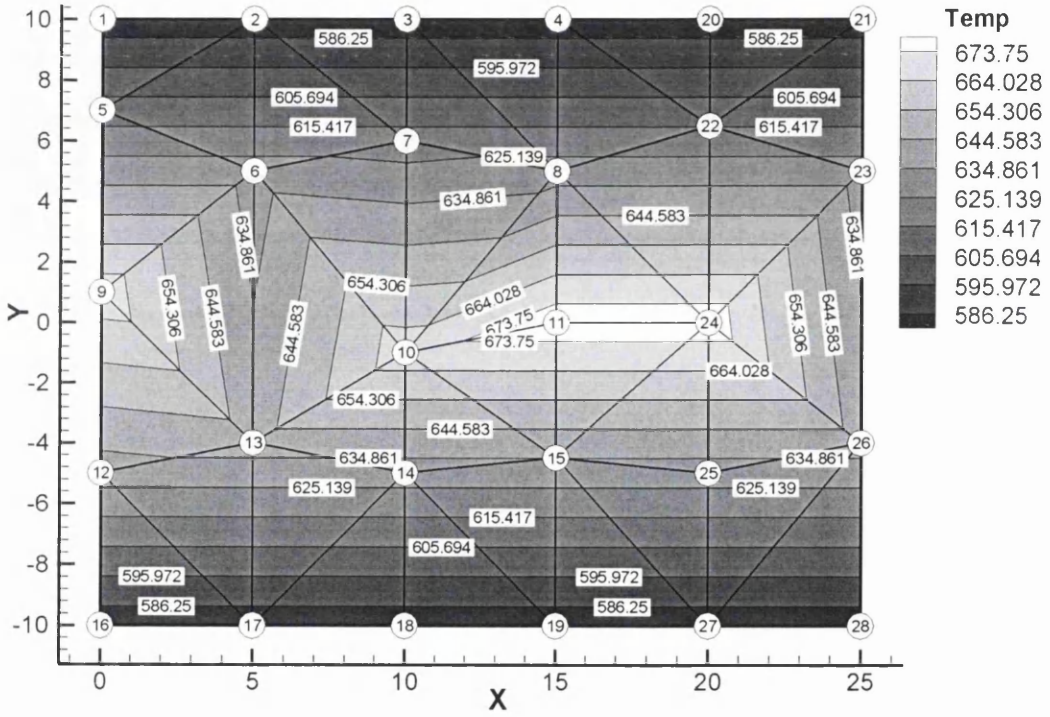

Figure 4.46: Temperature contours illustrating zigzag pattern

4.5.2 Results from double interpolation for gear blank casting using different point densities

This sub-section describes further case studies undertaken for gear blank casting using different mesh densities. Table 4.4 provides information of type of mesh used, total number of elements and nodes for gear Blank casting used earlier in Section 4.6.1 and 4.7.1.

Gear Blank Casting Model			
Type of Mesh	**Parts**	**Element Number**	**Node Number**
Coarse	Casting	647	388
	Mould	685	422
	Total	**1332**	**810**
Medium	Casting	3634	1970
	Mould	3052	1718
	Total	**6686**	**3688**
Fine	Casting	22700	11727
	Mould	16006	8459
	Total	**38706**	**20186**

Table 4.4: Table showing type of mesh, number of elements and nodes for Gear Blank casting

The discussion on error observed in interpolation result, which was explained in Section 4.8.1 is supported by the interpolation solutions obtained for casting models of gear blank casting with different point (mesh) densities [Figure 4.47 (a), Figure 4.48(a) and Figure 4.49(a)]. The temperature solutions obtained using double interpolation method for different mesh densities are shown in Figure 4.47(b), Figure 4.48(b) and Figure 4.49(b)]. These temperature solutions for three mesh densities are then enlarged from a part of casting and mould marked out by a dotted square as shown in Figure 4.48 (a). It is observed that with coarse mesh (Figure 4.47(b) and Figure 4.50), the zigzag and asymmetry is more pronounced compared to medium mesh (Figure 4.48 (b) and Figure 4.51). The interpolation solution obtained using a fine mesh provides more smooth temperature contours (Figure 4.49 (b) and Figure 4.52).

The reason for this being that the finer mesh provides a dense distribution of points that are used by the interpolation scheme for calculating geometric gathering information and obtaining distance and radius ratios. The higher density of points reduces the error in calculating distance ratio which in turn provides more accurate temperature result based on FE based temperature database and this then results in smoother contours.

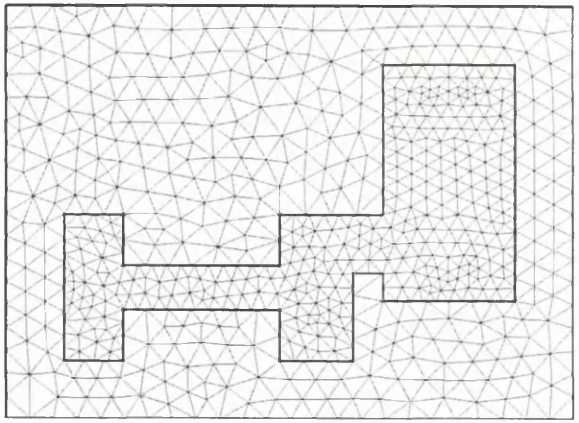

(a) Casting model showing mesh with 647 casting elements and 685 mould elements

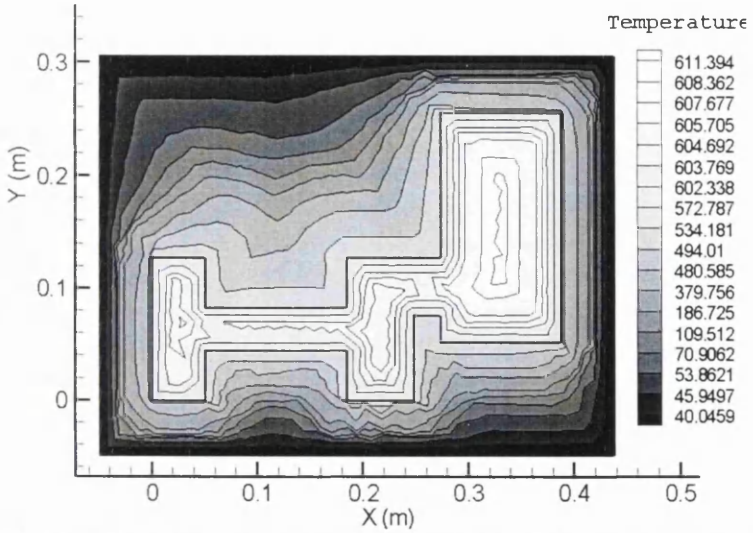

(b) Interpolated temperature contours for model with very coarse point density (mesh)

Figure 4.47: Gear Blank casting with coarse point density (mesh is only used to plot the contours where as points are used in the calculation procedure for the double interpolation method)

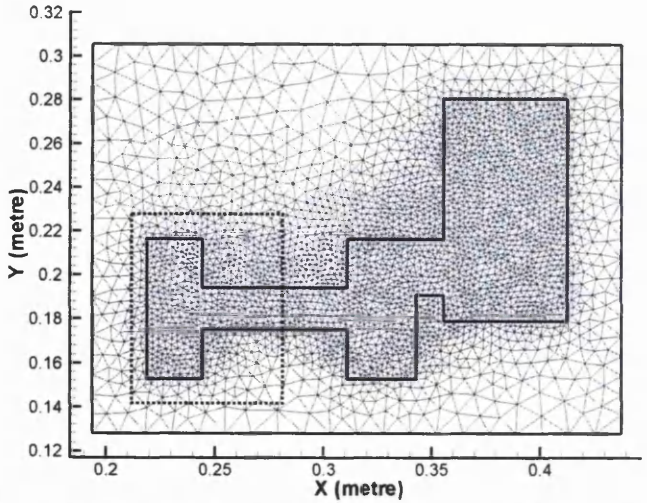

(a) Casting model showing mesh with 3634 casting elements and 3052 mould elements

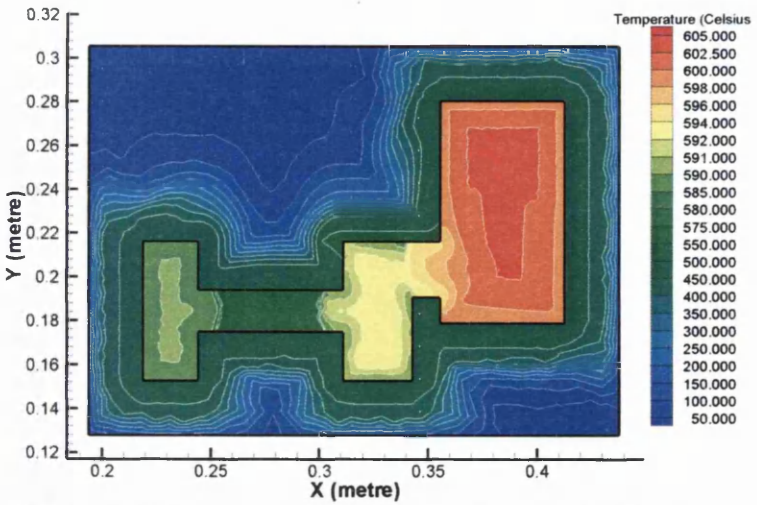

(b) Interpolated temperature contours for model with medium point density (mesh)

Figure 4.48: Gear Blank casting with medium point density (mesh is only used to plot the contours where as points are used in the calculation procedure for the double interpolation method)

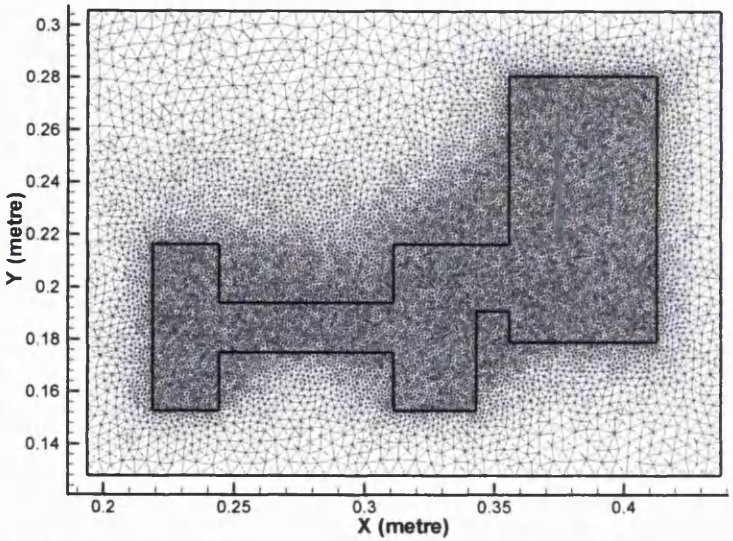

(a) Casting model showing mesh with 22700 casting elements and 16006 mould elements

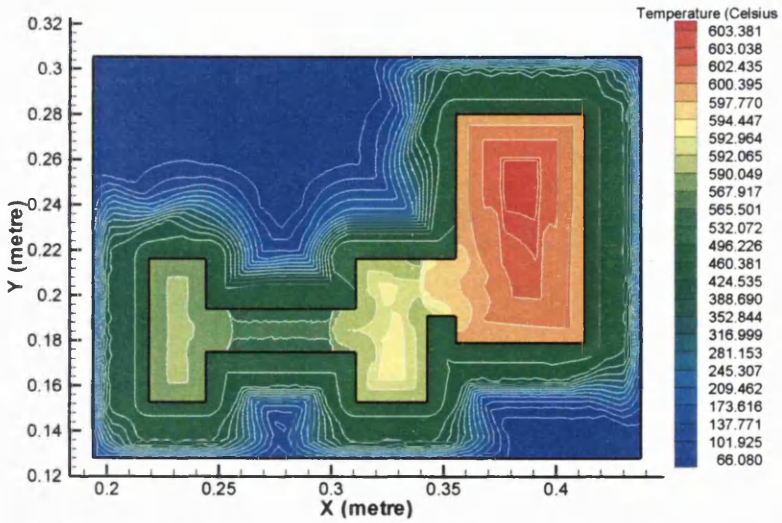

(b) Interpolated temperature contours for model with fine point density (mesh)

Figure 4.49: Gear Blank casting with fine point density (mesh is only used to plot the contours where as points are used in the calculation procedure for the double interpolation method)

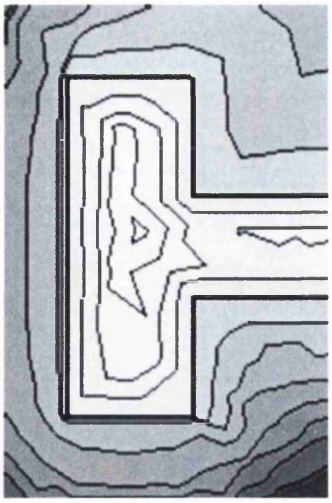

Figure 4.50: Enlarged section of Gear Blank casting with coarse mesh

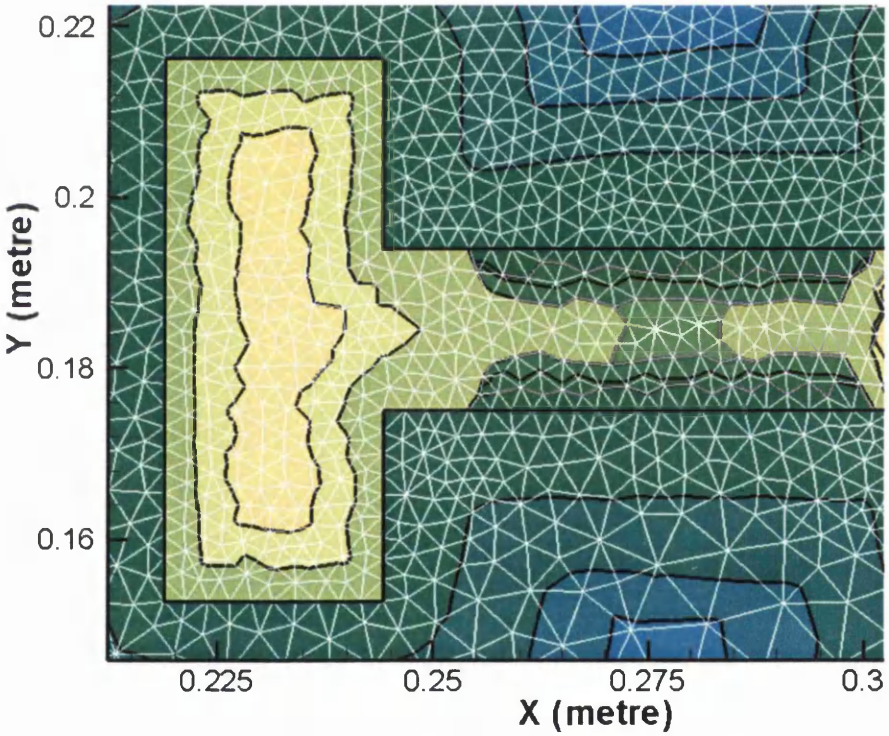

Figure 4.51: Enlarged section of Gear Blank casting with medium mesh

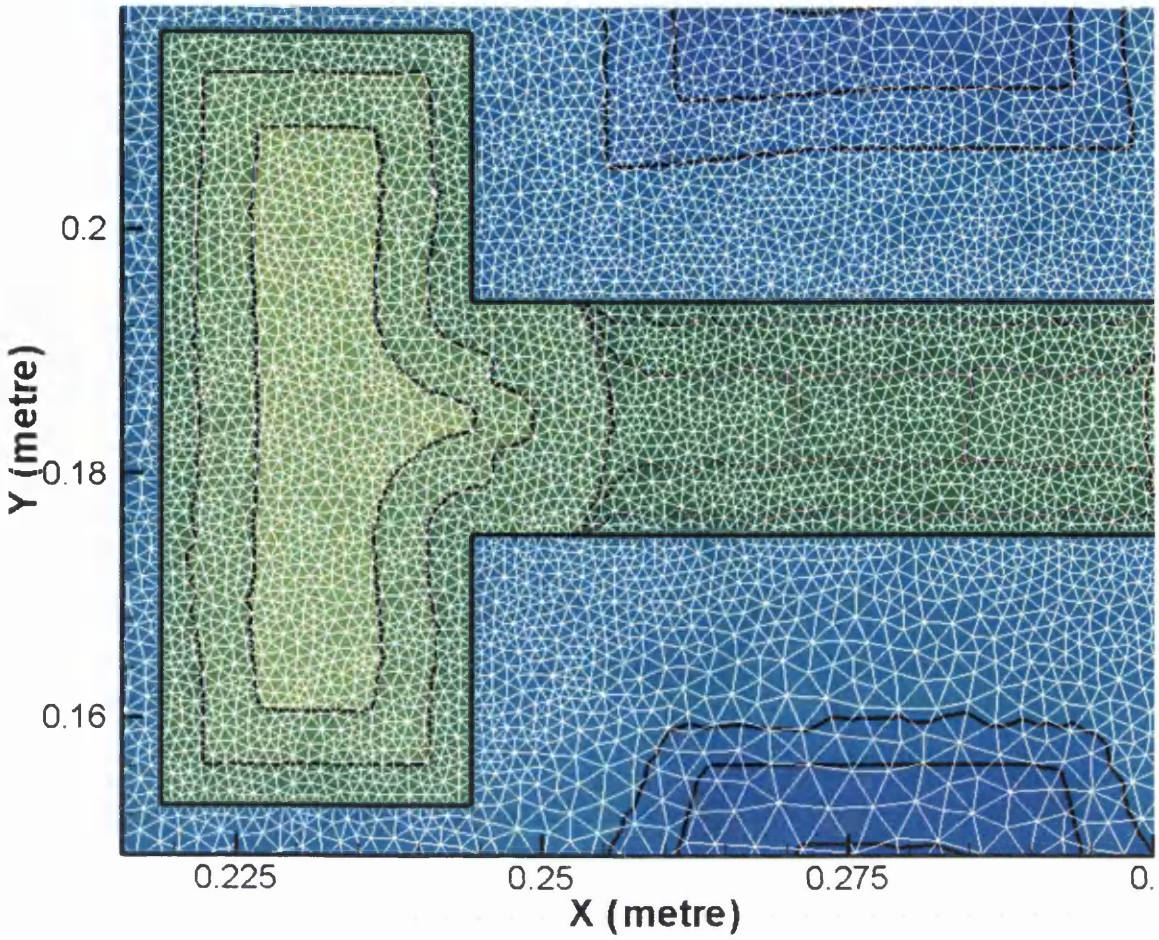

Figure 4.52: Enlarged section of Gear Blank casting with fine mesh

4.5.3 Variation in temperature profile through a section of gear blank casting model

The temperature profiles through a section of the gear blank casting model taken from the medial axis through the casting-mould interface to the mould boundary as shown by double pointed line in the dotted circle (Figure 4.53) were taken. Graphs shown in Figure 4.54 (a) and (b) illustrate the variation in temperature profile that has been obtained using double interpolation method through this selected section at eleventh time step for medium and fine point (mesh) densities.

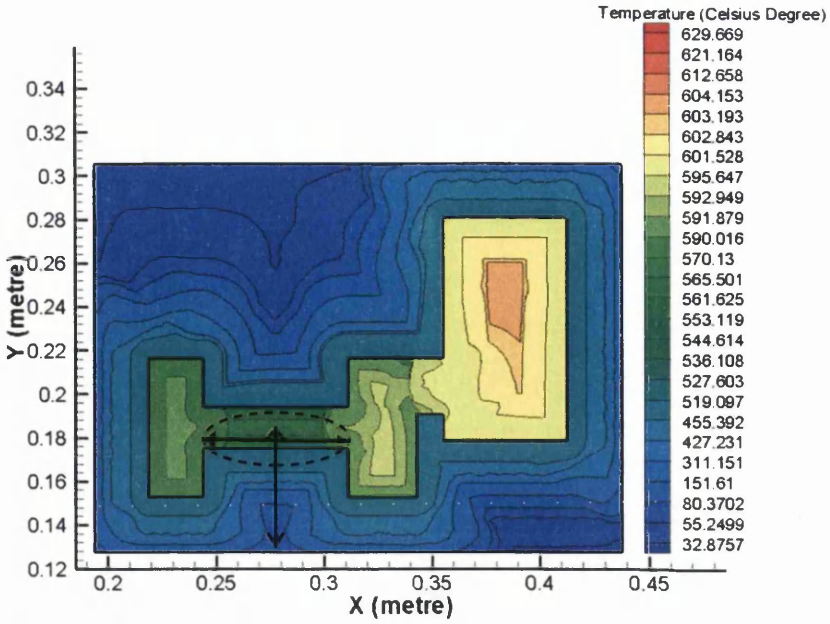

Figure 4.53: The sections of casting-mould model selected for showing variation in temperature profile

(a)

(b)

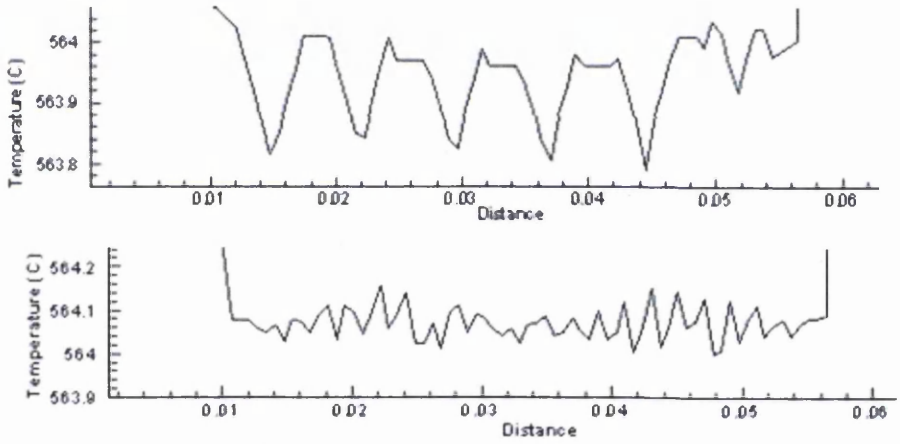

Figure 4.54: Graphs showing the variation in temperature profiles through the selected section of the model (a) with medium point (mesh) density and (b) with fine point density. Higher point density results in smoother temperature contours.

It is observed that the difference between the minimum and maximum temperatures at the edges of the 'zigzag' is greater in interpolated temperature solution with medium point (mesh) density as compared to fine point density. In this case the temperature difference with medium point density is observed to be slightly less than one and half times the temperature difference in edges of 'zigzag' generated by interpolated solution with fine point density. As the point density is increased, this temperature

difference is further reduced, thereby, resulting in smoother temperature contours. This also lends support to discussion on error generated by interpolation technique undertaken earlier in Section 4.5.1.

The other graph (Figure 4.55) showing temperature profile taken from a vertical section (vertical double arrow line in Figure 4.53) of the model of the gear blank casting that exhibited the 'zigzag' error conforms to temperature profile of the corresponding one-dimensional bar that is used by the interpolation algorithm.

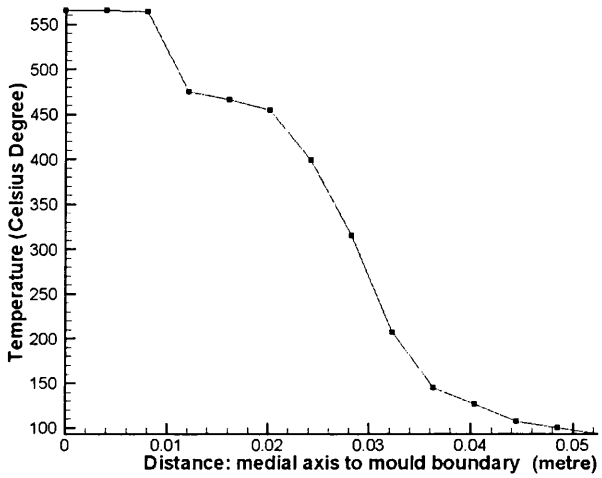

Figure 4.55: A graph showing the variation in temperature profile through a vertical section of the model at 11th time step

4.6 COMPARISON OF RUN TIME AND HUMAN INTERVENTION BETWEEN INTERPOLATION METHOD AND FINITE ELEMENT SOLUTION

4.6.1 Run time taken by the interpolation scheme

The run time including preparation, calculation and exporting of data file was recorded for different types of point densities for a case of Gear Blank casting that was discussed in detail in Section 4.6.1 and Section 4.7.1 and again in Section 4.8.2. The analysis was carried out on a Personal Computer having following specifications (Table 4.5).

Personal Computer Specifications	
Brand	Dell Workstation Precision 360
CPU	Intel Pentium 4 (3.00Ghz)
RAM	1.00 GB of RAM
Operating System	Windows XP Pro Service Pack 2

Table 4.5: Specifications of Personal Computer

The total number of nodes generated by the mesh generator for different point densities is presented separately for casting and mould in first four columns of Table 4.6. The time taken by the interpolation scheme for preparing geometrical data file, calculating the temperatures and exporting the Tecplot data file are summarised in Table 4.6. The interpolating, exporting and total time are then further represented graphically in Figure 4.56. It is observed that time increases linearly with the increase in number of points generated by the meshes of different densities. Since calculating time is only about 10% of the total time, further time savings can be effected by reducing the exporting time.

Gear Blank Casting				Interpolation time for 50 time-steps (seconds)			
Type of Mesh	Parts	Element Number	Node Number	Preparing time (calculate geom. Info.)	Calculating time (interpolation)	Exporting time (export all data files)	Total time
Medium	Cast	3634	1970	0.5	1	12	13.5
	Mould	3052	1718	0.5	2	10	12.5
	Total	**6686**	**3688**	**1**	**3**	**22**	**26**
Fine	Cast	22700	11727	1	9	73	83
	Mould	16006	8459	1	6	52	59
	Total	**38706**	**20186**	**2**	**15**	**125**	**142**
Very Fine	Cast	108958	55371	3	40	342	385
	Mould	211553	109185	3	78	670	751
	Total	**320511**	**164556**	**6**	**118**	**1012**	**1136**

Table 4.6: Interpolation time for Gear Blank casting with different mesh densities

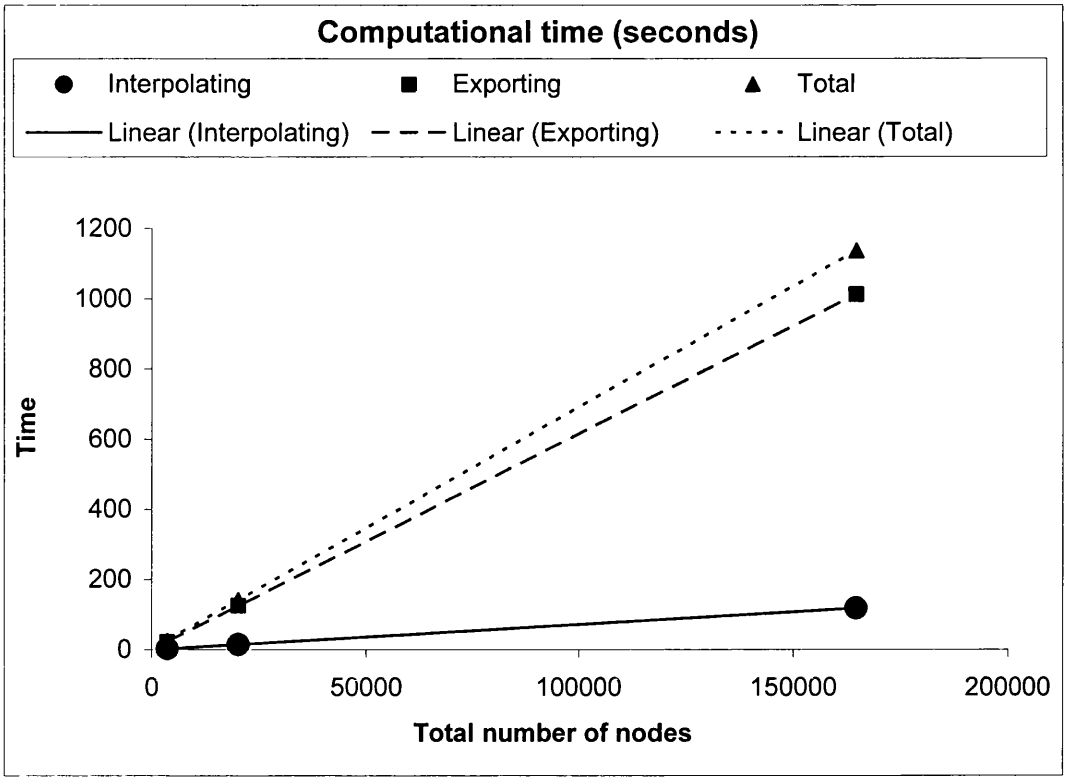

Figure 4.56: Graph showing time taken for interpolating, exporting and total time for different point densities (total number of nodes)

4.6.2 Comparison of run time and human intervention between a FE user and MAT based interpolation user

Table 4.7 provides the comparative human intervention time and inputs and the run time requirements on users using FE based solidification analysis and MAT based interpolation scheme for obtaining temperature solutions for castings.

Jobs	Tasks	Time	Auto/ Manual	FE User	Interpolation User
Modeling	Import file	5-10 min	Semi-auto	√	√
	Create new	1~2 hours	Manual	√	√
Geometric reasoning	MAT generation	10~30 sec	Auto		√
	Calculation of radius function	2~5 min	Semi-auto		√
	2D mesh generation	< 3 min	Auto	√	√
Calculation of geometrical information	Distance information (1D mesh)	1~5 sec	Auto		√
	Local thickness	1~5 sec	Auto		√
	Distance ratio	1~5 sec	Auto		√
Preparation of data file for solver	Mesh data (2D)	< 1 min	Auto	√	√
	Boundary Data	5-30 minutes	Semi-auto	√	
	Material Data	3~5 minutes	Manual	√	
Total pre-processing time				159 min	130 min
Solving time	Interpolation	26 sec			√
	FE	189 sec		√	
Total time				162 min	130.5 min

Table 4.7: Comparative Human intervention and Run time for FE and Interpolation users

The double interpolation scheme takes approximately 25% less time for a case of gear blank casting. The savings in time will however increase when the casting model becomes complex and involve denser mesh and application of complex boundary condition. On the other hand, once a database of temperature solutions has been created for a particular set of material

properties and boundary conditions, any shape and size of casting of same material can be analysed in shorter time and likely locations of hotspots can be predicted instantly.

4.7 ADVANTAGES OF INTERPOLATION SCHEME

The various advantages of MAT based interpolation scheme to predict casting temperature can be listed as under

1. One of the major advantages of this interpolation method is that it is fast in comparison to the conventional numerical simulation. The number of performed computer operations is linearly proportional to the number of mesh points in the casting. At a touch of a button, the whole simulation can be animated almost instantaneously.
2. The interpolation technique predicts relative variation in temperatures that compares well with the traditional numerical techniques and results obtained have same order of accuracy.
3. The interpolation scheme provides evolution of temperature profile in time since the spatial solution is time dependent, which is an added advantage over the Modulus Method.
4. Compared to geometric methods explained in Chapter 2, e.g. when compared to the Modulus Method, the current approach is advantageous as it is sensitive to material properties.

4.8 LIMITATIONS OF INTERPOLATION SCHEME

The MAT based interpolation scheme suffers from following limitations.

1. Despite its stated usefulness, this method is restrictive since only one type of boundary condition can be applied; either prescribed flux or prescribed temperature to the whole mould-cast assembly. Although, the interpolation algorithm can be expanded to incorporate varying and more complex boundary conditions by sectioning the cast-mould

assembly but that would defeat the very purpose and objective of providing a simple, fast and user friendly tool for Foundrymen.

2. The proposed method is less accurate compared to a numerical simulation method, particularly near the corners and sharp edges as is visible from the comparison shown in the cast studies. However the method always predicted correct hot spot location when compared to the Finite Element Method for all the geometries that were tested using the proposed scheme.

3. Like most geometric methods (like Modulus Method), it might invite criticism as it utilises the one-dimensional idealisation to solve two- or three- dimensional problems.

4.9 CLOSURE

A medial-axes-based solidification interpolation method has been proposed in this chapter. The method is a compromise between the full numerical casting simulation which is computationally expensive and the Modulus Method which is insensitive to the material properties and does not provide evolving temperature solutions. After a data bank of various temperature solutions from one dimensional bars has been created for a set of boundary conditions and particular material properties, the scheme then can provide instant solutions for casting of any shape and geometry as has been demonstrated through various case studies discussed in this chapter. The major advantages of this method are that it is fast and time saving, comprehensive and compares favourably with the conventional numerical simulation. The proposed method gives an instant "feel" of the design to its creator during the interrogation stage. The method can be effectively used as an add-on tool by the foundrymen to effect changes in the components, thus saving them precious time and costs during the design process. Since the objective of devising this technique is only to aid the technicians/draftsmen to make changes to the components, it is believed that such a technique, if used

wisely, can be useful in cutting down cost and time of the product development cycle, particularly in casting design and optimisation process.

But due to other limitations of this method, alternative techniques were studied to overcome the disadvantages posed by interpolation method. After a more rigorous literature review, another line of research was pursued to develop a method to predict solidification behaviour of the castings that was sensitive to material properties and boundary conditions while retaining elements of simplicity in its implementations. From the review of the literature in Chapter 2, it becomes apparent that some of the geometric techniques and geometric reasoning based methods hold a promise to answer some of the limitation faced in implementing the interpolation scheme. One such method known as the Heuvers' Circle method had traditionally been used by foundrymen to design castings but the method suffered from similar criticism because of its insensitivity to material properties and boundary conditions. This motivated further research to modify Heuvers' Circle method to take into account more realistic boundary conditions and different material properties of cast and mould. The next chapter will describe in detail the traditional Heuvers' Circle method and its modification to achieve the objective set out above.

REFERENCES

[1] J. P. Holman, "*Heat Transfer*", 7th Edition, McGraw-Hill Book Company, London, UK, 1992, pp 2-3.

[2] R. W. Heine and J. J. Uicker, "Risering by computer assisted geometric modeling", *AFS Transactions,* 1983, **91**, 127-136.

[3] Transcendata Europe Medial Object Technical Paper from their website http://www.fegs.co.uk/motech.html, 2002-2005, last accessed on 16th Jan 2006.

[4] http://www.fegs.co.uk/medial.html, 2002-2005, last accessed on 16th Jan 2006.

[5] Merlin Software Databank, School of Engineering, University of Wales Swansea, Swansea, UK, (Private communications)

[6] R. S. Ransing, W. K. S. Pao, M. P. Sood, C. Lin and R. W. Lewis, "An Enhanced Interpolation Algorithm using Medial Axis and its Application to Hotspot Prediction in a Mould-Casting Assembly", *International Journal of Cast Metals Research*, February 2005, Vol. 18, No. 1, pp. 1-12.

Chapter 5

A NOVEL APPROACH USING MODIFIED HEUVERS' CIRCLE METHOD FOR SOLIDIFICATION SIMULATION

CHAPTER LAYOUT
A method based on geometric reasoning techniques is proposed in this chapter to predict hot spots and make use of geometric parameters of the casting to obtain effective interface boundary conditions. This chapter carries on with the investigation of geometry based casting optimisation methods by coupling them with numerical simulation techniques to retain ease of use, speed and simplicity of geometric methods and at the same time achieve nearly same order of accuracy as offered by numerical methods. The work in this chapter is carried out in the context of literature on various geometric techniques that has been reviewed in Chapter 2 and essentially builds on the level of understanding that was attained on use of medial axis transformation techniques for solidification simulation in Chapter 3 and 4. This chapter first recaptures the limitations of various geometric reasoning based techniques including use of MAT for simulating solidification process from previous chapters. The chapter then goes on to briefly refresh the Medial Axis Transformation technique and discusses the conventional Heuvers' Circle methods and its limitations. The next section then proposes a modification to these two conventional techniques using Chvorinov's rule and implements a coupled approach using a numerical simulation method. Appendix A provides the justification for assumptions made in deriving the equation for obtaining effective values of interfacial heat transfer coefficient. The penultimate section then tests this newly developed approach on a simple casting geometry. The conclusions are then drawn from the research presented in this chapter for facilitating further testing and validation in next chapter.

5.1 INTRODUCTION

It was observed from literature reviewed that following on the experience gained over time using 'trial and error' methods and through undertaking expensive experiments, many 'dos' and 'don'ts' have evolved in the casting process. The classic example of this evolution is observed in Campbell's 10 rules [1], which are built on the four rules identified earlier. These rules consolidate the latest technological developments and facilitate production of high quality castings. Similarly his six feeding rules [2], which satisfy the heat transfer, volume, communication, thermal, geometrical and pressure criteria, are another example of work that has led and attracted further research in the field of castings which has already been discussed in the literature review.

The theoretical background on geometric methods was discussed in detail in Chapter 2 and then the medial axis transformation technique and its potential applications for solidification simulation using interpolation scheme were described in detail in Chapters 3 and 4. It was observed that these geometric methods (Chapter 2) and their innovation using an MAT based interpolation scheme (Chapter 3 and 4) pose certain limitations. These limitations and experience gained from using MAT technique for solidification simulation provided ground and an opportunity to further investigate other option for developing a coupled technique for thermal optimisation that uses MAT technique in combination with other geometric method and numerical simulation.

It was therefore, decided to explore other possibilities of using and modifying geometry based method, known as Heuvers' Circle method that hold promise to aid analysis of casting solidification process. This necessitates a description and analysis of the applications and limitations of the conventional Heuvers' Circle method thus paving way to propose a modification and its unification with MAT technique. These two geometry based methods are combined using Chvorinov's rule for predicting solidification time and achieving desired directional solidification in the castings. The newly developed approach is first tested on a simple two-dimensional casting geometry and the result is then validated using a FE based solidification analysis. It will be evident that

this method can constrain heat transfer coefficient values to yield more realistic values for foundry practices. The following chapter will then carry on with its further testing and validation using case studies on a variety of castings.

5.2 LIMITATION OF GEOMETRY BASED METHODS AND NEED FOR INNOVATION

As discussed in Chapter 2, in parallel with evolution of numerical optimization methods, some conventional approaches to solidification analysis have been driven by the casting geometry that essentially influences the sequence of solidification. These approaches simulate the solidification process using geometric parameters and link these parameters with the thermal properties of the metal, mould and heat transfer systems [1]. As discussed earlier in Chapter 2, one of the earliest optimization efforts was based on Modulus Method that had its origin in Chvorinov's classic rule [4] that related solidification time t_s of a casting to its modulus. The term modulus pertains to the ratio of heat content volume V to its heat transfer area A of the casting.

$$\textit{Solidification time } t_s = k\left(\frac{V}{A}\right)^2 \tag{5.1}$$

where k is a material constant depending on the cast and mould material. Derivatives of Chvorinov's rule given above in equation (5.1) have since been investigated and expanded by many researchers e.g. Wlodawer [4], Ravi and Srinivasan ([3],[5]), Tiryakioglu *et al.* ([6]-[8]), Berry *et al.* [9], Heine and Uicker [10], Neises *et al.* [11] and Luby *et al.* [12]. Their work has been discussed in detail in Chapter 2.

The various methods that have been developed over the years to model solidification pattern in solidifying castings have suffered from following limitations.

1 Trial and error methods based on experiments and intuitive and accumulated hands-on experience of foundrymen are quicker and easy to implement but do not always offer accuracy and optimal solution. The knowledge base often remains surrounded in 'mystique' and perishes or becomes unavailable with the movement of experienced foundrymen.

2 The FEM and FDM based numerical heat transfer/simulation packages provide detailed and accurate results but there are heavier computational and other costs attached to these methods. The costs include software prices, computational time and pre requisites of knowledge of material properties that is needed to use these softwares and interpret the results for implementation in foundries.

3 The numerical methods fail to assist foundrymen when there is a need to obtain quicker design iterations for rapid evaluation to optimise the solidification process.

4 On the other hand, the geometry based methods are simple, faster and relatively easier to implement but they don't always provide accurate results/predictions.

5 Most geometric methods offer only qualitative analysis and often invite criticism due to their insensitivity to material properties and boundary conditions.

6 Most of geometric methods based on Chvorinov's rule are only able to provide total solidification time for a casting without giving any transient details or local solidification times.

7 MAT based casting temperature approximation methods also assume uniform boundary conditions and rely on symmetry to predict relative solidification times. The MAT based interpolation

schemes proposed in Chapter 3 and 4 are also restrictive in application as only one type of boundary condition can be applied.

8 MAT based interpolation scheme also risks inviting criticism as it makes use of one-dimensional idealisation to solve two-dimensional problems. Many other geometric methods are 2D simplifications of 3D models.

It is thus gathered from discussion on various techniques to model solidification simulation that research in casting technology has been progressing towards achieving 'near optimal' solutions while attempting to keep the computational cost to minimum possible.

There was thus a compelling and strong case for using a coupled approach that inherits the speed of geometry based methods and also retains same order of accuracy as numerical techniques. The next section will now describe a similar approach which combines Chvorinov's rule with Heuvers' Circle method and Medial Axis Transformation technique with the Finite Element based simulation to predict casting temperature and provide optimal boundary conditions for further analysis. The research presented in this chapter aims to achieve these twin objectives in two FE simulations.

5.3 THE HEUVERS' CIRCLE METHOD

5.3.1 The Conventional Method

Heuvers' Circle Method ([4],[13],[14]) is also based on the modulus principle described earlier and implies that the modulus of a cross section must increase continuously in the direction of the feeder, if the freezing is to be prevented or steered directionally. As discussed in Chapter 2, Heuvers was the first to develop a practical method consisting of inscribing a series of circles (or spheres for three-dimensional castings) the diameter of which increases in the direction of the feeder head ([4],[13]). The underlying assumption is that larger the radius of the inscribed circle, longer is the time required for complete solidification in that part or section of the casting geometry. Figure 5.1 shows the largest inscribed circle in a L-shaped casting

and Figure 5.2 illustrates FE simulation results that confirm that the hotspot is located inside the largest inscribed circle.

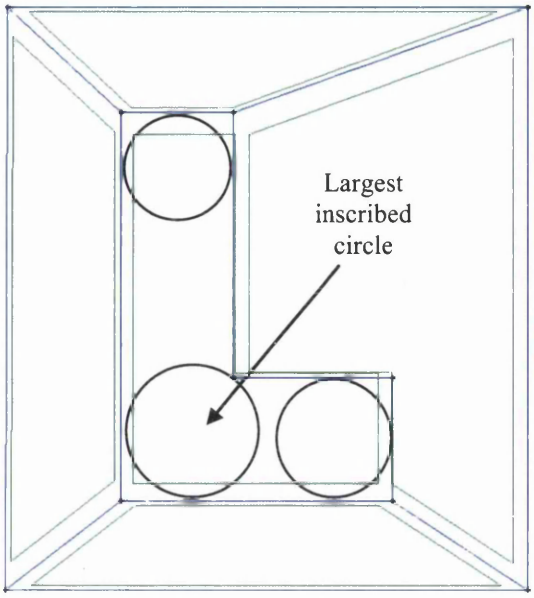

Figure 5.1: Prediction of hotspot using geometric reasoning based Inscribed Circle method in an L-shaped casting

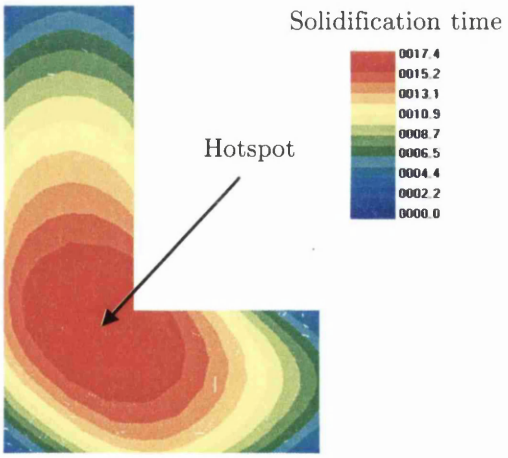

Figure 5.2: Hotspot location validated by FE based simulation which shows the hot spot inside the largest inscribed circle

Heuvers developed this method as an empirical test and applied it to sectional drawings to ensure conformity to principles of directional solidification [14]. A model of the casting is sketched to a scale of a 1:1 and

desired machining and contraction allowances are drawn in and then the circles are inscribed at points of intersections as is explained in Figure 5.3 and Figure 5.4. In the turbine wheel rim example (Figure 5.4), the padding additions have been designed on the basis of the Heuvers circles as they increase in diameter towards the feeder head.

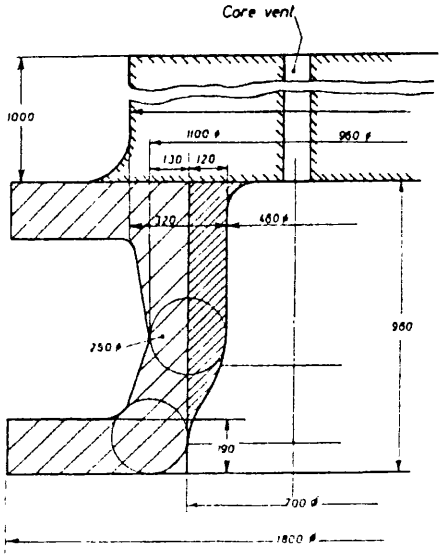

Figure 5.3: Double flange with Heuvers' circles up the feeder - Source: [4]

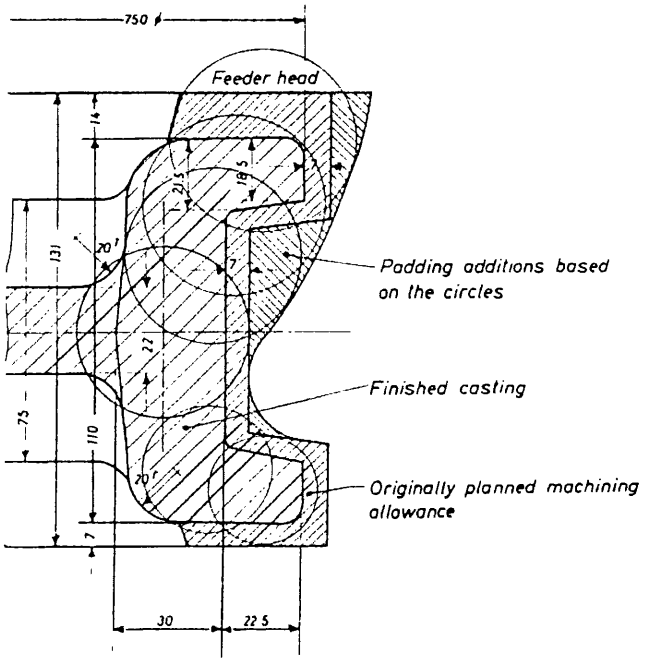

Figure 5.4: Heuvers' circles inscribed in turbine wheel rim - Source: [4]

5.3.2 Limitations of the Heuvers' Circle Method

In the previous example (Figure 5.3 and Figure 5.4.), the padding additions have been designed on the basis of the Heuvers circles as they increase in diameter towards the feeder head. The extent by which the diameters of these inscribed circles should increase was mostly solved 'intuitively' for unalloyed steels by earlier researchers. Invariably, the pad modulus was 1.1 times the modulus of the cross section in question. The padding thus added is essentially a correction to an erroneously designed casting and ultimately results in substantially increasing the size of the feeders [4]. As a result, the method invites criticism as such padding additions usually have to be removed through expensive machining operations. Criticism notwithstanding, the padding method remained one of the most important applications of the Heuvers' Circle method. Being purely geometric, the method could not suggest interface boundary conditions, which could otherwise be related to padding or insulation thickness and chills or die coating thickness. Like other geometric methods, Heuvers' circle method was also restricted in its application, as it remains a qualitative analysis, which is insensitive to material properties and boundary conditions e. g. the method would predict similar results for different materials and boundary conditions.

From the above discussions, it is concluded that this method on its own has limitations to its use. Due to these limitations, it was decided to utilize the Heuvers' circle method in combination with other geometric methods (MAT technique, Modulus method based on Chvorinov's rule) for the purpose of further research.

5.4 THE PROPOSED COMBINED METHOD

5.4.1 Background

As was observed earlier in this chapter and also in Chapter 2, Wlodawer [4] used the relationship between solidification time and modulus of the casting for designing the feeder in such a way that the modulus of the feeder is greater than that of the casting which ensured adequate feeding and casting soundness. This application of this concept was limited at that time to heavy steel castings in sand moulds. It was thus observed that to obtain a sound

steel casting in sand moulds, the temperature gradient must be at least 0.5^0C/cm length of the casting as the solidifying casting can still be fed from adjoining section of the casting that is 0.5^0C hotter. A section with a longer solidification time also has a larger modulus. Experiments showed [4] that modulus must be larger by a factor of about 1.1 to ensure the directional solidification with adequate feeding from thicker sections to thinner sections. Similarly the modulus for the feeder head must be at least 1.2 times larger than that of the casting or the modulus must increase by 10% from casting across the ingate to the feeder as given in equation (5.2) below [4].

$$M_{casting} : M_{neck} : M_{feeder} = 1 : 1.1 : 1.2 \qquad (5.2)$$

As discussed in Chapter 2, 3 and 4, the medial axis transform (MAT) of a two-dimensional region is a locus of the center of an inscribed disc of maximal diameter as it rolls within the domain while maintaining the contact with the domain boundary on at least two points, as shown in Figure 3.1 in Chapter 3. The centres of all these interior maximal discs are known as medial points. Figure 3.2 in Chapter 3 shows the extension of the concept to three dimensions, in which maximal spheres are inscribed. In this case the medial axis becomes a medial surface for a three dimensional object [15]. Thus it can be noted that for n-dimensional object, the medial-axes are (n-1)-dimensional entity of that region. The MAT provides us with the radius information for points located on its medial axes and it is this information that has been utilised for implementing a modified version of Heuvers' circle method.

5.4.2 Novelty in the proposed method

As discussed in earlier sections, the traditional numerical simulation methods are useful when the stated aim is to seek accuracy in predictions but even with the current age and efficiency of computer simulation tools and the advancements made in numerical simulation of casting processes, the optimisation procedures remain highly time consuming ([16],[17]). This study aims to propose an algorithm that inherits the advantages of geometric methods and at the same time derives a relative variation of heat transfer

coefficient values that helps in achieving the desired solidification pattern in castings. The method first predicts the hotspot using the Heuvers' circle method and then relates the geometric information to obtain effective interface boundary conditions and finally uses the Finite Element based numerical analysis to accurately simulate the optimized design.

The method utilizes the relationship between the Heuvers' circle method and a Medial Axis Transformation technique, which automatically calculates a series of inscribed circles for a given geometry. The technique proposes a geometric optimisation technique for ensuring directional solidification and relocating hotspots in the feeder. The approach outputs optimal values of interfacial heat transfer coefficients, which then can be used in the finite element analysis for further detailed and accurate simulation. When implemented, the method considerably cuts down the number of FE simulations needed to be performed during the design cycle.

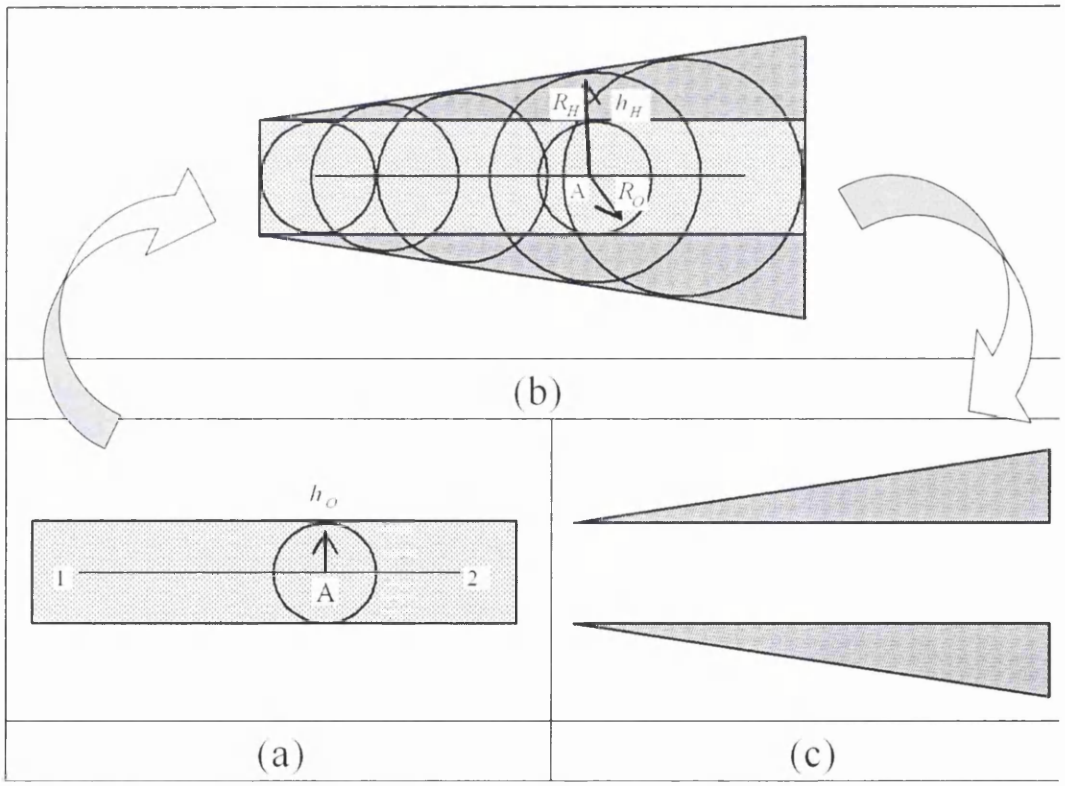

Figure 5.5: Heuvers' Circle Method: (a) original casting section, (b) the casting with Heuvers' circles and (c) the additional padding required as per Heuvers' circles

As deduced from earlier discussions on Heuvers' circle method, a casting, with a series of Heuvers' circles is in fact a new imaginary casting (Figure 5.5), whose modulus is increasing in the direction of the feeder. The aim is to obtain effective interface boundary conditions (IBCs) using the Heuvers' inscribed circle radius information in such manners that these IBCs can help achieve the same solidification pattern as would have been provided by the imaginary casting. One such option is to relate the geometric parameters (radius information) with the boundary conditions e.g. relating the modified Heuvers' radii to interfacial heat transfer coefficient (H_{Int}) to achieve the desired solidification pattern. If t_s is the solidification time, R is the radius of casting at a given point on its medial axis and h is the interfacial heat transfer coefficient, using Equation (5.1), it can be said that

$$t_s \propto R^2 \text{ if h is constant and } t_s \propto \frac{1}{h} \text{ if R is constant}^{1} \tag{5.3}$$

$$\therefore \text{ it can be inferred that } t_s \propto \frac{R^2}{h} \tag{5.4}$$

Now for the original casting, at point A on the medial axis (point A is defined in Figure 5.5 which also shows R_O and R_H), Equation (5.4) becomes

$$t_O \propto \frac{R_O^{\,2}}{h_O} \tag{5.5}$$

Hence, for an imaginary casting with increasing moduli, at point A on the medial axis,

$$t_H \propto \frac{R_H^{\,2}}{h_O} \tag{5.6}$$

[1] FE simulation of equivalent 2D models of one-dimensional bars has been undertaken to support this assumption. The details, results and discussions pertaining to five cases of 1D bars used for the FE analysis are given in Appendix A at the end of this chapter.

To achieve the same effect of increased thickness of the imaginary casting, the corresponding heat transfer coefficient value h_O needs to be modified to h_H if t_H and R_O are to be kept constant

$$\therefore t_H \propto \frac{R_O^2}{h_H} \tag{5.7}$$

Therefore, from equations (5.6) and (5.7),

$$\frac{R_H^2}{h_O} = \frac{R_O^2}{h_H} \tag{5.8}$$

$$\therefore h_H = h_O \left(\frac{R_O}{R_H} \right)^2 \tag{5.9}$$

where R_O and h_O are original radius and interfacial heat transfer coefficient, R_H and h_H are Heuvers' radius and the modified interfacial heat transfer coefficient respectively and t_O and t_H are original solidification time and one achieved after applying the Heuvers' circle method. The novelty and originality of the proposed method including Equation (5.9) has been appreciated by Prof. John Campbell in his book [1] on page 133-134 while describing Feeding Rule 5 (feed path requirement).

5.4.3 Implementation of the proposed method

Equation (5.9) provides the linkage between Heuvers' circles and the interface boundary conditions. After having derived an equation that can provide modified values of interfacial heat transfer coefficients using radius information, the next step is to implement this method and prove its workability on a casting section. The proposed method can now be used in a Foundry environment by implementing following steps as shown in Figure 5.6:

1. Identify possible hotspot locations within a casting geometry by assuming uniform solidification process. This can be achieved by applying the same heat transfer coefficient value across all metal-

mould interfaces. The simulation is run on a numerical software package [18].

2. Create a model of the casting in a CAD package and generate its medial axis [15].This provides a series of medial points across the length of medial axis and their respective inscribed radii.
3. Decide on a desired path of directional solidification that is intended to be followed to ensure sound casting without any defects.
4. Compute the Heuvers' radii for the selected points along the medial axis. This was accomplished using an Excel spreadsheet by increasing the original radius at 1 in 10 gradients along the medial axis as given in Equation (5.2). For this purpose, a start is made from the farthest point and then working towards the feeder following the directional solidification path decided in step 2 earlier.
5. Calculate the modified heat transfer coefficient values using Equation (5.9) for each of those sections along the desired path of solidification and apply these values as modified boundary conditions.
6. Undertake another Finite Element simulation with the modified heat transfer coefficient values to ensure that the desired directional solidification path is obtained.
7. Correlate the modified heat transfer coefficient values to real feeding design decisions such as insulation, padding, chills, die-coating thickness, location of feeders including other methods to keep the mould either cool or warm. All of these methods influence and help in steering the direction of solidification along desired path.

5.5 TESTING THE NEW METHOD

It was decided to test the method that has been discussed in preceding paragraphs on a simple hypothetical L-shaped casting geometry. The medial axis was generated using tools available in the CADfix package (Figure 5.7). Observing the radius information obtained from CADfix for this casting, it could be predicted that the hotspot is likely to be found at the junction of both arms in L-shaped casting as shown in Figure 5.1 as this is the centre of the largest inscribed circle in the casting. The finite element simulation with uniform solidification was then carried out using Merlin [18]. The initial

casting temperature for aluminium alloy (LM24) was kept at 650°C and mould (H13 alloy steel) was kept at 150°C initial temperature. The thermal Conductivity values of 186.28 W/mK and 33.9 W/mK were assumed for metal and mould respectively. The boundary conditions comprising a uniform interfacial heat transfer coefficient on cast-mould interface was assumed at 3000 W/m^2K and convection to ambient at 75 W/m^2K from exterior of mould to ambient at 20°C was considered.

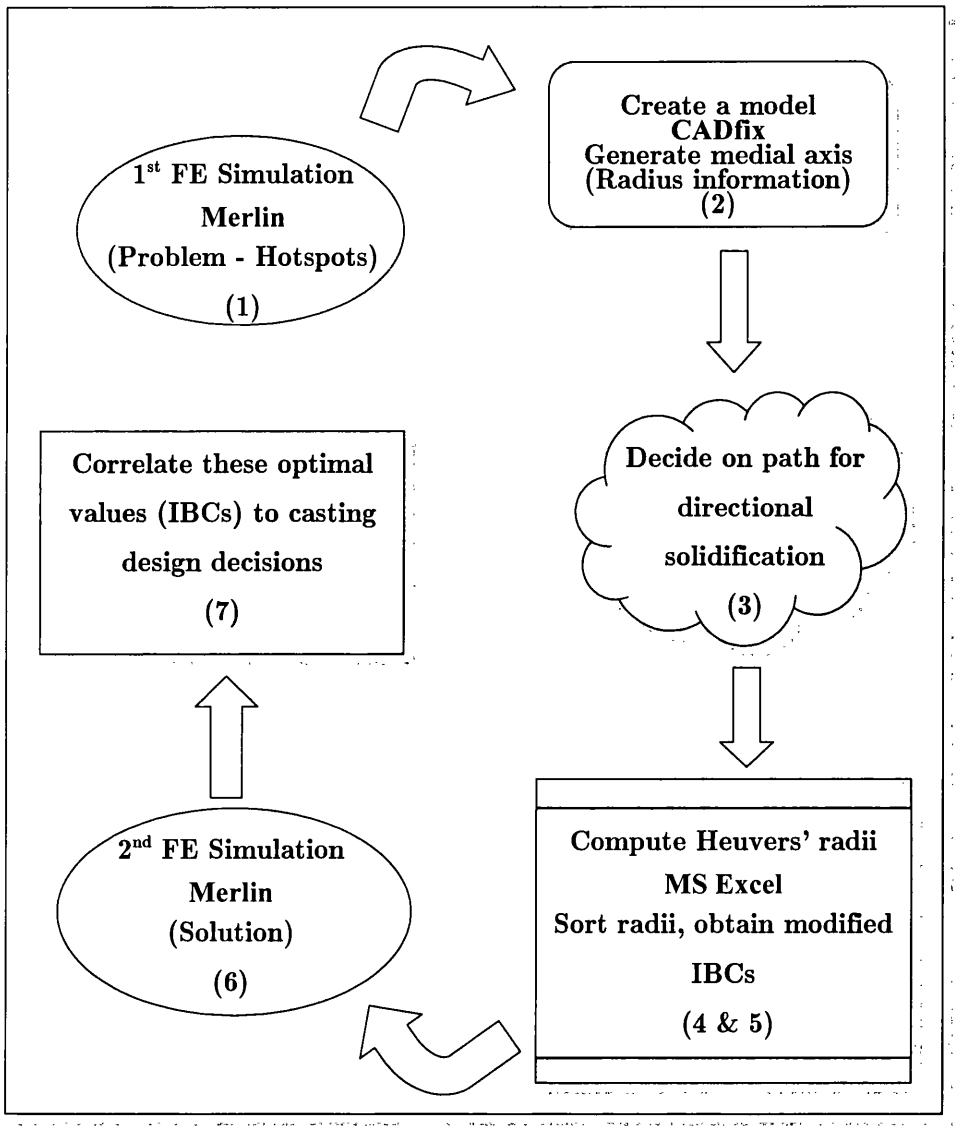

Figure 5.6: Flow diagram illustrating implementation of Modified Heuvers' Circle method

The solidification history from this FE simulation shows (Figure 5.8) a hotspot in this L-shaped casting which was in fact located inside the largest inscribed circle i.e. at same place as predicted by the geometric information

of the casting (Figure 5.1). The aim now is to move this hotspot from this location up along the vertical arm of the L shaped casting where the feeder is located using the new method.

The length of the medial axis, the relative distance between points and radii at few selected points on the medial axis were also obtained using the CADfix package [15]. To achieve directional solidification, it was assumed that the Heuvers' radii (R_H) be increased by 1 cm for every 10 cm length of the casting measured along the medial axis. Using this radius information, the Equation (5.9) gave us the modified values of interfacial heat transfer coefficient (h_H) which are given in Table 5.1 .

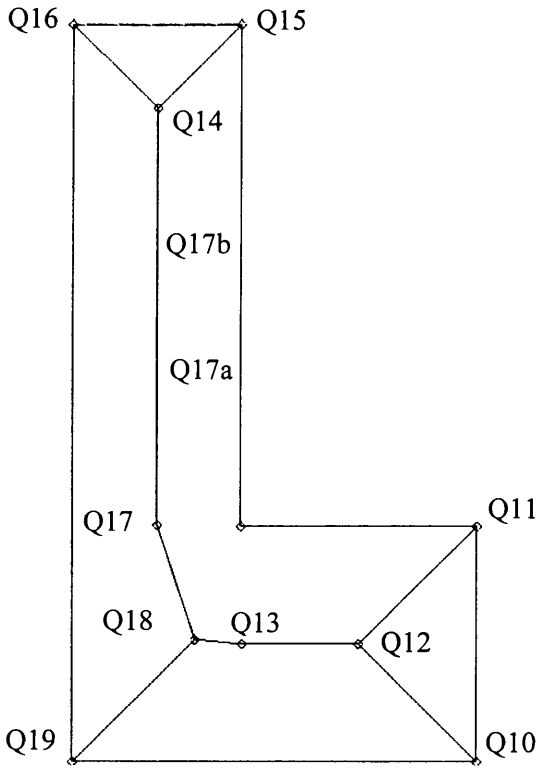

Figure 5.7: L-shaped casting geometry showing medial axis and medial points where Heuvers' radius was computed

The casting geometry was then subdivided into section and the modified values of interfacial heat transfer coefficients were then applied on respective surfaces of the cast-mould boundary. The finite element simulation was again carried out to observe the solidification behaviour of the casting. It is

observed that the hotspot has now moved towards the desired location (Figure 5.9) at the top of the vertical arm of the L-shaped casting geometry.

Points on Medial Axis	**Original IHTC h_o (W/m²K)**	**Original Radii (cm) R_o**	**Heuvers' Radii (cm) R_H**	**Modifying factor $(R_o/R_H)^2$**	**Modified IHTC h_H (W/m²K)**
Q12	3000.00	1.753	1.75	1.00	3000
Q13	3000.00	1.751	1.93	0.824	2472
Q18	3000.00	1.816	2.01	0.758	2274
Q17	3000.00	1.250	2.20	0.680	2040
Q17a	3000.00	1.250	2.33	0.287	861
Q17b	3000.00	1.250	2.59	0.232	696
Q14	3000.00	1.250	2.86	0.190	570

Table 5.1: L-shaped casting - Original and Heuvers' radii and corresponding original and modified values of interfacial heat transfer coefficients

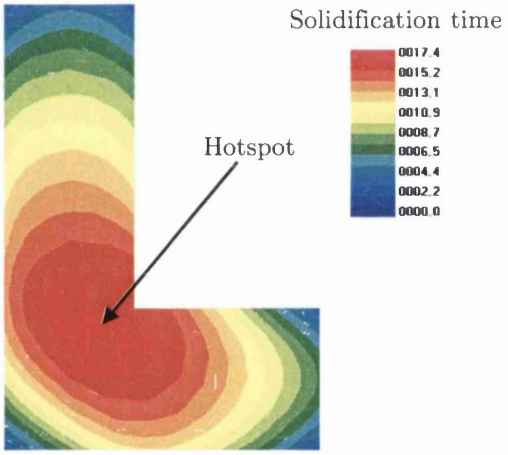

Figure 5.8: L-shaped casting - Solidification history showing freezing time contours from FE simulation with uniform Interfacial Heat Transfer Coefficient values on all boundaries

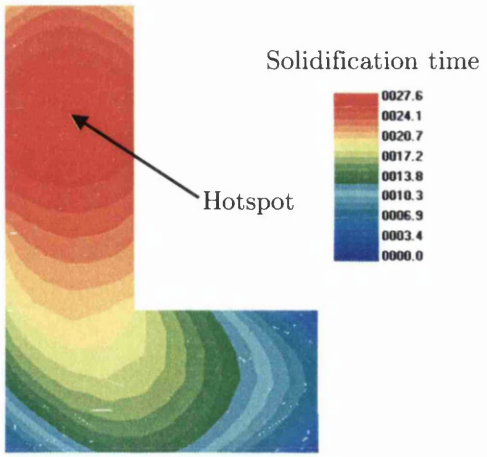

Figure 5.9: L-shaped casting - Solidification history showing freezing time contours from FE simulation with Heuvers radii based modified Interfacial Heat Transfer Coefficient values on selected surfaces of the casting

5.6 CLOSURE

The geometric reasoning techniques have often been criticized for their insensitivity to material properties and different boundary and metal-mould interface conditions. On the other hand, a complete numerical simulation can be computationally very expensive. In this chapter an innovative hybrid technique has been proposed that has advantages of both techniques. The Heuvers' circle method – a popular geometric reasoning technique of seventies has been innovatively used in combination with the Medial Axis Transformation technique to optimally design the thermal control with in a cast-mould system. The method can constrain heat transfer coefficient values to achieve better control over heat flux rate between cast and mould. Finite Element based optimisation techniques generally require a large number of simulation iterations to achieve this task. However, the method proposed in this chapter considerably brings down the number of FE simulations that needs to be performed during the casting design cycle. The method provides an important lead into the numerical values of interfacial heat transfer coefficients for facilitating more detailed numerical analysis, thereby saving precious time and resources. As a result of the proposed technique, it is estimated that foundry engineers will be able to achieve optimal feeding design in just TWO Finite Element simulations.

REFERENCES

[1] J. Campbell, *Castings Practice: The Ten Rules of Castings,* Butterworth-Heinemann, Oxford, UK, ISBN: 0750647914, May 2004.

[2] J. Campbell, *Castings 2nd Edition* Butterworth-Heinemann, Oxford, UK, 2003 p 210.

[3] B. Ravi and M. N. Srinivasan, "Casting Solidification Analysis by Modulus Vector Method", *International Journal of Cast Metals Research*, 1996, 9: 1-7.

[4] R. Wlodawer, "*Directional Solidification of Steel Castings*", Pergamon Press, Oxford, 1966

[5] B. Ravi and M. N. Srinivasan. "Feature-Based Castability Evaluation", *International Journal of Production Research*, 1995, Vol. 33 (12): 3367-3380.

[6] M. Tiryakioglu, E. Tiryakioglu and D. R. Askeland, "The Effect of Casting Shape and Size on Solidification Time: A New Approach", *International Journal of Cast Metals Research*, 1997, 9, 259-267.

[7] M. Tiryakioglu and E. Tiryakioglu, "A Comparative Study of Optimum Feeder Models for Castings", *International Journal of Cast Metals Research*, 2001, 14, 25-30.

[8] M. Tiryakioglu, E. Tiryakioglu and J. Campbell: *International Journal of Cast Metals Research*, 2002, vol. 14, pp. 371-375.

[9] J. Berry, V. Kondic and G. Martin, "Solidification times of simple shaped castings in sand models", *Modern Castings*, 1959, 36, 39

[10] R. W. Heine and J. J. Uicker, "Risering by Computer assisted Geometric Modeling", *AFS Transactions*, 1983, 91, 127-136.

[11] S. J. Neises, J. J. Uicker and R. W. Heine, "Geometric Modeling of Directional Solidification based on Section Modulus", *AFS Transactions*, 1987, 95, 25-30.

[12] S. C. Luby, J. R. Dixon and M. K. Simmons, "Designing with Features: Creating and Using Features Database for Evaluation of Manufacturability of Castings", *ASME Computer Review*, ASME, 1988: 285-292.

[13] J. Campbell, *Castings.* Reprinted series. Butterworth-Heinemann, Oxford, UK, 1997, 184-185.

[14] P. R. Beeley, "*Foundry Technology*", London, Butterworths, 1972, 125.

[15] http://www.fegs.co.uk/CAE.html, 2002-2005, last accessed on 16th Jan 2006 and http://www.fegs.co.uk/medial.html, 2002-2005, last accessed on 16th Jan 2006.

[16] R. S. Ransing and R. W. Lewis, "A Thermo-elasto-visco-plastic Analysis for Determining Air Gap and Interfacial Heat Transfer Coupled with the Lewis-Ransing Correlation for Optimal Feeding Design", *Modeling of Casting, Welding and Advanced Solidification Processes VIII*, Ed. BG Thomas and C. Beckermann, San Diego, USA, 1998: 731-738.

[17] R. S. Ransing and R. W. Lewis, "Optimal Design of the Die Coating Thickness Using the Lewis-Ransing Correlation", *International Journal of Cast Metals Research*, 1997, **9**, 269-277.

[18] http://www.swan.ac.uk/civeng/Research/casting/merlin/index.html, accessed in May 2005.

Appendix A

Finite Element Simulation of one-dimensional bars to support the assumption made in Equation 5.3 in Chapter 5

It was assumed in Equation 5.3 in Chapter 5 that $t_s \propto \frac{1}{h}$ if R is constant *i.e.* solidification time is inversely proportional to the interfacial heat transfer coefficient value if the casting shape and size remains constant. FE simulation of equivalent 2D models of one-dimensional bars was undertaken to support this assumption. The details pertaining to five cases of 1D bars used for the FE analysis are given in Table A.1.

Bar No.	Casting Length (cm)	Mould Length (cm)	Bar Thickness (mm)	Material (Casting and Mould)
1	5	5	5	LM25 and Sand
2	10	10	5	LM25 and Sand
3	5	10	5	LM25 and Sand
4	10	10	5	LM25 and H13
5	10	40	5	LM25 and H13

Table A.1: Details of 1D bars used for FE analysis

First Example

Two one-dimensional bars (Bar 1 and 2 in Table A.1) were created with an interface at the centre. These were 10 cm and 20 cm long and 5 mm thick with a casting-mould interface at 5 cm and 10 cm respectively. The bar dimensions for first bar are shown in Figure A.10. The bar was meshed and a mesh grid file was created. The bar had 36 elements and 40 nodes. It should be noted that although the bar has a finite thickness, it still approximates to 1D solution as there was only one linear element across the thickness and adiabatic conditions were applied on both sides of the thickness as shown in Figure A.11.

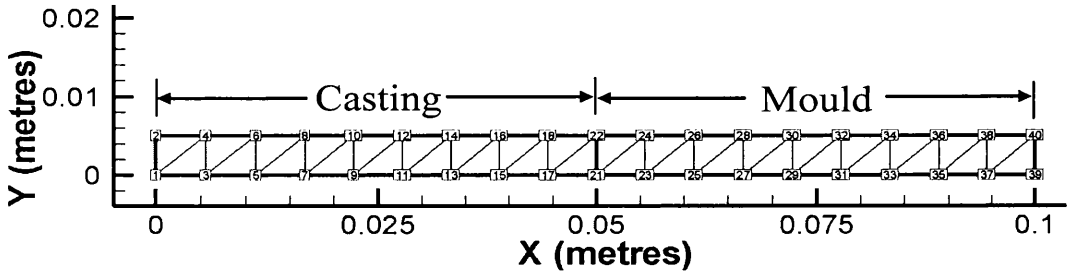

Figure A.10: 2D model of 1D bar with mesh result

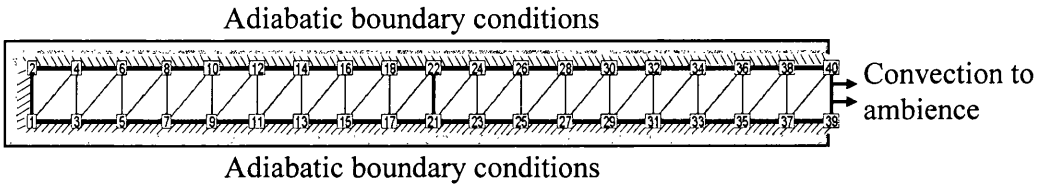

Figure A.11: Boundary conditions for 1D bar

Typical properties for the aluminium casting alloy (LM25) and sand casting process were used. The properties for aluminium alloy casting were: solid density $\rho_c = 2680$ kg/m^3, thermal conductivity $k_c = 186.3$ W/mK, specific heat $C_p = 1093$ J/kgK and for the sand mould were: $\rho_m = 1000$ kg/m^3, $k_m = 0.8$ W/mK and $C_{pm} = 709$ J/kgK [1]. The imposed boundary condition to the exterior of the mould was convection ($h_\infty = 200$ W/m^2K) to air at $T_\infty = 30^oC$. The sand was initially at 30^oC while the initial temperature of the molten aluminium (LM25) was at 650^oC.

The FE analysis was first carried out by assuming an inter-facial heat transfer coefficient value of $h_{\text{inf}} = 4000$ W/m^2K between the casting and the sand. The simulation was run for 5000 seconds and solidification results were analysed. Then a series of one-dimensional models of the same bars were analysed by varying interfacial heat transfer coefficient values (*i.e.* $h_{\text{inf}} = 3500, 3000, 2500, 2000, 1500, 1000, 500$ W/m^2K). The time taken for cast temperature at node '1' (Figure A.10) to reach the solidus temperature of 550^oC was recorded for both bars. (Note that as a result of boundary conditions, the temperature at node '1' was identical to the temperature value at node '2'). The results from this analysis for Bars 1 and 2 are given in

Table A.2 and are graphically demonstrated in Figure A.12.

Interfacial heat transfer coefficient (h_{inf} W/m^2K)	**Total Solidification time (seconds)**	
	Bar 1 (10cm long, Casting=5cm & Mould=5cm)	**Bar 2 (20 cm long, Casting=10cm & Mould=10cm)**
4000	542	2360
3500	592	2470
3000	626	2610
2500	664	2780
2000	720	3010
1500	792	3230
1000	985	3690
500	1480	4300

Table A.2: Time taken to reach solidus temperature at node '1' for Bar 1 and 2 for different values of interfacial heat transfer coefficient

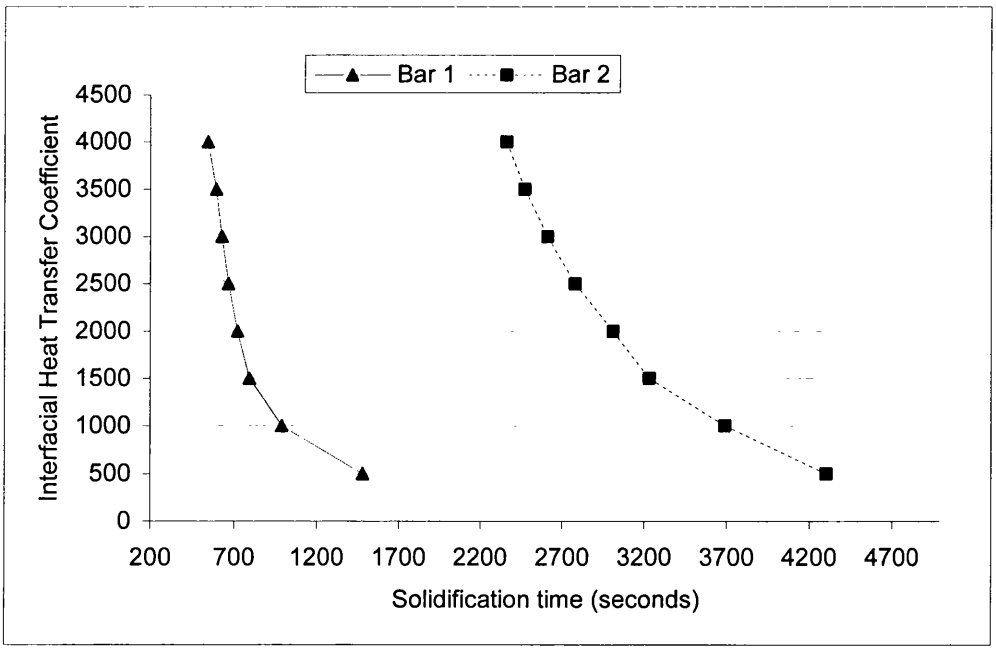

Figure A.12: Graph showing relationship of interfacial heat transfer coefficient values with the solidification time for Bar 1 and Bar 2

The results from both bars are consistent with each other and it is observed that the solidification time is inversely proportional to the variation in

interfacial heat transfer coefficient values. The increase in values of interfacial heat transfer coefficient increases the heat flux between the casting and the mould boundary thereby reducing the solidification time. It was also observed that the increase in length of 1D bar only resulted in the increase in the total solidification time and the nature of the graph remained the same.

Second Example

Another one-dimensional model of a bar was created with an increased mould length. This bar was 15 cm long with casting length of 5 cm and mould length of 10 cm and with 5 mm bar thickness. The 1D bar had 56 elements and 60 nodes Figure A.15. Material properties and boundary conditions similar to one assumed for first example were applied and the FE analysis was carried out for a series of bars with varying values of interfacial heat transfer coefficient. The results from Bar 3 were compared graphically with Bar 1 for studying the effect of increased value of mould length on the solidification time and these are shown in Table A.3 and Figure A.13.

Interfacial heat transfer coefficient (h_{inf} W/m^2K)	**Total Solidification time (seconds)**	
	Bar 1 (10cm long, Casting=5cm & Mould=5cm)	**Bar 3 (15 cm long, Casting=5cm & Mould=10cm)**
4000	542	771
3500	592	852
3000	626	933
2500	664	1000
2000	720	1060
1500	792	1120
1000	985	1260
500	1480	1670

Table A.3: Time taken to reach solidus temperature at node '1' for Bar 1 and Bar 3 for different values of interfacial heat transfer coefficient

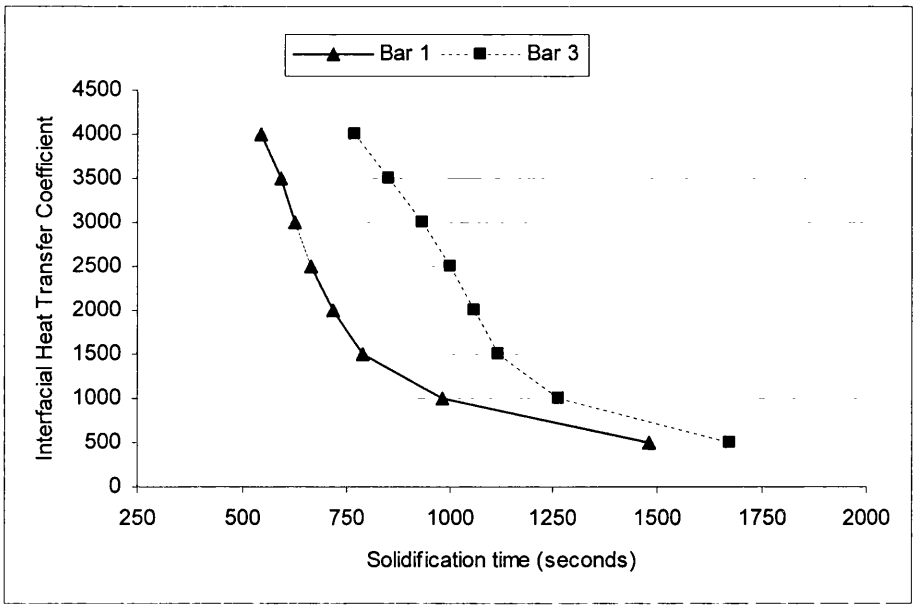

Figure A.13: Graph showing relationship of interfacial heat transfer coefficient values with the solidification time for Bar 1 and Bar 3

The increase in the solidification time as a result of increase in the mould length can only be associated with the low conductivity value of sand mould. The temperature values at node '39' (which is a node at the mould boundary as shown in Figure A.10) were plotted against the solidification time for Bar 1 which had solidified completely in 664 seconds when an interfacial coefficient value of $h_{inf} = 2500\ \mathrm{W/m^2}K$ was applied (Table A.3). It is observed that the temperature at node '39' at complete solidification was $258^{o}C$ (Figure A.14).

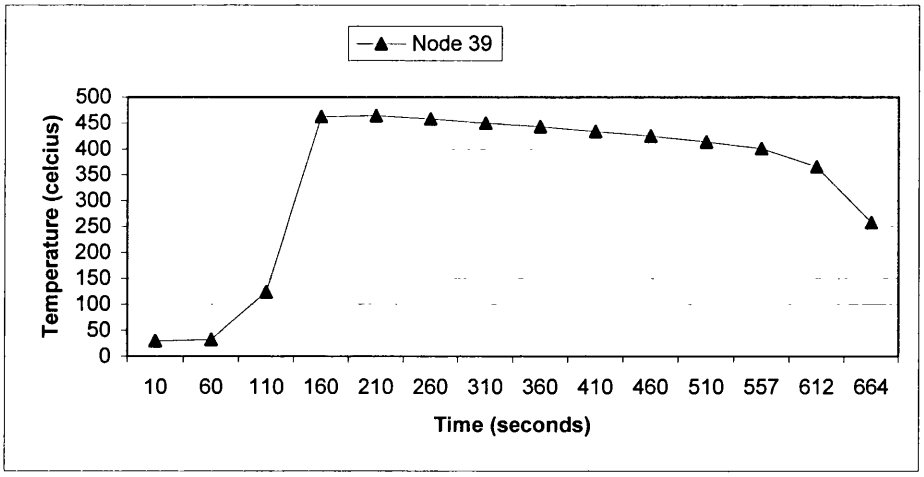

Figure A.14: Graph showing change in temperature at node '39' (mould boundary) at different time during the solidification for Bar 1

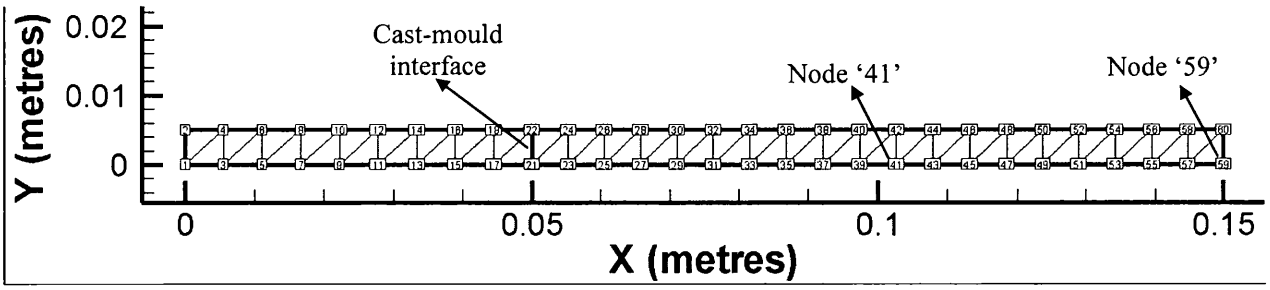

Figure A.15: Mesh result for Bar 3

Similar graph was now plotted for Bar 3 for temperature values at node '41' (almost half way through the mould length, which was mould boundary for Bar 1 in previous graph) and node '59' at mould boundary (Figure A.15). It is noticed that at same time (664 seconds) during the solidification, the temperature at node '41' was still $514^{o}C$ (Figure A.16) as against $258^{o}C$ noticed for Bar 1. The heat at this point still had to travel another 5 cm of mould length through the sand mould before being dissipated to surroundings through convection. Therefore, even though the increase in the mould length slightly increases the heat capacity of the sand mould, its low conductivity increases the solidification time for Bar 3 to 1000 seconds (Table A.3).

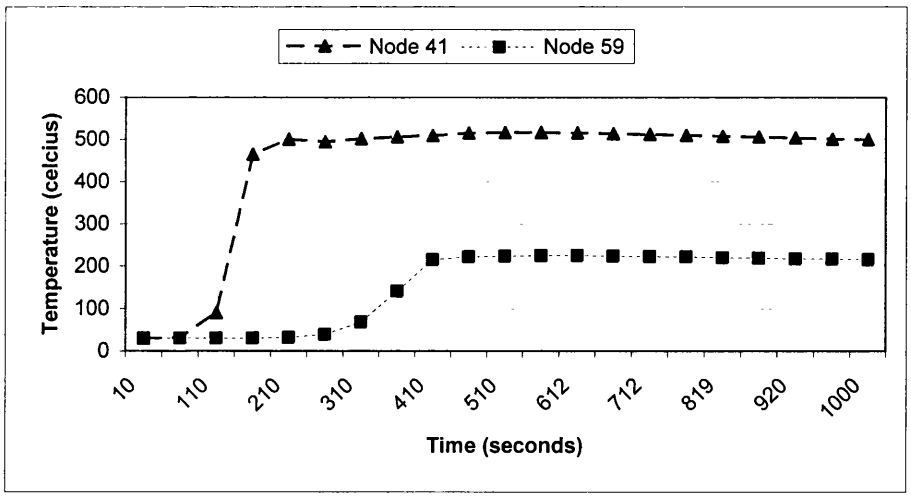

Figure A.16: Graph showing change in temperature at node '41' (half way through the mould and node '59' (mould boundary) at different time during the solidification for Bar 3

However, the solidification time is still observed to be inversely proportional to the variation in interfacial heat transfer coefficient values Figure A.13.

Third Example

Two more bars with varying mould length (Bar 4 and 5: Table A.1) were analysed using a different mould material. The casting was again assumed to be aluminium casting alloy (LM25) and the mould was assumed to be H13. Material properties for the aluminium cast were assumed to be same as used for Bar 1 and for the H13 mould, the properties were: $\rho_m = 7721\ \text{kg/m}^3$, $k_m = 33.9\ \text{W/mK}$ and $C_{pm} = 623\ \text{J/kgK}$ [1]. The initial temperature for mould was kept at 150^oC while the initial temperature of the molten aluminium (LM25) was at 650^oC.

The FE analysis was first carried out by varying the inter-facial heat transfer coefficient values between the casting and the mould (*i.e.* $h_{\text{inf}} = 9000,\ 8000,\ 7000,\ 6000,\ 5000,\ 4000,\ 3000,\ 2000,\ 1000\ \text{W/m}^2K$). The FE simulation was run for 5000 seconds and the time taken for cast temperature at node '1' to reach the solidus temperature of 550^oC was recorded. The results from this analysis are given in Table A.4 and are further graphically shown in Figure A.17.

Interfacial heat transfer coefficient (h_{inf} W/m^2K)	**Total Solidification time (seconds)**	
	Bar 4 (20cm long, Casting=10cm & Mould=10cm)	**Bar 5 (50 cm long, Casting=10cm, Mould=40cm)**
9000	670	620
8000	700	640
7000	720	670
6000	742	690
5000	772	710
4000	802	750
3000	822	790
2000	882	832
1000	1140	1120

Table A.4: Time taken to reach solidus temperature at node '1' for Bar 4 and 5 for different values of interfacial heat transfer coefficient

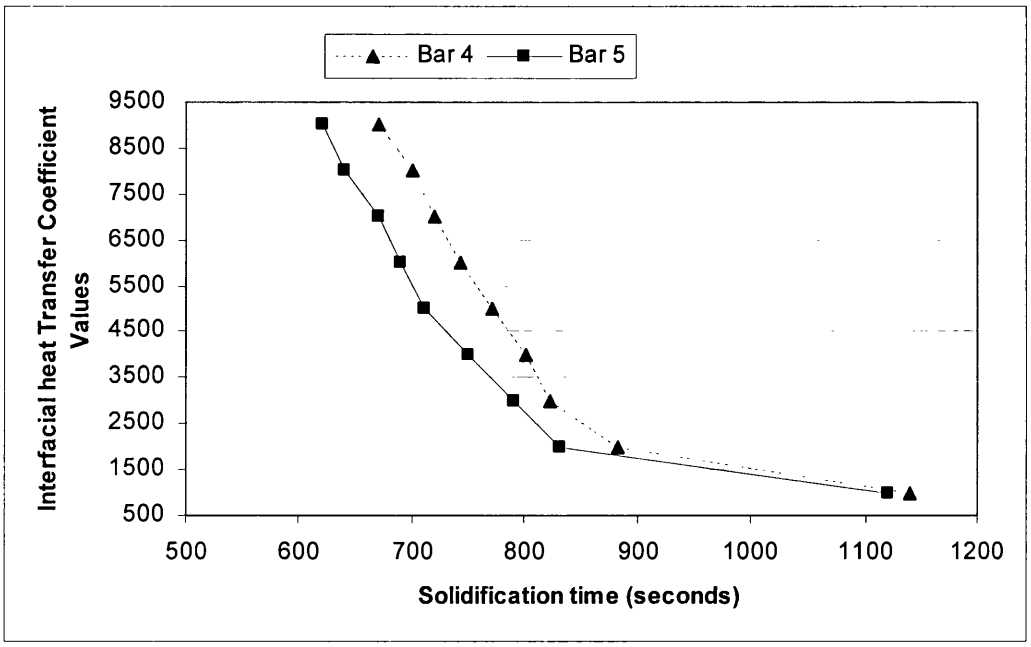

Figure A.17: Graph showing relationship of interfacial heat transfer coefficient with solidification time for Bar 4 and Bar 5

As opposed to Third Example when increase in length of sand mould increased the solidification time, it was observed that in case of H13 mould, increase in mould length (from 10 cm to 40 cm) brought down the time that was required for cast temperature to reach the solidus temperature at node '1'. This is because of the high conductivity value of the steel mould. The increased mould dimensions resulted in the higher heat capacity of the mould. This reduced the overall temperature in the mould thereby increasing the heat transfer across the cast-mould interface (Figure A.18 and Figure A.19). As a result, the solidification time was reduced.

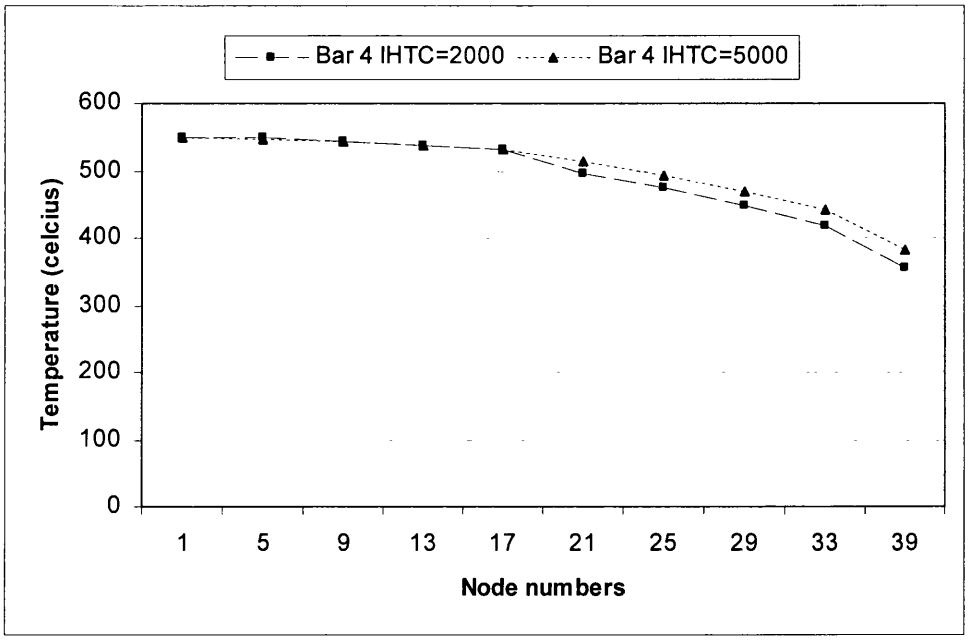

Figure A.18: Temperature distribution at various nodes in the casting and the mould for Bar 4 with two different values of interfacial heat transfer coefficients

($IHTC = h_{inf}$ = 2000 and 5000 W/m^2K)

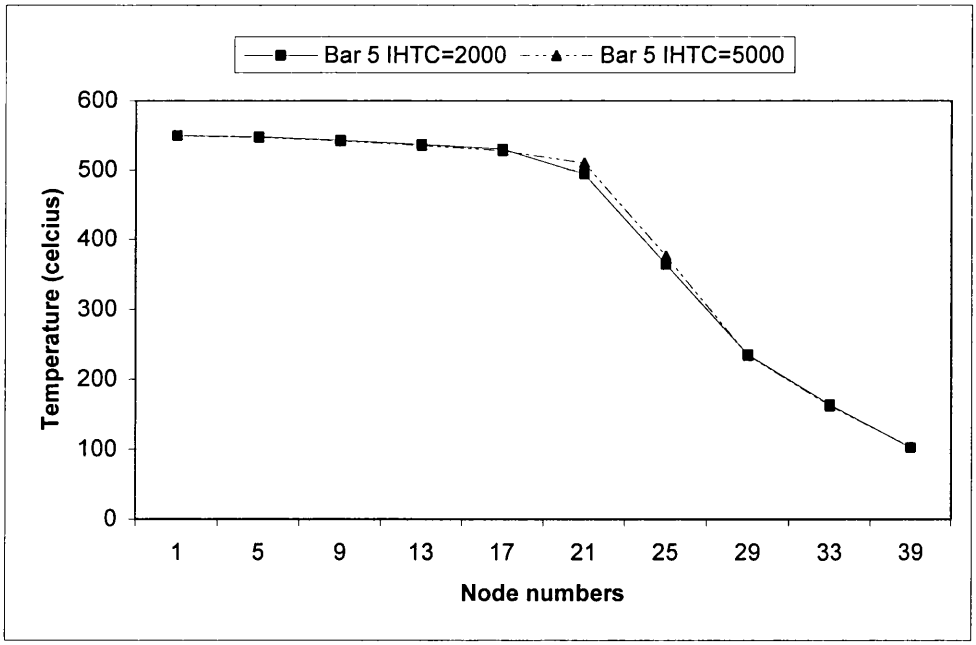

Figure A.19: Temperature distribution at various nodes in the casting and the mould for Bar 5 with two different values of interfacial heat transfer coefficients

($IHTC = h_{inf}$ = 2000 and 5000 W/m^2K)

It can be also noted that the change in values of interfacial heat transfer coefficients did not significantly influence the heat flux between the casting

and the mould. In this case too, it was noticed that the solidification time was inversely proportional to the variation in interfacial heat transfer coefficient values (Figure A.17).

Two more graphs were plotted for explaining the relationship between solidification time and values of interfacial heat transfer coefficients (h_{inf}). Now the solidification time (t_s) was plotted against values of $1/h_{inf}$ for Bar 1 and Bar 2 (with sand mould) and Bar 4 and Bar 5 (H13 mould) and these graphs are shown in Figure A.20 and Figure A.21.

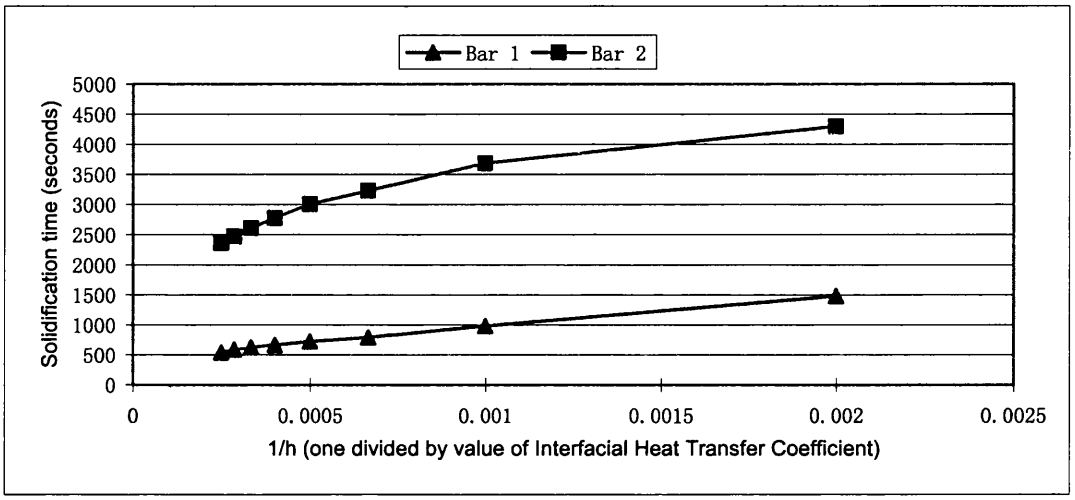

Figure A.20: Graph showing relationship of solidification time (t_s) with value of $1/h_{inf}$ for Bar 1 and Bar 2 (Sand mould)

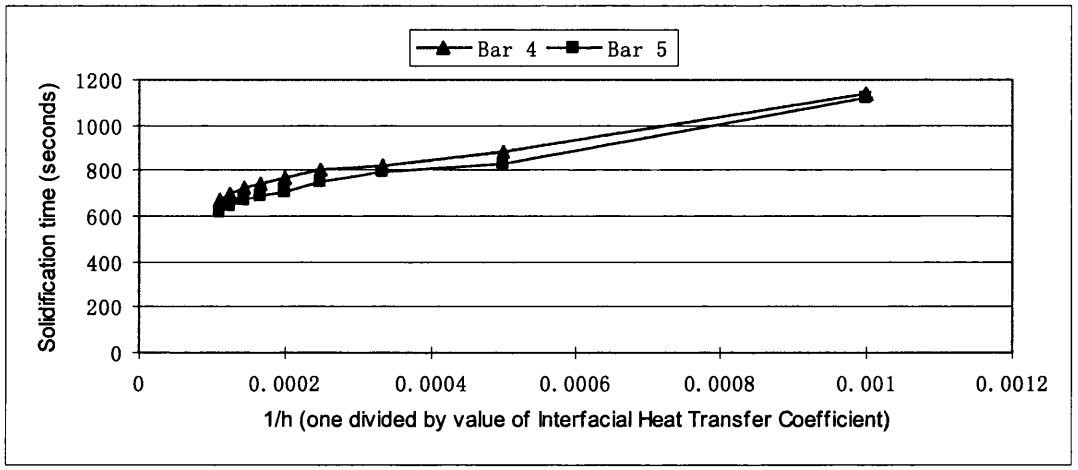

Figure A.21: Graph showing relationship of solidification time (t_s) with value of $1/h_{inf}$ for Bar 4 and Bar 5 (H13 mould)

It is observed that the relationship is more linear in case of H13 steel mould and less so for bars with sand mould.

Conclusion

It is observed from these examples that the assumption made in Equation 5.3 that $t_s \propto \frac{1}{h}$ is valid in many situations. The observations have been supported by an equivalent finite element analysis. The results obtained from these analyses demonstrate that the assumed relationship between solidification time and values of interfacial heat transfer coefficients is more valid and acceptable in case of castings with steel mould than those with sand mould.

REFERENCES

[1] Merlin Software Databank, School of Engineering, University of Wales Swansea, Swansea, UK, (Private communications), May 2003.

Chapter 6

COUPLED THERMAL OPTIMISATION USING MODIFIED HEUVERS' CIRCLE METHOD – RESULTS AND DISCUSSIONS

CHAPTER LAYOUT
A new approach was developed and proposed in Chapter 5 that successfully combined two geometric techniques with FE simulation to provide thermal control in a solidifying casting. This chapter now undertakes tests to validate the effectiveness and accuracy of this newly developed approach. A variety of casting geometries are selected for testing the method developed and proposed in the previous chapter. The coupled approach is first tested on simple geometries and is then further validated on more practical real life geometries including case studies on castings/geometries obtained from foundries. A parametric sensitivity study is also undertaken that discusses the sensitivity of the results with respect to input parameters. For three of the case studies on the casting sections tested in this chapter, results using some other techniques were already available in published literature. The remaining two case studies are performed on real castings obtained from foundries. The results for all these case studies are validated using FE based simulations. This is followed by a conceptualization of the approach to predict solutions for a three-dimensional geometry. The penultimate section then discusses the results and their interpretation and implementation through various design decisions in foundry situations. The conclusions are then drawn from the research presented in this chapter.

6.1 INTRODUCTION

The previous chapter proposed modifications to two well known geometric reasoning methods namely medial axis transformation technique and Heuvers' circle method using Chvorinov's classic rule. These two methods were combined to develop a new approach that coupled FE simulation to predict hot spots and utilised a geometric parameter (radius of inscribed circles) of the casting to obtain effective interface boundary conditions.

This chapter focuses on testing and validating the newly developed method that was proposed in Chapter 5 on a variety of casting geometries including conceptualising an approach for its applicability to three-dimensional casting objects. The chapter aims at successfully demonstrating the effectiveness of the proposed method to act as an elegant optimisation technique for optimal feeding design. For this purpose, each of the chosen casting geometries poses a different set of problems to check the robustness of the proposed technique. The results of the case studies are validated using an FE based solidification analysis. The new method considerably brings down the number of FE simulations that needs to be performed during the casting design cycle. This novel approach provides an important lead into the optimal numerical values of interfacial heat transfer coefficients for facilitating more detailed numerical analysis thereby, saving precious time and resources. The chapter closes with discussions on results and how the relative variation of interfacial heat transfer coefficients obtained from the method could be used in decision making on various design choices in real foundry environment.

6.2 VALIDATION OF THE PROPOSED MODIFIED HEUVERS' CIRCLE METHOD

6.2.1 First case study: Scaling of IHTC to achieve realistic values

It was discovered that sometimes, the modified interface boundary conditions as suggested by the new method (e.g. Table 5.1 in previous chapter) are not realistic in terms of their application in real foundry environment. In such a situation an algorithm needs to be developed to scale values either upwards or downwards, depending on individual foundry practices and type of casting and mould being used, to provide more realistic interface boundary

conditions. A gear blank casting geometry first used by Neises *et al.* [1] was chosen to test this situation and validate the method proposed in Chapter 5.

The original casting geometry was modified to generate a hotspot in main casting section on the left hand side (Figure 6.1). The medial axis was generated using the tools available in the CADfix package. The length of the medial axis, the relative distance between a few selected medial points and radii at these medial points on the medial axis were also obtained using the CADfix package [2] (Figure 6.1a). By observing the radius information from Table 6.1, it can be predicted that the hotspot is likely to be found at point Q174 (Figure 6.1a) on the medial axis in the left hand section of the casting as this is the centre of the largest inscribed circle in the casting with a radius of 5.63 cm. The other likely hotspots in sections with larger radius of 5.83 cm (point Q162) and 5.71 cm (point Q163 and Q166) are already located in the feeder.

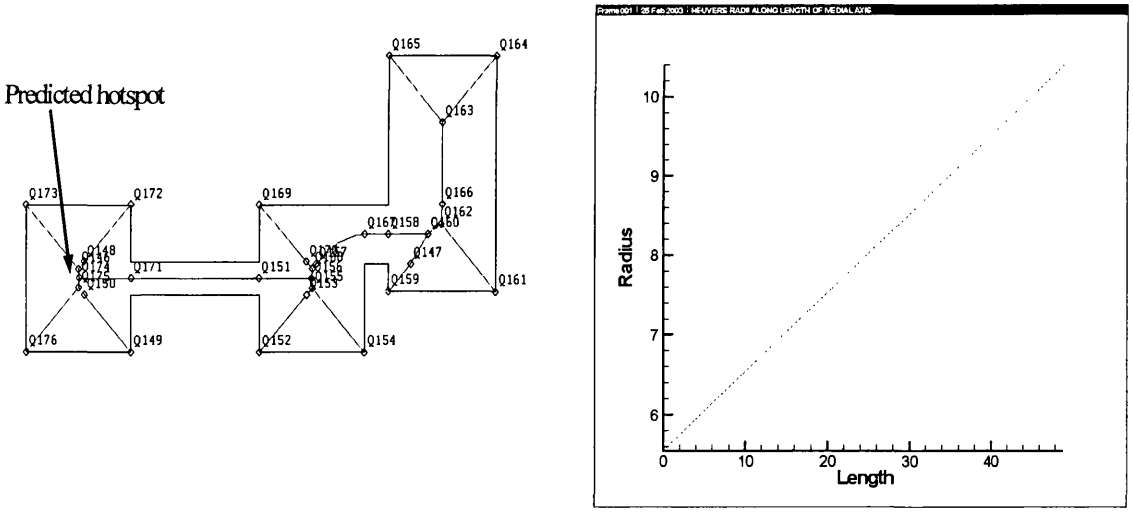

(a) (b)

Figure 6.1: (a) Gear Blank casting showing medial axis and radius points [1], (b) Graph plotted for radii against length along medial axis at 1 in 10 gradient

For achieving directional solidification, the Heuvers' radii (R_H) were increased by 1 cm for every 10 cm length of the casting measured along its medial axis. Using this radius information, the Equation 5.9 provides the modified values of interfacial heat transfer coefficient (h_H). Please see Table 6.1 for actual calculations.

Points on Medial Axis	Original IHTC h_o (W/m^{2}K)	Original Radii (cm) R_o	Heuvers' Radii (cm) R_H	Modifying factor $(R_o/ R_H)^2$	Modified IHTC h_H (W/m^{2}K)	Scaled up IHTC h_H (W/m^{2}K)
Q146	3000.00	5.55	5.55	1.00	3000	8550
Q174	3000.00	5.63	5.63	1.00	3000	8550
Q171	3000.00	1.40	6.16	0.05	155	442
Q171a	3000.00	1.40	6.82	0.04	126	360
Q151	3000.00	1.40	7.48	0.04	105	300
Q156	3000.00	5.61	8.00	0.49	1475	4204
Q168	3000.00	5.54	8.10	0.47	1403	4000
Q167	3000.00	2.54	8.72	0.08	255	725
Q158	3000.00	2.54	8.95	0.08	242	689
Q160	3000.00	4.93	9.37	0.28	830	2367
Q162	3000.00	5.83	9.53	0.37	1123	3200
Q166	3000.00	5.71	9.70	0.35	1040	2963
Q163	3000.00	5.71	10.40	0.30	904	2577

Table 6.1: Gear Blank Casting - Original and Heuvers' radii and corresponding original and modified values of interfacial heat transfer coefficients

The following material properties and boundary conditions (Table 6.2) were used to get the temperature profile and solidification pattern using the Finite Element Simulation method ([3],[4]).

Initial Casting Aluminium alloy (LM24) temperature	650° C
Initial Mould (H13 alloy steel) temperature	150° C
Thermal Conductivity for casting metal	186.28 W/mK
Original value interfacial heat transfer coefficient	3000 W/m^{2}K
Convection to ambient	75 W/m^{2}K
Ambient temperature	20° C

Table 6.2: Gear Blank Casting - material properties and boundary conditions

The solidification contours in Figure 6.2a show that the point Q174 on the medial axis on left hand side of the casting (please see Figure 6.1a)

represented a hotspot. This validated our earlier prediction on the location of the hotspot based purely on the radius information. The horizontal thinner section of the casting has solidified first blocking the metal flow path to left hand section and thus resulting in a hotspot. This hotspot needed to be moved into the feeder that is located on the right hand side of the casting. The casting boundary was then divided into segments and the modified interface boundary conditions (modified values of interfacial heat transfer coefficients (h_H) from Table 6.1) were then applied on respective segments around those points. Finally, the FE analysis was then carried out to check whether the desired solidification pattern was achieved (Figure 6.2b).

In real foundry environment, it may not be feasible to apply very low values of interfacial heat transfer coefficients on certain surfaces of casting boundary e.g. those ranging from 105-255 W/m^2K (Table 6.1) on thinner sections of the gear blank casting near points Q171, Q151, Q167 and Q158 (Figure 6.1a), where the amount of heat to be dissipated is far less compared to thicker sections of the casting. In order to achieve a realistic lower limit for heat transfer coefficient values, all modified values of heat transfer coefficients are uniformly scaled up as shown in the last column of the Table 6.1. The freezing time contours obtained from FE analysis (Figure 6.2c) after applying these scaled up values of IHTCs provided an optimal solution that exhibited similar pattern of accuracy and directional solidification and the hot spot was relocated and contained in the feeder section of the casting.

From Figure 6.2, it is observed that the hot spot has clearly and considerably moved from the left section of the casting (Figure 6.2a) into the feeder section (Figure 6.2b and c). The solidification history also exhibits an acceptable level of desired freezing pattern thus ensuring casting quality and soundness.

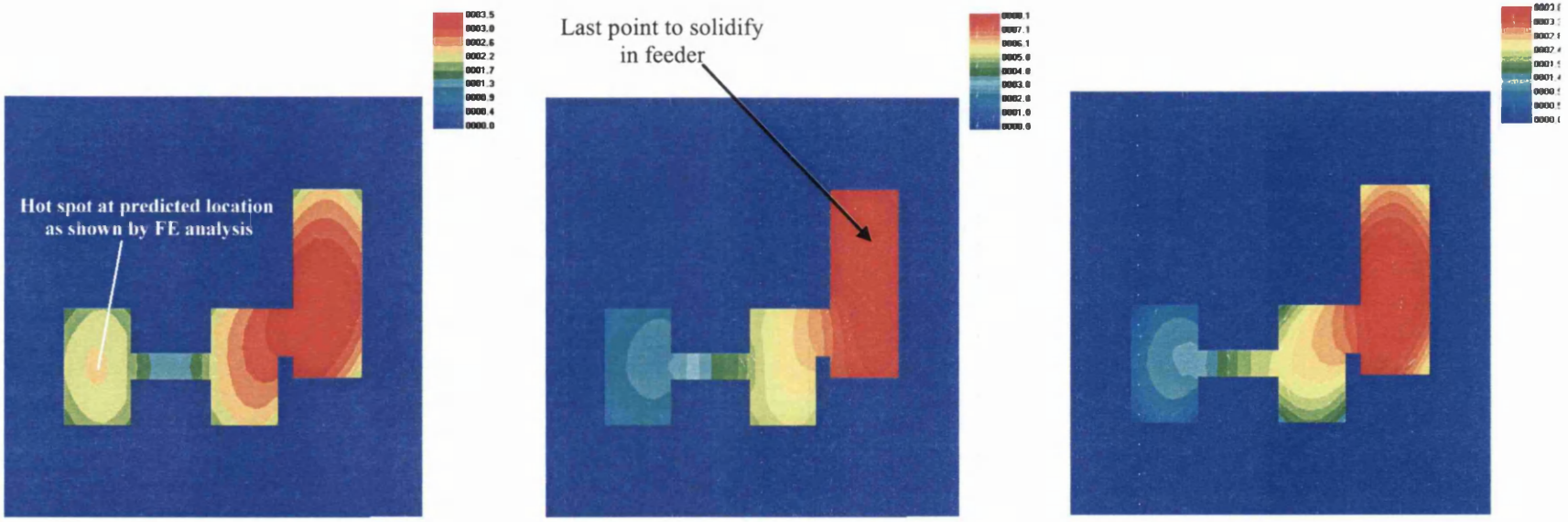

(a) (b) (c)

Figure 6.2: Gear blank casting - Solidification history showing freezing time contours using FE simulation (a) Solution with uniform Interfacial Heat Transfer Coefficient values on all boundaries and (b) Solution with Heuvers radii based modified Interfacial Heat Transfer Coefficient values on selected surfaces of the casting (c) Solution with scaled up Heuvers' radii based values

6.2.2 Parametric Sensitivity Study

This section will discuss the sensitivity of the result obtained with respect to the input parameters. The values of conductivity, specific heat and initial temperature were varied by ±30% and a series of FE simulations were carried out with these changed values of input parameters. The results of this parametric sensitivity study are presented through a case study that now follows.

6.2.2.1 Case Study

The gear blank casting used for the first case study in previous section was chosen to undertake this parametric sensitivity study for establishing effect of varying values of input parameters (conductivity, specific heat and initial temperature) on the solidification time and location of hotspot. The boundary conditions and material properties given in Table 6.1 and Table 6.2 were used for this study.

The values of conductivity (k) and specific heat (c) were changed by ±30% [4]. The initial temperature (*initial T*) was kept at 590, 650 and 800° C as applying value to an extent of -30% would have taken the initial temperature below the solidus and liquidus temperature.

All the permutations are given in Table 6.3 and the finite element simulations were carried out for each case. The temperature profiles and solidification pattern were analysed and the last column in Table 6.3 gives the solidification times for each of these cases.

Case No.	Thermal Conductivity (W/mK)	Specific Heat (J/kgK)	Initial Temperature (C)	Solidification Time (Seconds)
1	186.3	1093.0	650.0	16.81
2	186.3	1093.0	800.0	21.04
3	186.3	1093.0	590.0	12.99
4	186.3	1420.9	650.0	17.78
5	186.3	1420.9	800.0	23.22
6	186.3	1420.9	590.0	14.14
7	186.3	765.1	650.0	16.22
8	186.3	765.1	800.0	18.84
9	186.3	765.1	590.0	12.38
10	242.2	1093.0	650.0	15.70
11	242.2	1093.0	800.0	20.20
12	242.2	1093.0	590.0	12.38
13	242.2	1420.9	650.0	16.89
14	242.2	1420.9	800.0	22.18
15	242.2	1420.9	590.0	13.41
16	242.2	765.1	650.0	15.10
17	242.2	765.1	800.0	18.34
18	242.2	765.1	590.0	11.78
19	130.4	1093.0	650.0	17.27
20	130.4	1093.0	800.0	21.62
21	130.4	1093.0	590.0	13.59
22	130.4	1420.9	650.0	17.84
23	130.4	1420.9	800.0	24.19
24	130.4	1420.9	590.0	14.61
25	130.4	765.1	650.0	16.30
26	130.4	765.1	800.0	19.95
27	130.4	765.1	590.0	12.95

Table 6.3: Solidification time for a gear blank casting with varying values (-30%, typical and +30%) of thermal conductivity, specific heat and initial temperature

6.2.2.2 Effect of change in initial temperature on solidification time

Solidification time changed with a change in initial temperature for the same values of thermal conductivity and specific heat, *e.g.* Case number (1, 2 and 3). An increase of 23% in value of initial temperature increased the solidification time by about 25%. Similarly a 9% decrease in the value of initial temperature resulted in nearly 24% reduction in its solidification time. It is therefore, observed that for a particular set of boundary conditions and constant values of conductivity and specific heat, higher the initial temperature of the molten metal, more is the heat and internal energy in the casting that needs to be dissipated and therefore, longer it takes for the casting to solidify.

6.2.2.3 *Effect of change in value of specific heat on solidification time*

The value of specific heat assumed at 1093 J/kgK was changed by ±30% and the thermal conductivity and initial temperature were kept at 186.3 W/mK and 650°C respectively. It is observed from the results obtained from FE simulation (case number 1, 4 and 5) that there is slight change in solidification time with change in values of specific heat. The solidification time increased by 5.8% with an increase of 30% in value of specific heat and decreased by 3.5% with reduction of same magnitude in specific heat value. This is because the change in value of specific heat changes the heat capacity and as result the solidification time is slightly changed. If however, the latent heat is also taken into consideration (case number 4.1 and 5.1), the casting now has more heat energy to lose and hence the solidification time changes substantially (by nearly 30%).

6.2.2.4 *Effect of change in value of thermal conductivity on solidification time*

In this sensitivity study (case number 1, 6 and 7), value of the typical thermal conductivity assumed at 186.3 W/mK for LM24 was changed by ±30% and the specific heat and the initial temperature was kept constant at 1093 J/kgK and 650°C respectively. It is noticed that the solidification time increased by about 2.7% (17.27 seconds) when the thermal conductivity was reduced by 30%. On the other hand, an increase of 30% in its thermal conductivity value reduced the solidification time by about 6.6% (15.70 seconds).

Since it is known from the defining equation for the thermal conductivity [5] that the heat transfer rate is proportional to the normal temperature gradient

$$q = -kA\frac{\partial T}{\partial x}$$

where q is heat transfer rate, $\frac{\partial T}{\partial x}$ is the temperature gradient in the direction of the heat flow, k is called thermal conductivity of the material.

It is therefore, observed that the increase in thermal conductivity value increases the heat flow rate thereby, reducing the solidification time. On the other hand, application of reduced values of thermal conductivity reduces the heat flow rate thereby increasing the time that is required for complete solidification of the casting.

6.2.2.5 Effect of change of input parameters (k, c, initial T) on the location of the hotspot

It is observed that changing input parameters (thermal conductivity, specific heat and initial temperature) did not significantly influence the location of hotspot in the casting. In all cases (Figure 6.3 to Figure 6.6), hotspot was still located inside the feeder section which was the result achieved after applying the boundary conditions suggested by the proposed modified Heuvers' Circle method (Table 6.1). This demonstrates the robustness of the method proposed in Chapter 5 and 6.

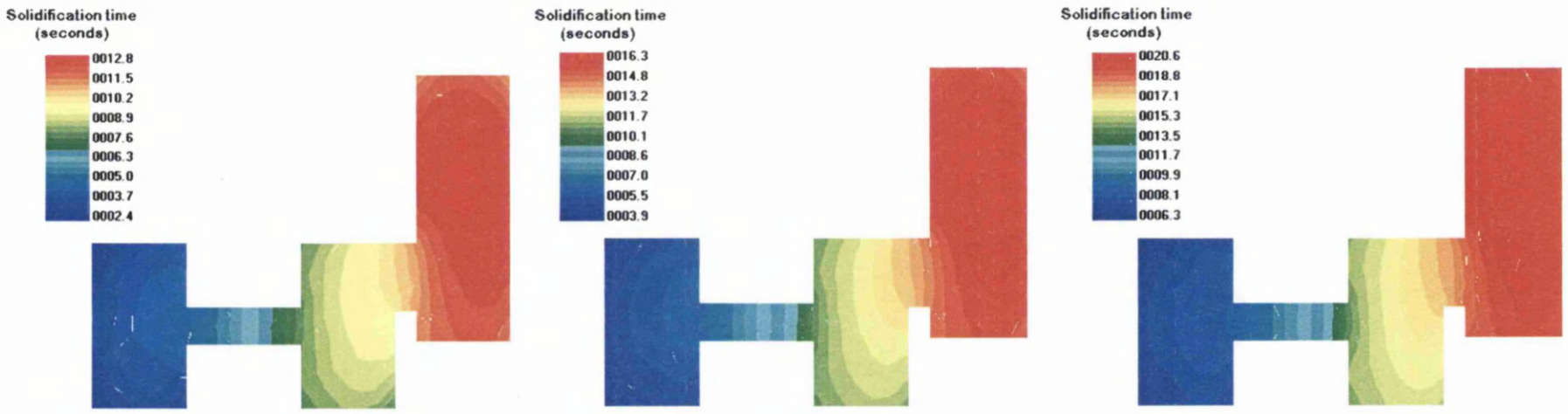

Initial temperature = 590° C (Case No. 3) Initial temperature = 650° C (Case No. 1) Initial temperature = 800° C (Case No. 2)

Figure 6.3: Solidification time contours showing location of hotspots for a gear blank casting with varying initial temperature values

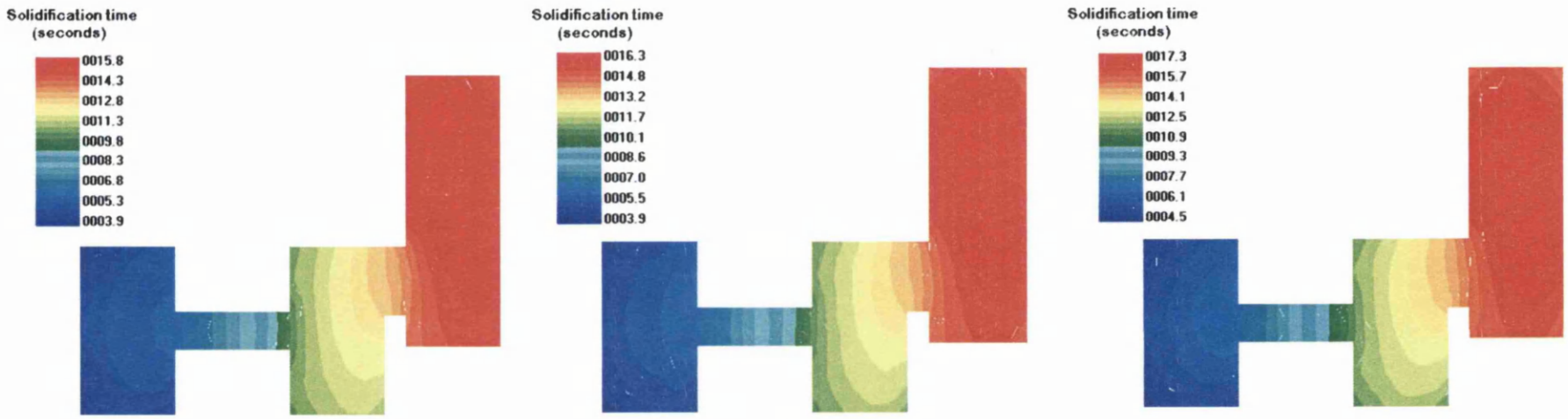

Specific heat = 765.1 J/kgK (Case No. 7) Specific heat = 1093.0 J/kgK (Case No. 1) Specific heat = 1420.9 J/kgK (Case No. 4)

Figure 6.4: Solidification time contours showing location of hotspots for a gear blank casting with varying values of specific heat

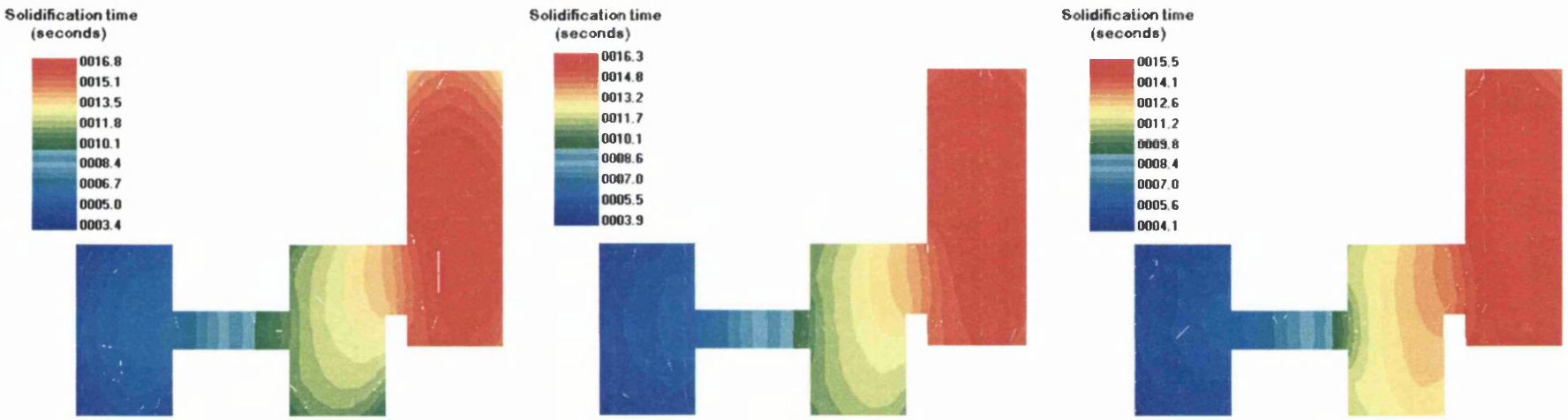

Thermal conductivity = 130.4 W/mK (Case No. 19)

Thermal conductivity = 186.3 W/mK (Case No. 1)

Thermal conductivity = 242.2 W/mK (Case No. 10)

Figure 6.5: Solidification time contours showing location of hotspots for a gear blank casting with varying values of thermal conductivity

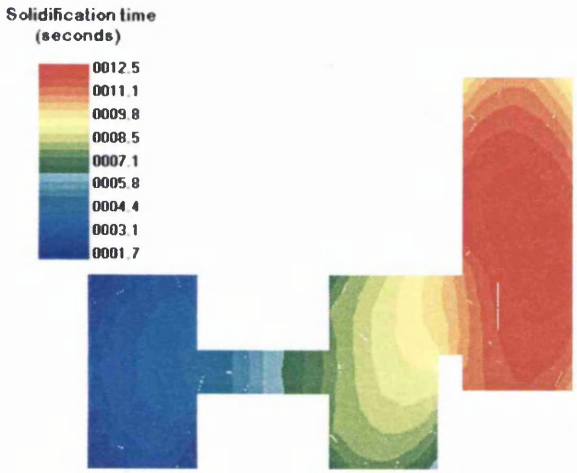

Thermal conductivity = 130.4 W/mK

Specific heat = 765.1 K/kgK

Initial temperature = 590° C

(Case No. 27)

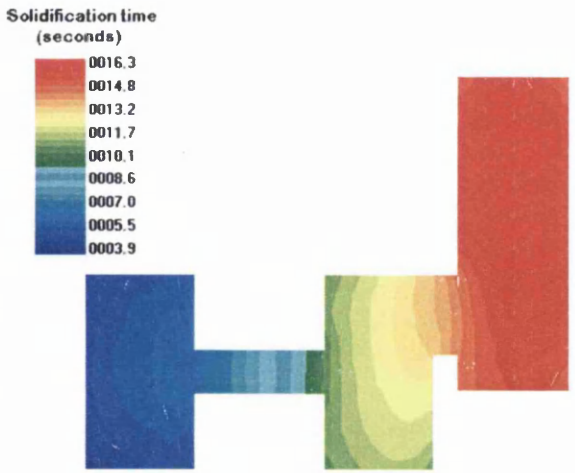

Thermal conductivity = 186.3 W/mK

Specific heat = 1093.0 K/kgK

Initial temperature = 650° C

(Case No. 1)

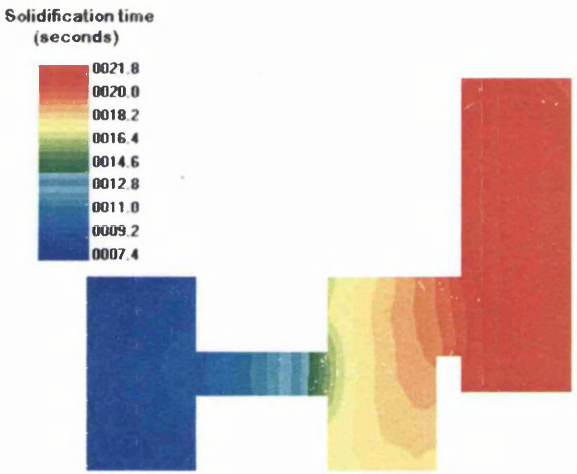

Thermal conductivity = 242.2 W/mK

Specific heat = 1420.9 K/kgK

Initial temperature = 800° C

(Case No. 14)

Figure 6.6: Solidification time contours showing location of hotspots for a gear blank casting with extreme values (-30%, typical and +30%) of thermal conductivity, specific heat and initial temperature

6.2.3 Second case study: Sorting technique for branched medial axis

The gear blank casting tested in previous section only had one main medial axis i.e. from point Q146 to Q163 (Figure 6.1a) apart from the side medial axis segments. Clearly, the method had worked accurately for this type of casting geometry but required to be further tested on a casting that had branched medial axis as shown in Figure 6.7. This casting had two feeders supplying liquid metal to the top and the bottom end of the casting. The cast metal was an aluminum alloy (LM24) with 615°C liquidus temperature. The mould was made of H13 alloy steel. The initial temperatures for casting and mould were assumed to be 650°C and 150°C respectively. The convection boundary condition of 75 W/m^{2}K was applied to the exterior of the mould and ambient temperature was assumed to be 20°C. The constant conductivity value of 186.28 W/mK and 33.9 W/mK were assumed for metal and mould respectively. A uniform interfacial HTC of 3000 W/m^{2}K was applied on all cast-mould interfaces for an initial Finite Element analysis. The solution obtained showed two hotspots representing two sections with largest inscribed circles, one each below the feeder neck at top and bottom (Figure 6.9a).

6.2.3.1 Technique for sorting Heuvers' radii for branched Medial Axis

As discussed in the previous section, the Heuvers' circle radii are increased at a rate of 10% along the medial axis. If the medial axis has more than one branch then at the junction, the proposed Heuvers' radius is found for each branch and the maximal value of the Heuvers' radius is chosen for the corresponding junction. This condition ensures that the junction point will solidify only after the corresponding branches have solidified. For example to ensure the directional solidification as shown in Figure 6.8, having a branched medial axes structure, the junction point G can only solidify after points A, B, C, D, E, and F. For this example, three Heuvers' radii will be obtained, one for each medial axis branch i.e. AB, CD and EF. Among these three choices, the proposed method selects the Heuvers' circle with the largest Heuvers' radius value [6].

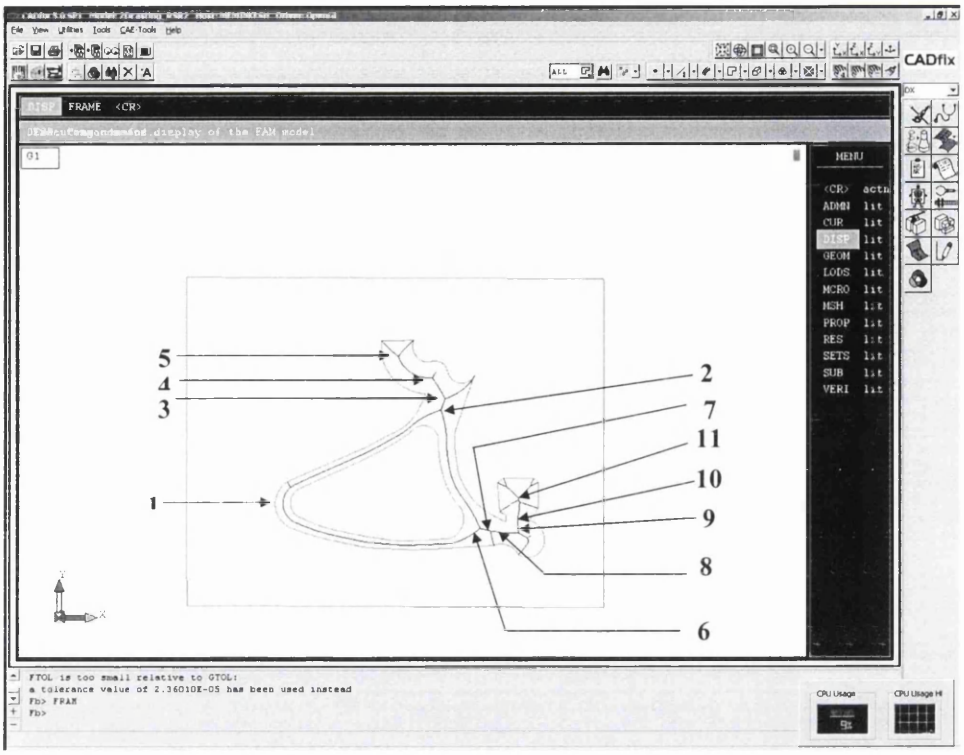

Figure 6.7: A two-dimensional casting section showing medial axis and important medial points obtained using CADfix [2]

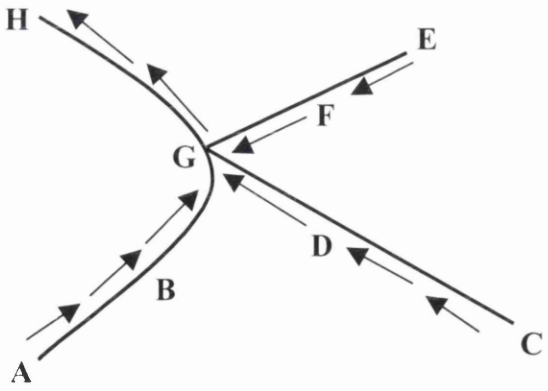

Figure 6.8: Selection of Heuvers' radii for branched medial axis: Arrows indicate the desired direction of solidification

Points On Medial Axis	Original IHTC h_o (W/m^{2}K)	Original Radii (cm) R_o	Heuvers' Radii (cm) R_H	Modifying factor $(R_o/ R_H)^2$	Modified IHTC h_H (W/m^{2}K)
Towards top feeder					
1	3000	8.10	8.10	1.0000	3000
2	3000	24.37	30.43	0.6414	1924
3	3000	24.14	31.82	0.5755	1727
4	3000	20.13	34.74	0.3358	1007
5	3000	19.02	39.57	0.2310	693
Towards bottom feeder					
1	3000	8.10	8.10	1.0000	3000
6	3000	21.39	33.00	0.4201	1260
7	3000	17.70	34.32	0.2660	798
8	3000	14.10	35.53	0.1575	472
9	3000	19.24	37.60	0.2618	786
10	3000	13.81	38.98	0.1255	377
11	3000	23.64	41.53	0.3240	972

Table 6.4: A 2-dimensional casting - Original and Heuvers' radii and corresponding original and modified values of interfacial heat transfer coefficients

Table 6.4 shows the calculation of Heuvers' radii for corresponding locations as shown in Figure 6.7. The corresponding modified heat transfer coefficients are also shown in the last column of Table 6.4. Figure 6.9(b) shows the solidification time contours from a FE simulation carried out after applying the modified heat transfer coefficient values for the second analysis. The result shows that both hotspots have moved into the feeder.

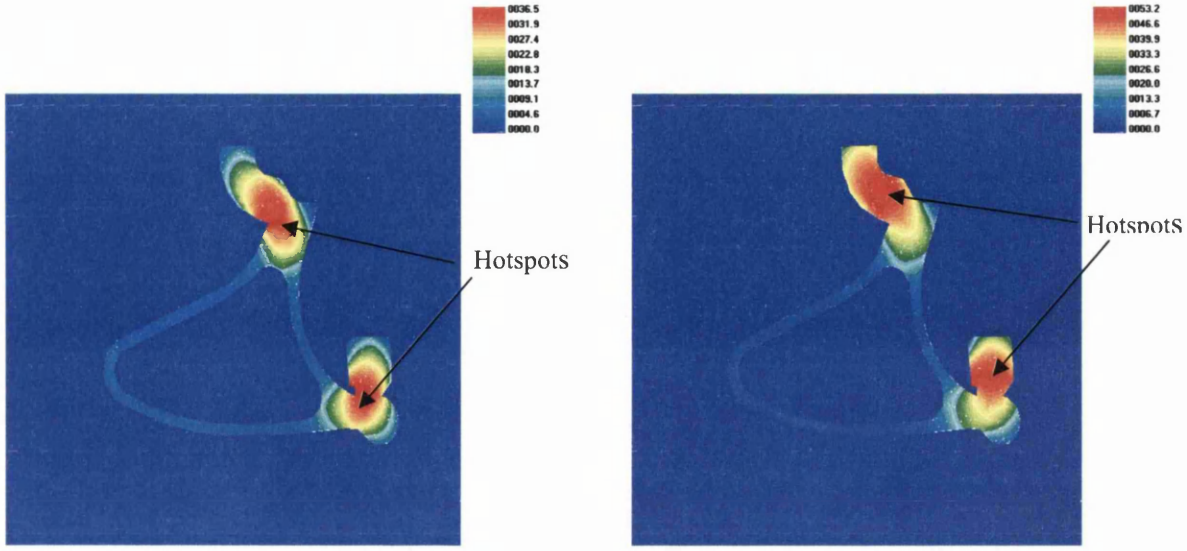

(a) (b)

Figure 6.9: A two-dimensional casting section - Solidification history showing freezing time contours using FE simulation (a) Solution with uniform Interfacial Heat Transfer Coefficient on all boundaries and (b) Solution with Heuvers radii based modified Interfacial Heat Transfer Coefficient on selected surfaces of the casting.

6.2.4 Third case study: Validation of sorting technique

A second example (Figure 6.10) with unequal medial axis branches has been chosen to demonstrate the robustness of proposed technique. The wheel geometry has been taken from published literature ([7],[8]) and the material properties and boundary conditions are kept same. The medial axis branch Q85-Q79-Q12-Q75 provided a larger value of Heuvers' radius compared to the other branch Q68-Q64-Q62-Q61-Q58-Q56-Q75 (Heuvers' radius of 29.30cm for the former against 27.77cm for the latter - Table 6.5). Therefore, the sorting algorithm chose the first branch (coming from below) at the junction point of two branches and carried on towards the feeder head as per procedure described for previous case studies.

Thereafter, same steps as outlined earlier were followed. Table 6.5 provides the details of original inscribed and Heuvers' radii and modified values of interfacial heat transfer coefficients. The modified interface boundary conditions were computed based on Heuvers' radii and using equation 5.9. After meshing the casting geometry (Figure 6.11), first and second FE

simulation were carried out first using uniform solidification and then with these modified boundary conditions. It is evident from Figure 6.12 b that desired solidification pattern was achieved and the hotspot moved from the casting section (Figure 6.12a) in to the feeder on the right hand side of the casting.

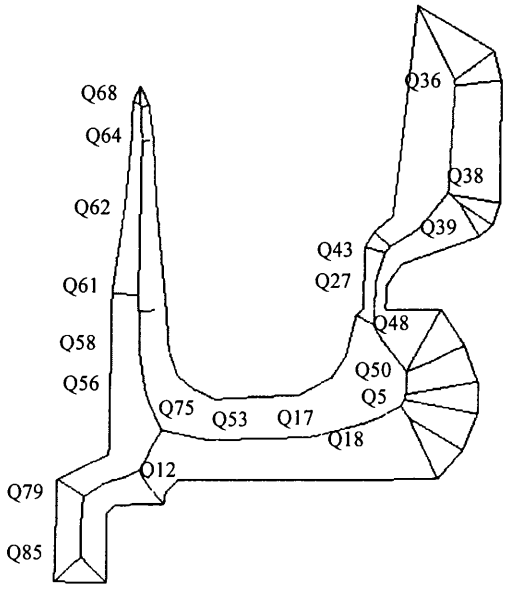

Figure 6.10: Wheel casting showing medial axis and medial points on main medial axis

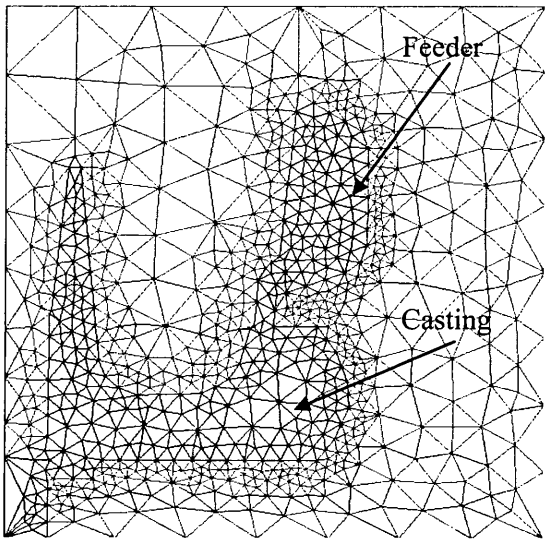

Figure 6.11: FE mesh created generated FE simulation software Merlin

Points On Medial Axis	Original IHTC h_o (W/m^{2}K)	Original Radii (cm) R_o	Heuvers' Radii (cm) R_H	Modifying factor $(R_o/ R_H)^2$	Modified IHTC h_H (W/m^{2}K)
Q85	3000	17.77	17.77	1.00	3000
Q79	3000	18.92	21.95	0.74	2229
Q12	3000	23.56	26.11	0.81	2443
Q75	3000	35.61	29.30	1.48	4431
Q53	3000	27.94	33.23	0.71	2121
Q17	3000	29.27	39.01	0.56	1689
Q18	3000	37.41	42.94	0.76	2277
Q5	3000	50.56	46.22	1.20	3590
Q50	3000	43.15	48.63	0.79	2362
Q48	3000	13.42	52.56	0.07	196
Q27	3000	7.82	55.37	0.02	60
Q43	3000	13.82	57.65	0.06	172
Q39	3000	22.96	61.27	0.14	421
Q38	3000	35.47	63.64	0.31	932
Q36	3000	30.92	71.38	0.19	563
Q68	3000	5.16	5.16	1.00	3000
Q64	3000	7.59	7.70	0.97	2915
Q62	3000	10.50	11.87	0.78	2347
Q61	3000	18.02	18.27	0.97	2918
Q58	3000	19.89	22.25	0.80	2397
Q56	3000	23.74	24.62	0.93	2789
Q75	3000	35.61	27.77	1.64	4933

Table 6.5: Wheel Casting - Original and Heuvers' radii and corresponding original and modified values of interfacial heat transfer coefficients

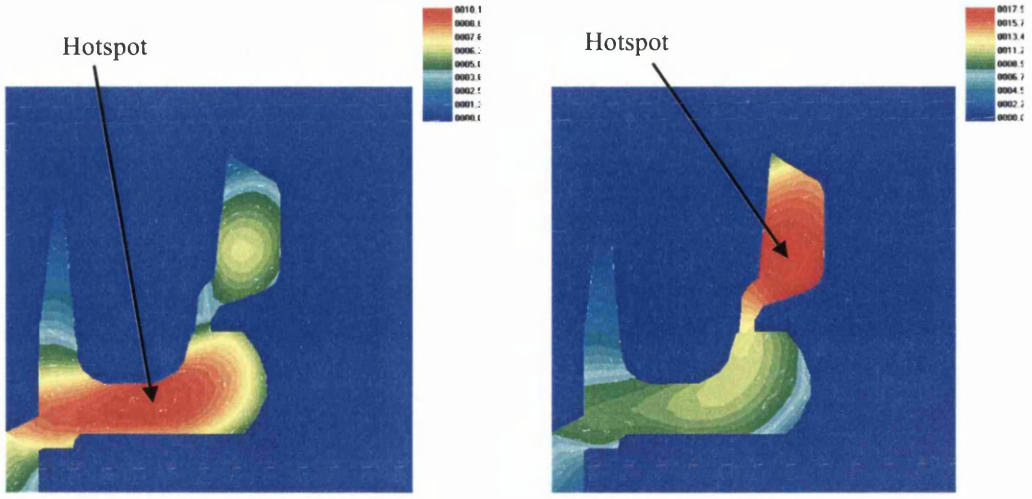

(a) (b)

Figure 6.12: Wheel casting - Solidification history showing freezing time contours using FE simulation (a) Solution with uniform Interfacial Heat Transfer Coefficient on all boundaries and (b) Solution with Heuvers radii based modified Interfacial Heat Transfer Coefficient on selected surfaces of the casting. Hot spot has moved into feeder in (b).

6.3 FOURTH CASE STUDY: A REALISTIC CASTING COMPONENT FROM FOUNDRY

6.3.1 The problem

During a visit and meeting with foundry engineers at Triplex Components Group on sharing experience, a casting component with a shrinkage defect was shown. In an effort to test this new approach on real life casting component, the foundry engineers were requested details of the casting. The casting geometry was modified to honour confidentiality and some details were suppressed. The model of the casting was generated using CADfix package. The models and location of defect is shown in Figure 6.13 and Figure 6.14. This cast component provided all the challenges and different situations that were visualized, discussed and solved in previous examples e.g. apart from a shrinkage defect, it also had many medial axes and needed a sorting technique and on the other hand, the casting also needed scaling process to yield more realistic boundary conditions.

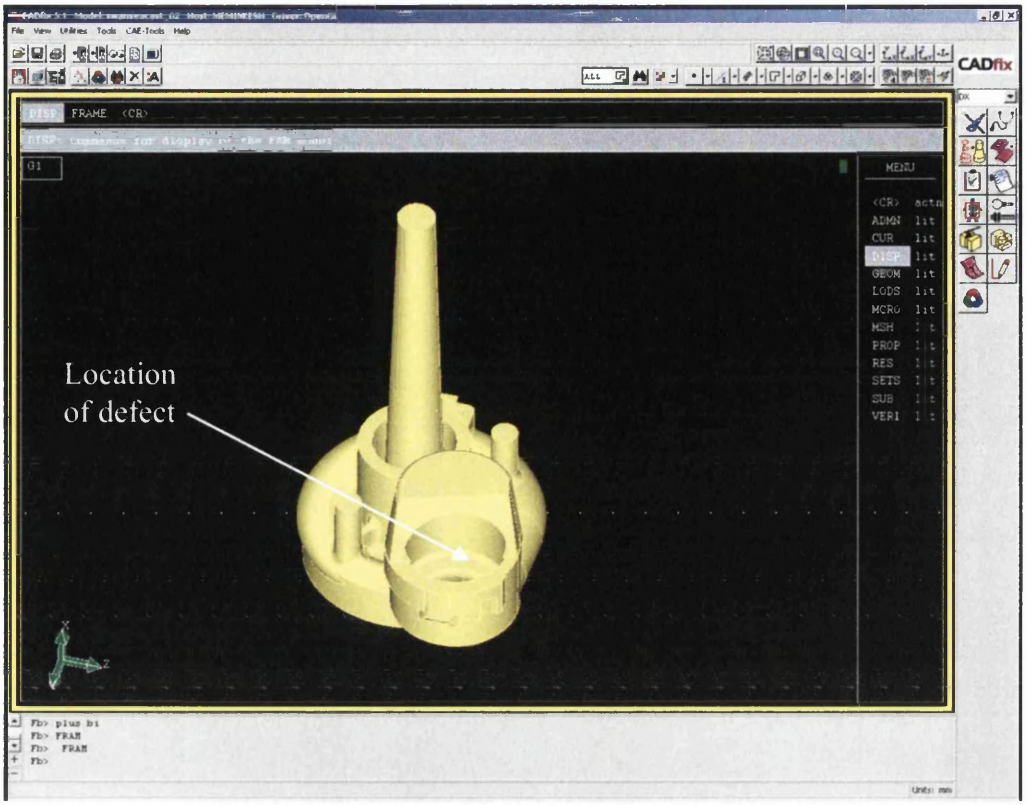

Figure 6.13: Model of the real life casting using CADfix

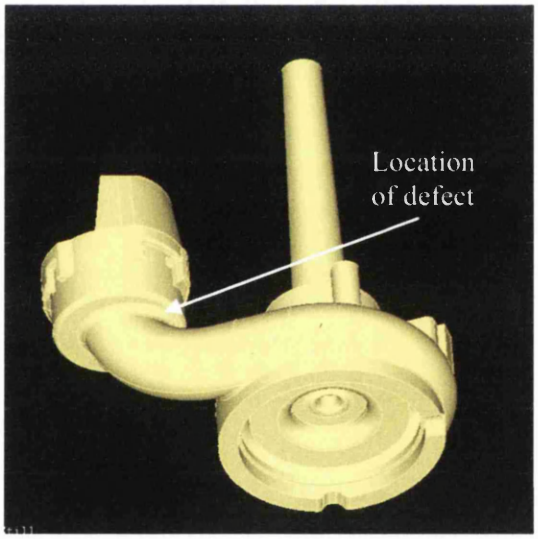

Figure 6.14: Model of the real life casting showing location of defect

6.3.2 The solution

The applicability of modified Heuvers' Circle method to different casting geometries was demonstrated in Section 6.2. Having had success with first three examples, it was decided to test and apply this newly devised method to this casting component from an industry. The aim again was to obtain

effective interface boundary conditions (IBCs) using the Heuvers' inscribed circle radius information in such a manner that these IBCs help us achieve the same solidification pattern as would have been provided by the Heuvers' imaginary casting.

6.3.3 Application of the Method

The method was then implemented by undertaking following steps:

1. Identify possible hotspot locations within a casting geometry by assuming a uniform solidification by carrying out first FE simulation.
2. Choose a desired directional solidification path. Then generate the medial axis and obtain radius information. Compute Heuvers' radii and obtain modified heat transfer coefficient values using the equation 5.9.
3. Undertake second FE simulation with the modified heat transfer coefficient values to ensure that the desired directional solidification path is obtained.
4. Correlate the modified heat transfer coefficient values to real feeding design decisions to obtain defect free casting.

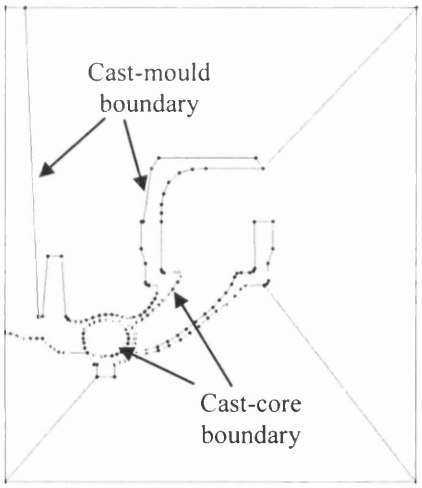

Figure 6.15: Simplified casting geometry created by using Merlin software for the FE analysis

6.3.3.1 Identifying the hotspot

The casting geometry was first simplified to obtain a desirable cross-section, which could be analysed through a finite element based simulation. The

rationale behind this was to include the part of casting with location of defect in the cross section for a two dimensional FE analysis (Figure 6.15).

After meshing the casting geometry, an axi-symmetric analysis along the central feeder was carried out. The following material properties and boundary conditions (Table 6.6) supplied by the foundry engineer[1] were used to obtain the temperature profile and solidification pattern using the Finite Element simulation method (Figure 6.16).

Initial Cast temperature Aluminum Alloy LM27	630°C
Initial Mould (sand) temperature	40°C
Convection to ambient	75 W/m^2K
Ambient temperature	25°C
Original interfacial heat transfer coefficient (IHTC) between casting & mould	2000 W/m^2K
Original interfacial heat transfer coefficient (IHTC) between casting & core	1000 W/m^2K

Table 6.6: Material properties and boundary conditions obtained from the foundry for FE analysis

This FE analysis resulted in a hotspot exactly at the same location as was found in the original casting component. This is the spot where the solidification time is 600 seconds, which solidifies later than other points with freezing times of 585 and 594 seconds at bottom and top ends respectively (Figure 6.16b) thereby resulting in a hotspot. This shrinkage defect at this hotspot in the casting needs to be moved and relocated in the feeder area so that main casting component solidifies progressively towards the feeder which should then be the last to solidify.

[1] Email communication from Dr. Henry Lo from Technical Centre, Triplex Components Group

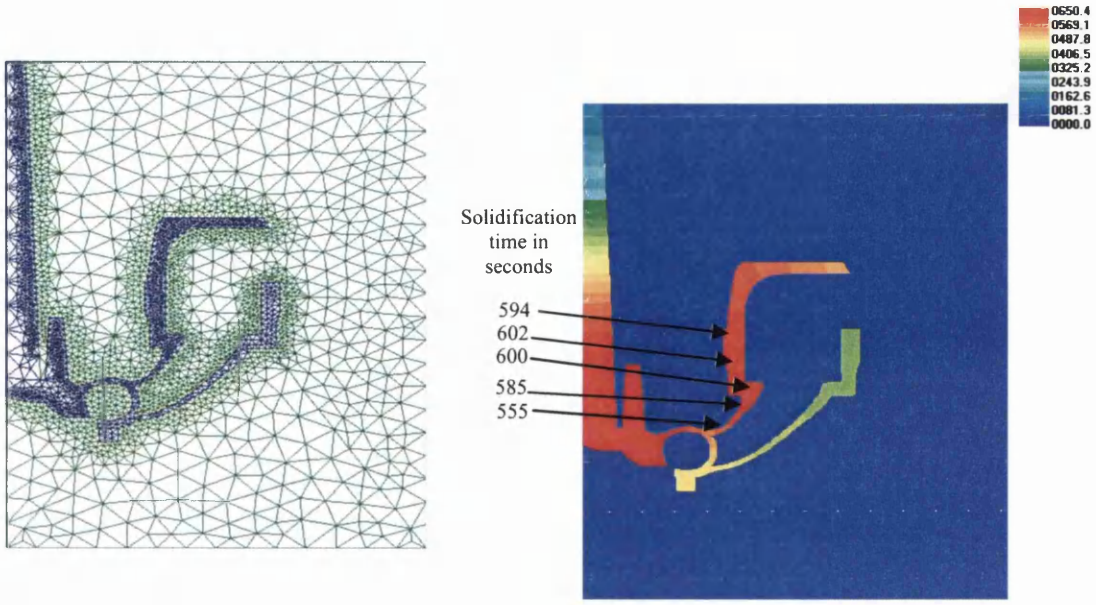

(a) (b)

Figure 6.16: Casting geometry showing (a) mesh for FE analysis and (b) solidification history from FE analysis carried out using Merlin with uniform interfacial heat transfer coefficients

6.3.3.2 Selecting desired directional solidification path and obtaining modified (Heuvers') interface boundary conditions

The medial axis was then generated using the tools available in the CADfix package (Figure 6.17). The length of the medial axis, the relative distance between points and radii at selected points on the medial axis were also obtained using the CADfix package. A desired path for directional solidification that would ensure adequate feeding and a defect free casting was chosen. Arrows and letters in Figure 6.17 denote this path. Using the radius information for selected points on the medial axes, the equation mentioned earlier generated modified values of interfacial heat transfer coefficient (h_H) for corresponding points along this path (Table 6.7).

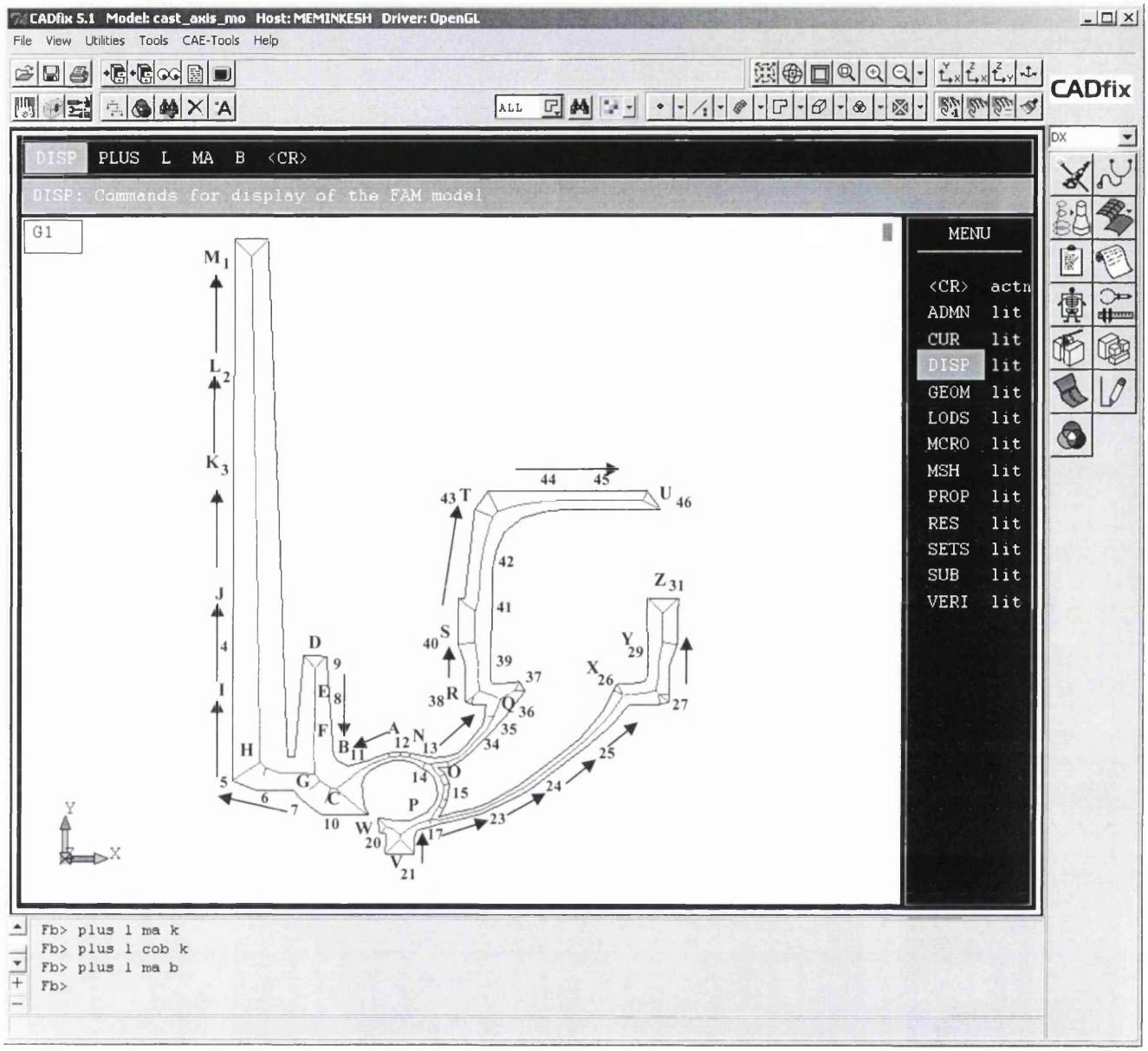

Figure 6.17: Casting geometry generated in CADfix showing medial axis and path of desired directional solidification. (Numbers are points on medial axis and letters denote path of solidification)

Points on Medial Axis	Medial Axis Node Number	Original Radius (cm) R_o	Length of Medial Axis Section(cm)	Heuvers' Radius (cm) R_H	Modifying Factor $(R_o/R_H)^2$	Original IHTC Cast-Mould h_o (W/m·K)	Modified IHTC Cast-Mould h_H (W/m·K)	Original Cast-Core IHTC=1000 then Modified h_H
1	2	3	4	5	6	7	8	9
A-B-C-G								
12	278	1.75		1.75	1.00	2000	2000.00	1000.00
11	180	3.03	13.66	3.12	0.95	2000	1891.14	945.57
10	102	10.80	12.52	4.37	6.11	2000	12226.65	6113.33
7	97	10.93	10.96	5.46	4.00	2000	8002.60	4001.30
D-E-F-G-H-I-J-K-L-M								
9	396	5.13		5.13	1.00	2000	2000.00	1000.00
8	223	6.85	22.28	7.36	0.87	2000	1733.27	866.64
7	97	10.93	22.07	9.56	1.31	2000	2611.72	1305.86
6	57	7.18	11.16	10.68	0.45	2000	903.83	451.92
5	44	11.60	12.41	11.92	0.95	2000	1893.70	946.85
4	345	10.49	50.21	16.94	0.38	2000	766.72	383.36
3	606	9.32	56.35	22.58	0.17	2000	340.82	170.41
2	852	8.16	56.35	28.21	0.08	2000	167.31	83.66
1	1033	7.14	48.30	33.04	0.05	2000	93.39	46.69
A-N-O								
12	278	1.75		1.75	1.00	2000	2000.00	1000.00
13	332	1.75	8.33	2.58	0.46	2000	918.14	459.07
14	363	3.05	9.49	3.53	0.75	2000	1491.33	745.66
P-O-Q								
17	190	3.20		3.20	1.00	2000	2000.00	1000.00
16	238	2.15	6.05	3.81	0.32	2000	638.40	319.20
15	315	2.71	9.34	4.74	0.33	2000	653.93	326.96
14	363	3.05	9.96	5.74	0.28	2000	565.53	282.76
32	384	2.07	3.00	6.04	0.12	2000	235.24	117.62
33	408	2.28	4.17	6.45	0.12	2000	249.69	124.85
34	473	1.75	13.01	7.75	0.05	2000	101.88	50.94
35	541	3.74	14.20	9.17	0.17	2000	332.45	166.23
36	583	6.34	7.88	9.96	0.41	2000	810.13	405.07
37	627	3.52		3.52	1.00	2000	2000.00	1000.00
36	583	6.34	7.21	4.24	2.23	2000	4469.82	2234.91
Q-R-S-T-U								
36	583	6.34		9.96	0.41	2000	810.13	405.07
38	569	5.81	9.39	10.90	0.28	2000	568.21	284.10
39	617	5.28	9.64	11.86	0.20	2000	396.12	198.06
40	664	6.86	10.70	12.93	0.28	2000	562.57	281.28
41	712	6.96	13.09	14.24	0.24	2000	477.51	238.75
42	804	5.08	18.51	16.10	0.10	2000	199.23	99.61
43	902	7.97	21.43	18.24	0.19	2000	381.92	190.96
44	991	4.26	21.89	20.43	0.04	2000	86.98	43.49
45	1056	3.76	25.98	23.03	0.03	2000	53.33	26.67
46	1086	3.76	16.03	24.63	0.02	2000	46.61	23.31
V-W								

21	85	6.01		6.01	1.00	2000	2000.00	1000.00
19	103	6.01	1.93	6.20	0.94	2000	1877.66	938.83
20	96	2.92		2.92	1.00	2000	2000.00	1000.00
19	103	6.01	6.92	3.61	2.77	2000	5535.85	2767.92
W-P-X-Y-Z								
19	103	6.01		6.20	0.94	2000	1877.66	938.83
18	150	2.42	7.84	6.99	0.12	2000	239.95	119.98
17	190	3.20	6.85	7.67	0.17	2000	347.94	173.97
22	202	1.46	4.13	8.09	0.03	2000	65.21	32.61
23	260	1.67	8.41	8.93	0.03	2000	70.00	35.00
24	477	2.10	32.04	12.13	0.03	2000	59.94	29.97
25	650	2.67	32.23	15.35	0.03	2000	60.48	30.24
26	755	4.72	21.77	17.53	0.07	2000	144.98	72.49
27	815	5.83	13.56	18.89	0.10	2000	190.57	95.29
28	857	4.28	9.50	19.84	0.05	2000	93.11	46.55
29	904	6.15	11.03	20.94	0.09	2000	172.52	86.26
30	925	6.25	5.98	21.54	0.08	2000	168.43	84.21
31	950	6.36	5.98	22.13	0.08	2000	165.12	82.56

Table 6.7: Original and Heuvers' method based modified radii and interfacial heat transfer coefficient (IHTC) values for fourth case study

However, in an actual foundry environment, it may not be feasible to apply very low and large number of values of interfacial heat transfer coefficients (last two columns of Appendix A) on certain boundary segments where the amount of heat to be dissipated is far less compared to thicker sections of the casting. There were nearly 64 such different values of interfacial heat transfer coefficients. In order to achieve realistic values of interfacial heat transfer coefficient, the nearly similar values of heat transfer coefficients were grouped together in two stages and averaged down to make them applicable to the casting geometry under investigation. These are given in Table 6.8.

Casting section showing path of directional solidification	Original Cast-Mould IHTC=2000 then Modified Cast-Mould IHTC (h_H) (W/m^2K)	Original Cast-Core IHTC=1000 then Modified Cast-Core IHTC (h_H) (W/m^2K)
A-B-C-G	2000-1800-12000	1000-900-6000
D-E-F-G-H-I-J-K-L-M	2000-1800-2600-2600-1800- 700-360-100-100	No core in these sections
A-N-O	900-500	500-240
P-O-Q	700-240	360-100
Q-R-S-T-U	500-360-500-240-100	360-240-240-100-100
V-W-P-X-Y-Z	2000-240-100-240-100	900-100-100-100-100

Table 6.8: Original and Heuvers' method based modified values of interfacial heat transfer coefficient (IHTCs) at various sections of the casting

6.3.3.3 FE analysis with modified interface boundary conditions

The cast boundary was then divided into segments (Figure 6.17). Now in this case instead of FE analysis with uniform solidification (using uniform heat transfer coefficients of 2000 W/m^2K on Cast-Mould interface and 1000 W/m^2K on Cast-Core interface), the modified interface boundary conditions (modified values of interfacial heat transfer coefficients (h_H) from Table 6.8 were applied on interface boundary in the respective surfaces around those points.

The second FE analysis was then carried out again to check whether the desired solidification pattern was achieved. The freezing time contours obtained from FE analysis after applying these modified values of IHTCs

provided an optimal solution and show that the problematic hotspot was moved from the location of defect up towards the feeder (Figure 6.18B). The solidification pattern now exhibits conformity to our desirable direction towards the top feeder with the lower casting sections solidifying first and then progressively freezing towards the feeder. This is evident from acceptable levels of freezing times of 598, 635, 655, 660 and 662 seconds obtained through the FE analysis (Figure 6.18B).

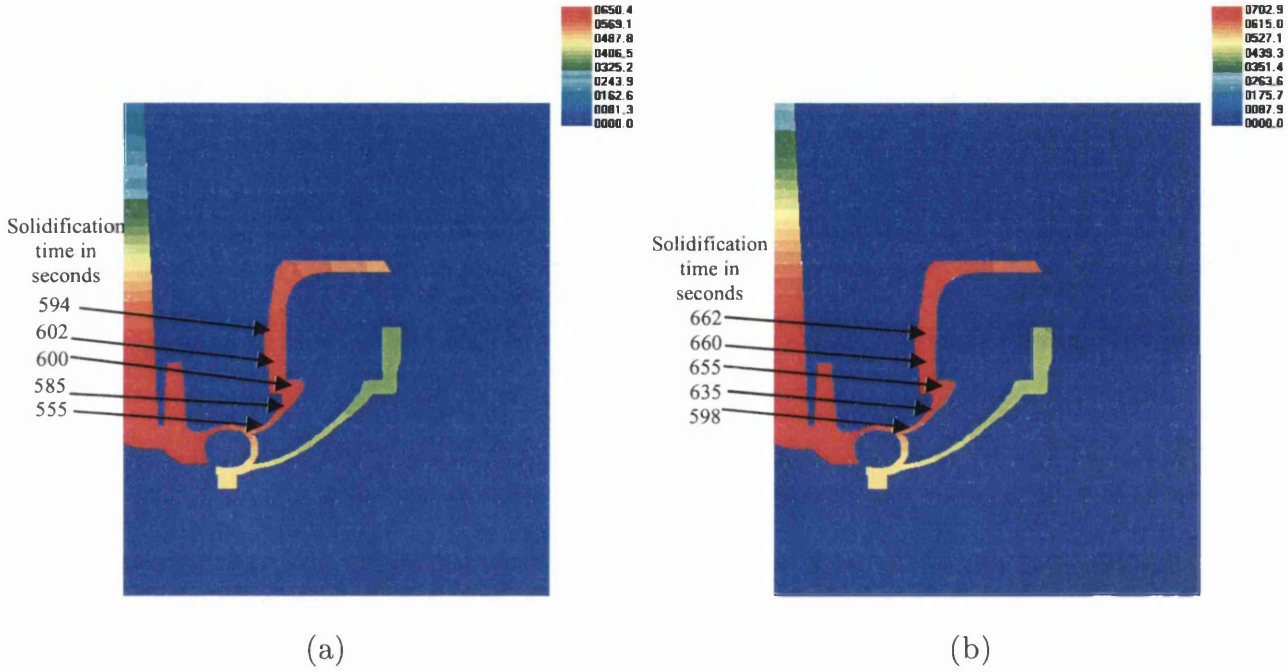

Figure 6.18: Solidification history from FE analysis carried out using Merlin (a) with uniform interfacial heat transfer coefficients and (b) with Heuvers based modified values of interfacial heat transfer coefficients

6.3.3.4 Correlating the modified heat transfer coefficient values to real feeding design decisions

This combined method suggests that the radius along the desired path should increase progressively at a gradient of 10% to ensure desired directional solidification. In this case, additional casting/feeder thickness needs to be provided, extending from sections Q along R and S towards T as suggested by Heuvers' radius values at points 36, 38, 39, 40 and 41 (Figure 6.17) towards feeder top (column 5 of table in Appendix A). This increased casting thickness will provide same amount of insulation as has been effected by the

modified values of interface boundary conditions derived from new method (Table 6.8) for an optimum solution. A larger feeder will provide sufficient metal flow to feed the casting part where shrinkage defect occurred. The additional thickness from the casting can be later machined off to get the original casting shape. Alternatively, as a more practical alternative, it will be advisable to enhance localized cooling in the area where shrinkage is experienced by place a chill to steer the solidification directionally from that particular casting section towards the feeder.

6.4 FIFTH CASE STUDY – REALISTIC CASTING COMPONENT FROM FOUNDRY WITH MULTIPLE MEDIAL AXES

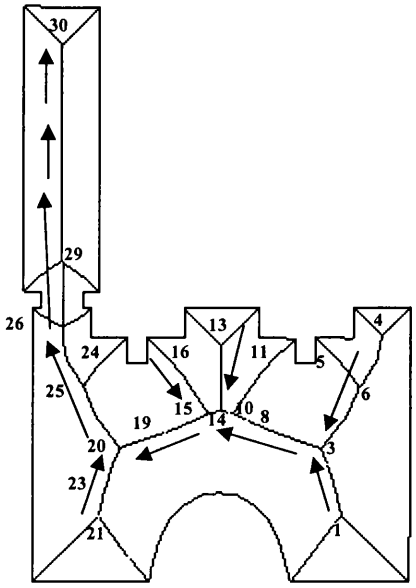

Figure 6.19: Casting geometry showing medial axes generated by CADfix and path of desired directional solidification is shown by arrows

Carrying on with the task of testing this method on more realistic casting components from practical foundry situations, another aluminium sand casting problem was selected. A two-dimensional cross section of the casting as shown in shown Figure 6.19 was chosen to test the proposed method [9]. For the purpose of this study, it was assumed that the casting is fed by a single feeder on the left hand-side as shown in Figure 6.20b and Figure 6.19. The material properties and boundary conditions that were used for this study are given in Table 6.9.

Cast metal	Aluminium alloy (LM 24)
Mould material	Sand
Initial Cast temperature	630°C
Initial Mould (sand) temperature	150°C
Thermal Conductivity	186.28 W/mK
Interfacial heat transfer coefficient	2500 W/m^2K
Convection to ambient	75 W/m^2K
Ambient temperature	25°C

Table 6.9: Material properties and boundary conditions for FE analysis

6.4.1 Application of modified Heuvers' Circle method

The procedure for implementing this new approach was outlined in section 5.4.3 in Chapter 5 and this was further established through three cast studies in Sections 6.2 and another case study on a real casting component in Section 6.3. Same steps were implemented for this casting component.

1. Identified the possible hotspot locations within a casting geometry by assuming uniform solidification. This was achieved by applying a same heat transfer coefficient value across all the casting-mould interfaces and carrying out an FE analysis using Merlin software (Figure 6.20 a and b). This FE analysis indicated a hotspot in the middle section of the casting. The aim is to use the thermal control in casting as suggested by the new approach to move the last point to solidify in the feeder section.

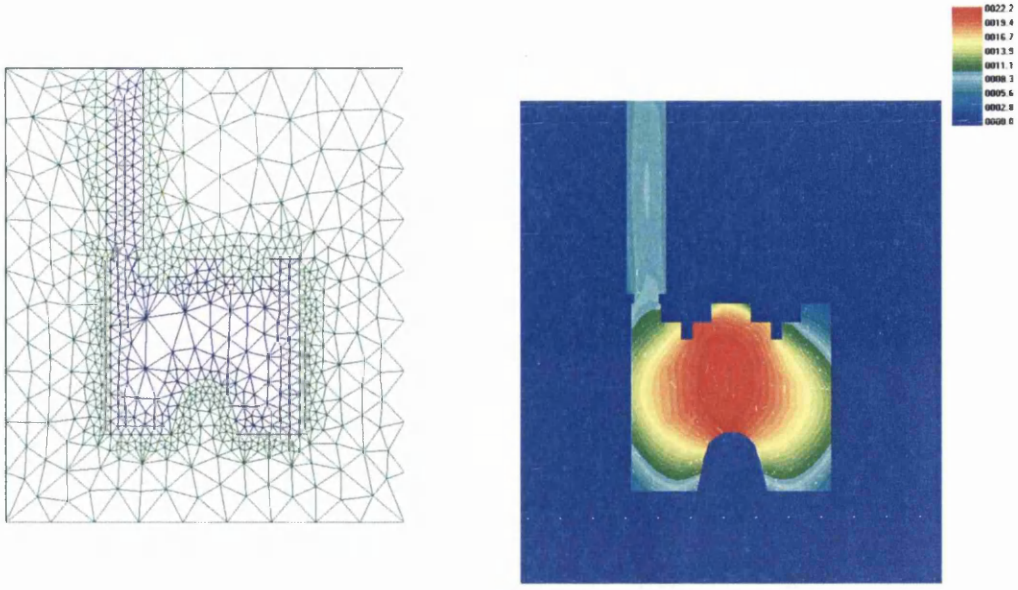

(a) (b)

Figure 6.20: (a) A two-dimensional casting geometry showing FE mesh generated using Merlin (b) Hotspot prediction using FE analysis with Merlin

2. The model of the casting was then created using CADfix and medial axes were generated. A path for desired directional solidification was then chosen starting from the farthest end towards the feeder (Figure 6.19) for implementing new technique and to obtain Heuvers' radii along that path on the medial axis.

3. The length of medial section between successive medial points and the radius information was then obtained for different medial points along the medial axis using CADfix. This information was then used to get values for Heuvers' radii which provided lead into modified values of interfacial heat transfer coefficients. These are computed and shown in Table 6.10 which is spread over next two pages.

Points On Medial Axis	Original Radius (cm) R_o	Length of Medial Axis Section (cm)	Heuvers' Radius (cm) R_H	Modifying factor $(R_o/R_H)^2$	Original IHTC h_o (W/m^{2}K)	Modified IHTC h_H (W/m^{2}K)
1	28.15		28.15	1.00	2500	2500.00
2	30.59	11.15	29.27	1.09	2500	2731.50
3	36.58	18.05	31.07	1.39	2500	3465.33
4	11.70		11.70	1.00	2500	2500.00
6	20.92	23.95	14.10	2.20	2500	5507.23
5	10.09		10.09	1.00	2500	2500.00
6	20.92	13.40	11.43	3.35	2500	8374.73
6	20.92		14.10	2.20	2500	5507.23
3	36.58	30.15	17.11	4.57	2500	11426.87
3	36.58		31.07	1.39	2500	3465.33
7	32.74	11.00	32.17	1.04	2500	2589.38
8	30.90	8.08	32.98	0.88	2500	2194.87
9	31.72	14.05	34.38	0.85	2500	2127.74
10	33.82	6.49	35.03	0.93	2500	2330.01
11	10.26		10.26	1.00	2500	2500.00
12	17.43	9.04	11.16	2.44	2500	6093.90
10	33.82	17.80	12.94	6.83	2500	17066.73
10	33.82		35.03	0.93	2500	2330.01
14	34.59	5.16	35.55	0.95	2500	2367.07
13	15.85		15.85	1.00	2500	2500.00
14	34.59	27.56	18.61	3.46	2500	8640.42
14	34.59		35.55	0.95	2500	2367.07
15	33.55	5.60	36.11	0.86	2500	2158.33
16	10.42		10.42	1.00	2500	2500.00
17	16.59	7.95	11.22	2.19	2500	5470.59
15	33.55	18.63	13.08	6.58	2500	16452.90
15	33.55		36.11	0.86	2500	2158.33
18	31.24	7.65	36.87	0.72	2500	1794.51
19	32.12	19.90	38.86	0.68	2500	1707.73
20	36.20	12.01	40.06	0.82	2500	2041.03
21	27.41		27.41	1.00	2500	2500.00
22	29.50	10.10	28.42	1.08	2500	2693.62
23	33.12	12.10	29.63	1.25	2500	3123.61
20	36.20	8.04	30.43	1.41	2500	3537.03

20	36.20		40.06	0.82	2500	2041.03
25	20.79	30.27	43.09	0.23	2500	581.94
24	10.43		10.43	1.00	2500	2500.00
25	20.79	12.76	11.71	3.15	2500	7885.55
25	20.79		43.09	0.23	2500	581.94
26	12.00	26.88	45.78	0.07	2500	171.78
27	8.99	14.70	47.25	0.04	2500	90.51
28	15.28	12.44	48.49	0.10	2500	248.22
29	15.75	1.02	48.60	0.11	2500	262.61
30	15.75	90.9	57.69	0.07	2500	186.37

Table 6.10: Original and Heuvers' radii and corresponding original and modified values of interfacial heat transfer coefficients for fifth case study

5. Finally applied these modified values on the respective surfaces of the casting and undertook another FE simulation with these modified heat interface boundary conditions to verify the solution for the problem posed earlier. As is very clear from Figure 6.21, the solution has ensured that the desired directional solidification was achieved and the hotspots that was earlier in the main casting component (Figure 6.21a) has now been relocated in the feeder (Figure 6.21b).

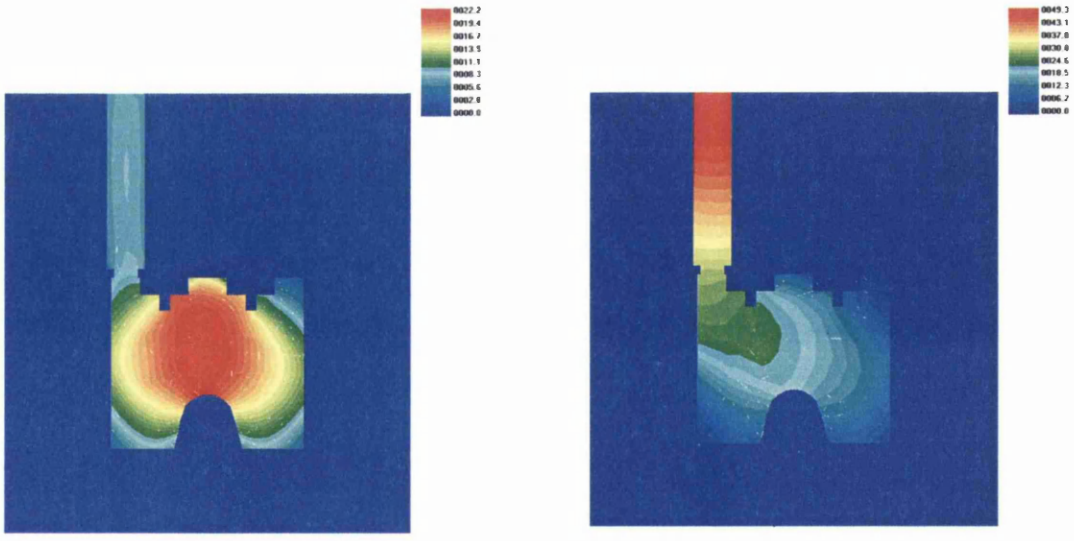

(a) (b)

Figure 6.21: Freezing time contours from FE simulation (a) Solution with uniform solidification and (b) Solution with modified interface boundary condition on selected surfaces of the casting. Hot spot has moved into the feeder in (b)

6.5 EXTENSION OF NEW COMBINED HEUVERS' CIRCLE METHOD TO THREE-DIMENSIONAL CASTING OBJECTS

This section aims at conceptualising the new approach developed in Chapter 5 and tested and validated in earlier sections of this chapter for its potential application to three-dimensional casting objects. It was earlier clarified that for a 3D object, the medial axis becomes a medial surface and inscribed circles assume the shape of inscribed spheres thereby providing the associated geometrical information such as radii of these inscribed spheres.

6.5.1 Case study – 3D L-shaped plate casting

For this purpose, a three dimensional L-shaped plate casting geometry was selected Figure 6.22 . Morthland *et al.* [10] had used a 2D approximation of similar L-shaped plate to present an optimised feeder design for this casting that ensured adequate feeding and thus eliminated the shrinkage porosity in its inner corner. The L-shaped plate used by these authors was of uniform thickness. However, real castings in foundry industry are rarely of such uniform dimensions and often have different thicknesses. In an effort to apply this approach to a realistic problem, this casting was slightly modified to have varying thickness all through the width and length of the plate. Some idea of this variation is illustrated through its 2D geometries as shown in Figure 6.22. This figure shows a 2D casting cross section (a), its geometry with medial axis (b) and finally only its medial axis with side branches.

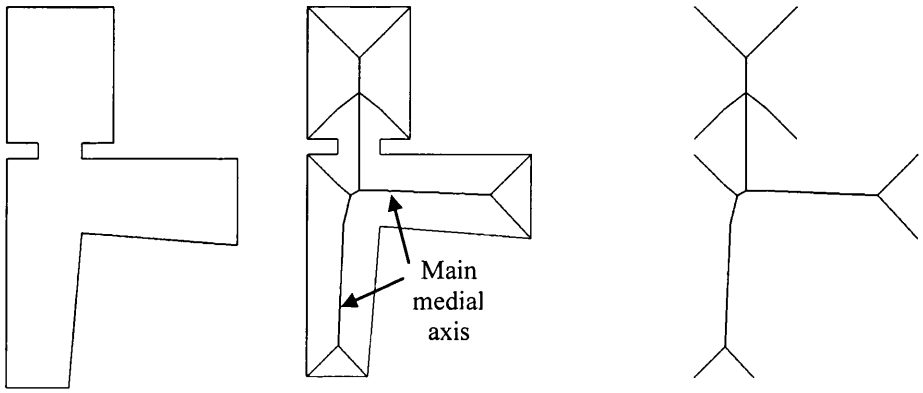

(a) Casting geometry (b) Casting with its medial axis (c) Medial axis only for the 2D L-shaped casting

Figure 6.22: Two-dimensional L-shaped casting geometry

The next step was to create a three-dimensional model from this 2D cross section. The model of the casting was created in CADfix and nearly similar dimensions were adopted as used by authors cited above [10]. The casting's length, width and thickness was taken as 400 mm, 250 mm and 100 mm respectively and then based on these basic dimensions, other dimensions were slightly increased to make it of varying thickness. Figure 6.23 provides dimensions of this 3D casting object.

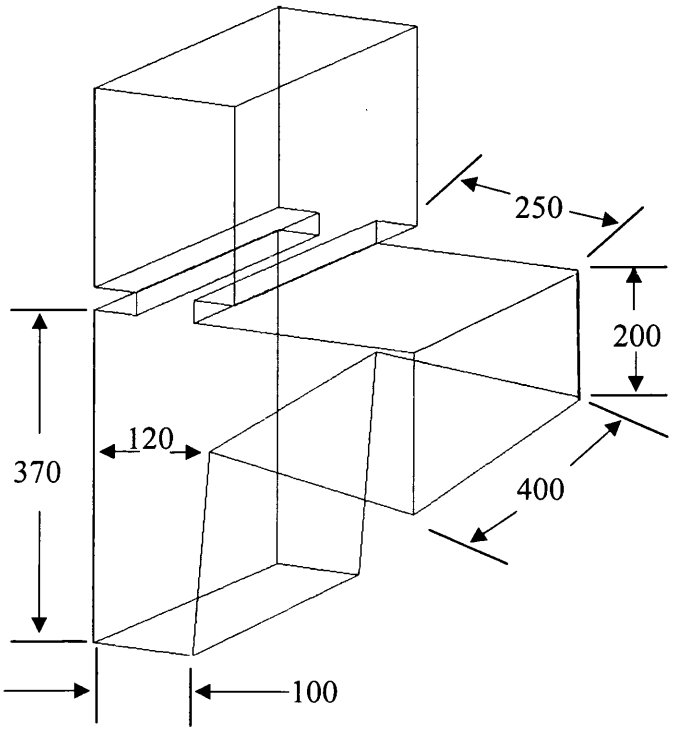

Figure 6.23: Three-dimensional frame of L-shaped casting showing dimensions in millimeters

In standard foundry practice, the feeders are usually cylindrical but in this particular case, the feeder was also approximated to be a long brick running along the length of the casting. The feeder neck's width and height were taken to be 70 mm and 25 mm respectively. The height and width of the feeder were assumed to be 220 mm and 170 mm respectively. The three-dimensional body of this casting is shown in Figure 6.24 which further depicts the varying thickness at different ends of the L-shaped plate.

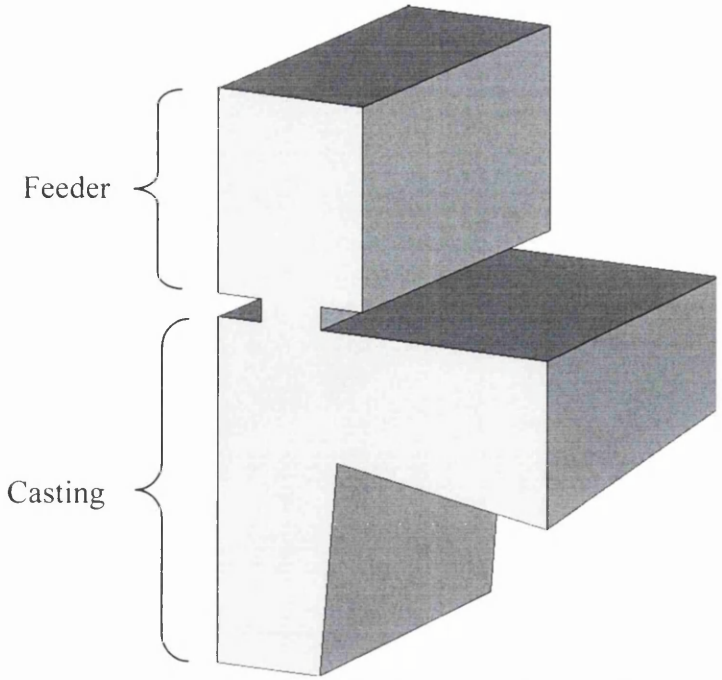

Figure 6.24: Three-dimensional body of the L-shaped casting created using CADfix

6.5.1.1 3D Medial surface and its medial axis

The next task now was to generate the medial surface for this 3D casting body. This task was hampered by software's inability and limitations in generating 3D medial surface. However, Figure 6.25 depicts the medial surface likely to be obtained from CADfix (a) and its medial surface frame of the same object is shown in Figure 6.25 (b).

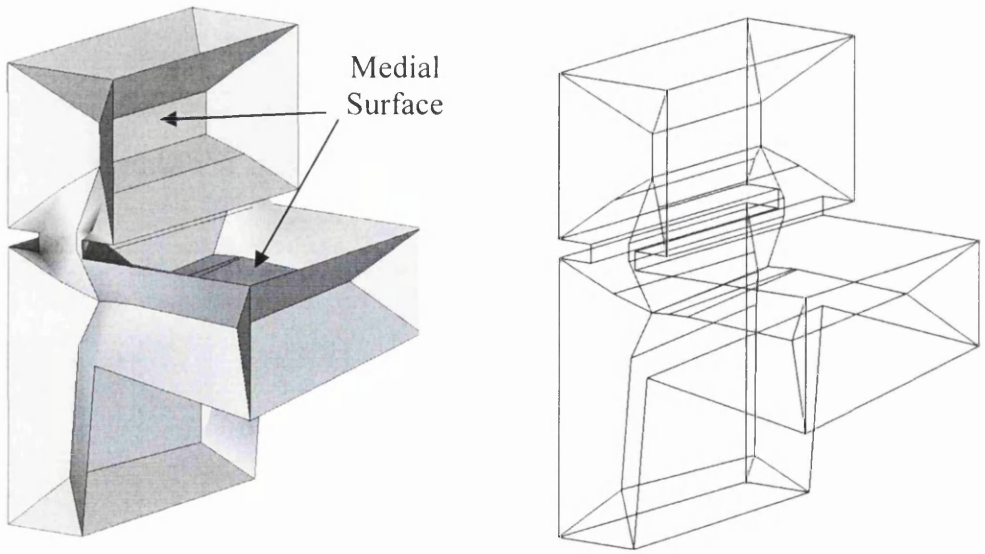

(a) Medial surface (b) Medial surface frame

Figure 6.25: Medial surface of the 3D L-shaped casting

It is observed from Figure 6.25 that medial surface is the skeletal representation of the 3D body and it contains important geometric information that can be utilised for applying the new approach similar to how it was applied to 2D castings using medial axis. The medial surface much like medial axis provides those important points along the length and width of the casting and the associated geometrical information (e.g. coordinates of the medial point and associated medial radius). But as is visible from the medial surface, much greater number of such points would be provided by the medial surface, owing to its three dimensions. This could then result in greatly increasing the computational work (for obtaining Heuvers' radii) and may also make the sorting algorithm more complex.

For resolving this problem, the medial surface is simplified and all smaller and inconsequential medial surfaces are discarded. This screening process leads to the main medial surface that contains all the points that are required by the new method as shown in Figure 6.26 (a). This simplified main medial surface is still able to provide all vital points and information to facilitate implementation of the new approach.

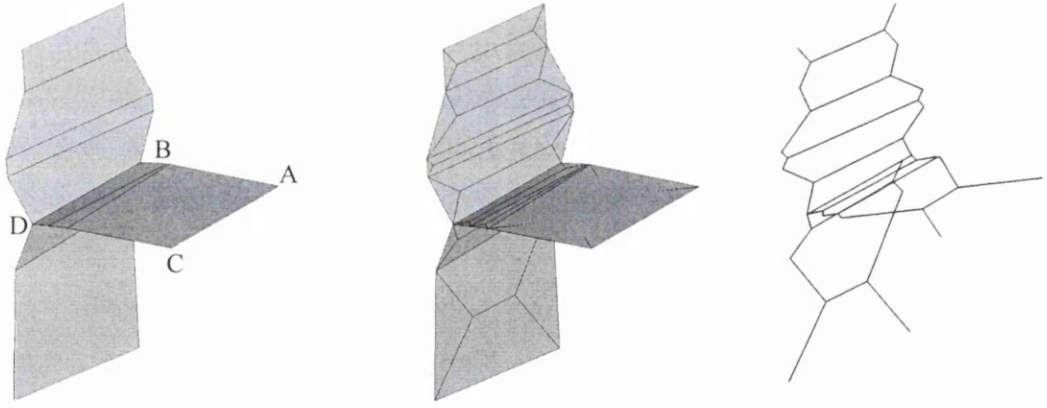

(a) Main medial surface obtained after rejecting inconsequential surfaces

(b) Medial axis generated for the main medial surface

(c) Medial axis only extracted from the main medial surface

Figure 6.26: Steps in obtaining important medial points for applying new approach

However due to variation in thickness along the width and length of the L-shaped plate casting as also due to other possible locations and shape of the feeder, the solidification may have to be steered e.g. from point A to B and C

to D as also from AB towards CD. The new approach presented earlier and its sorting algorithm will now demand more points along this directional solidification path to provide interface boundary conditions. This is now resolved by generating another medial axis of this main medial surface as shown in Figure 6.26 (b) and (c). This medial axis of the medial surface now provides sufficient medial points to seek associated geometric information for implementing the modified Heuvers' circle approach using medial axis transformation technique. Once all these important points are obtained and their associated radius information gathered from CADfix, the approach can be implemented using similar steps as outlined for earlier 2D case studies.

6.5.1.2 Application of method for 3D casting object

The applicability of this method to this 3D L-shaped plate is now further illustrated in this section. The desired path for steering the solidification is first chosen which is shown by letters and arrows in Figure 6.27. Since we have a brick shaped feeder that runs all along the length of the casting, the direction of solidification at any cross-section of this casting can be assumed to follow the path as shown in Figure 6.27. This would mean that casting starts solidifying beginning from section A through to B and similarly from section D through to E and then follows the path from C through the feeder neck F into the feeder G and finally H is the last point to solidify in the feeder.

As earlier mentioned, the casting is 400mm long and its thickness increases along all the three axes. For the purpose of applying this method on this particular casting, the radius information at above mentioned medial points (A, B, C, D, E, F, G and H) is taken at casting section lengths at 300mm and 100mm along the 'Z' direction (Figure 6.28).

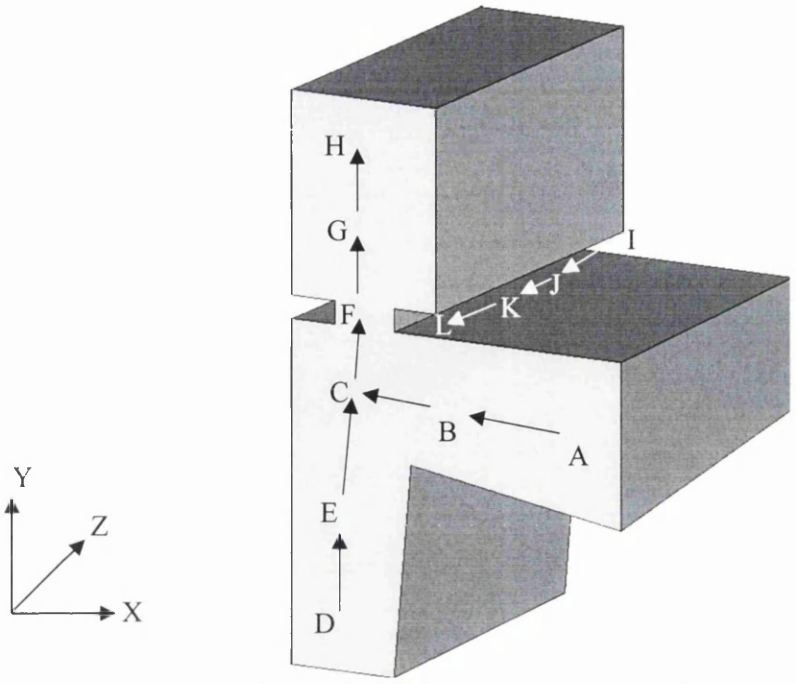

Figure 6.27: 3D L-shaped casting – Black arrows indicate the chosen path for steering solidification

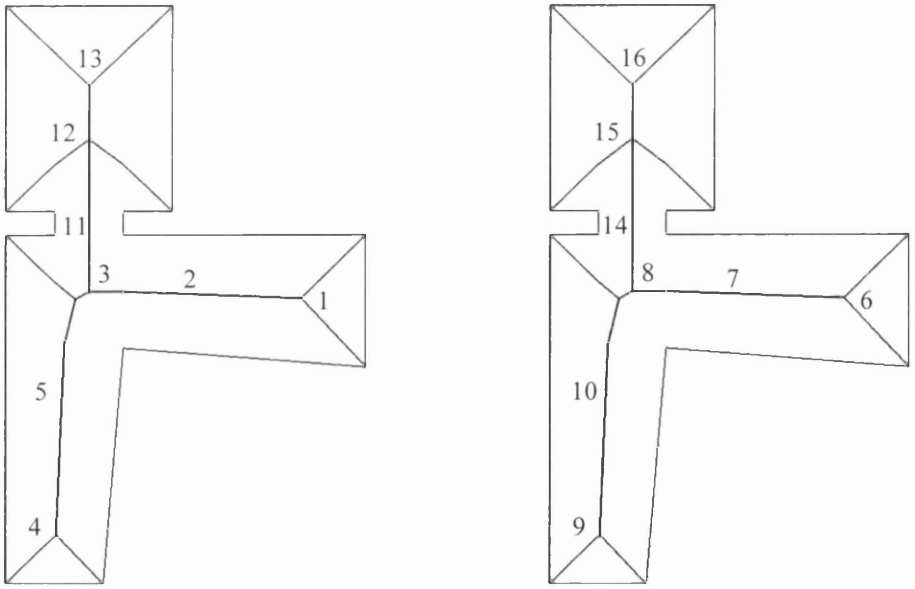

(a) Casting section at 'Z' = 300mm (b) Casting section at 'Z' = 100mm

Figure 6.28: Casting sections at different lengths showing medial points for extracting radius information (read with Table 6.11)

The radius information and length of the medial axis between respective medial points is also extracted from CADfix. From this, the Heuvers' radii

are computed and corresponding values of IHTC for exercising optimised thermal control in the casting are obtained. This information is given in Table **6.11**.

Points On Medial Axis		Original Radius (cm) R_o	Length of Medial Axis Section (cm)	Heuvers' Radius (cm) R_H	Modifying factor $(R_o/R_H)^2$	Original IHTC h_o (W/m^{2}K)	Modified IHTC h_H (W/m^{2}K)
At Z = 300mm							
A	1	8.81		8.81	1.00	2500	2500.00
B	2	7.43	11.66	9.98	0.55	2500	1386.77
C	3	8.21	10.84	11.06	0.55	2500	1377.58
D	4	5.29		5.29	1.00	2500	2500.00
E	5	6.17	12.80	6.57	0.88	2500	2204.85
C	3	8.21	13.80	7.95	1.07	2500	2666.20
At Z = 100mm							
A	6	7.93		7.93	1.00	2500	2500.00
B	7	6.81	11.66	9.10	0.56	2500	1401.31
C	8	7.96	10.84	10.18	0.61	2500	1528.52
D	9	5.20		5.20	1.00	2500	2500.00
E	10	5.84	12.80	6.48	0.81	2500	2030.56
C	8	7.96	13.80	7.86	1.03	2500	2564.02
Towards the Feeder at Z = 300mm							
C	3	8.21		11.06	0.55	2500	1377.58
F	11	3.50	7.50	11.81	0.09	2500	219.57
G	12	11.00	9.16	12.73	0.75	2500	1867.85
H	13	11.00	5.84	13.31	0.68	2500	1707.53
Towards the Feeder at Z = 100mm							
C	8	7.96		10.18	0.61	2500	1528.52
F	14	3.50	7.50	10.93	0.10	2500	256.35
G	15	11.00	9.16	11.85	0.86	2500	2155.67
H	16	11.00	5.84	12.43	0.78	2500	1957.87

Table 6.11: 3D L-shaped plate – Heuvers' radii and corresponding interface boundary conditions for optimised solution

6.5.1.3 Sorting technique for 3D application

The sorting of Heuvers' radii at a junction was guided by the same principle as has been described in Section 6.2.2.1 earlier. However, in case of a 3D cylindrical feeder at one particular end of the casting, the path for directional solidification will be different and in that case another dimension comes into

reckoning for steering solidification (solidification path I-J-K-L shown by white arrows in Figure 6.27). Now in this case, the desirable path for forcing solidification is from 1 to 2 in vertical section of the plate (Figure 6.29); then from 3 to 4 along the length of horizontal section of the plate and then gradually progressing from 5 through to 6 to 7 to 8 and finally 9 before the freezing contours enter the neck of the feeder at 10. The points at 11 and 12 in the feeder are the last sections to solidify thus ensuring adequate feeding for defect free casting. This would mean that junction or point 6 will only freeze after 3, 4 and 5 have solidified. Similarly casting section at 7 will solidify after 3, 4, 5, and 6 have solidified and so on. It is to be noted that unlike the long brick shaped feeder shown in Figure 6.29, we have assumed a cylindrical feeder just above sections 9. This section is the last to solidify in the casting, immediately followed by the neck of the feeder and finally sections 11 and 12 solidify in the feeder section. The sorting algorithm may then assume a 'tree' shape due to the nature of medial axis of the medial surface (Figure 6.26 c).

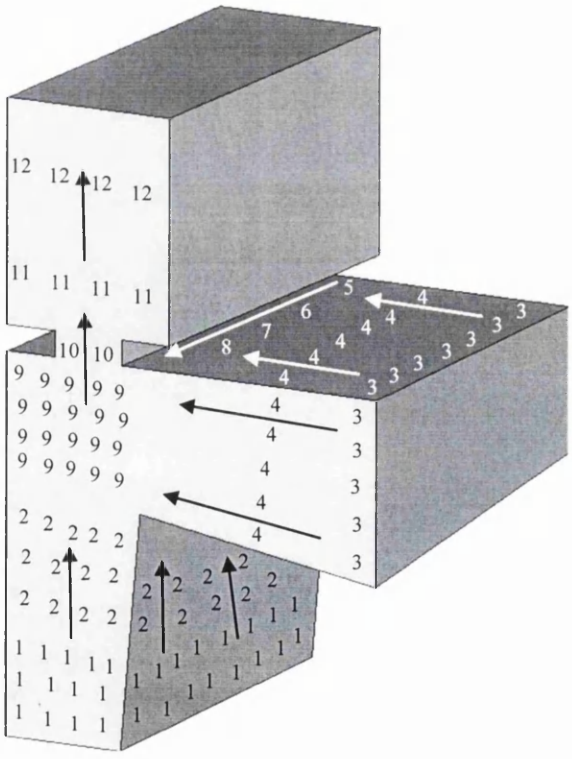

Figure 6.29: Schematic illustrating solidification stages, directional solidification that form basis for sorting technique for Heuvers' radii

It is clear from the above case study that once CADfix or similar software builds up its capability to provide robust three-dimensional medial surfaces and associated geometric information as easily as it does for 2D geometries, the method can be applied and extended with same speed and accuracy to three-dimensional casting objects too.

6.6 ASSESSMENT OF THERMAL GRADIENT ENSURING DIRECTIONAL SOLIDIFICATION USING MODIFIED HEUVERS' CIRCLE METHOD

As mentioned earlier, the goal set out and achieved by this method was to obtain a relative variation of IHTC along interface segments to ensure directional solidification in two FE simulations. It is gathered from above mentioned case studies that Heuvers' circles and radii were obtained by applying a standard 10% increase along the desired solidification path. This formed the basis for calculating modifying factor. This factor is in fact the radius ratio $(R_o/R_H)^2$, which is analogous to Chvorinov's modulus. Assuming uniform solidification initially for original geometry, the interface boundary conditions were obtained using this factor based on 10% gradient. This provided satisfactory results for all case studies as is evident from validation of results undertaken using FE simulations for each casting component studied. The method operated under following constraints

- A 10% increase is applied to obtain Heuvers' radii.
- The IHTC obtained after applying modifying factor based on above increase are checked to see if the value of $IHTC_{min}$ is realistic. If not, a scaling process was undertaken to obtain realistic values for $IHTC_{min}$.
- Based on this realistic value of $IHTC_{min}$, other values of IHTC are obtained and similar applicability check is again carried out for $IHTC_{max}$.

Now another case is considered wherein, for a particular geometry, the client or the foundry already has some values of IHTC and this practice needs to be effectively assessed using this technique. First example of gear blank casting is reconsidered for this purpose and Table 6.1 is reused (with IHTC value of

2500 W/m^{2}K instead of 3000 W/m^{2}K considered for the case study) for assessing this case. Based on client's practice (h_{Hc} in column 8 of Table 6.12) and by using equation derived for this technique (Equation 5.9 in previous chapter), the equivalent Heuvers radii (R_{Hc}) assumed by the client are calculated which are shown in column 9 of Table 6.12. From this, the percentage increase or decrease assumed by the client is calculated (Column 10).

Points on Medial Axis	Original Radii (cm) R_o	Heuvers' Radii (10%) (cm) R_H	Original IHTC h_o (W/m^{2}K)	Modifying factor $(R_o/R_H)^2$	Optimal (Heuvers') IHTC h_H (W/m^{2}K)	Client's optimal IHTC h_{Hc} (W/m^{2}K)	Value of Heuvers' radii R_{Hc} assumed by client	%age assumed by client
1	2	3	4	5	6	8	9	10
Q146	5.55	5.55	2500	1.00	2500	4000	4.39	
Q174	5.63	5.63	2500	1.00	2500	4000	4.45	
Q171	1.40	6.16	2500	0.05	129	200	4.95	9.41
Q171a	1.40	6.82	2500	0.04	105	170	5.37	6.35
Q151	1.40	7.48	2500	0.04	88	150	5.72	5.25
Q156	5.61	8.00	2500	0.49	1229	2200	5.98	5.09
Q168	5.54	8.10	2500	0.47	1169	2100	6.04	6.44
Q167	2.54	8.72	2500	0.08	212	400	6.35	4.93
Q158	2.54	8.95	2500	0.08	201	400	6.35	0.00
Q160	4.93	9.37	2500	0.28	692	1350	6.71	8.54
Q162	5.83	9.53	2500	0.37	936	1800	6.87	10.12
Q166	5.71	9.70	2500	0.35	866	1650	7.03	9.28
Q163	5.71	10.40	2500	0.30	754	1400	7.63	8.60

Table 6.12: Comparison of percentage increase for Heuvers' circles obtained from assuming uniform solidification and client's practice respectively

Now if the client practice has provided a defect free casting, then the method can be trained to adapt to client's percentage variation for prescribing Heuvers' geometry. For instance, by observing column 10 of Table 6.12, it may well be advisable to apply, say, 8% increase in Heuvers' radii instead of standard 10%. This is depicted by dotted circles in Figure 6.30. But if, on the other hand, the client practice has resulted in a defected casting, then the

client can be advised to adopt the optimal interface boundary conditions suggested by this method (Column 6)

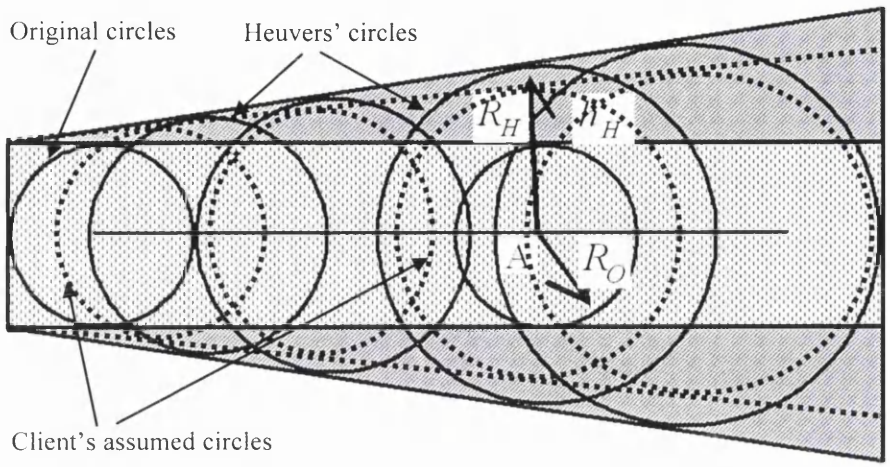

Figure 6.30: Assessment of client geometry and practiced optimal values using modified Heuvers' technique (read with Table 6.12)

Using this assessment, it becomes easier and convenient for the client to visualize and apply the modified boundary conditions derived from Heuvers' method taking in to consideration their own constraints or practices. At the same time the proposed method can be altered to adapt to existing foundry practices. The aim therefore, remains the same as set out while developing this method i.e. to obtain a relative variation of interface boundary conditions that are realistic and take existing norms and practices in to considerations.

6.7 DISCUSSION ON RESULTS

The last two chapters set out an objective of using a geometric reasoning based techniques and investigate their potential for application to casting problems in foundry situations. The medial axis transformation technique and Heuvers' circle method were selected from amongst other geometric methods because of the potential, scope, speed and ease of use that these two methods offered. These methods were combined with Chvorinov's classic rule on solidification to seek a new hybrid method. The newly developed method was then coupled with numerical simulation techniques to validate

effectiveness of the method and to build in accuracy element in the new method.

The hybrid method developed in this chapter not only predicts the hotspots in a solidifying casting but also effectively used geometric parameters (radius information of inscribed circles) to obtain effective boundary conditions. It is evident from the various case studies discussed in this chapter that the newly developed method provides an important information and lead into optimal numerical values of interfacial heat transfer coefficients. These values were then fed into FE simulation software to verify that the desired directional solidification pattern can be achieved. This can considerably bring down number of FE simulations during the casting design cycle.

As opposed to previous geometry based methods, this new method based on coupled approach has an added advantage as this takes into account the different material properties and is also sensitive to boundary conditions. This now provides an opportunity to interpret the results and values provided by this method and translate them into actions in real foundry situations to achieve optimal solutions.

The task can be accomplished by converting these optimal values provided by this method into design decisions in foundry industry. The relative variation of these values and numbers provides an indication on how to exercise that control in a solidifying casting by linking these to the heat flux at casting-mould interface. For example, higher values of interfacial heat transfer coefficients would suggest that more heat needs to be taken out from that particular section of the casting geometry by placing a chill. Therefore size and placement of chill can be guided by the values provided by the method. Similarly lower numbers would indicate a need for provision of insulation along that section. For different types of casting, these values/numbers will indicate a different design decision. Lower values in case of die casting will reveal need for increasing the die coating thickness along that particular length or section of the casting. In case of sand casting and other type of casting, these numbers or values of interfacial heat transfer

coefficients can guide placement of feeders and also their relative size. Higher values can also be indicative of need for providing cooling channels or increasing heat transfer from the mould through radiation by using fans. On the other hand, lower number in a section of a casting will warrant either heating the mould near that casting surface or providing padding or placing an additional adjacent casting to act as an additional heat source. A possible choice of such decisions for different types of casting is given in Table 6.13.

The important and critical information that this new method provides is the relative variation of these values/numbers across different sections of the casting geometry as this indicate the rate at which the heat needs to be taken out from the solidifying casting from those respective surfaces. It is this variation that will be the guiding principle in making and implementing various design decision discussed above and given in Table 6.13.

Choice of Design Decisions / **Type of Castings**	Feeders (Number, Size, Shape and Location)	Interface Conditions (IHTC, Chills, Insulations, padding)	Die Coating thickness	Mould & Outside (Cooling channels, Chills, Heating mould
Sand Casting	●	●		●
Gravity Die casting	●	●	●	●
Pressure Die casting	●		●	●
Investment Casting	●	●		●
Squeeze Casting	●		●	●

Table 6.13: Design decisions for different types of casting based on values of interfacial heat transfer coefficients obtained from new coupled approach

6.8 CLOSURE

The hybrid technique proposed in Chapter 5 that inherits the advantages of geometric and numerical methods was tested on a range of casting geometries in this chapter. The results were validated using FE simulations. The casting sections selected for undertaking case studies presented here posed different sets of problems to the method. The method was suitable improved to overcome these problems. In case of casting geometries with more than one medial axis or multiple medial axes, a sorting technique was developed and refined to selecting the most effective Heuvers' radius at junction of two medial axes. The unrealistic values of interfacial heat transfer coefficients provided by the method were scaled to yield to more realistic values that can be implemented in foundry settings. The proposed method was validated on a variety of casting geometries with different boundary conditions and it was shown that it provided the correct and optimal solution in two FE simulations. The method was then extended to three-dimensional casting objects and a conceptual framework was provided to demonstrate its successful application to 3D castings. As the capability of the CAD based software to provide a robust medial surface for three-dimensional casting objects builds up, the method can be applied to any 3D castings with same degree of success. The results were discussed and a framework was also proposed to assess design of any casting using this method and on how this relative variation of heat transfer coefficient values could be linked to various casting design decision in foundry situations.

REFERENCES

[1] S. J. Neises, J. J. Uicker and R. W. Heine, "Geometric Modeling of Directional Solidification based on Section Modulus", *AFS Transactions*, 1987, 95, 25-30.

[2] http://www.fegs.co.uk/CAE.html, last accessed on 16th Jan 2006. http://www.fegs.co.uk/medial.html, last accessed on 16th Jan 2006.

[3] http://www.swan.ac.uk/civeng/Research/casting/merlin/index.html, accessed in May 2005.

[4] Merlin Software Databank, School of Engineering, University of Wales Swansea, Swansea, UK, (Private communications).

[5] J. P. Holman, "*Heat Transfer*", 7th Edition, McGraw-Hill Book Company, London, UK, 1992, pp 2-3

[6] R. S. Ransing, M. P. Sood and W. K. S. Pao, "Computer Implementation of Heuvers' Circle Method for Thermal Optimization in castings, *International Journal of Cast Metals Research,* 2005, vol. 18, no 2, pp. 119-126.

[7] R. W. Lewis, M. T. Manzari, R. S. Ransing and D. T. Gethin, "Casting shape optimisation via process modelling", *Materials and Design* 2000, vol. 21 (4), pp. 381-386.

[8] R. W. Lewis, M. T. Manzari, R. S. Ransing and D. T. Gethin, "The optimal design of interfacial heat transfer coefficients via a thermal stress model", *Finite Elements in Analysis and Design,* 2000, vol. 34, pp. 193-209.

[9] R. W. Lewis, M. R. Ransing and R. S. Ransing, An approach for casting defect analysis employing finite element design optimisation, medial axis transformation and neural networks", *International Journal of Cast Metals Research,* 2002, vol. 18, pp. 41-53.

[10] T. E. Morthland, P. E. Byrne, D. A. Tortorelli and J. A. Dantzig, "Optimal riser design for metal castings", *Metallurgical and Materials Transactions,* 1995, 26B: 871-885.

Chapter 7

CONCLUSIONS

7.1 CONCLUSIONS

The work presented in this thesis constitutes the main body of research carried out to develop a new technique for solidification simulation by using Medial Axis Transformation technique in combination with other geometric reasoning and numerical methods. The aspects of casting solidification researched, developed, refined and modified were:

- Review of various techniques and methods employed in the field of casting solidification to develop an informed understanding of their advantages and limitations with regard to their applicability to contemporary casting problems.

- Develop techniques for employing MAT and associated geometric information to predict hotspots and temperatures during casting solidification. Learning from its application to casting geometries and resulting limitations, bring about enhancements for better results.

- Develop a new effective technique based on MAT and the Heuvers' Circle method and combine it with FE based simulation software and test and validate results on a variety of casting geometries.

Motivated by the potential and the unique and useful data structure that it offered and learning from its previous applications, the medial axis transformation (MAT) technique was investigated for its application to analyse casting solidification. Following achievements were accomplished successfully:

1. A new MAT based single interpolation technique for solidification simulation was presented. The technique was then expanded to

account for effect of mould in a cast-mould assembly. Enhancements were implemented in the proposed interpolation scheme to overcome limitations posed by its first version and in addition to distance ratio used for earlier algorithm; the radius ratio was also incorporated. The scheme solves one-dimensional heat conduction equations for cast and mould and then uses the geometric information provided by MAT through a double interpolation scheme to successfully predict hotspots and also simulate temperatures distribution contours in a solidifying casting. Once the data bank from FE simulation of one-dimensional bars is created, any casting geometry can be assessed for its design. Case studies were carried out to test the method on foundry castings applying realistic material properties and boundary conditions and the results were compared with numerical solutions and actual casting defects. The technique always predicted the correct location of hotspots, the most likely locations for occurrence of casting defects. The evolution of temperature distribution profiles provided by the technique compared favourably with the results obtained from FE simulations for same castings or published in literature. The scheme presented is a compromise between full numerical simulation, which is computationally expensive and the modulus method, which is insensitive to material properties and does not provide evolving temperature solutions.

2. Encouraged by the results achieved during the development of abovementioned scheme, as also owing to the limitations and the constraints under which the MAT based interpolation scheme operated, the MAT technique was further investigated. During this phase of research, MAT was used with another popular geometry based technique called Heuvers' Circle method. Based on Chvorinov's classic rule and modulus method, a new equation was derived for using radius and other geometric information obtained from MAT of the casting models to obtain effective interface boundary conditions for optimal solution. The method can constrain heat transfer coefficient values to yield more realistic values for foundry practice. The results

from this development were then validated using FE based solidification simulation software and published results.

3. This innovative hybrid method was tested on range of two-dimensional casting geometries and the technique was further improved to overcome problems posed by each of these cases. The castings studied included those from already published literature and realistic casting components from the foundries. A sorting technique was developed for selecting effective Heuvers' radii in castings with multiple medial axes. The scaling of values of interface heat transfer coefficients was adopted to provide realistic interface values for exercising desired thermal control in the cast-mould assembly. The inability of CADfix to generate robust three-dimensional models of castings impeded progress towards application of this scheme to 3D castings. However, within the limited capability of the CAD software, a case study was presented to conceptualise and demonstrate applicability of the modified Heuvers' Circle method to a 3D casting object. A framework was then provided on how this relative variation of heat transfer coefficient values could be linked to various casting design decision in foundry situations.

Thus it is observed that the research in casting optimisation has always been following these two parallel lines with no serious effort for their combination emerging from the reviewed literature. It is in the backdrop of this perspective that the research undertaken, accomplished and presented in this thesis assumes significance. The proposed method inherits the respective advantages of geometric and numerical methods and, at the same time, derives a relative variation of heat transfer coefficient values that helps in achieving the desired solidification pattern in castings.

To the best of author's knowledge, this was the first instance when the geometric reasoning based techniques have been combined with numerical simulation to predict hotspots and casting temperatures. Also for the first time, an effective technique has been developed that retains simplicity, ease

of use, speed, accuracy and sensitivity to material properties and boundary conditions, is robust and is still capable of providing optimal solutions in two FE simulations. The techniques proposed in this thesis have a useful potential to contribute significantly in helping the Product Life cycle Management (PLM) designer for undertaking a quick manufacturability assessment of casting components as set out in Section 1.1 of Chapter 1.

The progress made and this achievement has been acknowledged by Prof. J. Campbell on page 133-134 of his recent book [1] where he describes the technique and procedure proposed in Chapter 5 and 6. He further describes the proposed scheme as follows

> *"Failure to provide sufficient modulus gradient towards the feeder can be countered in various ways by (i) ..... describes a further option, (iv) in which he proposes a change in heat transfer coefficient. The latter technique is a valuable insight because it is easily and economically computed by a geometric technique, and so contrasts with the considerable computing reserves and efforts required by finite element and finite difference methods. ..... This simple technique has elegance, economy and power and is strongly recommended.*
>
> *Depending on the conditions, this failure of the modulus principle can be either a problem or a benefit. ..... the technique described above is unusual since it successfully takes this problem into account"*

7.2 FUTURE WORK

The foundations for a unified approach combining and inheriting advantages of both streams of casting optimisation (geometric and numerical) has, in essence, been laid to develop a robust technique capable of providing optimised solution for casting solidification in two FE simulations. As is the case with most research initiatives, significant achievements have been made

but certain aspects of related issues require further research. The issues involved are:

- The interpolation scheme presented needs to be tested for different material properties to expand its data bank that is used by the interpolation algorithm to improve its scope and application.

- At present, the scheme operates under limited and uniform boundary conditions and therefore, needs further development to operate under more varied and complex boundary conditions.

- There is a need to develop a robust medial axis generation tool that can provide medial axis for three-dimensional objects with same ease as it does for 2D geometries.

- The newly developed method needs to be further tested on more 3D casting objects. As the complexity offered by the casting shape increases, the number of medial axes and volume of associated geometric information will increase. This may necessitate development of a fast and advanced sorting algorithm for selecting the most effective Heuvers' radii at junction points of such medial axes.

- More studies are needed to link the modifying factor obtained from Heuvers' radii with the actual design decisions with in foundry settings. The relative variation of this factor and suggested heat exchange between cast and mould needs to be linked to decision making on location and shape and size of feeders, placement of chill or insulations, die-coating thickness etc for different types of casting.

The Grand Challenge for the Optimisation and Artificial Intelligence community is to develop a computer that not only is capable to optimise the entire casting process but could also learn from the failures, provide corrective actions automatically and evolve with time. In particular, it is

envisaged that the intelligent factory of future should have the following capabilities:

1. monitor all process control parameters
2. capture real time process data from a network of distributed sensors
3. analyse data and suggest feedback/corrective action - if necessary - on its own initiative.
4. keep traceability and control of all and each of the casting/mould produced in the foundry
5. allow changes of the process parameters 'on demand'

A possible methodology for future design process is summarized in Figure 7.1. The aim is to develop self-learning algorithms that can not only learn the entire 'cause and effect' relationships from past examples but also use this knowledge to optimally design the process by taking into account all process, design and material parameters.

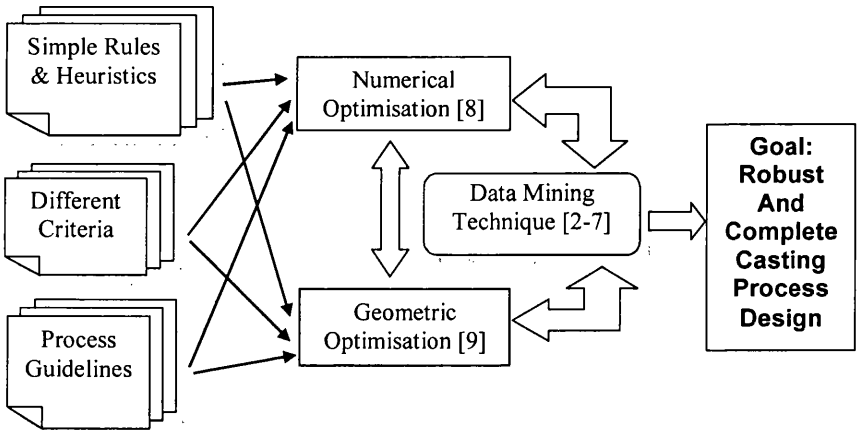

Figure 7.1: Optimal design of the entire casting process

The unified approach presented in this thesis is a step forward in the direction of completing this overall picture.

REFERENCES

[1] J. Campbell, *Castings Practice: The Ten Rules of Castings,* Butterworth-Heinemann, Oxford, UK, ISBN: 0750647914, May 2004.

[2] R. S. Ransing, M. N. Srinivasan, "Computer Aided Analysis for the Identification of Causes of Defects in Foundry", 10th Annual Convention of IIF, Madras, February 1991: 285-291.

[3] M. R. Ransing, Issues in learning cause and effect relationships from examples : with particular emphasis on casting processes, Ph.D. Thesis, University of Wales Swansea, UK , 2002.

[4] R.S. Ransing and R. W. Lewis, "Recognizing Patterns in Rejection Data for Diagnosis", *International Journal of Cast Metal Research,* 1998, 10, 207-219.

[5] M. R. Ransing, R. S. Ransing and R. W. Lewis, "Computer Methods for Analysis of Defects", *24th BICTA Conference on Investment Casting, Oxford,* 6-8 June 1999: 14-1:14-18.

[6] R. S. Ransing, M. R. Ransing and R. W. Lewis, "Limitation of Neural Networks Technique for Analysing Cause and Effect Relationship in Manufacturing Process - A Case Study", *Proceedings of Data Mining Conference*, Rio, Brazil, Editors: N. F. F. Ebecken, C. A. Brebbia and A. Zanasi, December 2003, ISSN: 1470-6326: 501-510.

[7] R. S. Ransing, M. R. Ransing and R. W. Lewis, "Defect Analysis: From Human Expert to Intelligent Computers", *11th World Conference on Investment Casting,* Edinburgh, UK, 23-26 May 2004, Paper 7:71-7.4.

[8] R. S. Ransing and R. W. Lewis, "Optimal Design of the Die Coating Thickness Using the Lewis-Ransing Correlation", *International Journal of Cast Metals Research*, 1997, Vol. 9: 269-277.

[9] R. S. Ransing, M. P. Sood and W. K. S. Pao, "Computer Implementation of Heuvers' Circle Method for Thermal Optimisation in Castings", *International Journal of Cast Metals Research,* 2005, Vol. 18, no 2, 119-126.